EFFECTS OF SLOPE ROUGHNESS ON WAVE RUN-UP ON COMPOSITE SLOPES

Prepared by

JERRY L. MACHEMEHL and JOHN B. HERBICH

Coastal and Ocean Engineering Division

TEXAS A&M UNIVERSITY

TAMU-SG-70-222 August 1970 COE Report No. 129

EFFECTS OF SLOPE ROUGHNESS ON WAVE RUN-UP ON COMPOSITE SLOPES

by

Jerry L. Machemehl and John B. Herbich
Coastal and Ocean Engineering Division
Texas A&M University

Partially supported by the National Science Foundation
Sea Grant Program
Institutional Grant GH-59 to
Texas A&M University

Sea Grant Publication No. TAMU-SG-70-222
Coastal and Ocean Engineering Division
Report No. 129 - C.O.E.

August 1970

ABSTRACT

A comprehensive study of the wave run-up (R) phenomena on single and composite slopes was conducted in order (1) to determine the effects of slope roughness (r) on regular and irregular wave run-up (R) on composite sections, (2) to determine the effects of slope roughness (r) on the velocity distribution in the uprush zone, (3) to investigate the energy loss in the uprush zone due to turbulence and bottom dissipation and (4) to compare regular and irregular wave run-up (R) on roughened slopes with wave run-up (R) on smooth slopes.

Monochromatic wave tests were run using wave periods (T) of 1.00 sec, 1.56 sec and 1.86 sec in water depths (d) of 1.2 ft, 1.5 ft and 1.8 ft. Equivalent deep water wave heights (H_e') were varied from 0.113 ft to 0.443 ft while the mean wave energy densities (E_μ) were varied from 0.0006 ft^2/sec^{-1} to 0.0165 ft^2/sec^{-1}. Wind (irregular) wave tests were run in water depths (d) of 1.2 ft, 1.5 ft and 1.8 ft. Wave periods varied from 0.72 sec to 0.83 sec, while equivalent deep water wave heights (H_e') varied from 0.290 ft to 0.396 ft and the mean wave energy densities (E) varied from 0.0100 ft^2/sec^{-1} to 0.0228 ft^2/sec^{-1}.

Three model structures [single (1 on 1-1/2 slope, composite (1 on 1-1/2 slopes with 1.5 ft berm) section and composite (1 on 1-1/2 slopes with 3.0 ft berm) section] were studied in a wind, water-wave flume. Three roughness conditions (smooth, parallel strips, and a symmetric block pattern) were investigated.

The following conclusions were drawn from the study:

1. The water depth affected the relative wave run-up (R) of the long waves ($\lambda >> d$, $H_o' << d$).

2. The reflecting capability (power) of the single (1 on 1-1/2 slope was not significantly affected by the slope roughness (r).

3. The reflecting capability (power) of the composite (1 on 1-1/2 slopes with berm) section was not significantly affected by the slope roughness (4).

4. The elevation of the berm with respect to the still water level had a significant effect on the reflecting capability (power) of the composite (1 on 1-1/2 slopes with berm) section.

5. The maximum reduction of wave run-up (R) occurred with the water depth equal to the berm elevation.

6. The parallel strip roughness element was the most efficient dissipator of the wave run-up (R) energy on the composite (1 on 1-1/2 slopes with berm) section.

7. The wave uprush velocity (V_u) on the smooth (1 on 1-1/2) slope was approximately seven-tenths of the wave celerity ($V_u = 0.7C$).

8. The slope roughness (r) reduced the maximum relative uprush velocity (V_u/C) on the 1 on 1-1/2 slope.

9. Due to the changing mean velocity in the uprush zone the level of turbulence could not be measured.

10. No significant difference between monochromatic wave run-up (R) and wind wave run-up (R) was noted on either the single (1 on 1-1/2) slope or the composite (1 on 1-1/2 slopes with berm) section.

A new method of determining wave run-up (R) using the mean wave energy density (E_μ) is proposed.

PREFACE

Research described in this report was conducted as part of the research program in Coastal and Ocean Engineering at Texas A&M University.

The report is primarily written by the senior author in partial fulfillment of the requirement for the Ph.D. degree.

The review of this report by Professors W. B. Davis, R. E. Schiller, Jr., E. A. Hiler and R. O. Reid was very much appreciated.

The research set fourth in this report was partially supported by the U.S. Army Coastal Engineering Research Center, Washington D. C., by the U.S. Army Engineer District, Galveston, by the W. G. Mills Memorial Fellowship and by the National Science Foundation Sea-Grant Program, Institutional Grant GH-59 to Texas A&M University.

TABLE OF CONTENTS

Page

Page

INTRODUCTION

Storm flooding has caused extensive damage in coastal areas for centuries. Seawalls, breakwaters, and dikes have been built in recent years to protect densely populated and highly industrialized coastal areas from destructive storms. In 1953, waves from a major North Sea storm breached the coastal dikes and seawalls in The Netherlands and England. This storm caused a great loss of life, extensive damage to property, and inundation of vast areas of cultivated land.

A thorough inspection of the dikes and seawalls after the storm revealed structural failure resulting from rearface erosion caused by substantial overtopping.

To prevent structural failure from overtopping, it is imperative that accurate information on wave run-up (vertical height of the limit of uprush reached by a wave on a slope) be determined for various wave and structural characteristics. An accurate assessment of the wave run-up (R) is essential for economic and safe design of a coastal structure.

The primary objectives of this study were:

1. To determine the effects of slope roughness (r) on regular and irregular wave run-up (R) on composite sections.
2. To determine the effects of slope roughness (r) on the velocity distribution in the uprush zone.

The citations on the following pages follow the style of the *Journal of the Waterways and Harbors and Coastal Engineering Division*, Proceedings of the American Society of Civil Engineers.

3. To investigate the energy loss in the uprush zone due to turbulence and bottom dissipation.

4. To compare regular and irregular wave run-up (R) on roughened slopes with wave run-up (R) on smooth slopes.

REVIEW OF LITERATURE

Wave Run-up (R)

Before presenting the available wave run-up (R) theories, it is important to describe what physically happens when a wave or wave train propagates from deep water to the shore. As a wave is propagated shoreward on the continental slope its wave length (λ) is shortened while its wave height (H) first decreases slightly and then increases. As the wave steepness (H/λ) reaches a certain limiting value for breaking [which depends on the relative depth (d/λ)] the wave breaks and a substantial amount of energy is dissipated. The wave may continue to break as a nonsaturated breaker (depending on the wave characteristics and bottom contour) or it may form a nonbreaking wave of smaller height (H) and continue to advance shoreward while growing in steepness. As a wave reaches very shallow water, it falls into the category of a shallow water wave ($\frac{d}{\lambda} < \frac{1}{25}$). The shallow water wave may become a bore with its height decreasing as it advances shoreward and finally it runs up the beach. If the wave steepness (H/λ) fails to reach the limiting value for breaking [which depends on the relative depth (d/λ)] the wave simply advances to the shore without breaking and runs up the beach or structure.

Theories for Nonbreaking Waves

When a long wave ($\frac{d}{\lambda} < \frac{1}{25}$) with small amplitude is propagated toward a steep slope the wave will not break seaward of the slope.

This wave is called a nonbreaking wave. If the bottom friction is neglected, the nonbreaking wave will be totally reflected by the steep slope. In the case of a vertical wall the wave run-up (R) will be equal to the wave height (H) of the original wave:

$$\frac{R}{H} = 1.0 \quad \ldots\ldots\ldots\ldots \quad (1)$$

For the case of a uniform slope and infinite depth ($d = \infty$) Miche[34], using linear theory, developed the following equation:

$$R/H = \sqrt{\pi/2\alpha} \quad \ldots\ldots\ldots\ldots \quad (2)$$

in which α is the slope angle. For a slope terminating at a finite depth Miche[35] derived the equation:

$$R/H = 1 + \pi \frac{H}{\lambda} \frac{1}{\tanh \frac{2\pi d}{\lambda}} \left(1 + - \frac{3}{4 \sinh^2 \frac{2\pi d}{\lambda}} - \frac{1}{4 \cosh^2 \frac{2\pi d}{\lambda}} \right). \quad (3)$$

by applying correction terms to Equation (1). Equation (3) loses its validity for a small relative depth since it predicts an infinite relative runup $\frac{R}{H} \to \infty$. In this case the wave run-up (R) must be approximated by solitary wave theory. Using solitary wave theory Wallace [49] investigated wave reflection from a vertical wall. He found the wave run-up (R) to be two and a half times the solitary wave height (H):

$$R/H = 2.5 \quad \ldots\ldots\ldots\ldots \quad (4)$$

For the case of a sloping beach rather than a vertical wall,

the superelevation terms found in Equation (3) are added to Equation (2) to obtain the equation:

$$R/H = \sqrt{\pi/2\alpha} + \pi \frac{H}{\lambda} \frac{1}{\tanh \frac{2\pi d}{\lambda}} \left(1 + \frac{3}{4 \sinh^2 \frac{2\pi d}{\lambda}} - \frac{1}{4 \cosh^2 \frac{2\pi d}{\lambda}} \right) \ldots \quad (5)$$

which is valid for moderate to steep slopes (S > 1 on 30). Equation (5) also loses its validity for a small relative depth since it predicts an infinite relative run-up ($R/H \to \infty$).

The propagation of waves in water of nonuniform depth was studied on the basis of linear theory by Lewy[33] and Issacson[20]. In these studies the bottom and the water surface were taken as the boundaries of a sector in a complex plane. The potential function satisfying the boundary conditions on the sector were determined by the method of reflections in the theory of complex variables.

For a nonuniformly sloping beach (slowly varying depth) Keller[28] matched the geometrical optics theory in deep water (which yields an approximate solution in deep water) to the linear, standing wave theory, (which yields an approximate solution near shore) to obtain the equation:

$$\frac{R}{H} = \frac{A}{2} = \frac{1}{2} \left(\frac{2\pi}{\alpha} \right)^{1/2} \frac{(Ko \sinh^2 \gamma Ko + \gamma Ko)^{1/2}}{\cosh \gamma Ko} \quad \gamma >> 1 \quad \ldots \quad (6)$$

in which α is the slope angle of the beach at the shore line, γ is

the dimensionless wave frequency ($2\pi/T\sqrt{g/d}$), Ko is the root of the equation:

$$Ko \tanh \gamma Ko = 1.0 \quad \ldots\ldots\ldots \quad (7)$$

For a uniformly sloping beach (particular bottom profile for which the equations of the linear shallow water theory can be solved explicitly for all values of the dimensionless wave frequency) Keller[27] derived the equation:

$$\frac{R}{H} = \frac{A}{2} = \left(J_0^2 \ \frac{2\gamma}{\alpha} + J_1^2 \ \frac{2\gamma}{\alpha} \right)^{-1/2} \quad \ldots\ldots \quad (8)$$

in which J_0 and J_1 are Bessel functions, and γ is the dimensionless wave frequency ($2\pi/T\sqrt{g/d}$).

To obtain results for nonlinear shallow water waves on a uniformly sloping beach, Keller and Keller[27] devised a numerical solution (method of finite differences) to solve the initial boundary value problem and calculate wave run-up (R) numerically. The method enabled an incident wave to be introduced into a one dimensional model bounded by the shoreline. Their results showed fair agreement with the analytical results for waves of low frequency but not for higher frequencies.

To improve the agreement with analytical results at higher frequencies, Keller and Keller[26] used a finite difference scheme of higher order accuracy. The discrepancies between the numerical and analytical results still occurred at the highest frequencies (which were still somewhat below those at which the analytical

results ceased to be valid).

Carrier[6] combined nonlinear shallow water theory with the linear dispersive theory for deep water to obtain the equation:

$$\frac{R}{H} = \frac{2.1}{\alpha^{1/2} X_o^{1/6}} \quad \ldots\ldots\ldots \quad (9)$$

which related run-up to the wave height at the point X_o for the case of a horizontal bottom for $0 < X < X_o$ and a delta function bottom elevation at $X = 0$.

Theories for Breaking Waves

No generally applicable wave run-up theory exists for breaking waves. Breaking is a nonconservative process and the breaking point is a mathematical singularity.

Bore run-up theory. Run-up of a bore on a beach was investigated in a sequence of papers by Ho and Meyer[15], Shen and Meyer[44], Ho, Meyer and Shen[16]. The bore run-up (R) was found to be independent of slope (S):

$$R = \frac{U_o^2}{2g} \quad \ldots\ldots\ldots \quad (10)$$

in which U_o is the horizontal velocity component at the instant the bore reached the shoreline. (This conclusion was also arrived at separately by Freeman and Le Mehaute'[18].) By using an approximation proposed by Whitham[52] the horizontal velocity (U_o) was calculated from bore behavior prior to its intersection with the beach. Keller, Levine, and Whitham[25] compared solutions for bore run-up

based on the approximations of horizontal velocity (U_o) by Whitham with numerical solutions obtained by integrating the nonlinear shallow water equations (see Stoker[47]) by finite differences. They found good agreement between the two methods of computing the bore run-up (R).

Nonsaturated breaker theory. Le Méhauté[32] first introduced the new concept of saturated and nonsaturated breakers. His theory overcomes a difficulty previously encountered in the long wave theory which resulted in the premature prediction of bores. Le Méhauté concluded that a solitary wave carries a maximum amount of energy towards the shore and that if excess energy exists in the wave, it will be dissipated in a spilling breaker. Also, if excess energy exists it will be carried along (by a bore instead of a spilling breaker) and will cause wave run-up (R). The following conclusions were drawn from this theory in which S is bottom slope and f_* is a friction coefficient:

(1) If $S < 0.01\ f_*$, the wave does not break due to bottom friction and viscous dissipation and there is no wave run-up (R).

(2) When $0.01\ f_* < S < (0.02 + 0.01\ f_*)$, the wave breaks as a spilling breaker and the energy dissipated by the breaker increases as the bottom slope increases. All the wave energy is dissipated before reaching the shoreline and there is no significant wave run-up (R).

(3) When $S > (0.02 + 0.01\ f_*) \simeq 0.02$, the breaker becomes saturated and becomes a fully developed bore. In this case, the maximum wave run-up (R) is experienced. Le Mehaute's theory therefore only predicts when appreciable wave run-up (R) will be experienced.

Numerical methods. Amein[2] investigated the motion of periodic long waves in shoaling water and their run-up on a sloping beach. His theoretical study was confined to waves with periods ranging from 30 seconds to several minutes (waves generally associated with tsunami and explosion waves arriving in coastal waters).

The wave propagation was determined by the first-order linear small amplitude surface wave theory away from the shore and by the first-order nonlinear shallow water theory near the shore. The calculations by the linear theory were made by using Friedrich's[9] second asymptotic representation while the calculations by the nonlinear theory were made by using a finite difference scheme based on the method of characteristics. Amein coupled the bore equations to the equations of the nonlinear theory in his numerical procedure to calculate the wave run-up on a dry slope.

Experimental Investigations

Due to the complexity of this phenomenon, theory alone has not always been able to accurately predict wave run-up heights (especially true if the wave breaks seaward of the shore). Present knowledge has been acquired only through the painstaking effort of both theorists and experimentalists. Analysis and experiment have merged as tools in scientific research to supplement the available theories in the understanding of this complicated problem.

Significant parameters. In formulating the physical laws which govern a natural phenomenon it is normal practice to form

dimensionless parameters from the variables involved in the problem. The dimensionless parameters evolved can then be studied under closely controlled laboratory conditions and solutions to the problem derived. In an investigation to determine the height of wave run-up (R) on a rough impermeable continuous slope, the following variables are important:

a. Geometric variables
   - Wave run-up, R
   - Wave height, H
   - Wave length, λ
   - Depth of water, d
   - Relative roughness, r
   - Structure slope, α

b. Dynamic variables
   - Wave celerity, C
   - Wave energy, E

c. Fluid properties
   - Mass density, ρ
   - Dynamic viscosity, μ

The general equation may be written as follows:

$$f_1 (R, H, \lambda, d, r, \alpha, C, E, \rho, \mu) = 0 \quad . . . \quad (11)$$

Utilizing the Buckingham π- theorem the following dimensionless parameters were obtained:

$$f_2 \left(\frac{R}{H}, \frac{H}{\lambda}, \frac{H}{d}, \frac{H^2C^2\rho}{E}, \frac{HC\rho}{\mu}, \alpha, r \right) = 0 \quad . . . \quad (12)$$

Where R/H relates the wave run-up (R) to incident wave height (H), H/λ and H/d relate the wave run-up (R) to wave length (λ) and water depth (d), respectively, $\frac{H^2C^2\rho}{E}$ is an energy term which is approximately equal to $\tanh \frac{2\pi d}{\lambda}$, $\frac{HC\rho}{\mu}$ is a form of the Reynolds Number,

α is (a characteristic of) the slope and r is a term describing the surface roughness.

These parameters must then be investigated to determine their effect upon the wave run-up (R) on a slope or structure.

Investigation by Bruun. A study was conducted by Bruun[5] to determine the effects of structural shape and characteristics on wave run-up (R) and wave reflection. Single slopes, composite slopes, and composite slopes with berms were investigated (see Fig. 1). For a single impermeable slope Bruun found (1) that the slope should be greater than 1 on 1.5 to facilitate breaking and (2) that the maximum effect of a roughness element appears on a 1 on 2 slope. For an impermeable composite slope with berm he found (1) that the berm elevation should be at or near storm water level, (2) that the berm should (for practical reasons) be horizontal or inclined forward and (3) that a composite section with stilling basin was very effective in reducing wave uprush.

Investigation by Granthem. Granthem[11] investigated constant-slope structures for the purpose of determining experimentally (1) the effect of slope angle (α) and side slope porosity (n) on wave run-up (R) and (2) to investigate the effect of wave steepness (H/λ) and relative depth (d/λ) on wave run-up (R). A series of wave uprush tests were run in the 60 ft U of C (University of California) wave tank for slope angles (α) ranging from 15° to 90°, wave heights (H) from 0.075 ft to 0.307 ft, water depths (d) from 0.98 ft to 1.23 ft, and for wave steepness ratios ($\frac{H}{\lambda}$) from 0.012 to 0.112.

(a) Composite slope

(b) Composite slope with variable berm

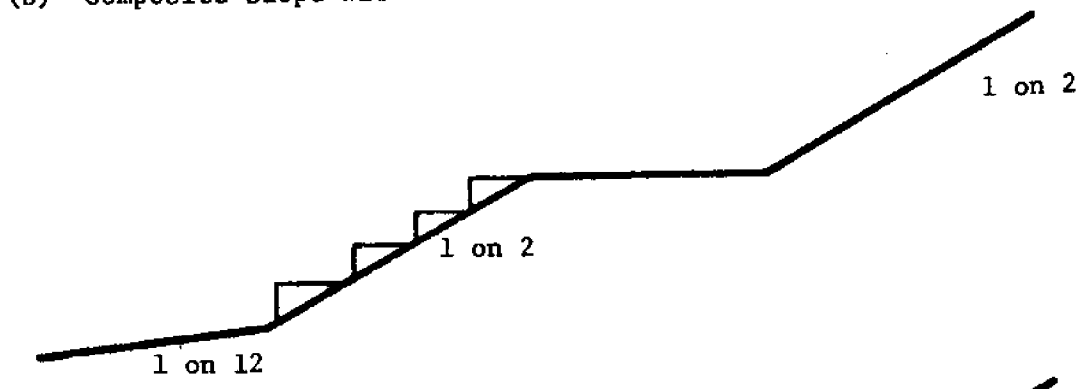

(c) Composite slope with steps

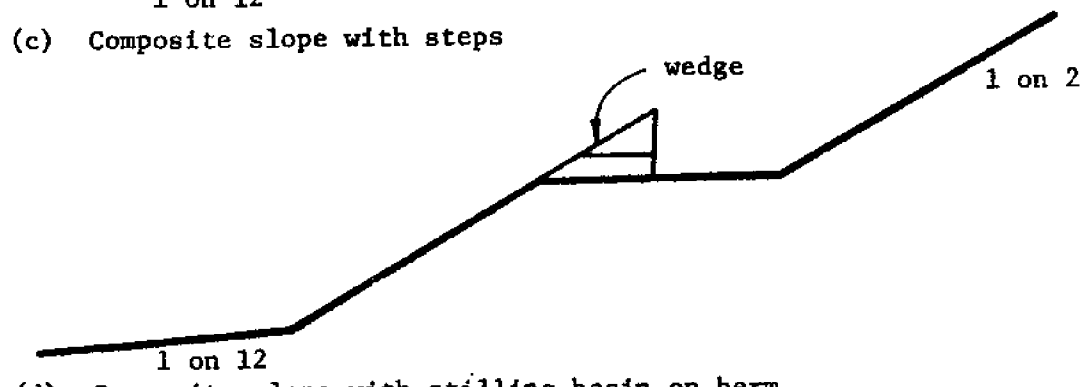

(d) Composite slope with stilling basin on berm

FIG. 1.--MODEL STRUCTURES TESTED BY BRUUN[5]

The constant slope models used by Granthem consisted of a smooth flat surface with a porosity n = 0% and two specially constructed model slopes of 1-1/2 inch maximum angular stone and well rounded pea gravel with porosities n = 32.6% and n = 28.9%, respectively. From the investigation Granthem concluded that (1) as structure porosity (n) increases, the wave run-up (R) decreases, (2) as the wave steepness (H/λ) increases, the wave run-up (R) increases, and (3) as the relative depth (d/λ) decreases, the wave run-up (R) increases. Granthem also found that for a given incident wave the maximum wave run-up (R) will occur when the slope angle is approximately 30° and that if there is any variation from this slope in either direction, the wave run-up (R) will decrease.

Investigation by Hall and Watts. Hall and Watts[12] investigated wave run-up (R) from solitary waves on an impermeable single slope. Tests were conducted in the B.E.B. (Beach Erosion Board) wave tank (85 ft long, 14 ft wide and 4 ft deep) using a wave generator producing a single horizontal push. Slope angles (α) tested ranged from 5° to 45°, water depths (d) from 0.5 ft to 2.25 ft and wave heights (H) from 0.005 ft to 0.5 ft. Results from the run-up (R) experiments were presented in the form:

$$\frac{R}{d} = f_1(S) \left(\frac{H}{d}\right)^{f_2(S)} \quad \ldots\ldots\ldots \quad (13)$$

in which $f_1(S)$ and $f_2(S)$ are empirically-determined functions of the slope (S). The functions obtained by Hall and Watts are shown in Table 1.

TABLE 1.--EMPIRICAL COEFFICIENTS AND EXPONENTS FOR USE WITH RELATIVE RUN-UP EQUATION BY HALL AND WATTS[12]

Slope (1)	f_1 (S)[a] (2)	f_2 (S)[a] (3)
$0.09 < S < 0.2$	$11.00\ S^{0.67}$	$1.90\ S^{0.35}$
$0.20 < S < 1.0$	$3.05\ S^{0.13}$	$1.15\ S^{0.02}$

[a]After Hall and Watts[12].

Investigation by Kaplan. Kaplan[24] investigated tsunami run-up (R) on smooth continuous slopes. His preliminary tests in the B.E.B. wave tank (96 ft long, 1.5 ft wide and 2 ft deep) showed that for a given wave height (H) the initial wave will give the maximum run-up (R) while the wave run-up (R) from the following waves are significantly reduced by backwash. For continuous slopes of 1 on 30 and 1 on 60, and for a vertical type reflecting wall, and 1 on 2 dike type wall installed at the shore line on the 1 on 60 slope Kaplan obtained the empirical equations in Table 2.

Investigation by Sibul. An experimental investigation was conducted by Sibul[45] to determine the quantity of water pumped over an impermeable uniform slope by wave action. A series of tests were conducted in the U of C (University of California) wave research laboratory wave tank (60 ft long, 3 ft deep, and 1 ft wide) for smooth and roughened 1 on 2 and 1 on 3 slopes. Wave run-up (R) in

TABLE 2.--EMPIRICAL EQUATIONS FOR RELATIVE WAVE RUN-UP BY KAPLAN[24]

Slope (1)	Relative run-up[a] (2)
1 on 30 slope	$R/H = 0.381\ (H/\lambda)^{-0.316}$
1 on 60 slope	$R/H = 0.206\ (H/\lambda)^{-0.315}$
1 on 60 slope with reflecting type wall	$R/H = 0.436\ (H/\lambda)^{-0.285}$
1 on 60 slope with 1 on 2 dike type wall	$R/H = 0.418\ (H/\lambda)^{-0.283}$

[a]After Kaplan. The wave length (λ) is defined as twice the distance between the first noticeable rise of the water and the maximum.

each test was equal to the elevation of the crest of the structure when the latter was just high enough to prevent overtopping. Sibul found maximum wave run-up (R) occurring at the wave steepness $(\frac{H}{\lambda})$ which caused breaking at the edge of the structure. When the breaking point moved seaward of the structure the wave run-up (R) decreased. With the wave breaking seaward of the structure he found a decrease in the wave run-up (R) with decreasing wave steepness $(\frac{H}{\lambda})$. For a given wave condition the critical wave steepness $(\frac{H}{\lambda})$ which caused breaking on the structure was higher for the 1 on 2 slope than for the 1 on 3 slope.

Investigation by Sibul. Wave run-up (R) from wind generated waves was first investigated by Sibul[46] in the U of C (University of California) wave tank (60 ft long, 1 ft wide, and 1.28 ft deep). Wave uprush tests were conducted on smooth continuous 1 on 3 and 1 on 6 slopes rising above a 1 on 10 bottom slope. Comparing wave run-up (R) from wind generated waves with wave run-up (R) from mechanically generated waves Sibul found no significant difference in relative run-up $(\frac{R}{H})$ on the 1 on 6 slope for low wind velocities (V). On the 1 on 3 slope, however, he found a 30 per cent increase in the relative run-up $(\frac{R}{H})$ from the wind generated waves.

Sibul found the breaker location affecting the wave run-up (R). With the breaking point at the edge of the structure the wave run-up (R) was at a maximum. When the breaking point moved seaward the wave run-up (R) decreased. Sibul states that for the 1 on 3 slope the deep water extended much closer to the edge of the structure

than for the 1 on 6 slope, thus allowing the waves to approach closer to the structure before breaking. He further states that this caused the higher run-up (R) values on the 1 on 3 slope.

Investigation by Saville. Saville[43] analyzed run-up (R) data from a comprehensive test program conducted jointly by W.E.S. (Waterways Experiment Station) and B.E.B. W.E.S. used a large wave flume (120 ft long, 5 ft wide, and 5 ft deep) to collect wave run-up (R) data for a vertical wall, a curved wall (based on the Galveston seawall section), a similar curved wall with a recurvature at the top, smooth slopes of 1 on 3 and 1 on 1-1/2, a step-faced wall of 1 on 1-1/2 slope, and a riprap faced wall of 1 on 1-1/2 slope (one layer of riprap on an impermeable base) as shown in Fig. 2. All of the structures were fronted by a 1 on 10 beach slope during testing. Wave heights (H) were varied from 0.17 ft to 0.70 ft, while the wave periods (T) ranged from 0.63 seconds to 3.64 seconds. Water depths (d) at the toe of the structures were varied from 0.00 ft to 0.53 ft. B.E.B. used a smaller wave flume (96 ft long, 1.5 ft wide, and 2 ft deep) to collect wave run-up (R) data on smooth slopes of 1 on 1-1/2, 1 on 2-1/4, 1 on 3, 1 on 4, and 1 on 6. The structures were fronted by a 1 on 10 beach slope. Wave heights (H) were varied from 0.03 ft to 0.58 ft while the wave periods (T) ranged from 0.61 seconds to 4.70 seconds. Water depths (d_2) at the toe of the structures were varied from 0.00 ft to 1.25 ft. In addition smooth slopes of 1 on 10 and 1 on 30 were tested for one depth.

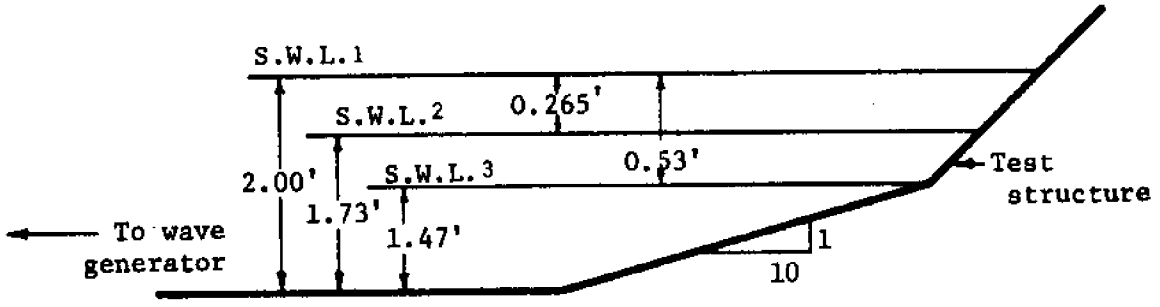

a. Waterways Experiment Station

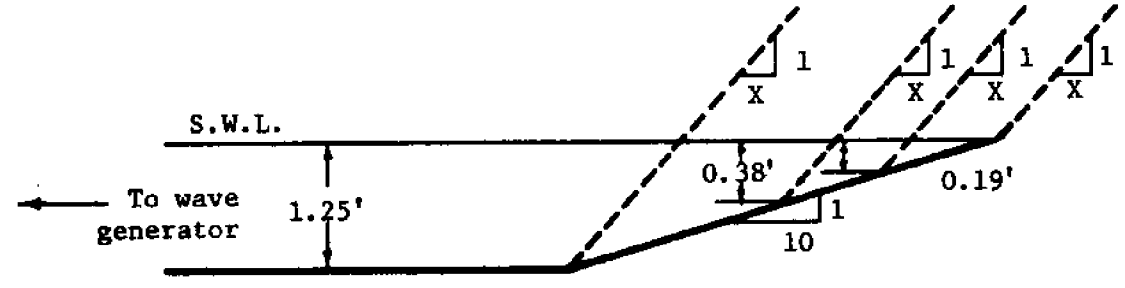

b. Beach Erosion Board

FIG. 2.--MODEL STRUCTURES TESTED BY WATERWAYS EXPERIMENT STATION AND BEACH EROSION BOARD

The first tests were run to determine the effect (if any) of depth (d) on wave run-up (R). Saville found run-up (R) increasing with depth of structure until a depth-height ratio (d/H_o') of between 1 and 3 was reached.

Evaluating wave run-up (R) for various structures, Saville found the vertical wall more efficient in reducing wave run-up (R) than slopes steeper than 1 on 4 (for all conditions except that of zero depth at the structure toe). He attributed this decrease in wave run-up (R) to the fact that the waves (horizontal) momentum must be changed instantaneously to vertical momentum to carry the wave up the wall (some momentum may be carried downward if the wave breaks on the wall) whereas on a slope the waves (horizontal) momentum changes gradually to vertical momentum. Saville found the highest relative run-up (R/H_o') values on the curved walls.

Investigation by W.E.S. An experimental investigation was conducted by W.E.S.[51] (Waterways Experiment Station) to obtain information relative to wave run-up (R) and overtopping of levees. A series of wave uprush (R) tests were conducted on 1:30-scale section models in the W.E.S. wave tank (94 ft long, 1.0 ft wide, and 1.5 ft deep). The tests were run to determine the effects of (1) levee slope (α) on wave run-up (R), (2) water depth at toe of beach (d_1) on wave run-up (R), (3) water depth at toe of levee (d_2) on wave run-up (R), (4) various combinations of berms on wave run-up (R) and overtopping, and (5) various combinations of composite slopes on wave run-up (R) and overtopping. A series of single and

composite slopes ranging from 1 on 20 to 1 on 2 with a beach slope of 1 on 10 were tested.

W.E.S. found the magnitude of wave run-up (R) to be a function of the wave steepness ($\frac{H}{\lambda}$), slope of levee (α), geometry of levee face, water depth at toe of beach slope (d_1), water depth at toe of levee (d_2), roughness (r) and permeability (n) of levee face, wind speed (V), and time relative to wave period (T) required for water that runs upslope for a given wave to return downslope.

The equation for relative run-up (R) can be expressed as:

$$R/H = f\left(\frac{H}{\lambda},\ \alpha,\ d_1 \text{ and } d_2,\ \begin{matrix}\text{berm}\\ \text{width,}\end{matrix}\ \begin{matrix}\text{slope}\\ \text{geometry,}\end{matrix}\ \begin{matrix}\text{wave}\\ \text{backwash}\end{matrix}\right) \quad . \ . \ . \qquad (14)$$

in which d_1 and d_2 are water depth at toe of beach slope and water depth at toe of levee section, respectively. The following conclusions were drawn from the study:

(1) Water depth at the beach toe (d_1) had a negligible effect on wave run-up (R).

(2) Wave run-up (R) increased as wave steepness (H/λ) decrease [for the range ($0.03 < H/\lambda < 0.08$)].

(3) Wave run-up (R) decreased as water depth at the levee toe (d_2) decreased.

(4) Wave run-up (R) decreased as the berm width increased.

(5) An increase in water depth at the break in grade of a composite levee slope resulted in a decrease in run-up (R).

(6) Wave run-up (R) decreased as levee slope (α) decreased.

(7) Wave run-up (R) data was not affected (to a measurable extent) by scale effect.

Investigation by Wassing. Wassing[50] summarized model investigations on wave run-up (R) carried out in the Netherlands over a twenty-year period. His summary included wave run-up (R) on smooth and roughened impermeable slopes (straight, convex, berm dike, and berm dike with stilling basins). As reported by Wassing, the wave run-up (R) was governed by (1) wave characteristics in front of the dike, (2) the direction of wave propagation, (3) the slope of the dike (α), (4) the shape of the dike, (5) the character of the dike facing and (6) the artificial foreshore conditions. Of particular interest herein was the influence of the dike berm and the character of the dike facing. The equation for run-up (R) that was developed can (for clarification of the influence of this factor) be rewritten as:

$$\frac{R}{H} = \phi \, f\left(\alpha, \frac{H}{\lambda}, \frac{B}{\lambda}, \text{Type of facing, and so forth}\right) \quad . \; . \; . \qquad (15)$$

where the value of ϕ was taken as unity for a revetment of neatly set stones. Values of ϕ for various kinds of artificial roughness are summarized by Wassing.

From various model tests on berm dikes it was found that the berm width should be approximately 1/4 λ.

Investigation by Savage. Savage[39, 40] investigated wave run-up on smooth, roughened, and permeable structures of constant slope. The objectives of his study were to determine the effects of

roughness (r) and permeability (n) on wave run-up (R). A series of wave run-up (R) tests were run in the C.E.R.C. (Coastal Engineering Research Center) wave tank (96 ft long, 1.5 ft wide and 2 ft deep) for slopes ranging from 1 on 30 to a vertical wall, wave heights (H) from 0.001 ft to largest stable height, and wave periods (T) from 0.5 sec to 5 sec. A constant water depth (d) of 1.25 ft was used in all tests. Savage found the magnitude of wave run-up (R) to be a function of the deep water wave steepness (H_o'/T^2), the structure slope (α), the mean diameter of the roughness material (d_1) or the permeability of the slope material (n), and the form of wave breaker which, in turn, depends on the behavior and timing of the backwash from the proceeding wave. The equation for relative wave run-up can be expressed as:

$$\frac{R}{H} = f_1\left(\frac{H_o'}{T^2},\ \alpha\ ,d' \text{ or } n,\ \begin{matrix}\text{Form of the}\\ \text{breaker}\end{matrix}\right) \quad \ldots\ldots \qquad (16)$$

in which H_o' is the equivalent deep water wave height, T is the wave period and d' is the particle diameter of the roughness material.

Evaluating wave run-up (R) on smooth slopes, Savage found the highest relative run-up (R/H_o') for steep waves occurring on a slope in the order of 1 on 2 and the highest relative run-up (R/H_o') for waves of low steepness occurring on a slope in the order of 1 on 4. From his investigation of roughened and permeable slopes he found (1) that the effect of slope roughness (or permeability) increases with an increase in the roughness (or permeability), (2) that the

effect of a constant roughness (or permeability) on a given slope increases with decreasing wave steepness (H_o'/T^2) and that (3) the effect of a constant roughness (r) or permeability (n) increases as the slope flattens.

Discussion by Hunt. In 1953, Hunt[19] summarized all the equations (known to him) being utilized to compute wave run-up (R) on a seawall. From his review of the wave run-up (R) phenomenon he proposed the equations shown in Table 3 be used in seawall design.

Investigation by Hudson. Hudson[18] investigating wave run-up (R) on a model breakwater found the relative run-up (R/H) to be a function of breakwater slope (α), wave steepness (H/λ) and, to some extent, the hydraulic roughness (r) of the breakwater surface. A series of wave uprush tests were run for slopes ranging from 1 on 1-1/4 to 1 on 5 with relative depths (d/λ) from 0.10 to 0.50. Hudson found the effects of relative depth obscured by a wide range of scatter in the observed values of wave run-up (R). He attributes this scatter to the complexity of defining and observing the phenomenon of wave motion on a roughened slope.

Although his tests were not designed specifically to study the effects of hydraulic roughness (r) on wave run-up (R), he conducted wave uprush (R) tests on breakwater sections composed of 0.10 lb and 0.30 lb stones. For a 1 on 4 slope Hudson found the effects of hydraulic roughness (r) negligible while on a 1 on 5 slope the wave run-up (R) was reduced 20 per cent. Hudson states that this phenomenon can probably be explained by the fact that waves tend to

TABLE 3.--EMPIRICAL EQUATIONS FOR RELATIVE WAVE RUN-UP BY HUNT[19]

Wave and structure conditions (1)	Relative run-up (R/H) (2)	Limitations and assumptions (3)
Wave run-up on a continuous sloping impermeable structure	$R/H = \frac{2.3 \tan \alpha}{(H/T^2)^{1/2}}$	$i^2 < H/T^2$ $H \approx H_o'$
Wave run-up (surging wave) on a continuous sloping impermeable structure	$R/H \quad 3$	$i^2 < H/T^2$ $H \approx H_o'$
Wave run-up on a composite slope	$R/H = \frac{2.3}{(H/T^2)^{1/2}} \frac{\tan \alpha_1 + \tan \alpha_2}{2} S$	SWL at the break in slope $i^2 < H/T^2$ $H \approx H_o'$ $S \approx 0.8$ to 0.9
Wave run-up on a continuous (roughened) sloping impermeable structure	$R/H = \frac{2.3}{(H/T^2)^{1/2}} \tan \alpha \ (r)$	$i^2 < H/T^2$ $H \approx H_o'$

break more readily on flatter slopes which provide a greater distance over which energy losses can occur. Hudson also states that his tests are not sufficient to determine fully and accurately the effects of hydraulic roughness (r) on wave run-up (R), and that additional tests are necessary.

Discussion by Saville. Saville[41] discussed the dependency of relative run-up (R/H) on relative depth (d/λ). He points out the fact that both wave height (H) and wave length (λ) are dependent on the relative depth (d/λ) in which they are measured and that a wave run-up (R) curve independent of relative depth (d/λ) will produce an anomaly of wave run-up (R) values for a particular wave train (depending on where the wave characteristics are measured). Saville also suggests that there is a tendency for relative run-up (R) to decrease with decreasing wave steepness (H/λ) below a critical steepness value (although this conclusion is largely dependent on the location of a single point).

Investigation by Adam. An experimental investigation was conducted by Adam[1] to determine the height of wave run-up (R) on smooth and roughened structures of constant slope for wave heights in the same dimensional range as the slope riprap material. A series of wave uprush (R) tests were run in the University of Manitoba wave tank (44 ft long, 3 ft wide, and 2.33 ft deep) for slopes ranging from 1 on 30 to a vertical wall, wave heights (H) from 0.075 ft to 0.580 ft and wave periods (T) from 1.0 to 4.0 seconds. A constant water depth (d) of 1.50 feet was used in all the tests. The riprap

material used in the tests on roughened slopes ranged in size from 0.021 ft (1/4 in.) to 0.50 ft (6 in.). From the investigation Adam concluded that (1) as the wave steepness (H_o'/T^2) decreased, the effect of slope roughness on wave run-up (R) increased, (2) as the roughness coefficient ($H_o'T^2/d^2$) [actually the reciprocal of a dimensionless roughness coefficient] decreased, the effect of slope roughness on wave run-up (R) increased and (3) that for a constant wave steepness (H_o'/T^2) and roughness coefficient ($H_o'T^2/d$), the effect of slope roughness increased as the slope decreased. Adam also found maximum wave run-up (R) occurring on a 1 on 4 (or 1 on 6) slope for waves of low steepness ($H_o'/T^2 = 0.005$) and on a 1 on 1 (or 1 on 2) slope for waves of high steepness ($H_o'/T^2 = 0.400$).

Investigation by Herbich *et al.* To determine the limitations of Saville's method for predicting wave run-up on composite beaches Herbich *et al.*[14] investigated the effect of berm width (B) on wave run-up (R). A composite structure (1 on 4 slopes) with variable berm) was studied in the F.E.L. (Fritz Engineering Laboratory) wave tank (67.5 ft long, 2 ft deep, and 2 ft wide). Shallow water waves with periods (T) ranging from 0.67 to 1.67 sec and with wave heights (H_o') ranging from 0.09 to 0.34 ft were generated in the study.

The theoretical values of wave run-up (R) predicted by Saville's method[42] were compared with experimental values from the study. The theoretical values compared favorably with experimental values for berm to wave length ratios (X/λ) less than 0.15. For berm to wave

length ratios (X/λ) greater than 0.15 there was little agreement as the experimental run-up (R) remained approximately constant while the predicted values decreased.

Investigation by Hosoi and Mitsui. An experimental investigation was conducted by Hosoi and Mitsui[17] to determine the effect of breaking waves on the run-up (R) on composite slopes. A series of wave uprush tests were run with composite slopes (see Fig. 3) in the 368 ft P.W.R.I. (Public Works Research Institute) wave tank for deep water wave heights (H_o') ranging from 0.32 ft to 2.14 ft, water depths (d) from 3.28 ft to 4.6 ft and for wave steepness ratios (H_o'/λ_o) from 0.005 to 1.0. Results of the tests indicated that the relative run-up (R/H_o') was a function of the characteristic of the breaker within the range of $d/H_o' = 2.3$ to 11.7.

Investigation by Jordaan. Theoretical and experimental studies were conducted by Jordaan[23] to determine maximum wave uprush (R) from an impulsively generated wave train (wave train of continuously decreasing periodicity and varying amplitude). The tests were conducted in the N.C.E.L. (Naval Civil Engineering Laboratory) wave basin (94 ft by 92 ft and 3 ft deep). Three rigid beach sections of 1:5, 1:15, and 1:24 provided with smooth, fine-grained and coarse-grained strips were tested to determine the relative effects of surface roughness on wave run-up (R). A plunger in the form of a paraboloid of revolution about the axis of symmetry was used to create the wave train by displacement or impact.

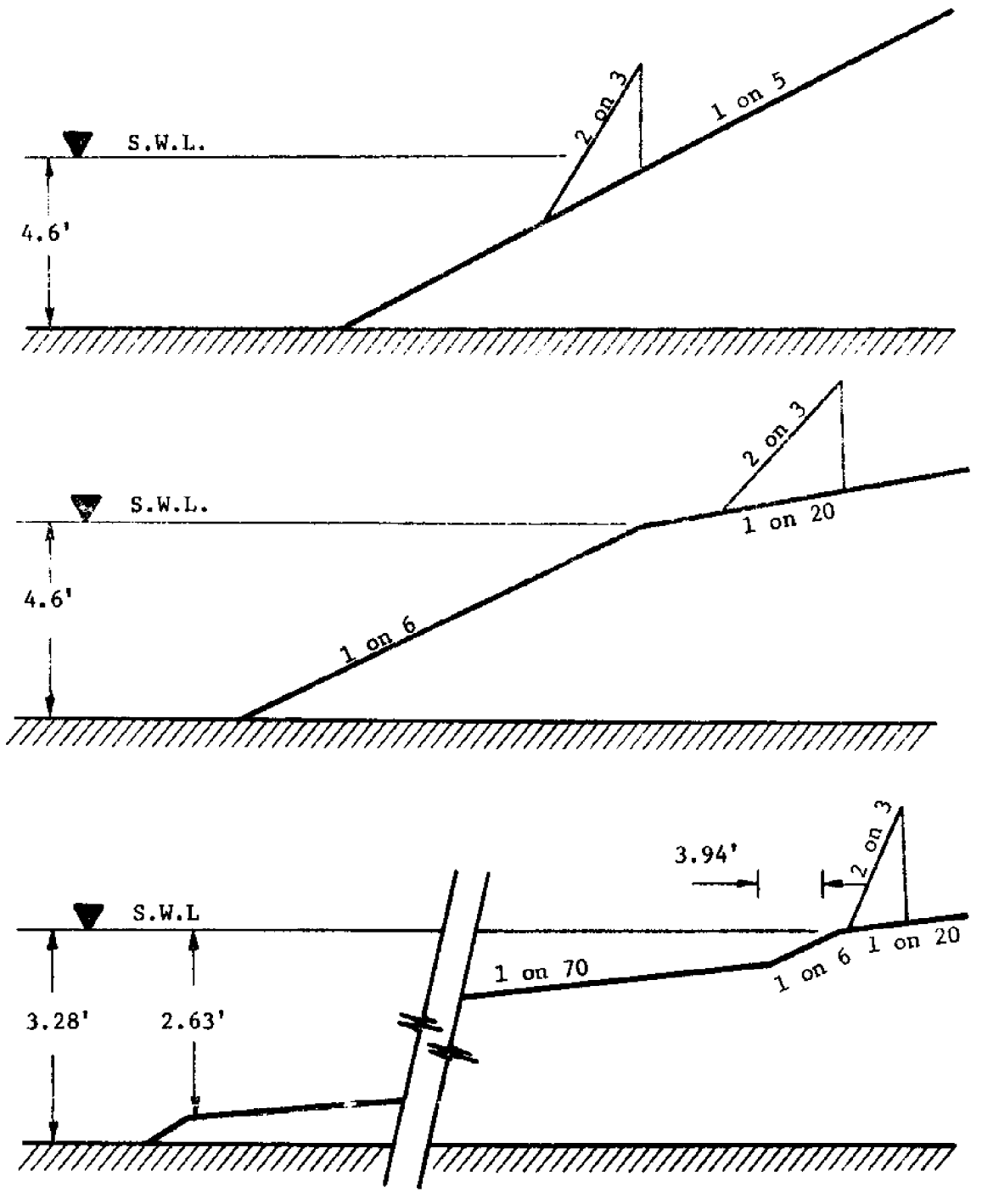

FIG. 3.--MODEL STRUCTURES TESTED BY HOSOI AND MITSUI[17]

In the impulsively generated wave train Jordaan found maximum run-up (R) produced by the leading wave. The momentum of the subsequent wave was then reduced by the backwash of the leading wave. In the experiments on the 1 on 15 slope Jordaan found significant wave run-up (R) from every third or fourth wave.

Investigation by Van Dorn. Van Dorn[48] investigated wave run-up (R) on beaches of arbitrary slope. His objectives were to develop a method of predicting wave run-up (R) on a beach, given only the slope of the beach (assumed uniform and impermeable) and the characteristics of the offshore incident waves (where the wave height is substantially independent of depth) and to determine whether an individual wave in a dispersive system can be treated independently (without regard to its neighbor) or whether some cumulative effect of the wave train is of importance in a wave prediction scheme.

Investigations by Le Méhauté *et al.* Le Méhauté *et al.*[31] investigated the behavior of gravity waves on gentle slopes to obtain a better understanding of the behavior of explosion-generated waves on a gentle slope. A series of tests were conducted in the N.E.S.C O. (National Engineering Science Company) wave flume (190 ft long, 4 ft wide and 4 ft deep) using a 1 on 107 bottom slope. The waves dissipated their energy completely prior to reaching the shore line, thus verifying the nonsaturated breaker theory proposed by Le Méhauté[32]. Run-up (R) in each test series was equal to the wave set-up (due to mass transport).

Investigation by Multer. An experimental investigation was conducted by Multer[37] to determine how the basic laboratory variables (generator stroke, period, and water depth) influenced wave run-up (R). Tests were run in the C.E.R.C. (Coastal Engineering Research Center) 72-ft wave tank. Multer found wave run-up (R) varying with test location in the tank. He concluded that this unusual variation of wave run-up (R) with distance from the wave generator was caused by the interaction of primary and secondary waves. He concluded that the relative position of the primary and secondary waves (wave going out of phase, waves coming into phase rapidly, waves coming into phase slowly or waves out of phase) had a major effect on wave run-up (R) and that the run-up (R) could be changed by as much as a factor of 3 because of this effect.

Two distinct questions were raised by Multer's investigation of wave run-up (R). First, what exactly is the relationship between experimental results obtained in a wave tank and a hydraulic occurrence in a real sea (the interrelationship between the random phase effect in a real sea and the phase effect in a wave tank is not well understood), and second, what amount should be taken of the phase effect in laboratory investigations?

Multer attempted to describe the phase effect by introducing the parameters θ and H_2/H_1. His equation for relative run-up can be expressed as:

$$\frac{R}{H_1} = f_1\left(\frac{H_1}{gT^2}, \frac{H_1}{d}, \frac{H_1}{H_2}, \theta \right) \quad \ldots\ldots\ldots\ldots \quad (17)$$

in which θ is the phase angle between the primary and secondary waves and H_1 and H_2 are respectively the heights of the primary and secondary waves. Attempts by Multer to evaluate Equation 17 have shown that the parameters are difficult to separate and that a complete analysis would require a complex procedure.

Investigation by Robson. An experimental investigation was conducted by Robson[38] to determine (1) if an oscillation (seiche) could be induced by an incident train of waves in the water over an offshore submerged shelf, and (2) if so, the effect of the wave system on the wave run-up (R) on an impermeable beach. The tests were conducted in the N.C.E.L. wave flume (100 ft long and 2 ft wide). A horizontal shelf (with aluminum shavings packed underneath the shelf to minimize reflections) was installed 75 ft from the wave generator. A plywood beach with a slope of 1 on 10 extended upward from the level of the shelf.

Tests were run with various combinations of wave period (0.6 to 3.7 sec), depth of water(8 to 24 in.), depth of water over the shelf (2 to 6 in.) and length of shelf (4 to 8 ft). Run-up heights (R) and wave amplitudes (n) [over the shelf] were obtained for sixteen runs. A plot of wave run-up (R) *versus* wave amplitude (n) showed considerable data scatter and no clear trend of run-up (R) with respect to the length of the shelf was observed. The scatter of the data was attributed to (1) too-small instrument signal (signal was taped and then played back to a direct writing oscillograph) in some cases, (2) need for refining the wave gauge, (3)

variable initial motion of the wave generator and (4) variable amplitude of shelf oscillation for a given incident-wave amplitude.

In two of the test runs Robson correlated maximum wave run-up (R) with other than the first wave (probably due to mass oscillation of seiching). He concluded from his investigation that the increase in wave run-up (R) due to seiching could be significant, especially since incident dispersive waves in nature would be higher and would develop greater on-shore mass transport.

Discussion by Haws. Haws[13] discussed wave run-up (R) results obtained for a wind-generated spectrum. He states that no direct relationship has been found to exist between individual wave heights (H) and run-up (R) values in a wind-generated wave train.

Investigation by Jackson. Jackson[21] investigated wave run-up and run down) on model rubble-mound breakwaters constructed of rough and smooth quarrystones, quadripods, tetrapods, hexapods, tribars, modified cubes, and truncated tetrahedrons. Run-up tests were conducted in the W.E.S. wave flume (119 ft long, 5 and 12.5 ft wide, and 4 ft deep) for a limited range of wave conditions. Jackson found a wide range of scatter in the measured values of wave run-up (and run down). He attributed this scatter to difficulties in defining and observing the extent of run up (and run down) on a rough, porous, sloping surface, and the complexities of wave motion on rubble-mound slopes. For increasing values of wave steepness (H/λ) and slope angle ($\cot \alpha$) Jackson found a decrease in relative run-up (R/H). However, for slopes greater than 1 on 3 he found that

the breakwater slope had less effect on wave run-up (R) than wave steepness (H/λ). Jackson did not find any appreciable reduction in wave run-up due to slope roughness or method of placement of armor stone. From the meager run-up (R) data collected he concluded that his data was accurate enough for determining design crown elevations for proposed, rubble-mound breakwaters where overtopping could not be tolerated.

Investigation by Bowen *et al.* Wave set-up on a smooth 1 on 12 slope was measured by Bowen *et al.*[4] in the S.I.O. (Scripps Institution of Oceanography) wave flume (130 ft long, 1.65 ft wide, and 2.46 ft deep). Bowen found the maximum set-up on the slope to be of the order of the wave amplitude. He found the wave run-up (R) to be in good agreement with the empirical equations given by Hunt[19].

Summary by Le Méhauté. In 1968, Le Méhauté[30] summarized theories for breaking and nonbreaking waves. From his review of the wave run-up (R) phenomena, he proposed the general equation:

$$\frac{R}{H} = f\left(\alpha, \frac{2\pi d}{\lambda}\right) + g\left(\frac{H}{\lambda}, \frac{2\pi d}{\lambda}\right) - k\left(\alpha, \frac{2\pi d}{\lambda}, \frac{H}{\lambda}\right) \quad . \quad . \quad . \quad . \quad . \qquad (18)$$

in which the function $f\left(\alpha, \frac{2\pi d}{\lambda}\right)$ is the run-up contribution by linear approximations, $g\left(\frac{2\pi d}{\lambda}, \frac{H}{\lambda}\right)$ is the correction due to superelevation by nonlinear effects and $k\left(\alpha, \frac{2\pi d}{\lambda}, \frac{H}{\lambda}\right)$ is the reduction in relative run-up due to the loss of energy in breaking and bottom dissipation.

Investigation by Miller. Miller[36] investigated the run-up (R) of an undular surge ($\mathcal{F} \leq 1.35$) and a fully developed bore ($\mathcal{F} \geq 1.55$) on four slopes, each with three different bottom roughnesses in the U of Ch (University of Chicago) wave tank (63 ft long, 1.16 ft wide, and 3.0 ft deep). For each combination of slope and bottom roughness he developed a linear equation of the form:

$$\frac{R}{H_3} = f_1 (\sin \alpha, f_*) + f_2 (\sin \alpha, f_*) \frac{H_3}{d} \quad . \ . \ . \quad (19)$$

in which H_3 is the height of the wave measured from the channel bottom, d is the undisturbed water depth, α is the slope angle, f_* is a dimensionless friction coefficient, and f_1 and f_2 are functions. The functions obtained by Miller are shown in Table 4. In all tests Miller found the bore strongly affected by slope (α) and bottom roughness. He also found a general disagreement between theory (based on nonlinear long-wave equations) and his experimental results. In particular, he found that Equation 10 was not valid for the conditions tested (Equation 10 neglects bottom friction).

Methods for Determining Wave Run-up on Composite Slopes

A method for determining wave run-up (R) on composite slopes from laboratory-derived curves for single slopes was first presented by Saville[42]. His method was one of successive approximations which involved the replacement of the actual composite slope with a hypothetical slope obtained from the breaking depth (d_b) and an

TABLE 4.--FUNCTIONS FOR USE WITH RELATIVE RUN-UP EQUATION BY MILLER[36]

Condition (1)	$f_1 (\sin \alpha_1 f_*)$ (2)	$f_2 (\sin \alpha_1 f_*)$ (3)
Undular surge $H_3/d \leq 1.35$ ≤ 1.25	$-3.151 - 15.00 \sin \alpha + 27.88 f_*$	$3.03 + 14.54 \sin \alpha - 22.12 f_*$
Fully developed bore $H_3/d \geq 1.75$ ≥ 1.55	$-0.182 - 9.60 \sin \alpha + 11.82 f_*$	$1.57 + 6.96 \sin \alpha + 9.33 f_*$

estimated wave run-up (R) value. Saville found the wave run-up (R) predicted by his method to be generally within 10 per cent of experimental values except for the longest berms tested. The indications were that, after a horizontal berm had reached a certain width, further widening had no significant effect in reducing wave run-up (R). Saville found the reduction in berm effectiveness (for berm widths greater than 1/4 λ) to be caused by the phenomenon of water 'set-up' on the berm. This 'set-up' of water (increase in water depth on the berm) was caused by the forward transport of water by waves. Saville found wave run-up (R) affected by reformed waves or surges on the berm.

Modification of Saville's method was first proposed by Hosoi and Mitsui[17]. Due to the characteristics of breakers they proposed that the relationship between cot α and R should be:

$$\cot \alpha = \frac{X_b + X_r}{d_b + R} \qquad \ldots\ldots\ldots\ldots \quad (20)$$

where X_b is the horizontal distance from breaking point to the toe of the structure and X_r is the horizontal distance from the toe of the structure to the extent of maximum wave run-up (see Fig. 3).

RESEARCH APPARATUS AND PROCEDURES

This study was conducted in the Hydromechanics Laboratories of the Civil Engineering Department, Texas A&M University.

Research Apparatus

Wind, water-wave flume. The experiments were conducted in a wind, water-wave flume (Fig. 4). The wave flume consisted of four basic sections: (1) wave generating section, (2) air inlet section, (3) main channel section, and (4) wave absorbing section. The wind, water-wave flume was 120 ft long, 3 ft deep, and 2 ft wide. The bottom was constructed of 3/16 in. steel plate while the walls were 3/8 in. plate glass panels. The glass wall panels allowed an unobstructed view of the wave phenomena over the entire length of the wave flume.

The wave generating section provided a space for the pendulum wave generator (used to generate monochromatic waves) as well as a space for a reservoir and energy absorber behind the paddle push plate. The reservoir (behind the paddle push plate) kept the water depth variation small during operation of the pendulum generator. The wave absorber (behind the paddle push plate) eliminated undesirable unsteady dynamic loading on the paddle push plate by reducing wave reflections from the reservoir.

The air inlet section provided a space for the air inlet. This section was located 10.5 ft downstream of the pendulum generator.

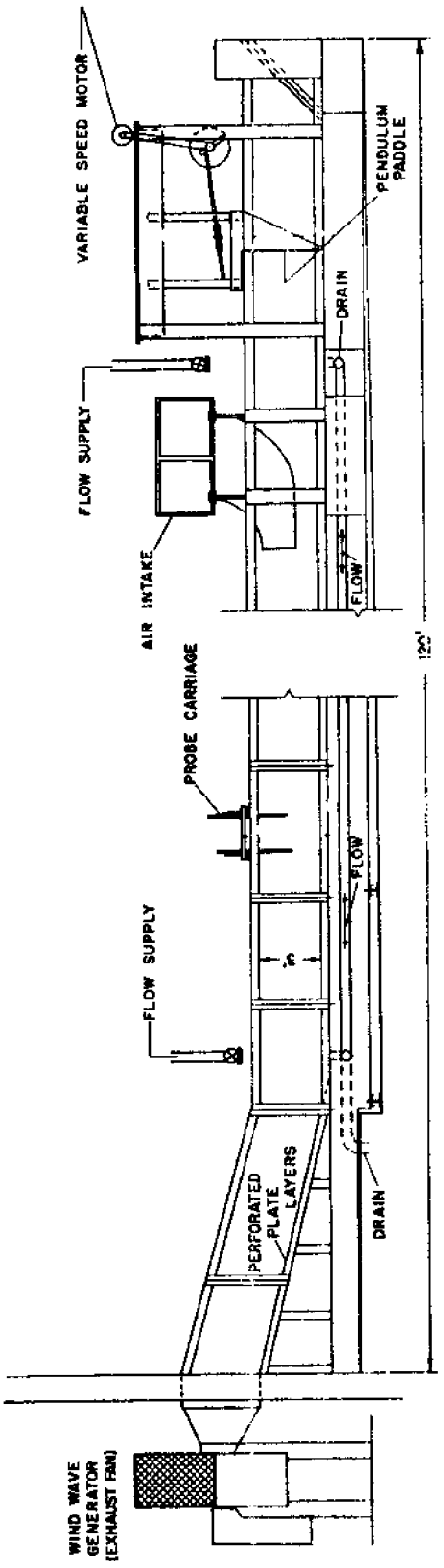

FIG. 4.--SCHEMATIC OF WIND, WATER WAVE FLUME

The main channel and test section was 90 ft long and consisted of 9 glass wall sections (10 ft each) of 3/8 in. standard plate glass. The joints between the glass wall panels were filled with permagum (commercial sealant). All internal joints (joints between glass wall panels) were made flush to reduce wall disturbances of either water or air stream. The flume was covered over its entire length with 5/16 in. fiber board during wave flume operation. The joints between fiber board top sections were taped to insure air tightness.

The wave absorber section provided a space for an energy absorber to eliminate wave reflections from the end of the wave flume.

Wave generators. The monochromatic wave generator shown in Fig. 5 was of the pendulum type, with provisions for variation of wave amplitude and frequency. The pendulum generator was attached eccentrically by a push rod to a 1.5 ft diameter driving disk as shown in Fig. 5. The driving disk was driven by a model ACMG 903 air cooled adjust gear unit which was rated at 3 horsepower at 1800 rpm. The speed control of this unit was achieved by employing a high performance silicon controlled rectifier controller (Model 4-58-3). At 1800 rpm (max. speed) the speed varied no more than minus 17 rpm with full load applied. The governing factor for the accuracy of the control system was the inherent drift due to noise in the circuit (specified at ± 1 rpm at all speeds). The wave period (monochromatic waves) was varied by changing the run speed of

NONOCHROMATIC (REGU

the variable speed drive unit thus enabling a continuous range of wave periods from 0.75 seconds to 5.00 seconds. The wave height (monochromatic waves) was changed by varying the eccentricity of the connecting rod on the driving disk. This allowed a continuous range of wave heights to be generated (from very small heights on the order of 0.001 ft to the largest stable wave height for a given water depth and wave period).

The irregular (wind) wave generator shown in Fig. 6 was an American Standard airfoil bladed exhaust fan. The fan (running at full speed) exhausted 14,400 standard cubic ft of air per minute from the wave flume while operating against pressures varying from 1/4 in. water gauge to 2 in. water gauge. At 1/4 in. static pressure the fan unit required 2.69 bhp to turn 787 rpm while exhausting 14,400 cubic ft of air per minute. At 2 in. static pressure the fan unit required 6.50 bhp to turn 950 rpm while exhausting the same volume.

Air inlet. The air stream for wind waves entered the wave channel through an elbow air inlet located at 10.5 ft from the pendulum generator. The elbow air inlet was constructed of 1/8 in. aluminum plate (the requirement for height adjustment of the air inlet with respect to the water surface dictated a light weight structure for the air inlet) and was provided with four jacking screws for height adjustment. To reduce contamination of the free water surface by dust, the air stream was filtered with standard furnace filters as shown in Fig. 7. The air inlet has an 840 square

FIG. 6.--IRREGULAR (WIND) WAVE GENERATOR

in. throat opening at the filter section which contracts to a 456 square in. opening in the channel. The contraction is advantageous since it not only keeps the head loss through the elbow small but provides a larger entrance area to reduce the entrance losses through the filter. Three turning vanes are provided in the contracted turning section to insure uniformity of the velocity distribution when entering the test section of the wave flume.

Wave absorber. The wave (energy) absorber was located at the beach end of the wave channel on a 15° slope as shown in Fig. 8. The wave absorber was constructed of 5-1/16 in. perforated aluminum plates spaced 3/4 in. apart. The top of the energy absorber was constructed 3 ft above the bottom of the wave flume. Reflection coefficients for the energy absorber (for various wave periods) are given in Table 5.

Wave filter. The wave filter was located 10 ft from the monochromatic wave generator. The wave filter was constructed of No. 4 wire mesh in a corrugated design as shown in Figs. 9 and 10. The purpose of the filter was to reduce the effects of multiple reflections between the monochromatic wave generator and the wave absorber (or model structure when in the wave flume). Resonance was thus avoided and the generated wave was very stable. The wave filter also inserted a friction force into the fluid in such a way that harmonics of high frequency were also absorbed.

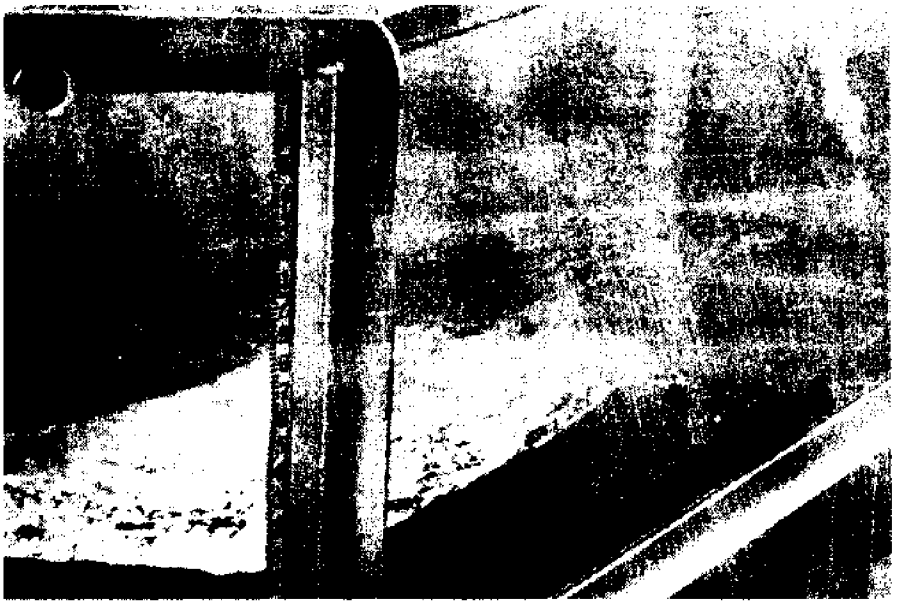

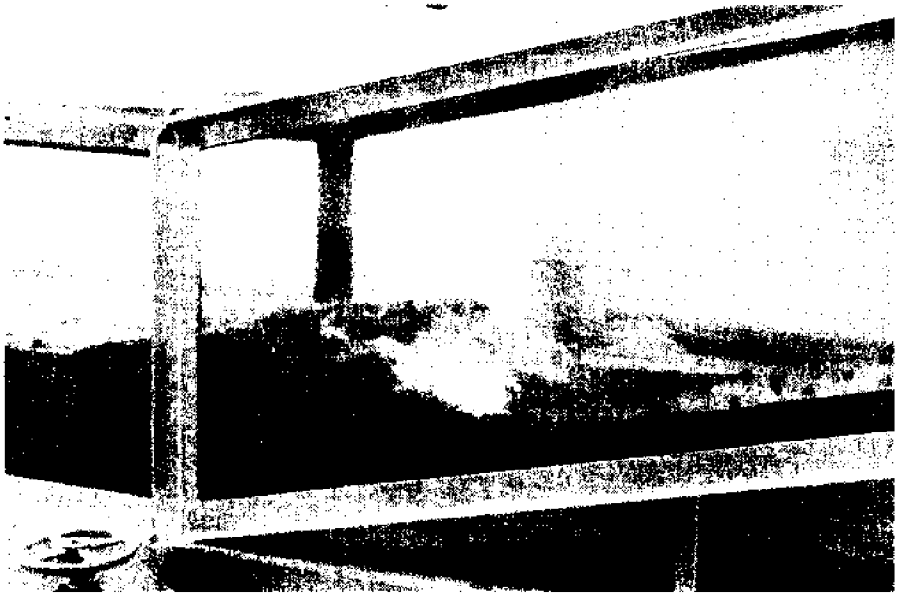

FIG. 8.--WAVE (ENERGY) ABSORBER

TABLE 5.--REFLECTION COEFFICIENTS FOR WAVE ABSORBER

Run number (1)	Relative depth $\frac{d}{\lambda}$[a] (2)	Wave steepness $\frac{H}{\lambda}$ (3)	Coefficient of reflection $C_r = H_r/H_i$ (4)
1	0.094	0.0037	0.286
2	0.067	0.0018	0.454
3	0.051	0.0085	0.429
5	0.094	0.6092	0.200
6	0.067	0.0043	0.391
7	0.051	0.0012	0.560
8	0.179	0.0404	0.062
9	0.142	0.0280	0.143
10	0.094	0.1700	0.230
11	0.067	0.0068	0.023
12	0.179	0.0364	0.068
13	0.142	0.0249	0.048
14	0.090	0.0123	0.156
15	0.067	0.0059	0.313

[a] $d = 1.8'$.

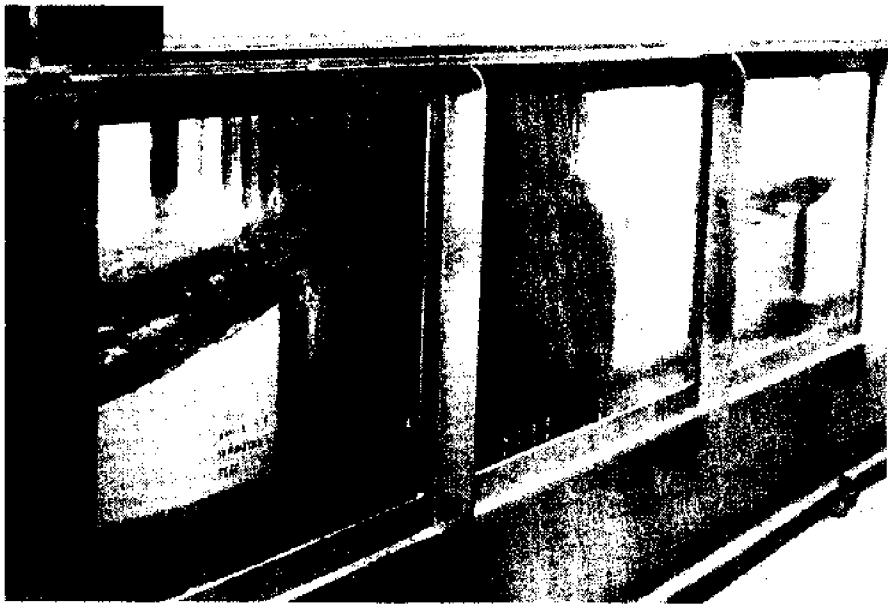

FIG. 9.--WAVE FILTER

(Wave entering wave filter)

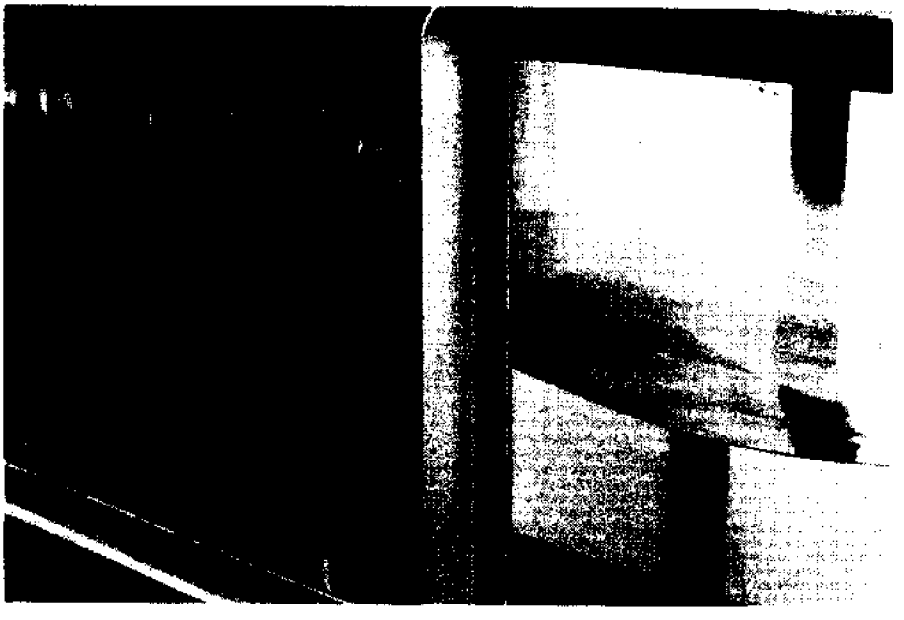

Wave leaving wave filter

FIG. 10.--WAVE FILTER

Research Instrumentation

Wave height sensor. A capacitance type wave height sensor with bridge circuit was used with a Model 321 Sanborn Dual Channel Carrier Amplifier Recorder as shown in Fig. 11 to obtain a water surface-time history. The capacitance type wave height sensor was constructed of 3/16 in. brass rod and No. 20 polythermaleze insulated wire. The polythermaleze sensing wire spaned across a "C" frame as shown in Figs. 12 and 13. One end of the sensing wire was embedded in an epoxy cement plug on the "C" frame while the other end was connected to the capacitance probe bridge.

The capacitance type wave sensor measured the electrical capacitance existing between the two conductors (the insulated wire and the surrounding water). The polythermaleze insulated wire provided the dielectric medium. Variation in water depth due to the passage of a surface-wave disturbance (at the air-water interface) was sensed by the change in the capacitance with the capacitance bridge. The output voltage of the bridge was proportional to the change in water depth (only when the change in the capacitance was small).

The capacitance bridge used with the sensor was designed by Dr. A. Miller of Sanborn Instrument Company. The two basic requirements of the capacitance bridge were (1) that the phase angle of the bridge output relative to the excitation voltage be small ($> 10°$) and (2) that the input impedance of the bridge circuit be in the

FIG. 11.--PORTABLE 2-CHANNEL CARRIER/RECORDER

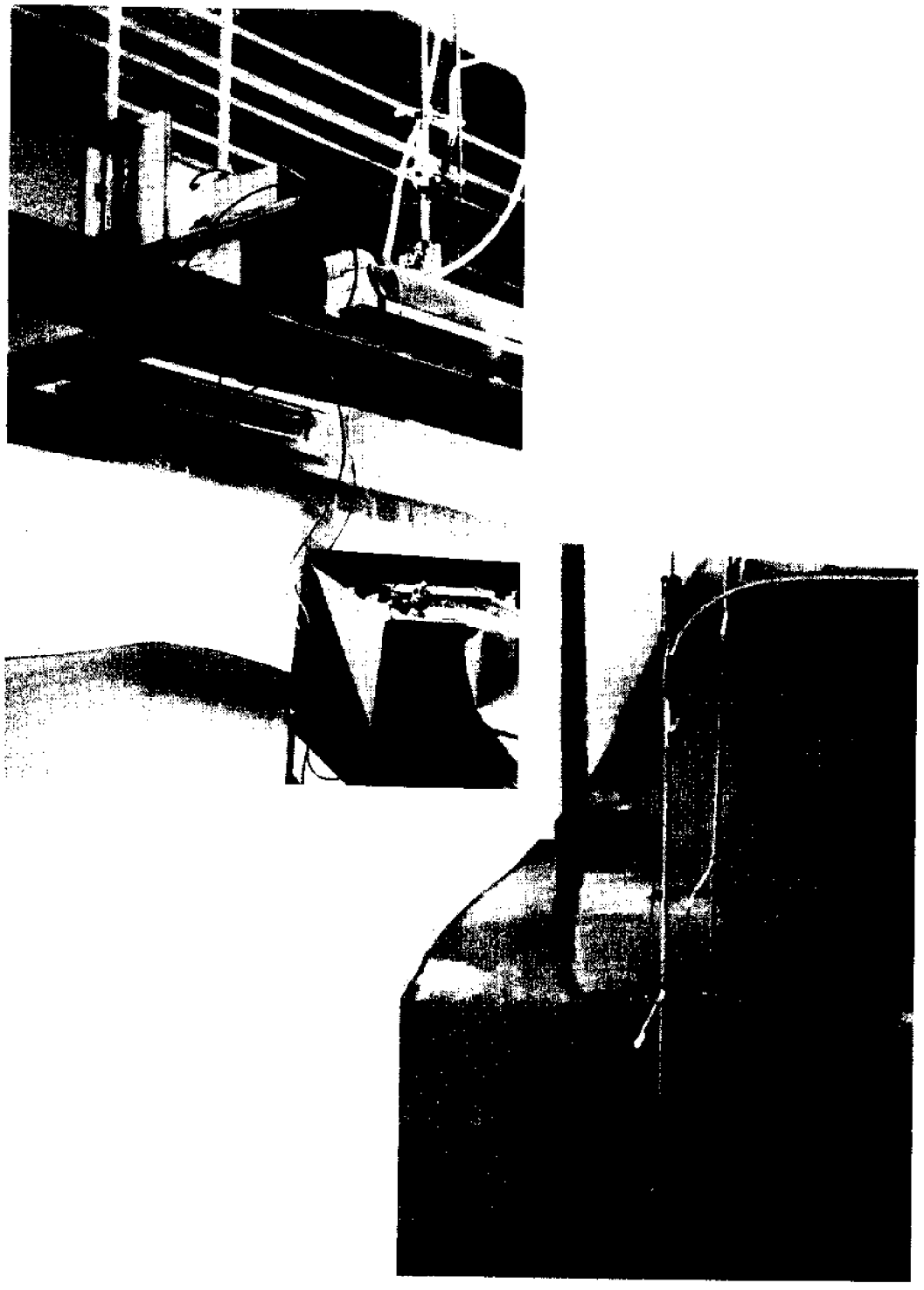

FIG. 12.--CAPACITANCE WAVE HEIGHT SENSOR AND
SANBORN CARRIER AMPLIFIER RECORDER

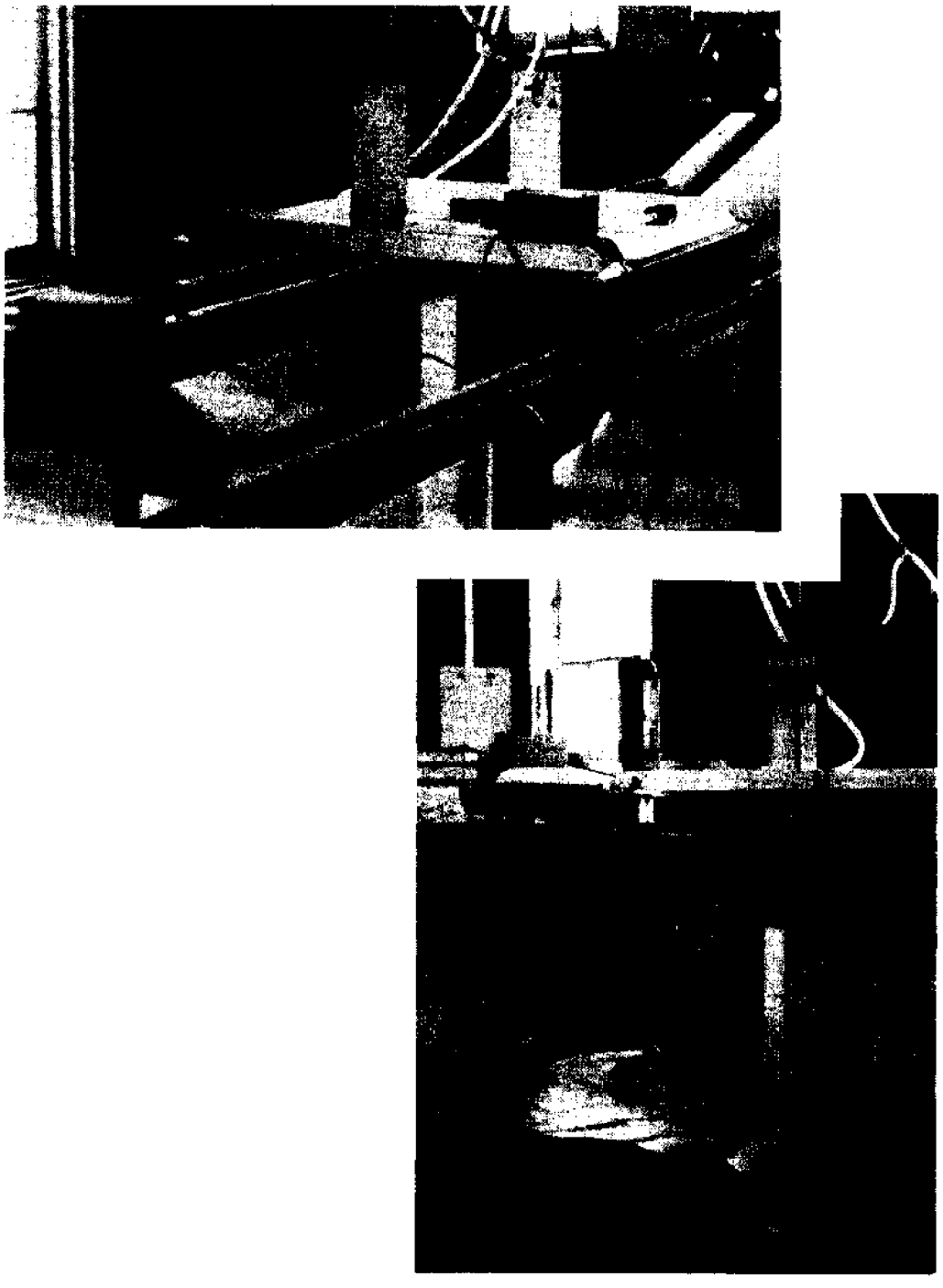

FIG. 13.--INSTRUMENT CARRIAGE WITH PRANDTL TUBE AND CAPACITANCE WAVE HEIGHT SENSOR

neighborhood of 200 ohms rather than in the range of 1000 to 5000 ohms.

The capacitance gauge was used for the following reasons:

1. Reflections from the wave-height sensor were minimized.
2. Flow disturbance (from sensing element and support) was minimized in water and air stream.
3. The sensor was stable and linear with adequate sensitivity (full scale deflection for 0.2 ft of wave height).
4. The sensor responded rapidly with negligible time lag in an unsteady state application.
5. The sensor was simple, inexpensive and easily repairable.
6. Dissolved minerals did not affect the gauge calibration.

Velocity and turbulence sensor. A hot-film sensor was used with a Model 1050 Thermo-systems anemometer and a Honeywell visicorder as shown in Fig. 14 to obtain uprush and dnrush (hereafter means velocity downrush on the slope) velocity profiles. The hot-film sensor constructed by Thermo-systems Inc. was essentially a conducting film on a ceramic substrate. The hot-film sensor was used with the Model 1050 Thermo-systems anemometer to measure the rate of heat transfer between the sensor and the environment. As the flow velocity past the hot-film sensor increased the sensor was cooled with a resulting decrease in resistance. This resistance decrease caused the voltage to decrease thus changing the input to the amplifier. The phase of the amplifier was such that a decrease in voltage caused an increase in the output of the

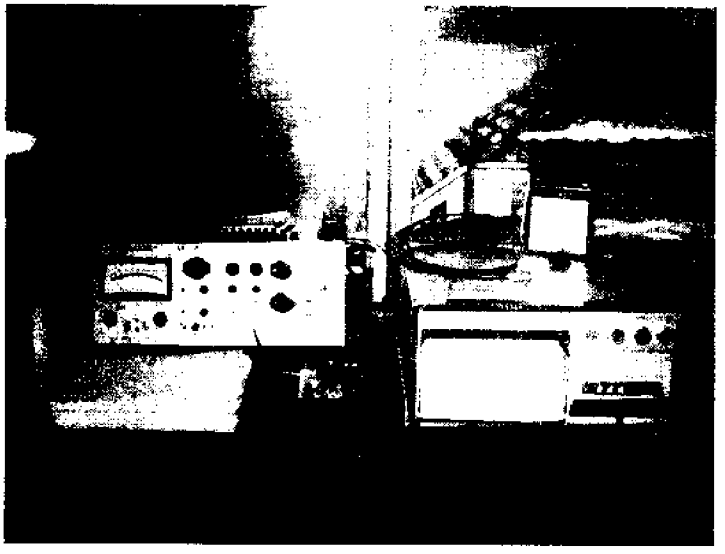

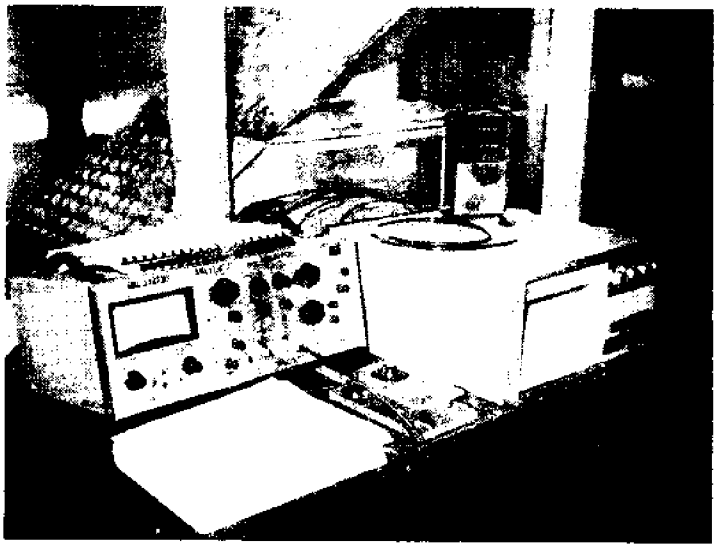

FIG. 14.--THERMO-SYSTEMS CONSTANT TEMPERATURE ANEMOMETER (LEFT) AND HONEYWELL VISICORDER (RIGHT)

amplifier to increase the current through the sensor. The amplifier had a sufficient gain to keep inputs very close to the balanced condition. Changes in resistance were immediately corrected by an increase or decrease in the current through the sensor. The output of the constant temperature anemometer was thus the voltage required to drive the necessary current through the sensor.

The hot-film sensor with constant temperature system was used for the following reasons:

1. The constant temperature system provided a direct D.C. output.
2. The sensor was not burned-out from rapidly changing velocities or a change from a water environment to an air environment.

Measurements

Wave characteristics. The capacitance-type wave height sensor with bridge circuit was used with a Model 321 Sanborn Dual Channel Recorder as shown in Figs. 11, 12 and 13 to obtain a water surface-time history. With the recorder statically calibrated (by raising and lowering the wave height sensor a known distance) the wave height of a monochromatic wave train was read directly from the trace within ± 5 per cent of the wave height.

The wave period was determined by recording with an electric timer fifty complete cycles of movement of the monochromatic (pendulum) wave generator.

Depth measurements. The stillwater depth was recorded from a

staff gauge mounted on a glass wall section of the wind, water wave flume.

Velocity measurements (air). A Pitot-static tube (O.D. 5/32 in. I.D. 1/16 in.) of the standard Prandtl design as shown in Fig. 15 was used to measure the wind velocities above the free water surface. The differential pressure on the Pitot-static tube was read to ± 0.005 ft on a differential inclined manometer containing an indicating fluid with a specific gravity of 1.00, and to 0.004 ft on a Pace CD-25 commercial pressure transducer indicator as shown in Fig. 15. The manometer readings were converted to velocities by assuming a coefficient of unity for the Pitot-static tube (assumption was verified by comparing the Pitot-static tube with a calibrated Prandtl tube). The Pitot-static tube was mounted on an instrument carriage designed so that point velocities could be taken at any point in the air stream at the centerline of the wave channel.

Velocity measurements (uprush zone). A Thermo-systems hot-film sensor was used with a Model 1050 Thermo-systems anemometer to measure the turbulent velocity signal in the uprush zone. The constant temperature anemometer instantaneously measured fluid flow parameters in the uprush zone by sensing the heat transfer rate between the sensor and environment. The anemometer output signal was related to flow characteristics by applying King's Law[29]

$$E_a^2 \approx [A' + B' (\rho \bar{V})^{1/n} (t_s - t_e)] \quad \ldots\ldots\ldots \quad (21)$$

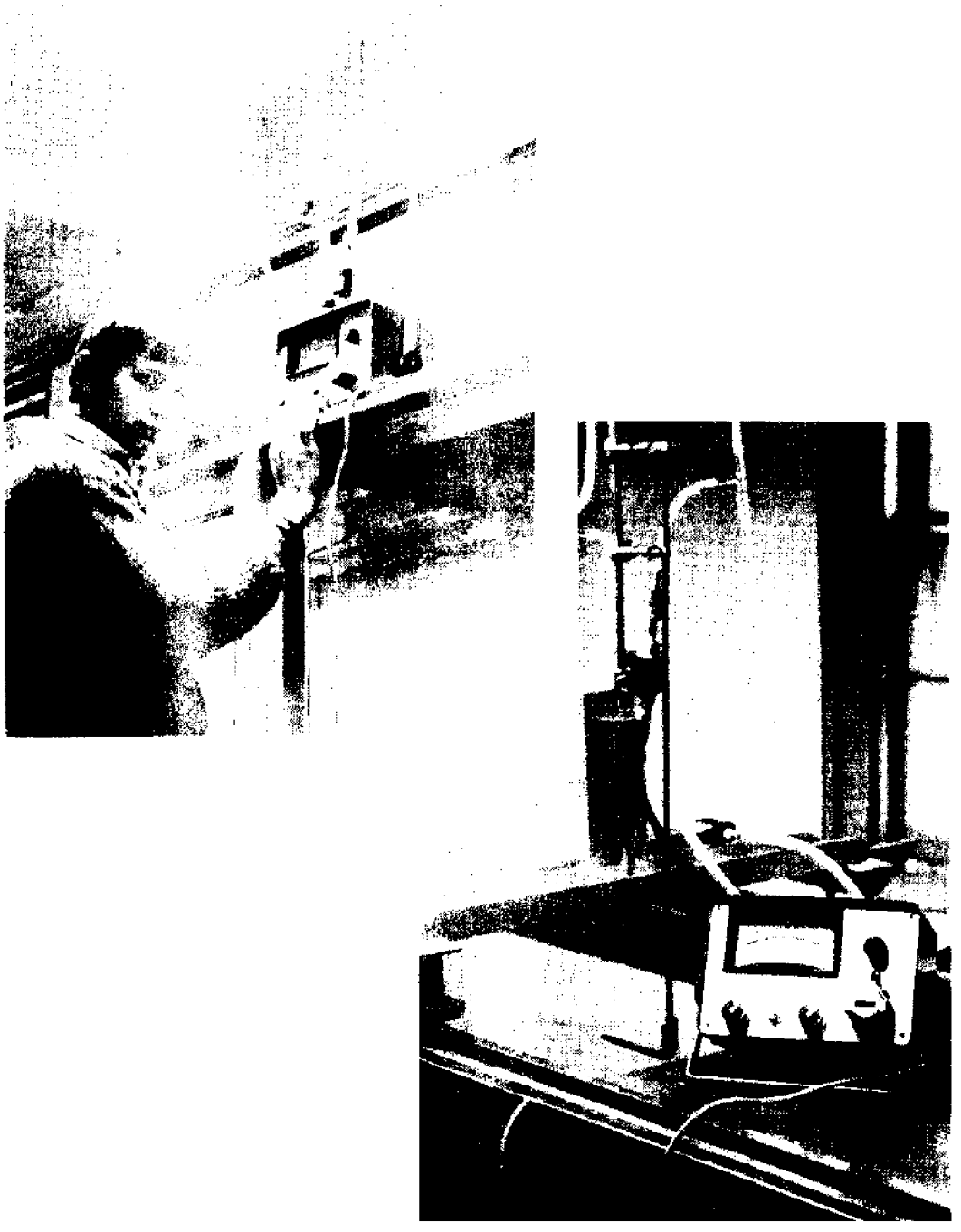

FIG. 15.—PRANDTL TUBE AND PACE CD-25 TRANSDUCER INDICATOR

in which E_a is the anemometer bridge D. C. Voltage A' and B' are constants which depend upon the sensor and flow characteristics. $\overline{V}$ is the temporal mean velocity, n is an exponent that varies with range and fluid (usually about 2), t_s and t_e are respectively sensor surface temperature and fluid (environment) temperature. By assuming a constant fluid density and by operating the anemometer at a constant overheat ratio, Equation 21 reduced to:

$$E^2 = A' + B' \sqrt{\overline{V}} \quad . . . . . \quad (22)$$

in which the notations are the same as previously defined. A high response Honeywell visicorder (XY Plotter) was used to record the D.C. voltage output from the constant temperature anemometer.

A Pitot-static tube (O.D. 5/32 in. - I.D. 1/16 in.) of the standard Prandtl design was used with an inclined manometer to calibrate the hot-film sensor. The hot-film sensor was mounted alongside the Pitot-static tube in a constant flow region of a small recirculating water flume. The bridge output D.C. voltage was recorded on the high response Honeywell visicorder at the same time the inclined manometer was being read. The flow velocity in the recirculating water flume was varied from 0.0 ft/sec to 4.5 ft/sec. Readings from the anemometer and the inclined manometer were recorded through the flow range. The calibration tests were replicate three times. A calibration curve for the hot-film sensor was developed from the recorded data. A considerable amount of D.C. drift occurred during calibration due to debris in the water recirculating

flume. By cleaning the sensor with a soft artist's brush the drift problem was eliminated until the next piece of debris changed the heat transfer property of the sensor. During sensor operation in the uprush zone this problem was not encountered due to the washing action of the uprush and dnrush which kept the sensor free of debris.

Turbulence measurements (uprush zone). The Thermo-systems Model 1050 anemometer with hot-film sensor was used to measure the turbulent velocity signal in the uprush zone. It was originally planned to connect a true RMS voltmeter to the anemometer output to measure the root mean square average of flow fluctuations (*i.e.*, turbulence) but due to the rapidly fluctuating temporal velocity and the discontinuities in the velocity signal it was concluded that the RMS voltmeter (with averaging time constant less than half the wave period) would be invalid. Attempts to make meaningful computations using existing equations proved equally as frustrating. The major problem was the nature (and the length) of the phenomena on the slope.

Criteria for Modeling Wave Run-up

Similitude considerations. The generation, propagation, and terminal effects (including kinematics, dynamics and run-up of gravity water waves) are governed by the Froude similitude relationship:

$$V_r^2 = Y_r \quad \ldots\ldots\ldots\ldots \quad (23)$$

where V_r is the velocity ratio and Y_r is the vertical-scale ratio between two geometrically similar events. This law relates inertia to gravity forces, and if both these forces are simulated in the same proportion in model and prototype then all dependent effects will also be in the correct scale relationship.

In modeling the wave run-up (R) phenomena a Froude scale reduction resulted since higher viscous damping forces were experienced in the model. The scale reduction considered permissible was therefore limited by the Reynolds criterion that turbulent flow in nature should be modeled by turbulent flow in nature.

The model structures in the study were constructed geometrically similar to prototype structures since a distorted model would violate the similitude criterion with respect to a steep slope, wave steepness (H_o'/T^2) and wave length to depth ratios (λ_o/d).

The criterion considered in the modeling of the wave run-up phenomena are shown in Table 6.

Model composite section. The model structure was constructed in three separate sections as shown in Fig. 16. The forward slope section (see Fig. 16) was constructed of 1/2 in. marine plywood with 2 × 4 in. bracing to keep the section from warping. Three coats of epoxy paint were applied to the forward slope section to keep the laminated layers from separating. Scales for reading wave run-up were secured on the slope as seen in Fig. 30 (page 92). During testing the forward slope section was secured to the bottom

TABLE 6.--MODELING CRITERION

Criteria (1)	Decision (2)
1. Froude law $V_r^2 = Y_r$	Use to model wave run-up (R) since force of gravity is predominate.
2. Undistorted scale $L_r = Y_r$	Use undistorted scale Breaking effects are important.
3. Smallest permissible vertical scale	For a nondispersive wave propagation a vertical scale not less than 1 on 100 is permissible.

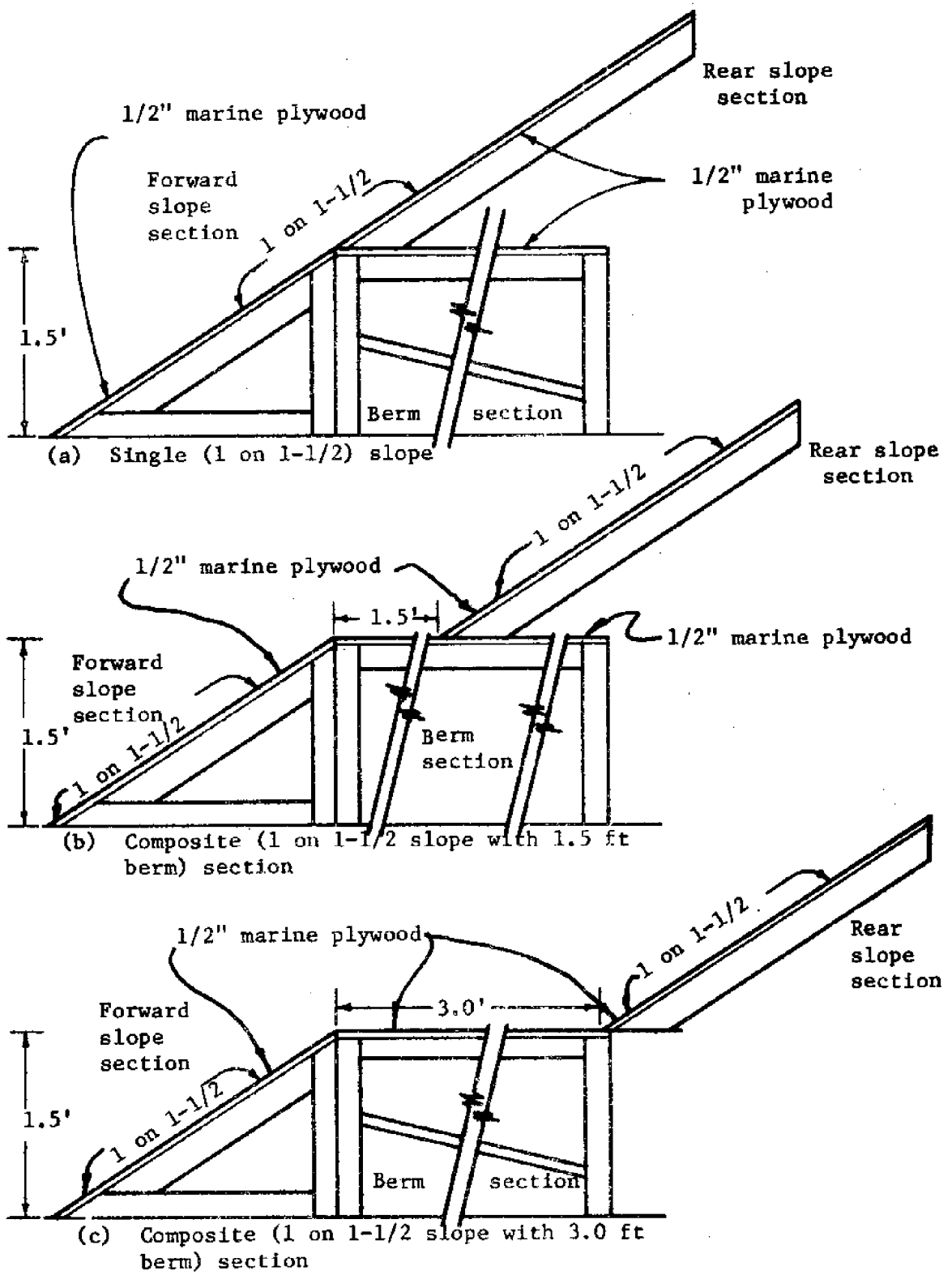

FIG. 16.--MODEL COMPOSITE SECTION

of the wave flume to prevent movement. The berm section (see Fig. 16) was also constructed of 1/2 in. marine plywood with 2 × 4 in. bracing. The berm section was 3.0 ft wide and half flume depth in height. The berm section was painted with three coats of epoxy paint. Scales were also applied to the berm so that berm width adjustments could be easily made. During testing the berm section was secured to the bottom of the wave flume to prevent movement.

The rear slope section (see Fig. 16) was constructed of 1/2 in. marine plywood with 1 × 4 in. bracing. Three coats of epoxy paint were applied to the rear slope. The rear slope was also supplied with scales for reading wave run-up. During testing the rear slope section was secured to the berm section (by nailing) and to the walls of the specially designed test section.

Leakage between the slope sections was reduced with permagum. Considerable care was necessary to level the berm section and set the slopes correctly to avoid any lateral component of wave motion that might excite the transverse modes of oscillation in the tank.

Artificial roughness. A series of parallel strips and blocks as shown in Fig. 17 were used to create artificial roughness in the study. The strips and blocks were attached to the model structures in the configurations shown in Fig. 17. The equivalent sand roughness (K) was estimated from Fig. 18 to be 0.026 ft for both the parallel strips and the regular spaced blocks. For the smooth slopes the equivalent sand roughness (K) was estimated to be 0.005 ft.

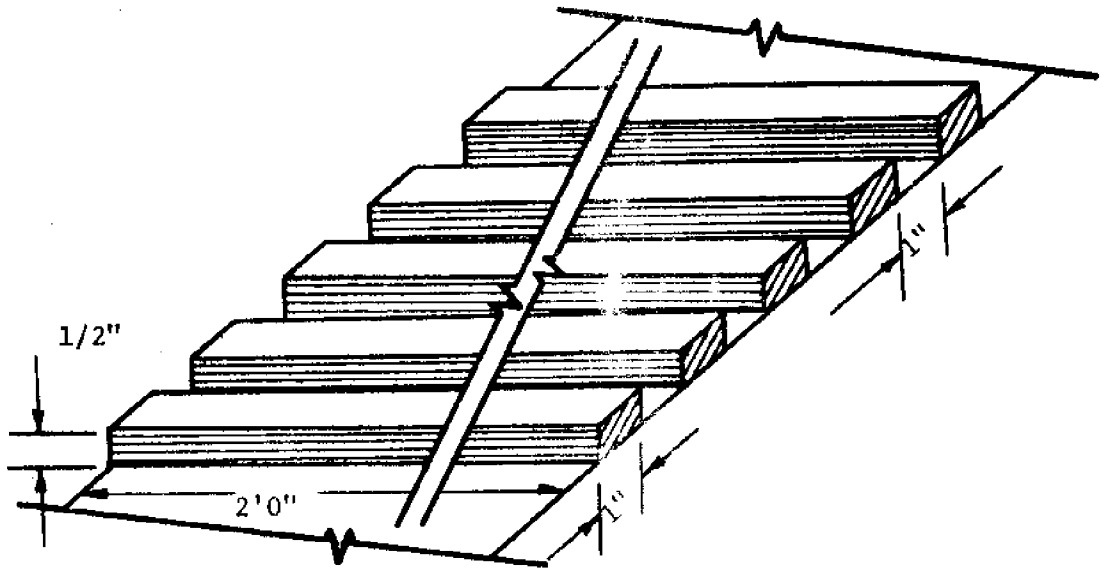

(a) Parallel strips

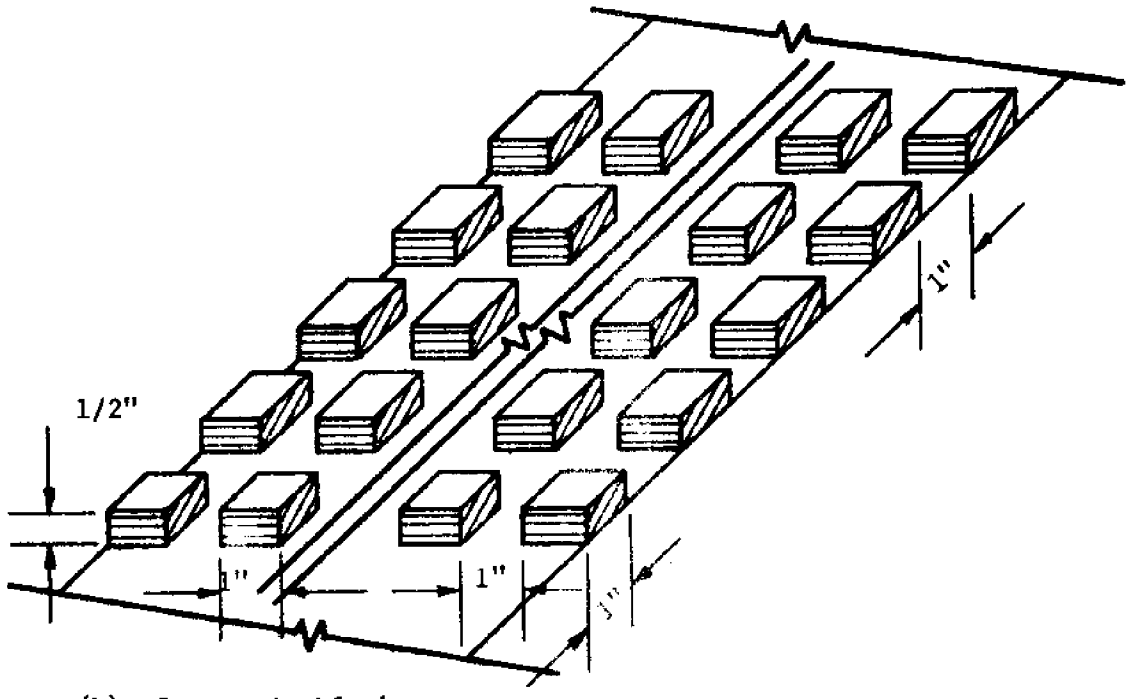

(b) Symmetric block pattern

FIG. 17.--MODEL COMPOSITE SECTION

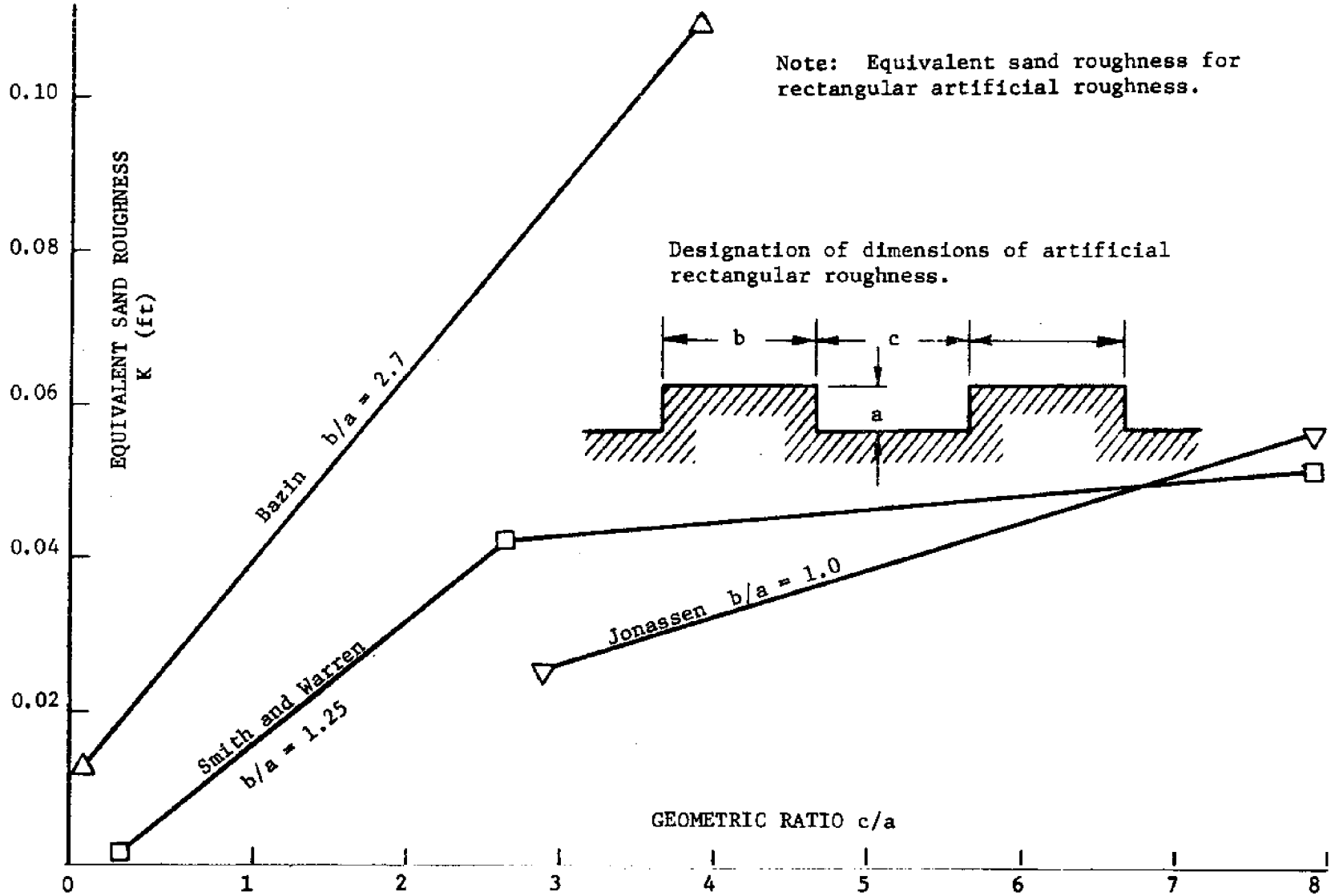

FIG.18.--EQUIVALENT SAND ROUGHNESS (K) AS A FUNCTION OF GEOMETRIC RATIO (c/a) by Johnson[22]

The ratio of roughness element height, a, to the deep water wave height, H_o', varied from 0.09 to 0.24.

Test Program

Monochromatic waves. Preliminary tests (calibration tests) were conducted in the research wave channel to establish wave parameters (H, λ, T) for the test program. During the calibration tests secondary waves (secondary wave crests) were observed in the wave channel. Since these waves were not of permanent form and would have an appreciable effect on wave uprush (R) data, a relationship developed by Galvin[10] was used to predict the formation of secondary wave crests. Galvin found secondary waves occurring at depth-to-wave length ratios (d/λ) less than 0.1 and height-to-depth ratios (H/d) greater than 0.05 (see Fig. 19). In accordance with these parameters the preliminary tests were run and the wave parameters were established for the test program. The test program shown in Table 7 was developed and used in this study.

Wind (irregular) waves. Wind generated wave tests were conducted in the research wave channel to establish irregular wave parameters (H_e, f) for the test program. The wave statistics were evaluated from a surface-time history record with a power (energy) spectra. An equivalent wave height was developed for the irregular wave train from the equation:

$$H_e = \left\{\frac{8}{T}\int_0^T n^2 dt\right\}^{\frac{1}{2}} \qquad \ldots\ldots\ldots \qquad (24)$$

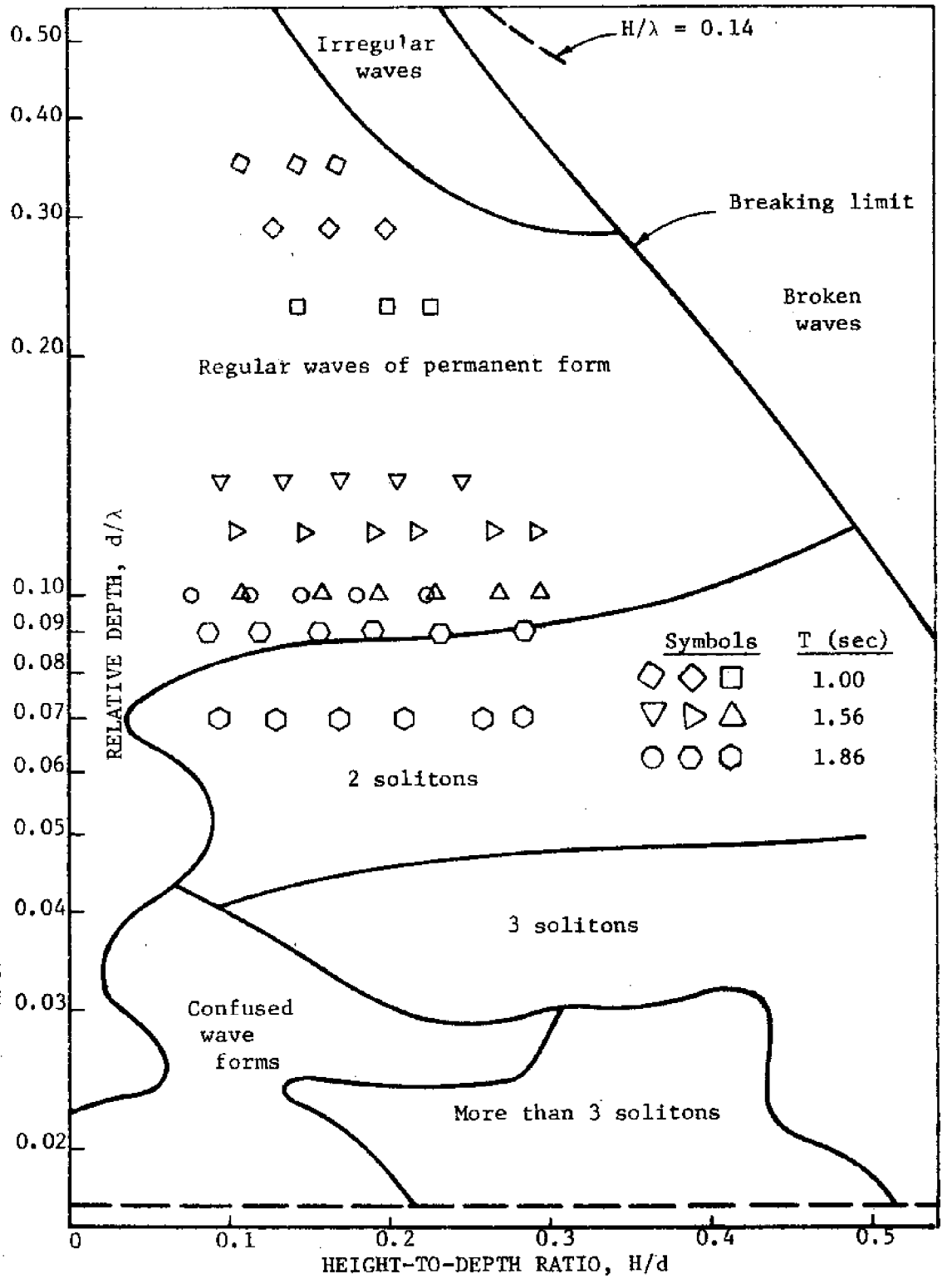

FIG. 19.--RELATIONSHIPS FOR WAVES OF PERMANENT FORM by Galvin[10]

TABLE 7.--TEST PROGRAM

Test series / Run number (1)	Water depth d (ft) (2)	Structures to be tested (3)	Roughness elements to be tested (4)	Tests to be conducted (5)
67/1,4,7 46/10,13,16, 19,22,25 39/27,30,33, 36,39,42	1.2	Single (1 on 1-1/2)slope	Parallel strips Symmetric block pattern	Wave uprush Wave reflection Uprush and dn-rush velocity
		Composite (1 on 1-1/2 slopes with 1.5 ft berm) section	Parallel strips Symmetric block pattern	
		Composite (1 on 1-1/2 slopes with 3.0 ft berm) section	Parallel strips Symmetric block pattern	
67/2,5,8 46/11,14,17, 20,23,26 39/28,31,34, 37,40,43	1.5	Single (1 on 1-1/2)slope	Parallel strips Symmetric block pattern	Wave uprush Wave reflection Uprush and dn-rush velocity
		Composite (1 on 1-1/2 slopes with 1.5 ft berm) section	Parallel strips Symmetric block pattern	
		Composite (1 on 1-1/2 slopes with 3.0 ft berm) section	Parallel strips Symmetric block pattern	
67/3,6,9 46/12,15,18, 21,24 39/29,32,35, 38, 41	1.8	Single (1 on 1-1/2) slope	Parallel strips Symmetric block pattern	Wave uprush Wave reflection Uprush and dn-rush velocity
		Composite (1 on 1-1/2 slopes with 1.5 ft berm) section	Parallel strips Symmetric block pattern	
		Composite (1 on 1-1/2 slopes with 3.0 ft berm) section	Parallel strips Symmetric block pattern	

where H_e is the equivalent wave height, η is the water surface displacement, T is the wave period and t is time.

Wave energy spectra. Techniques of power spectrum analysis developed by Blackman and Tukey[3] for use in communications engineering were used to evaluate the wave records [see wave profiles shown in Figs. 104 through 117 and Figs. 118 through 123 (Appendix III)]. One hundred waves in each test series [see Table 9 (Appendix III)] were digitized and punched on IBM cards for analyzing. Power spectrum computations [see Figs. 124 and Table 11 (Appendix IV] were performed on the University's IBM 360/65 computer. Wave spectra for test series 67/1 through 39/43 [see Table 9 (Appendix III)] and test series A/1 through C/6 [see Table 10 (Appendix III)] are shown in Figs. 125 through 133 (Appendix IV) and Figs. 134 through 139 (Appendix IV), respectively.

Wave statistics for test series 67/1 through 39/43 are given in Tables 9 (Appendix III) and 19 (Appendix VI) while power, spectra statistics are given in Table 12 (Appendix IV). Wave statistics for test series A/1 through C/6 are given in Tables 10 (Appendix III) and 20 (Appendix VI) while power spectra statistics are given in Table 13 (Appendix IV).

To verify the use of the power spectrum technique the measured wave statistics from test series 67/1 through 39/43 were compared with computed wave statistics. In all tests the wave statistics were in good agreement.

Experimental Procedure

Calibration tests. Preliminary tests were conducted in the wave channel without a model structure in place. Both monochromatic (regular) waves of permanent form shown in Figs. 104 through 117 (Appendix III) and wind (irregular) waves shown in Figs. 118 through 123 (Appendix III) were generated with various periods, heights, and lengths as given in Tables 9 and 10 (Appendix III). A surface-time history of each wave was obtained on the Sanborn Dual Channel Carrier Amplifier-Recorder. The surface-time history records were evaluated and the test program was developed.

Monochromatic (regular) wave tests. A series of wave run-up (R) tests were conducted with the composite structure secured in the wave channel. The tests outlined in the test program shown in Table 7 were run. Uprush (from monochromatic waves with the same amplitude, period, and length as in the calibration tests) was measured by visual observation of two staff gauges mounted on the model structure. Wave uprush (R) was defined, and measured, as the distance from the still water level to the point where the entire face of the structure was wetted. Spray resulting from breaking waves, which progressed past the point of wave uprush (R) was not included in the measurements. In each test run, the wave run-up (R) data was obtained for ten waves before the reflections from the structure interferred with the record. Observation of the surface-time history record indicated that the reflected energy of the waves appeared in the record after

approximately 9 or 10 waves had impinged on the structure. After recording wave run-up (R) from 10 waves the pendulum generator was stopped and the surface disturbances allowed to dampen out prior to initiating a new test run (monochromatic wave uprush (R) data was replicated three times).

A series of wave uprush velocity (V_u) tests were also run with the structure secured in the wave channel. The tests outlined in the test program shown in Table 7 were run. Uprush and dnrush velocities (velocity profiles) were measured with the Thermo-Systems Constant Temperature Anemometer and a Honeywell Visicorder. Uprush and onrush velocity profiles were recorded as shown in Figs. 140 through 183. Maximum uprush (V_u) and dnrush (V_d) velocities (evaluated from the velocity profiles) are given in Table 23 (Appendix VII). Wave uprush (V_u) and dnrush (V_d) profiles were obtained for 10 waves before the reflections from the structure confused the record.

Wind (irregular) wave tests. A series of wave run-up (R) tests were conducted with wind generated waves as outlined in the test program shown in Table 7. The model composite structure was secured in a special test section to reduce the "venturi effect" over the structure. With the wave channel covered over its entire length a train of irregular waves were generated using the irregular wave generator. The wave run-up (R) was measured by visual observation of the staff gauges through a transparent section. Spray, resulting from the irregular waves, was not included in the uprush (R)

measurements. After recording wave run-up of 30 (or more) waves the irregular wave generator was cut off and the surface waves were allowed to dampen out prior to initiating a new test run (irregular wave uprush data was replicated two times). The water 'set-up' produced by the pressure anomaly, etc. when the irregular wave generator was in operation was measured and subtracted from the wave run-up (R) readings on the single slopes and composite sections.

ANALYSIS OF DATA AND DISCUSSION OF RESULTS

Mechanisms of Energy Dissipation

Wave energy striking a coastal protective structure (seawall, breakwater, etc.) is dissipated primarily by:

1. Reflection
2. An increase in the potential energy, that is, wave run-up
3. Heat
    a. Generated by the turbulence of the breaking of the wave
    b. Generated by the roughness of the structure
    c. Generated by the mixing in the voids of a permeable structure

Hunt[19] has stated that the key to proper design of a seawall is an insight in these mechanisms of energy dissipation.

Wave Energy Dissipation on a Single (1 on 1-1/2) Slope

Relative wave run-up (R/H_o'). To establish a standard for comparison purposes and to verify the work of previous investigators, a series of wave run-up (R) tests were run using a smooth (1 on 1-1/2) slope. Wave run-up (R) data for both monochromatic (regular) waves and wind (irregular) waves was obtained for the smooth (1 on 1-1/2) slope configuration shown in Fig. 30 (page 92).

The monochromatic (regular) wave tests were run using wave periods (T) of 1.00 sec, 1.56 sec. and 1.86 sec in water depths (d)

of 1.2 ft, 1.5 ft and 1.8 ft. Equivalent deepwater wave heights (H_o') were varied from 0.113 ft to 0.443 ft for the water depths tested [see Table 9 (Appendix III)].

The wind (irregular) wave tests were run using surface wind velocities ($V_{0.30}$) of 39.8 ft/sec, 41.3 ft/sec and 54.5 ft/sec obtained for water depths of 1.2 ft, 1.5 ft and 1.8 ft, respectively. The equivalent wave periods (T) obtained from the wave energy spectrum were 0.77 sec, 0.72 sec and 0.83 sec for water depths of 1.2 ft, 1.5 ft and 1.8 ft, respectively, while the equivalent deep water wave heights (H_e') obtained from the wave energy spectrum were respectively 0.330 ft, 0.313 ft and 0.387 ft [see Table 10 (Appendix III)].

The mean wave energy density (E_μ) was obtained from the wave energy spectrum for both the monochromatic (regular) waves and for the wind (irregular) waves. For the monochromatic (regular) waves the mean wave energy density (E_μ) varied from 0.0006 ft^2/sec^{-1} to 0.0165 ft^2/sec^{-1} while for the wind (irregular) waves the mean wave energy density (E_μ) varied from 0.0131 $ft^2/sec^{-1}$to 0.0232 ft^2/sec^{-1} [see Tables 9 and 10 (Appendix III)].

Relative wave run-up (R/H_o' and R/H_e') was calculated from the wave run-up (R) tests for both the monochromatic (regular) waves and the wind (irregular) waves [see Tables 15, 16, 17 and 18 (Appendix VI)]. Each relative run-up value (R/H_o' and R/H_e') was plotted as a dependent variable for its respective incident mean wave energy density (E_μ) which was plotted as an independent variable.

Relative wave run-up (R/H_o' and R/H_e') values for water depths (d) of 1.2 ft, 1.5 ft and 1.8 ft are shown respectively in Figs. 20, 21 and 22. From the relative monochromatic wave run-up (R/H_o') data for each water depth (d) an empirical equation expressing the relative run-up (R/H_o') in terms of the oncoming wave energy density (E_μ) was obtained from a multiple least squares regression analysis of the data [see Table 21 (Appendix VI) for statistics]. The empirical equations:

$$d = 1.2 \text{ ft}, \quad \frac{R}{H_o'} = 1.94\, E_\mu^{0.0104} \quad \ldots\ldots\ldots \quad (25)$$

$$d = 1.5 \text{ ft}, \quad \frac{R}{H_o'} = 1.68\, E_\mu^{-0.0379} \quad \ldots\ldots\ldots \quad (26)$$

$$d = 1.8 \text{ ft}, \quad \frac{R}{H_o'} = 1.75\, E_\mu^{-0.0409} \quad \ldots\ldots\ldots \quad (27)$$

were obtained respectively from 465, 453 and 392 monochromatic wave run-up (R) values. Due to the nature of the monochromatic wave run-up (R) phenomena there was a distribution (scatter) of the monochromatic wave run-up (R) values for each mean wave energy density (E_μ). Envelope curves (lines) were arbitrarily drawn to enclose the relative monochromatic wave run-up (R/H_o') data. The envelope curves delineated the deviation of the data from the best fit line obtained from the regression analysis. For the 1.2 ft water depth the relative monochromatic wave run-up (R/H_o') values deviated as much as 30 per cent above and 19 per cent below the best fit line for the data. For the 1.5 ft and 1.8 ft water depths the relative

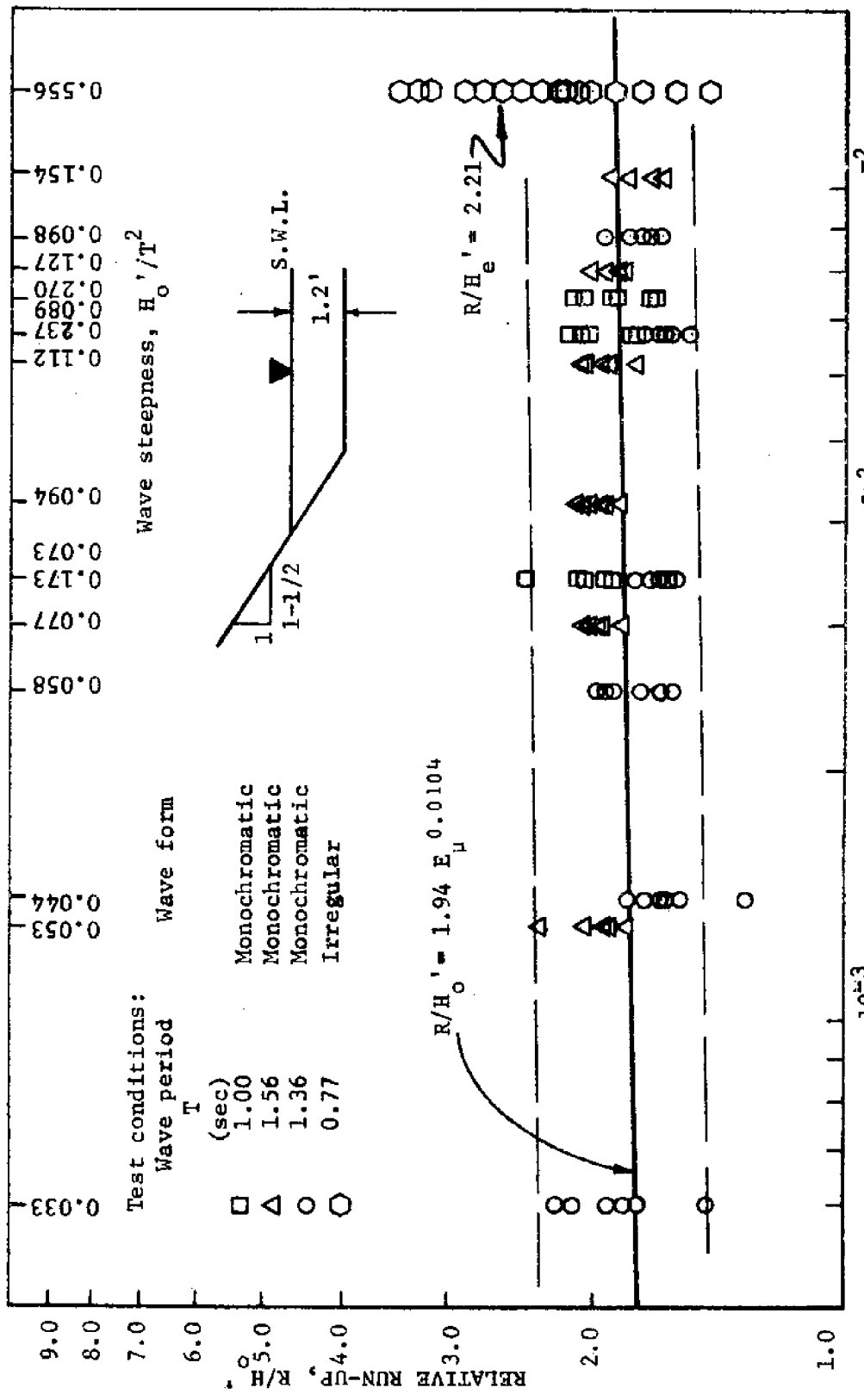

FIG. 20.--RELATIVE RUN-UP ON A SMOOTH 1 ON 1-1/2 SLOPE (d = 1.2 ft)

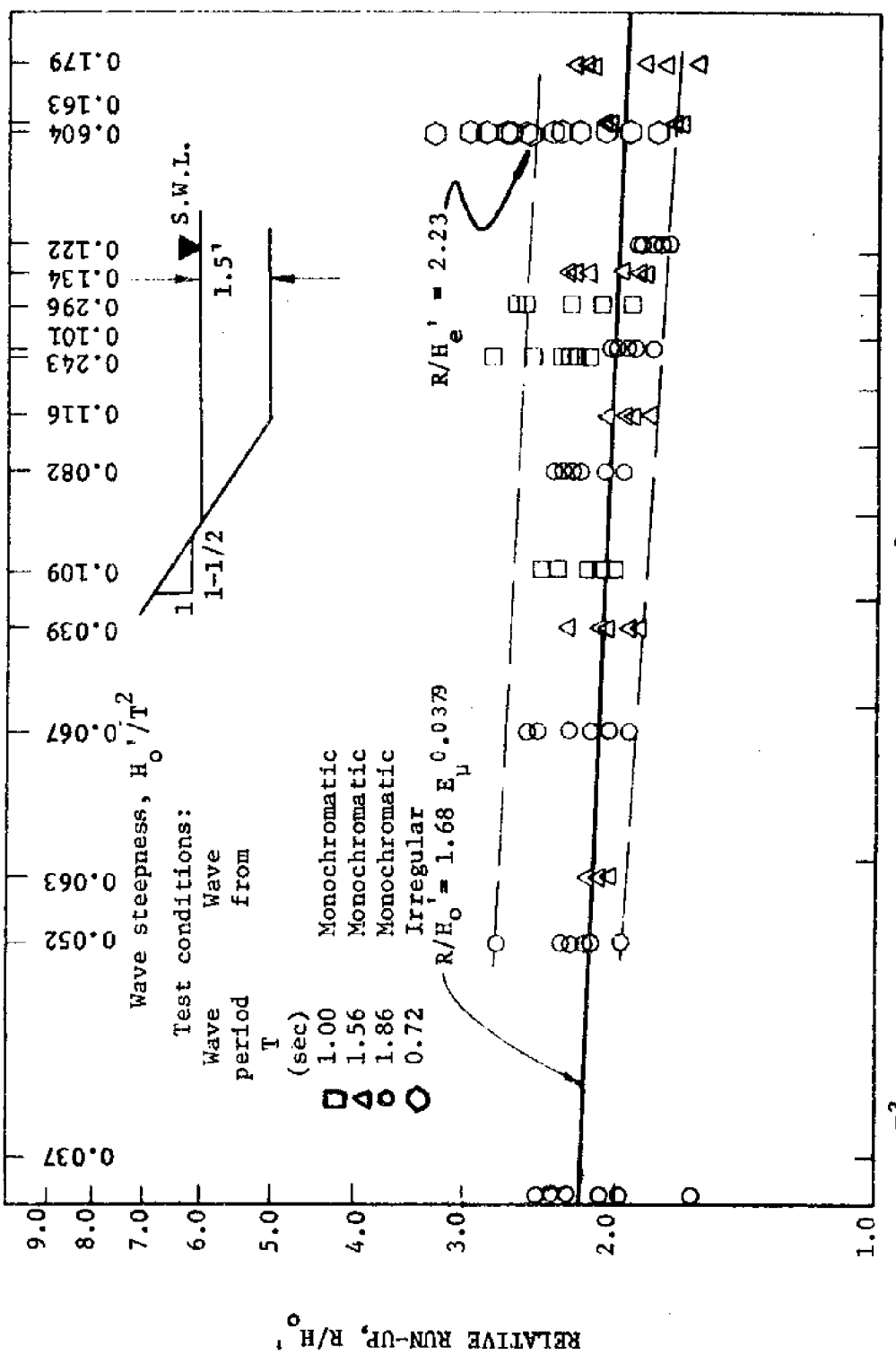

FIG. 21.--RELATIVE RUN-UP ON A SMOOTH 1 ON 1-1/2 SLOPE (d = 1.5 ft)

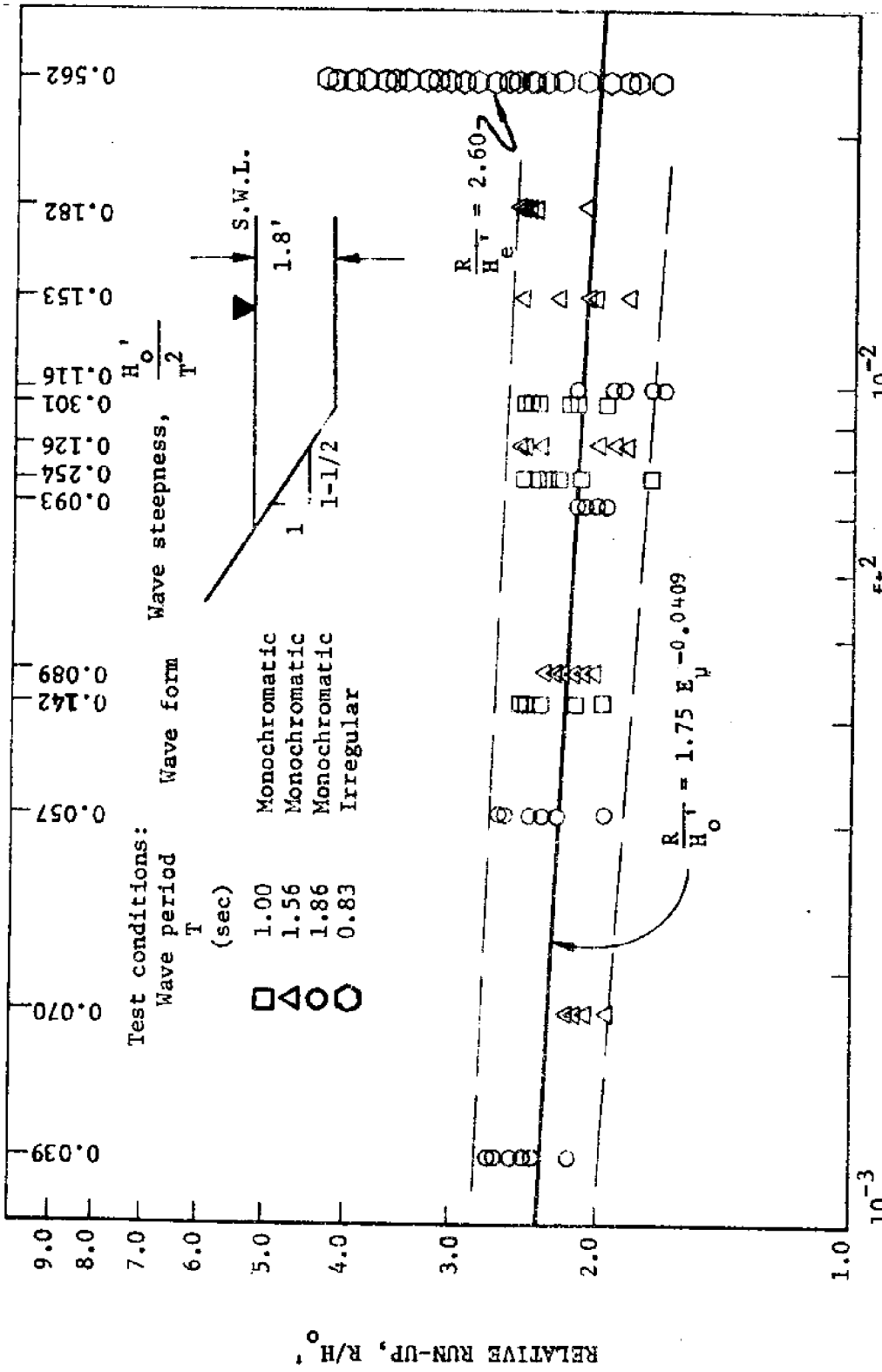

FIG. 22.--RELATIVE RUN-UP ON A SMOOTH 1 ON 1-1/2 SLOPE (d = 1.8 ft)

monochromatic wave run-up (R/H_o') values deviated 22 per cent above and 12 per cent below and 23 per cent above and 18 per cent below, respectively. Due to the scatter of the data the correlation coefficients were very low (< 0.1) for all depths. A high probability (0.341) of a Type I error existed for the 1.2 ft water depth [see Table 21 (Appendix VI)]. Analysis of variance was computed for each water depth. Results of the F test are shown in Table 22 (Appendix VI). From the relative wind wave run-up (R/H_e') data for each water depth (d) an average relative wave run-up (R/H_e') value was computed for the oncoming mean wave energy density (E_μ). The average relative wave run-up (R/H_e') values:

$$d = 1.2 \text{ ft} \qquad E_\mu = 0.0131 \frac{ft^2}{sec^{-1}} \qquad \frac{R}{H_e'} = 2.21 \quad . . . . . \quad (28)$$

$$d = 1.5 \text{ ft} \qquad E_\mu = 0.0138 \frac{ft^2}{sec^{-1}} \qquad \frac{R}{H_e'} = 2.23 \quad . . . . . \quad (29)$$

$$d = 1.8 \text{ ft} \qquad E_\mu \quad 0.0232 \frac{ft^2}{sec^{-1}} \qquad \frac{R}{H_e'} = 2.60 \quad . . . . . \quad (30)$$

were obtained from 90 wave run-up (R) readings taken in each test series [see Table 18 Appendix VI)].

A study of the relative run-up values (R/H_o' and R/H_e'):

$d = 1.2$ ft	$\frac{R}{H_o'} = 1.91$	(31)
$E_\mu = 0.0131 \frac{ft^2}{sec^{-1}}$	$\frac{R}{H_e'} = 2.21$	(28)
$d = 1.5$ ft	$\frac{R}{H_o'} = 1.96$	(32)
$E_\mu = 0.0138 \frac{ft^2}{sec^{-1}}$	$\frac{R}{H_e'} = 2.23$	(29)
$d = 1.8$ ft	$\frac{R}{H_o'} = 2.02$	(33)
$E_\mu = 0.0232 \frac{ft^2}{sec^{-1}}$	$\frac{R}{H_e'} = 2.60$	(30)

indicates that the average relative wave run-up (R/H_e') of wind waves was slightly greater than the relative wave run-up (R/H_o') of monochromatic waves. Due to the scatter of the data this slight increase was not considered significant.

Wave reflection. To establish a standard for comparison purposes and to determine the reflecting capability (power) of a smooth (1 on 1-1/2) slope, a series of wave reflection (H_r/H_i) tests were run using monochromatic (regular) waves.

The wave reflection tests were run using wave periods (T) of 1.00 sec, 1.56 sec and 1.86 sec in water depths of 1.2 ft and 1.8 ft. (Tests were not run with a 1.5 ft water depth.) Equivalent deepwater wave heights (H_o') were varied from 0.113 ft to 0.443 ft while the mean wave energy densities (E_μ) varied from 0.0006 ft^2/sec^{-1}

to 0.0165 ft^2/sec^{-1}, respectively, for the water depths tested [see Table 9 (Appendix III)].

The reflecting capability (power) of the smooth (1 on 1-1/2) slope was evaluated from wave records obtained by moving the instrument carriage containing the wave height sensor through a train of waves to obtain the incident and reflected wave heights. A reflecting coefficient (ratio of the reflected wave height to the incident wave height) was calculated for each test run [see Table 14 (Appendix V)]. Each reflecting coefficient (*i.e.*, coefficient of reflection) value ($C_r = H_r/H_i$) was plotted as a dependent variable for its respective incident mean wave energy density (E_μ) which was plotted as an independent variable as shown in Fig. 23. Fig. 23, therefore represents the reflecting capability (power) of the smooth (1 on 1-1/2) slope.

As the mean wave energy density (E_μ) increased from 0.001 ft^2/sec^{-1} to 0.01 ft^2/sec^{-1} the reflecting capability (power) was decreased approximately 19 per cent.

Uprush and dnrush velocities (V_u and V_d). To establish a standard for comparison purposes and to determine maximum velocities in the uprush zone on a smooth (1 on 1-1/2) slope, a series of wave uprush and dnrush velocity (V_u and V_d) tests were run using monochromatic (regular) waves.

The uprush and dnrush velocity tests were run using wave periods (T) of 1.0 sec, 1.56 sec and 1.86 sec in water depths (d) of 1.2 ft,

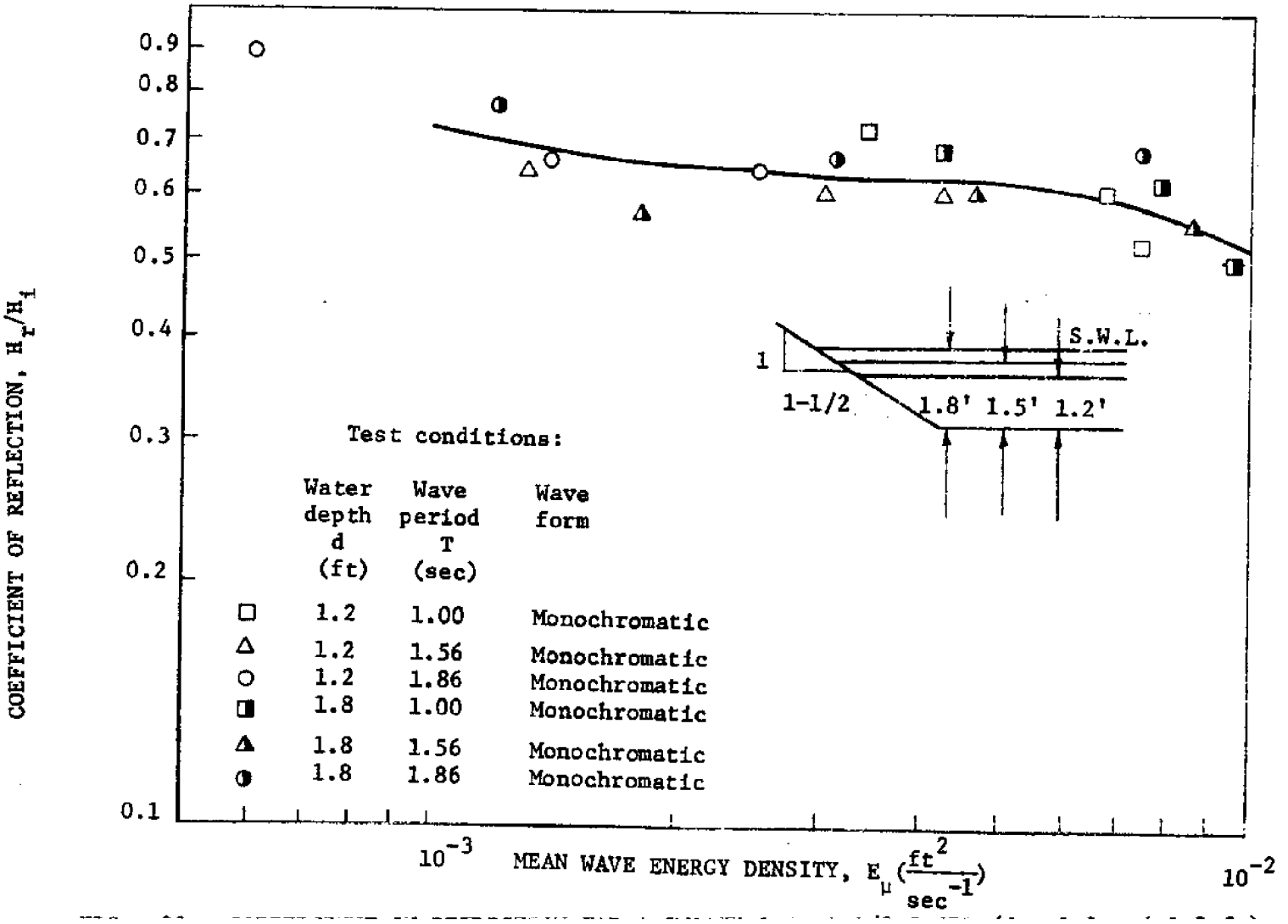
COEFFICIENT OF REFLECTION, H_r/H_i
0.9
0.8
0.7
0.6
0.5
0.4
0.3
0.2
0.1
10^{-3}
10^{-2}
MEAN WAVE ENERGY DENSITY, E_μ ($\frac{ft^2}{sec^{-1}}$)
S.W.L.
1
1-1/2
1.8' 1.5' 1.2'
Test conditions:
Water depth d (ft)
Wave period T (sec)
Wave form
1.2 1.00 Monochromatic
1.2 1.56 Monochromatic
1.2 1.86 Monochromatic
1.8 1.00 Monochromatic
1.8 1.56 Monochromatic
1.8 1.86 Monochromatic

1.5 ft and 1.8 ft. Equivalent deepwater wave heights (H_o') were varied from 0.113 ft to 0.443 ft while the mean wave energy densities (E_μ) varied from 0.0006 ft^2/sec^{-1} to 0.0165 ft^2/sec^{-1}, respectively, for the water depths tested [see Table 9 (Appendix III)].

Velocities in the uprush zone were evaluated from profiles obtained using the turbulent velocity sensor (hot-film sensor). In the first series of tests to measure the uprush and dnrush velocities the sensor was maintained at a height of 0.035 ft above a slope gauge reading of 0.05 ft, thus the velocity component parallel to the slope (just above the S.W.L.) was measured. In the second series of tests, the sensor height was varied from 0.035 ft to 0.255 ft, thus the velocity component parallel to the slope at various heights was obtained. The maximum uprush and dnrush velocities (V_u and V_d) were evaluated from profiles for each run of the first test series [see Table 23 and Figs. 140 through 154 (Appendix VII)].

A relative uprush velocity (V_u/C) value and a relative dnrush velocity (V_d/U) value was obtained for each test run and plotted as a dependent variable for its respective incident mean wave energy density (E_μ) which was plotted as an independent variable as shown in Figs. 24 and 25.

As the mean wave energy density (E_μ) increased from 0.001 ft^2/sec^{-1} to 0.01 ft^2/sec^{-1} the relative uprush velocity (V_u/C) increased from 0.59 to 0.75 as shown in Fig. 24. Due to the scatter of the relative dnrush velocity (V_d/C) it was not evaluated (see Fig. 25).

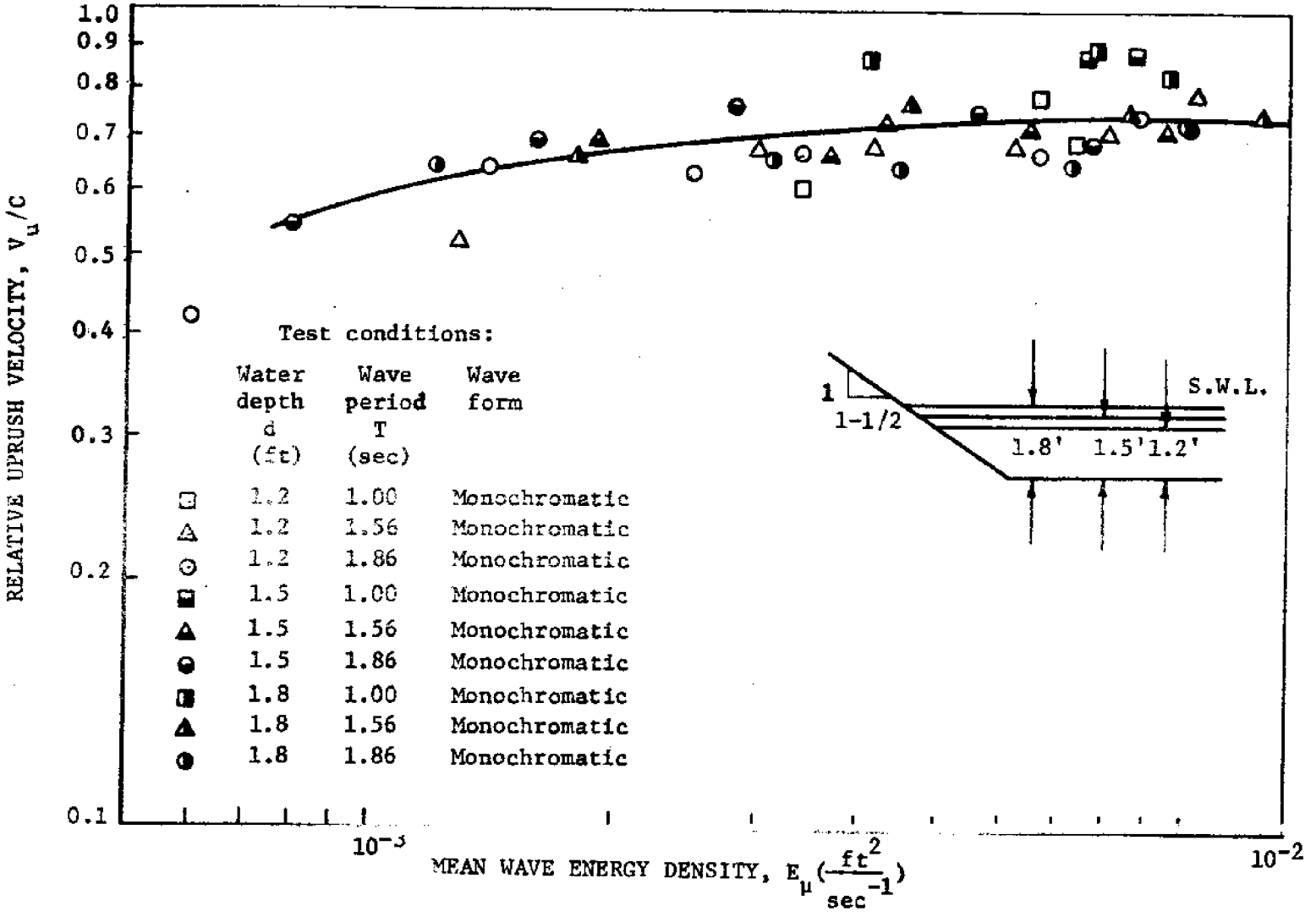

FIG. 24.--RELATIVE UPRUSH VELOCITY FOR A SMOOTH 1 ON 1-1/2 SLOPE (d = 1.2, 1.5 and 1.8 ft)

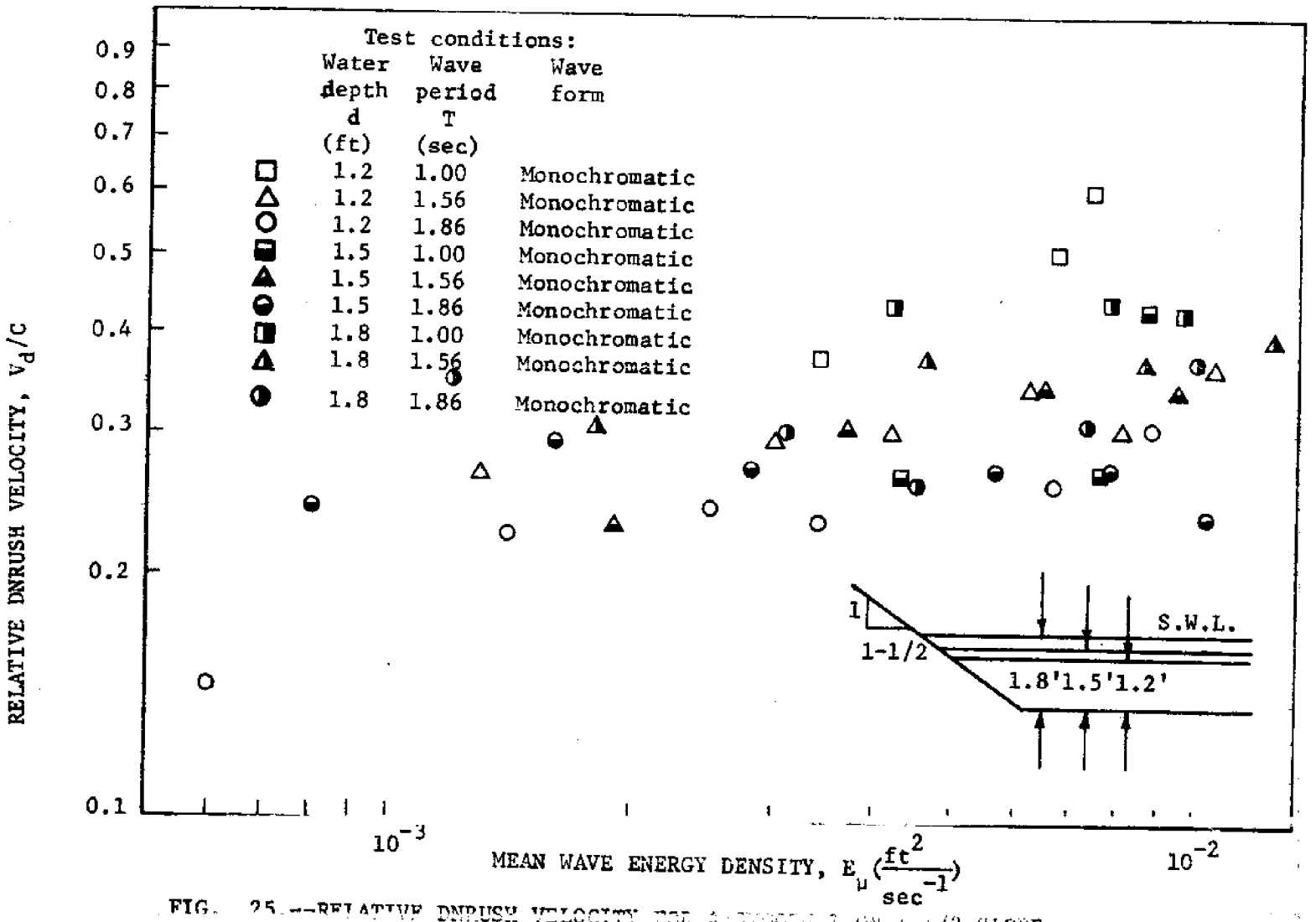

FIG. 25.--RELATIVE DNRUSH VELOCITY FOR A SMOOTH 1 ON 1-1/2 SLOPE
(d = 1.2, 1.5 and 1.8 ft)

The uprush and dnrush velocity distribution for the 1.2 ft water depth is shown in Figs. 140 through 154 (Appendix VII).

Effect of water depth (d) on relative wave run-up (R/H_o'). The effect of water depth (d) on relative wave run-up (R/H_o') on a smooth (1 on 1-1/2) slope was studied by comparing relative wave run-up (R/H_o') data from the three water depths (d) tested (see Fig. 26). The comparison was made between the best fit curves (lines) obtained from least squares regression analysis of the data.

Some effect of water depth (d) on relative wave run-up (R/H_o') was noted in the lower range of mean wave energy densities (E_μ), but since the correlation coefficients from the best fit curves (lines) were very low (< 0.1) the differences in relative wave run-up (R/H_o') were not considered significant. A study of Fig. 26 suggests a strong possibility that water depth (d) may have a pronounced effect on relative wave run-up (R/H_o') in low wave energy densities (E_μ) representing long waves ($d << \lambda$) with small wave heights ($H_o' << d$).

Effect of significant parameters (d/λ, H_o'/d and H_o'/T^2) on relative wave run-up (R/H_o'). The effects of three significant parameters (d/λ, H_o'/d and H_o'/T^2) on relative wave run-up (R/H_o') were studied. The relative wave run-up (R/H_o') data was plotted as a dependent variable for its respective relative wave energy density (E_μ/C^2T^3), which was plotted as an independent variable as shown in Figs. 27, 28 and 29. (At this point, it should be noted that by nondimensionalizing the mean wave energy density (E_μ) with the

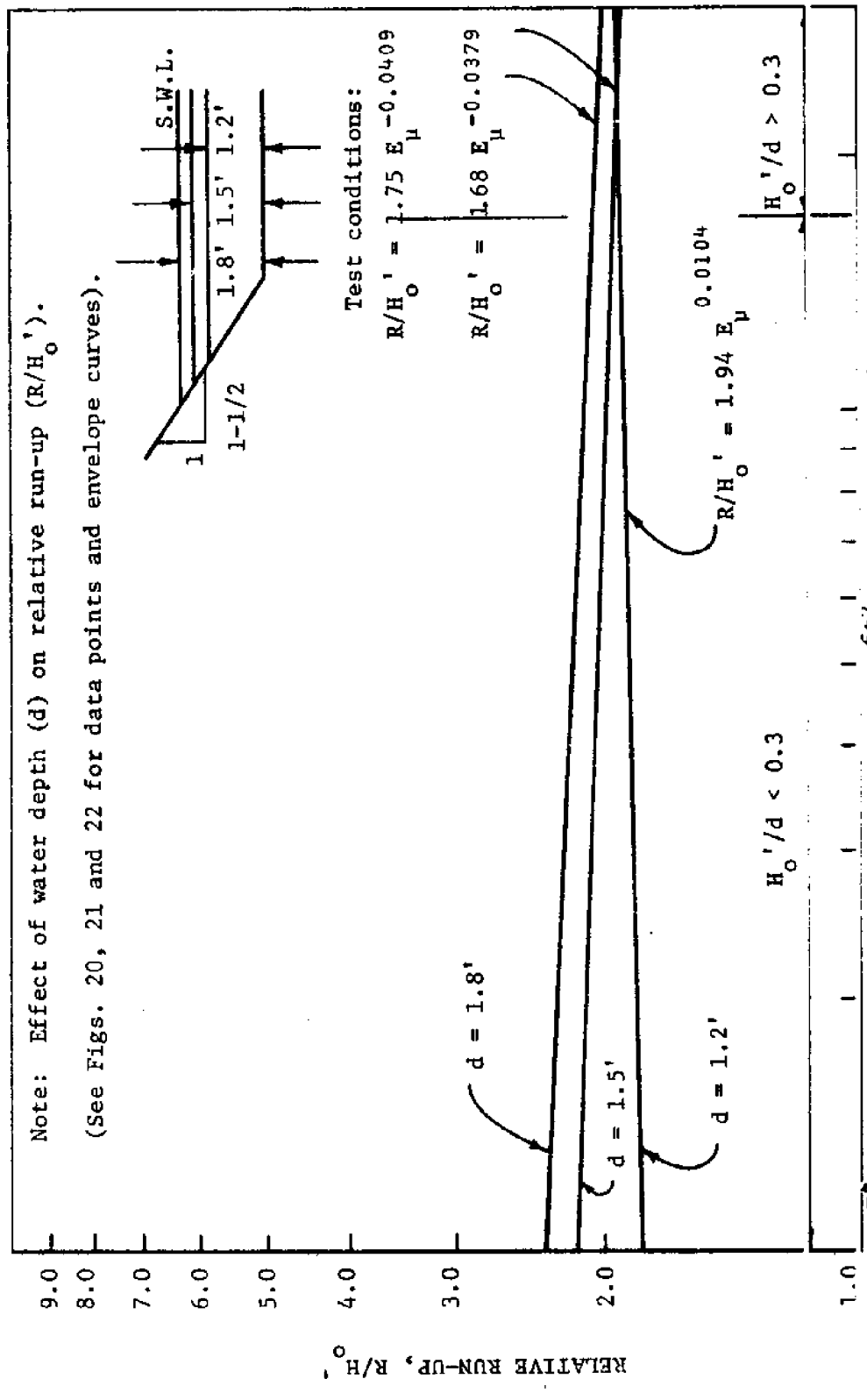

26.—RELATIVE RUN-UP ON A SMOOTH 1 ON 1-1/2 SLOPE (d = 1.2, 1.5 and 1.8 ft.)

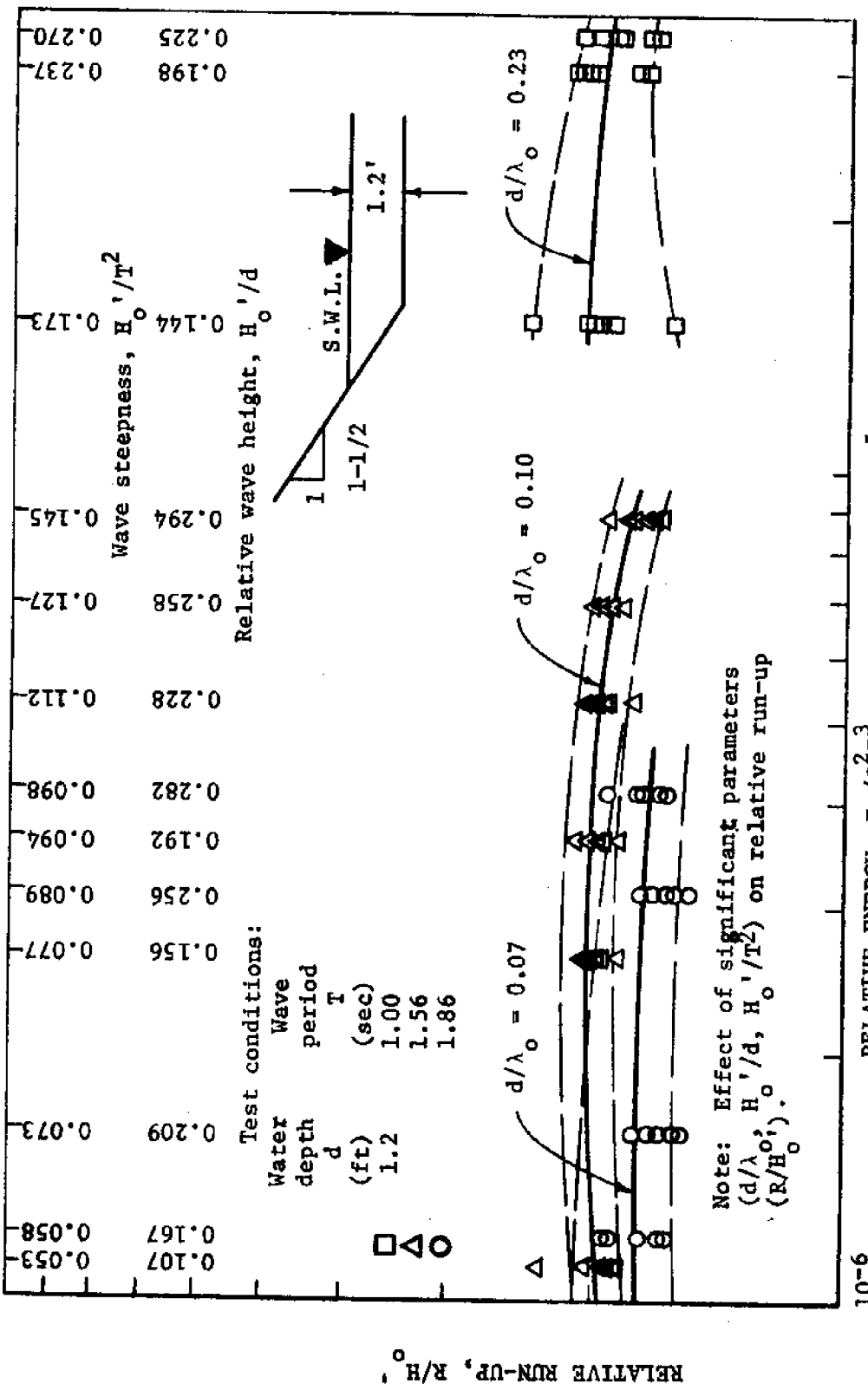

FIG. 27.--RELATIVE RUN-UP ON A SMOOTH 1 ON 1-1/2 SLOPE (d = 1.2 ft.)

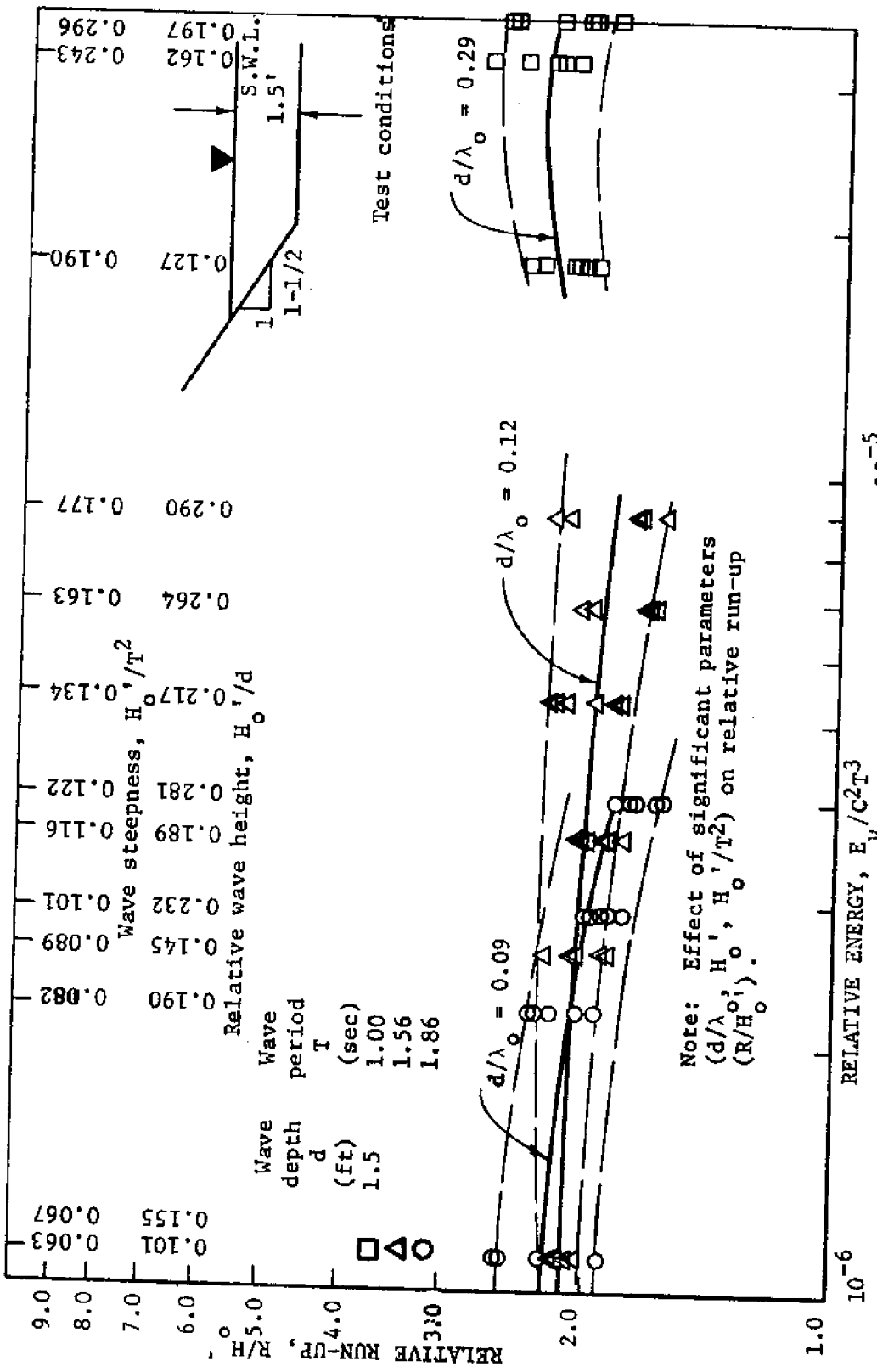

FIG. 28.--RELATIVE RUN-UP ON A SMOOTH 1 ON 1-1/2 SLOPE (d = 1.5 ft)

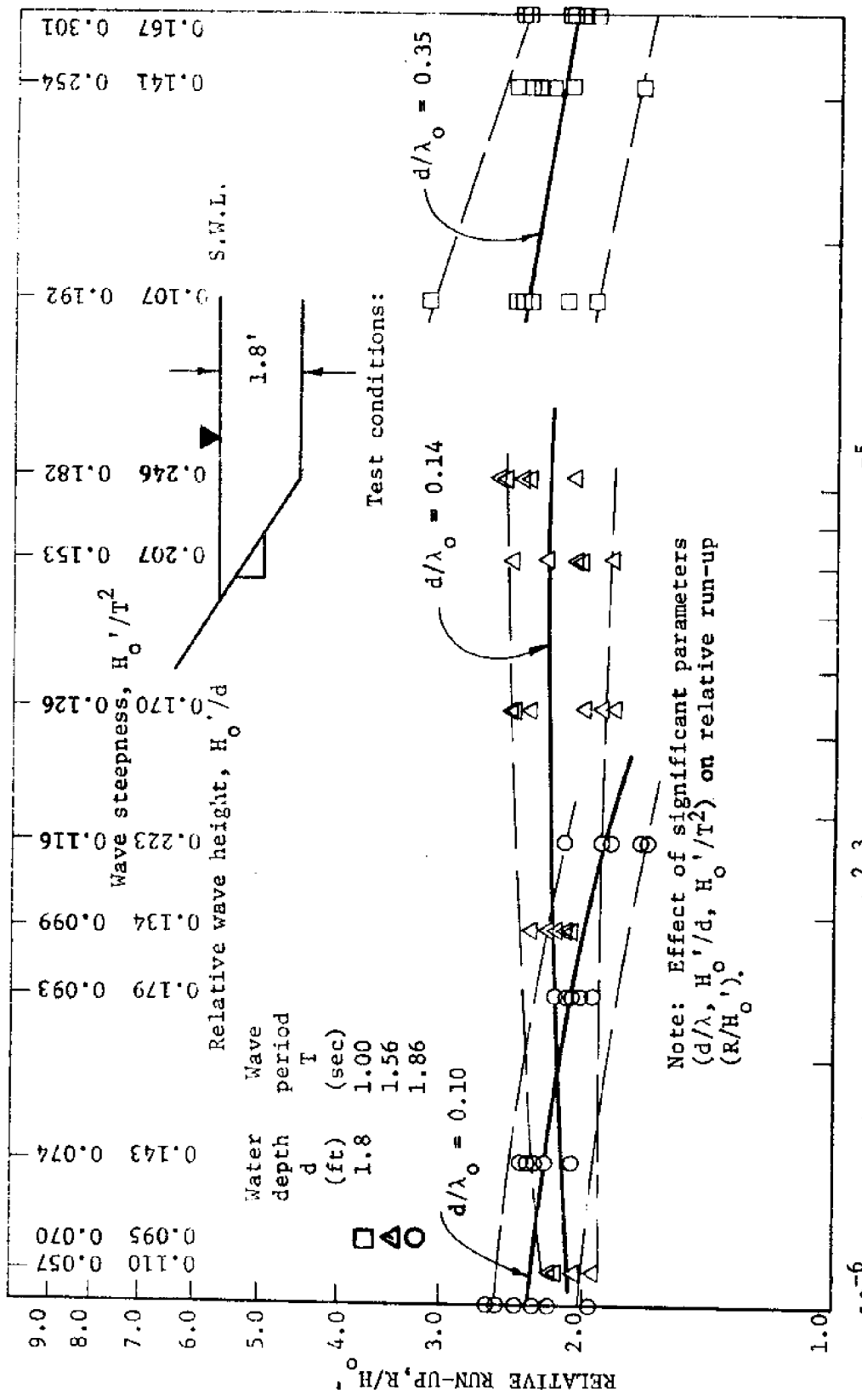

FIG. 29.--RELATIVE RUN-UP ON A SMOOTH 1 ON 1-1/2 SLOPE (d = 1.8 ft)

time (t) variable the wave steepness (H_o'/T^2) values were ordered by magnitude).

Arbitrary curves for each relative depth (d/λ) were developed as shown in Figs. 27, 28, and 29. Since these curves were independent of each other, it was concluded that the relative wave run-up (R/H_o') was affected by the relative depth (d/λ) parameter:

$$\frac{R}{H_o'} = f\left(\frac{d}{\lambda}, \cdots\right) \quad \ldots\ldots\ldots \quad (34)$$

As the wave steepness (H_o'/T^2) and the relative wave height (H_o'/d) increased for each constant relative depth (d/λ), the relative wave run-up (R/H_o') increased to a maximum value for a particular wave steepness (H_o'/T^2) and relative wave height (H_o'/d) and then decreased. It was therefore concluded that the relative wave run-up (R/H_o') was affected by the wave steepness (H_o'/T^2) and the relative wave height (H_o'/d) parameters:

$$\frac{R}{H_o'} = f\left(\frac{H_o'}{T^2}, H_o'/d, \ldots\right) \quad \ldots\ldots \quad (35)$$

Physical observations. The following significant observations were made and recorded during testing:

1. The leading edge of the wave run-up (R) was observed to be irregular (see Fig. 30).

2. The phenomena of transverse waves was unexpectedly (and unavoidably) observed at various times during testing although the wave lengths were not harmonics of the wave flume width.

3. Wave reflection was observed in the wave flume

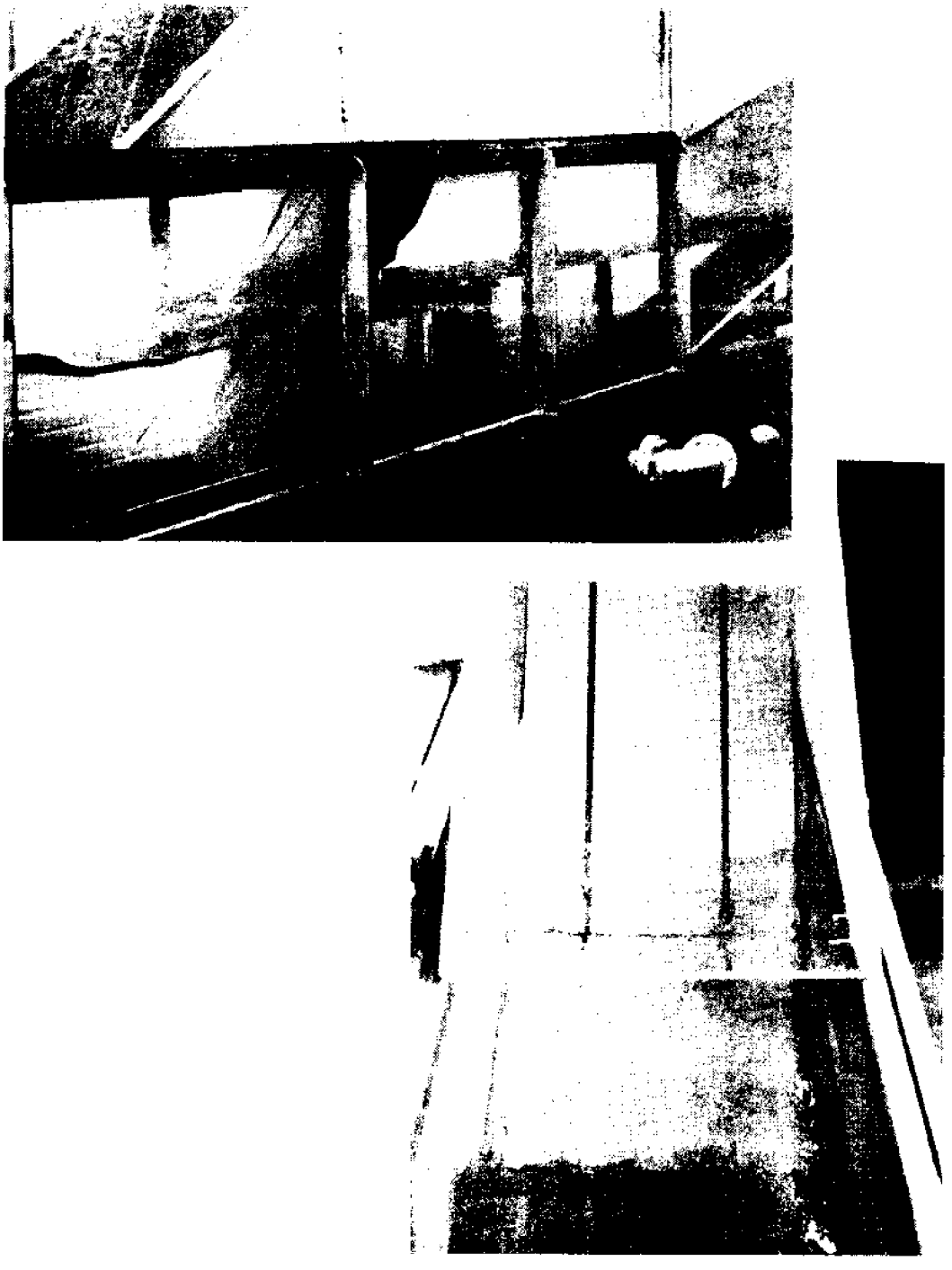

FIG. 30.--MONOCHROMATIC (REGULAR) WAVE RUN-UP ON A SINGLE (1 ON 1-1/2) SLOPE

shortly after the leading wave was reflected.

4. A water 'set-up' was observed in the wave flume during the testing using the wind (irregular) waves.

5. A considerable spray up the slope was observed during the wave run-up (R) tests using the wind (irregular) wave generator even though the 'venturi' effect was eliminated by providing a comparable flow way above the slope (see Fig. 30).

Wave Energy Dissipation on a Single (1 on 1-1/2) Roughened (Strips) Slope

Relative wave run-up (R/H_o'). To determine the effects of slope roughness on wave run-up (see objectives 1 and 4), a series of tests were run using a (1 on 1-1/2) slope containing parallel surface strips. Wave run-up (R) data for both monochromatic (regular) waves and wind (irregular) waves was obtained for the roughened slope configuration shown in Fig. 41 (page 113).

The monochromatic (regular) wave tests were run using wave periods (T) of 1.00 sec, 1.56 sec and 1.86 sec. In water depths (d) of 1.2 ft, 1.5 ft, and 1.8 ft equivalent deepwater wave heights (H_o') were varied from 0.113 ft to 0.443 ft for the water depths tested [see Table 9 Appendix III)].

The wind (irregular) wave tests were run using surface wind velocities ($V_{0.30}$) of 39.8 ft/sec, 41.3 ft/sec and 54.5 ft/sec obtained for water depths of 1.2 ft, 1.5 ft and 1.8 ft, respectively. The equivalent wave periods (T) obtained from the wave energy

spectrum were 0.72 sec, 0.77 sec and 0.83 sec for water depths of 1.2 ft, 1.5 ft and 1.8 ft, respectively, while the equivalent deep-water wave heights (H_e') obtained from the wave energy spectrum were, respectively, 0.287 ft, 0.296 ft and 0.344 ft [see Table 10 (Appendix III)].

The mean wave energy density (E_μ) was obtained from the wave energy spectrum for both the monochromatic (regular) waves and for the wind (irregular) waves. For the monochromatic (regular) waves the mean wave energy density (E_μ) varied from 0.0006 ft^2/sec^{-1} to 0.0165 ft^2/sec^{-1} while for the wind (irregular) waves the mean wave energy density (E_μ) varied from 0.0124 ft^2/sec^{-1} to 0.0200 ft^2/sec^{-1} [see Tables 9 and 10 (Appendix III)].

Relative wave run-up (R/H_o' and R/H_e') was calculated from the wave run-up (R) tests for both the monochromatic (regular) waves and the wind (irregular) waves [see Tables 15, 16, 17 and 18 (Appendix VI)]. Each relative run-up value (R/H_o' and R/H_e') was plotted as a dependent variable for its respective incident mean wave energy density (E_μ) which was plotted as an independent variable.

Relative wave run-up (R/H_o' and R/H_e') values for water depths (d) of 1.2 ft, 1.5 ft and 1.8 ft are shown, respectively, in Figs. 31, 32 and 33. From the relative monochromatic wave run-up (R/H_o') data for each water depth (d) an empirical equation expressing the relative run-Up (R/H_o') in terms of the oncoming wave energy density (E_μ) was obtained from a multiple least squares regression analysis

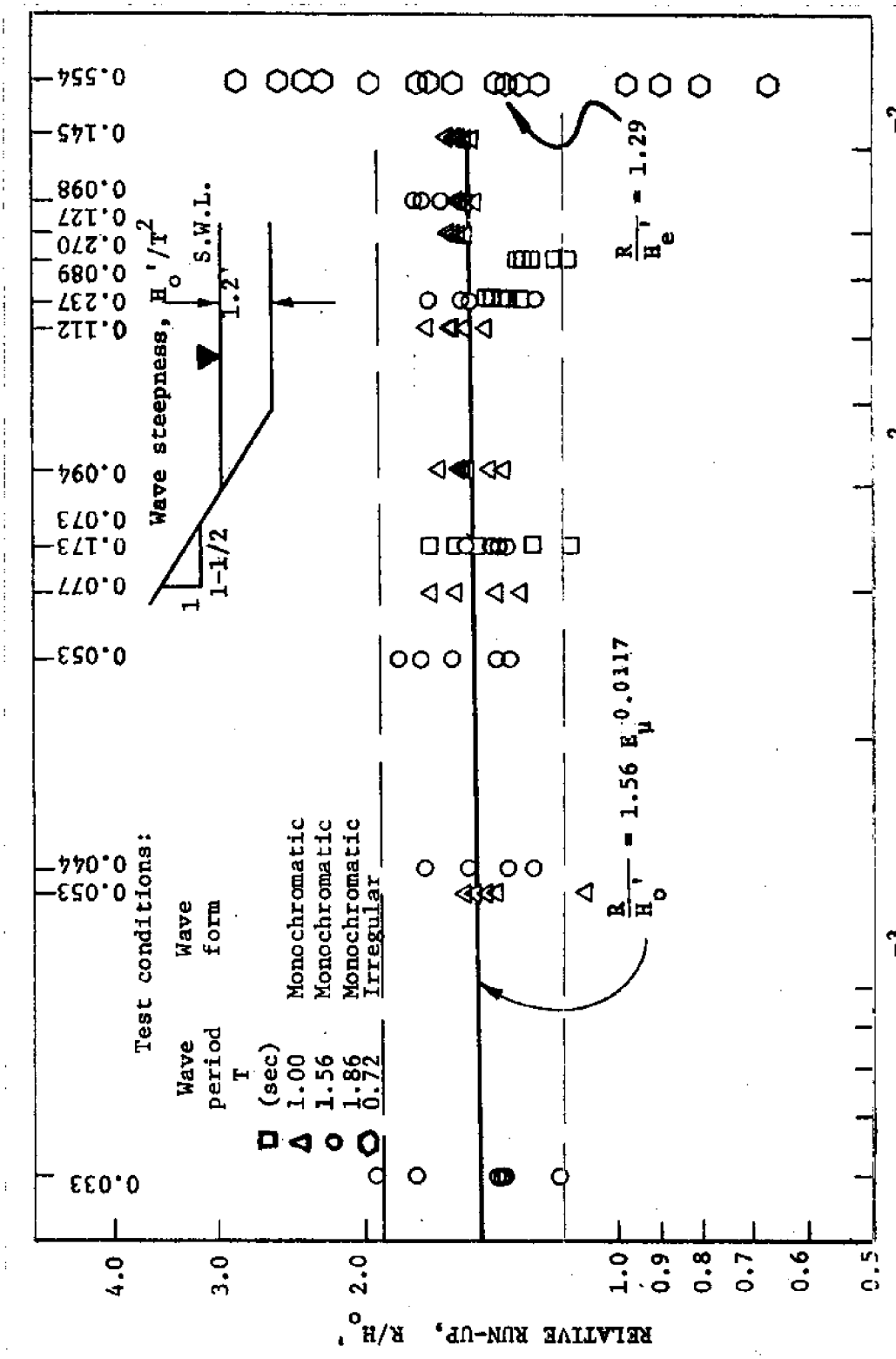

FIG. 31.--RELATIVE RUN-UP ON A ROUGHENED (STRIPS) 1 ON 1-1/2 SLOPE (d = 1.2 ft)

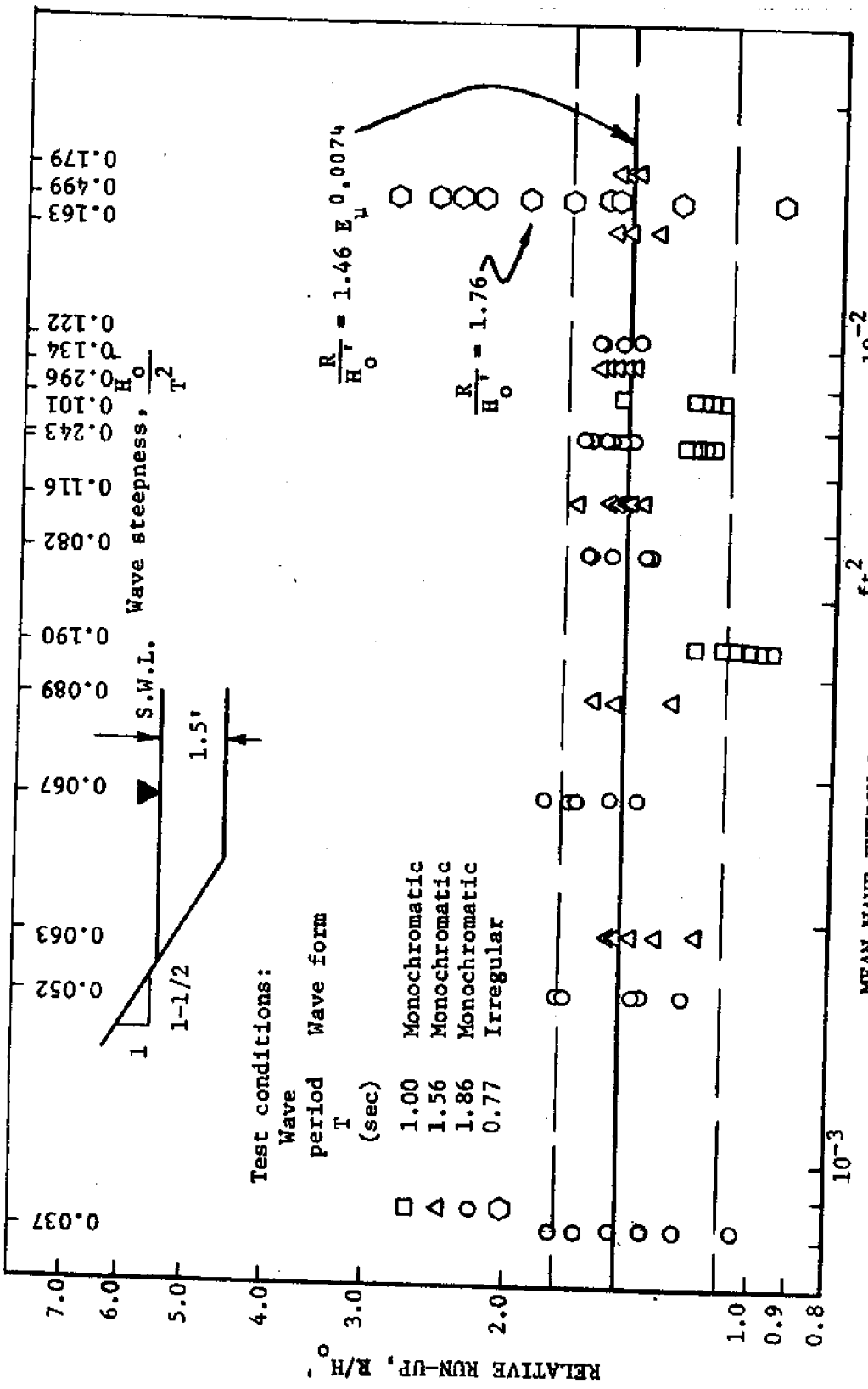

FIG. 32.--RELATIVE RUN-UP ON A ROUGHENED (STRIPS) 1 ON 1-1/2 SLOPE (d=1.5 ft)

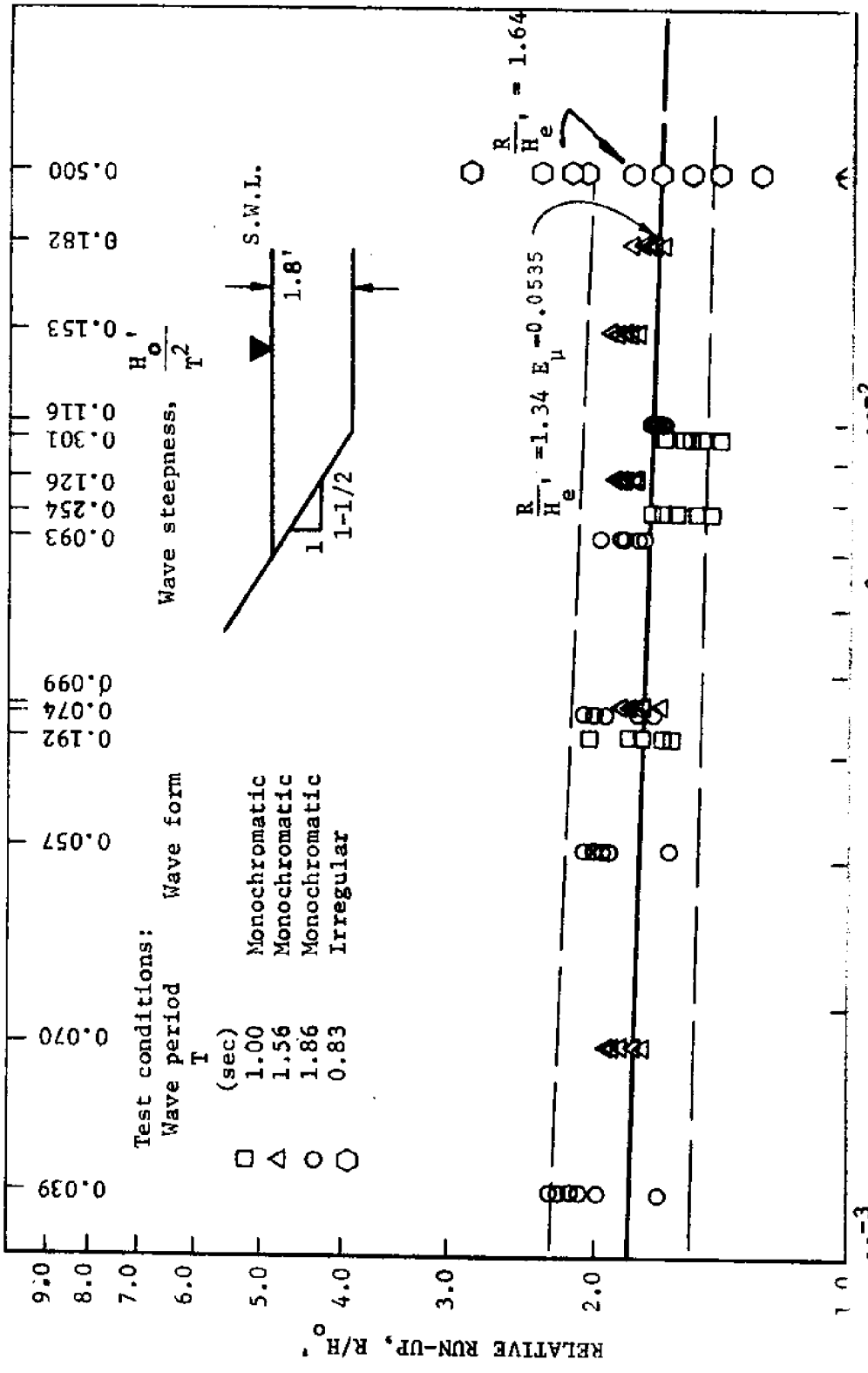

FIG. 33.--RELATIVE RUN-UP ON A ROUGHENED (STRIPS) 1 ON 1-1/2 SLOPE (d = 1.8 ft)

of the data [see Table 21(Appendix VI) for statistics]. The empirical equations:

$$d = 1.2 \text{ ft} \qquad R/H_o' = 1.56\, E_\mu^{0.0117} \quad \ldots\ldots \quad (36)$$

$$d = 1.5 \text{ ft} \qquad R/H_o' = 1.46\, E_\mu^{0.0074} \quad \ldots\ldots \quad (37)$$

$$d = 1.8 \text{ ft} \qquad R/H_o' = 1.34\, E_\mu^{-0.0535} \quad \ldots\ldots \quad (38)$$

were obtained, respectively from 449, 449, and 390 monochromatic wave run-up (R/H_o') values. Due to the nature of the monochromatic wave run-up (R) phenomena there was a distribution (scatter) of the monochromatic wave run-up (R) values for each mean wave energy density (E_μ). Envelope curves (lines) were arbitrarily drawn to enclose the relative monochromatic wave run-up (R/H_o') data. The envelope curves delineated the deviation of the data from the best fit line obtained from the regression analysis. For the 1.2 ft water depth the relative monochromatic wave run-up (R/H_o') values deviated as much as 32 per cent above and 20 per cent below the best fit line for the data. For the 1.5 ft and 1.8 ft water depths the relative monochromatic wave run-up (R/H_o') values deviated 21 per cent above and 25 per cent below and 24 per cent above and 16 per cent below, respectively, Due to the scatter of the data the correlation coefficients were very low (< 0.1) for all depths. A high probability (0.527) of a Type I error existed for the 1.5 ft water depth [see Table 21 (Appendix VI)]. Analysis of variance was computed for each water depth. Results of the F test are shown in

Table 22 (Appendix VI). From the relative wind wave run-up (R/H_e') data for each water depth (d) an average relative wave run-up (R/H_e') value was computed for the oncoming mean wave energy density (E_μ). The average relative wave run-up (R/H_e') values:

$$d = 1.2 \text{ ft} \qquad E_\mu = 0.0124 \frac{ft^2}{sec^{-1}} \qquad \frac{R}{H_e'} = 1.29 \quad . . . . . \quad (39)$$

$$d = 1.5 \text{ ft} \qquad E_\mu = 0.0152 \frac{ft^2}{sec^{-1}} \qquad \frac{R}{H_e'} = 1.76 \quad . . . . . \quad (40)$$

$$d = 1.8 \text{ ft} \qquad E_\mu = 0.020 \frac{ft^2}{sec^{-1}} \qquad \frac{R}{H_e'} = 1.64 \quad . . . . . \quad (41)$$

were obtained from 90 wave run-up (R) readings taken in each test series [see Table 18 (Appendix VI)].

Comparing the relative run-up values (R/H_o' and R/H_e'):

$d = 1.2$ ft, $E_\mu = 0.0124 \frac{ft^2}{sec^{-1}}$

$$\frac{R}{H_o'} = 1.50 \quad . . . . . \quad (42)$$

$$\frac{R}{H_e'} = 1.29 \quad . . . . . \quad (39)$$

$d = 1.5$ ft, $E_\mu = 0.0152 \frac{ft^2}{sec^{-1}}$

$$\frac{R}{H_o'} = 1.47 \quad . . . . . \quad (43)$$

$$\frac{R}{H_e'} = 1.76 \quad . . . . . \quad (40)$$

$d = 1.8$ ft $\qquad \frac{R}{H_o'} = 1.70$ . . . . . (44)

$E_\mu = 0.0200 \frac{ft^2}{sec^{-1}}$

$\frac{R}{H_e'} = 1.64$ . . . . . (41)

indicates that the average relative wave run-up of wind waves (R/H_e') was approximately the same as the relative wave run-up (R/H_o') of the monochromatic waves.

Wave reflection. To determine the effects of slope roughness on the reflecting capability (power) of a slope, a series of wave reflection (H_r/H_i) tests were run using a (1 on 1-1/2) slope containing parallel surface strips. Wave reflection (H_r/H_i) data for monochromatic (regular) waves was obtained for the roughened slope configuration shown in Fig. 41 (page 113).

The wave reflection tests were run using wave periods of 1.00 sec, 1.56 sec, and 1.86 sec in water depths of 1.2 ft, 1.5 ft and 1.8 ft. Equivalent deepwater wave heights (H_o') were varied from 0.113 ft to 0.443 ft while the mean wave energy densities (E_μ) varied from 0.0006 ft^2/sec^{-1} to 0.0165 ft^2/sec^{-1}, respectively, for the water depths tested [see Table 9 (Appendix III)].

The reflecting capability (power) of the roughened (1 on 1-1/2) slope was evaluated from wave records obtained by moving the instrument carriage containing the wave height sensor through a train of waves to obtain the incident and reflected wave heights. A reflecting coefficient (ratio of the reflected wave height to the incident

wave height) was calculated for each test run [see Table 14 (Appendix V)]. Each reflecting coefficient (*i.e.*, coefficient of reflection) value ($C_r = H_r/H_i$) was plotted as a dependent variable for its respective incident mean wave energy density (E_μ) which was plotted as an independent variable as shown in Fig. 34. Fig. 34 therefore represents the reflecting capability (power) of the slope containing parallel strips.

As the mean wave energy density (E_μ) increased from 0.001 ft^2/sec^{-1} to 0.01 ft^2/sec^{-1} the reflecting capability (power) was decreased approximately 8 per cent.

Energy dissipation by turbulence and bottom friction. The level of turbulence (intensity of turbulence) was increased with the introduction of parallel surface strips. The parallel strips served to generate turbulence.

The effect of turbulence and bottom friction on the wave run-up (R) could not be measured due to the fluctuating nature of the uprush velocity. Since the effect of turbulence on the wave run-up (R) was coupled with the effect of drag on the wave run-up (R) the combined effect was studied. In all cases the combined effects of drag and increased turbulence reduced the wave run-up (R).

Uprush and dnrush velocities (V_u and V_d). To determine the effects of slope roughness on maximum velocities in the uprush zone (see objective 2) a series of tests were run using a (1 on 1-1/2) slope containing parallel surface strips. Wave uprush and dnrush

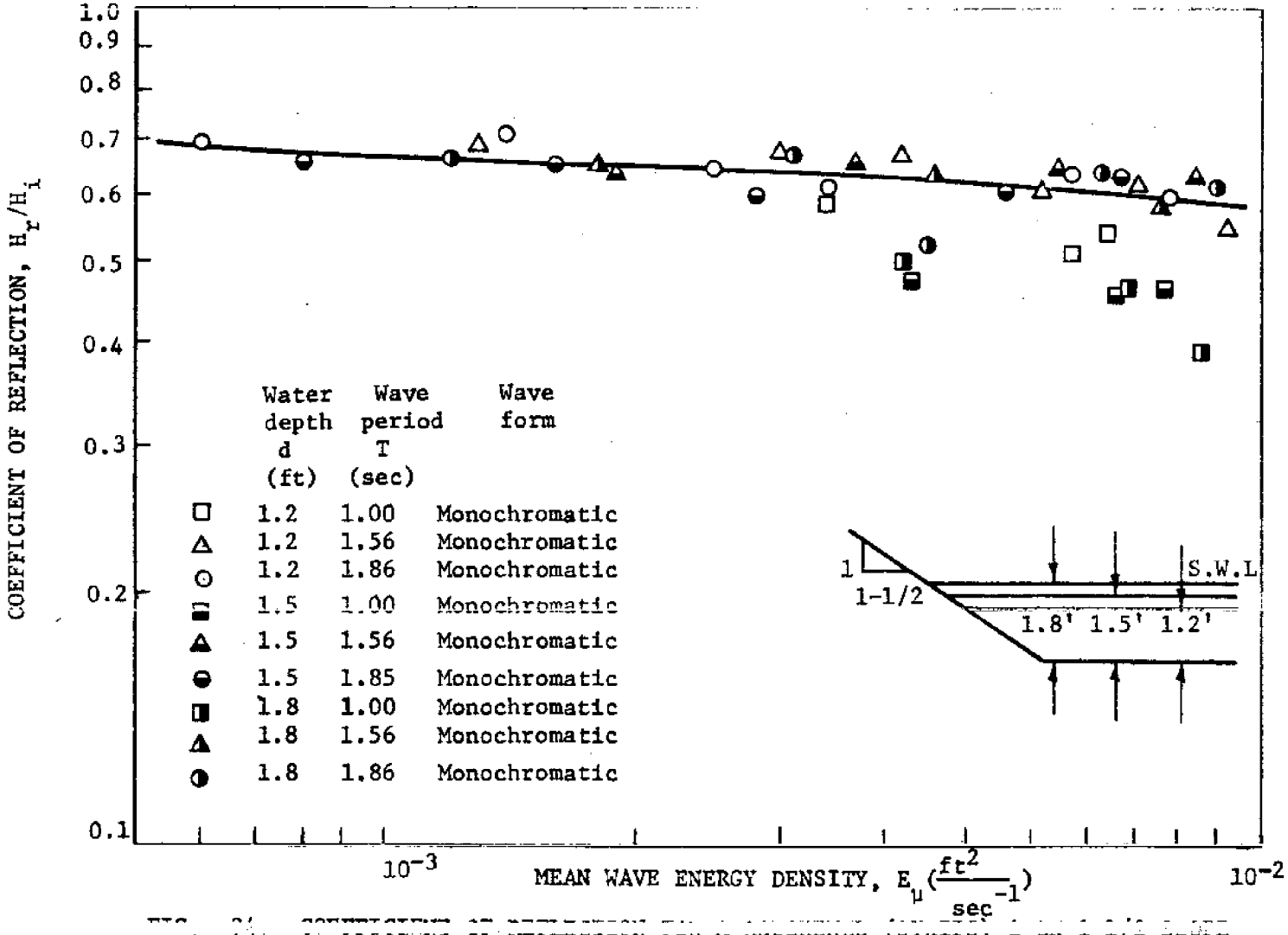

(d = 1.2, 1.5 and 1.8 ft)

velocity (V_u and V_d) data for monochromatic (regular) waves were obtained for the roughened slope configuration shown in Fig. 41 (page 113).

The uprush and dnrush velocity tests were run using wave periods (T) of 1.00 sec, 1.56 sec and 1.86 sec in water depths (d) of 1.2 ft, 1.5 ft and 1.8 ft. Equivalent deepwater wave heights (H_o') were varied from 0.113 ft to 0.443 ft while the mean wave energy densities (E_μ) varied from 0.0006 ft^2/sec^{-1} to 0.0165 ft^2/sec^{-1}, respectively, for the water depths tested [see Table 9 (Appendix III)].

Velocities in the uprush zone were evaluated from profiles obtained using the turbulent velocity sensor (hot-film sensor). In the first series of tests to measure the uprush and dnrush velocities the velocity sensor was maintained at a constant height of 0.035 ft above a slope gauge reading of 0.05 ft. The velocity component parallel to the slope (just above the S.W.L.) was measured. In the second series of tests, the sensor height was varied from 0.035 ft to 0.255 ft, thus the velocity component parallel to the slope at various heights was obtained. The maximum uprush and dnrush velocities (V_u and V_d) were evaluated from profiles for each run of the first test series [see Table 23 (Appendix VII) and Figs. 155 through 168 (Appendix VII)].

A relative uprush velocity (V_u/C) value and a relative dnrush velocity (V_d/C) value was obtained for each test run and plotted as a dependent variable for its respective incident mean wave energy density (E_μ) which was plotted as an independent variable as shown in Figs. 35 and 36.

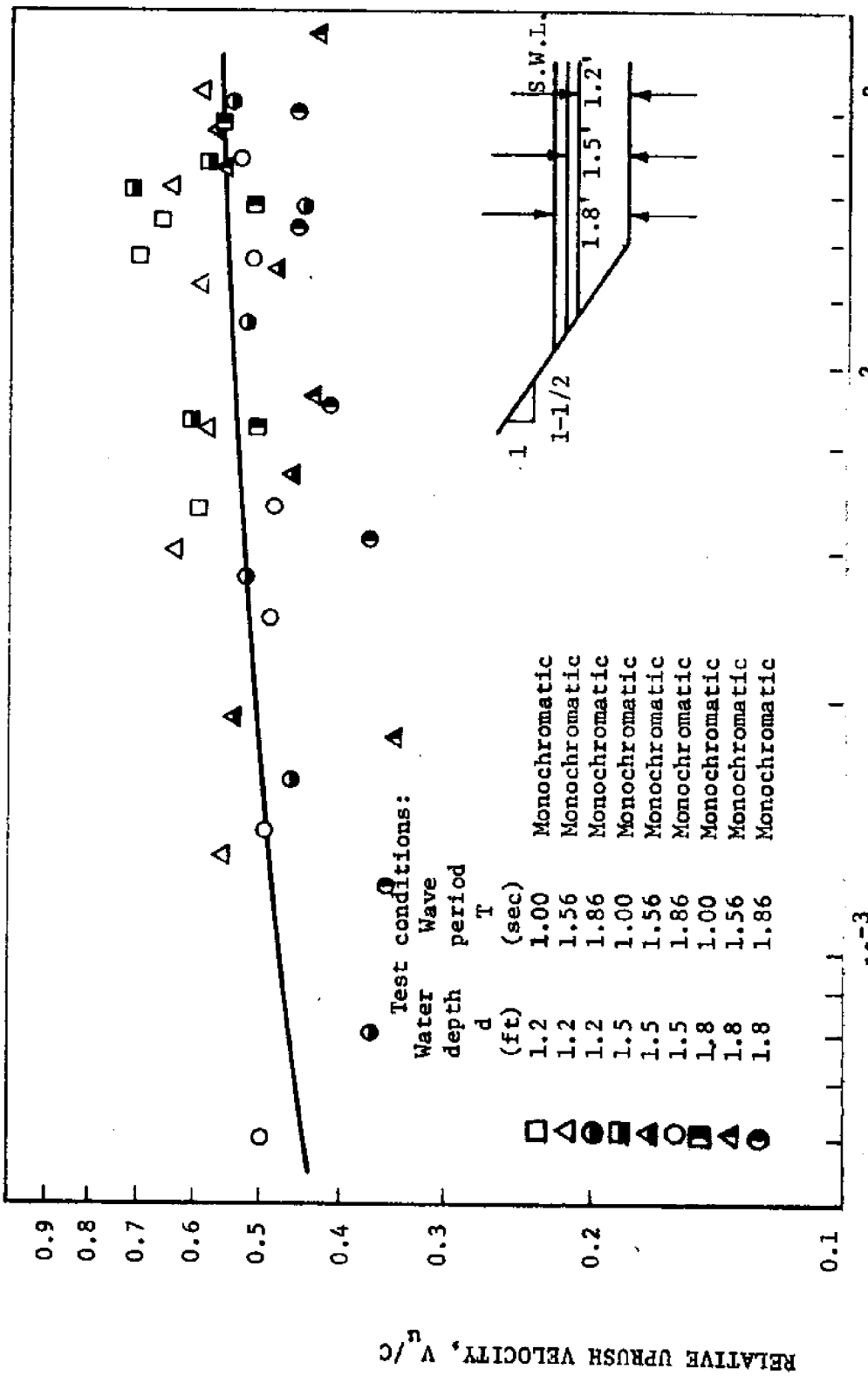

FIG. 35.--RELATIVE UPRUSH VELOCITY FOR A ROUGHENED (STRIPS) 1 ON 1-1/2 SLOPE (d = 1.2, 1.5 and 1.8 ft)

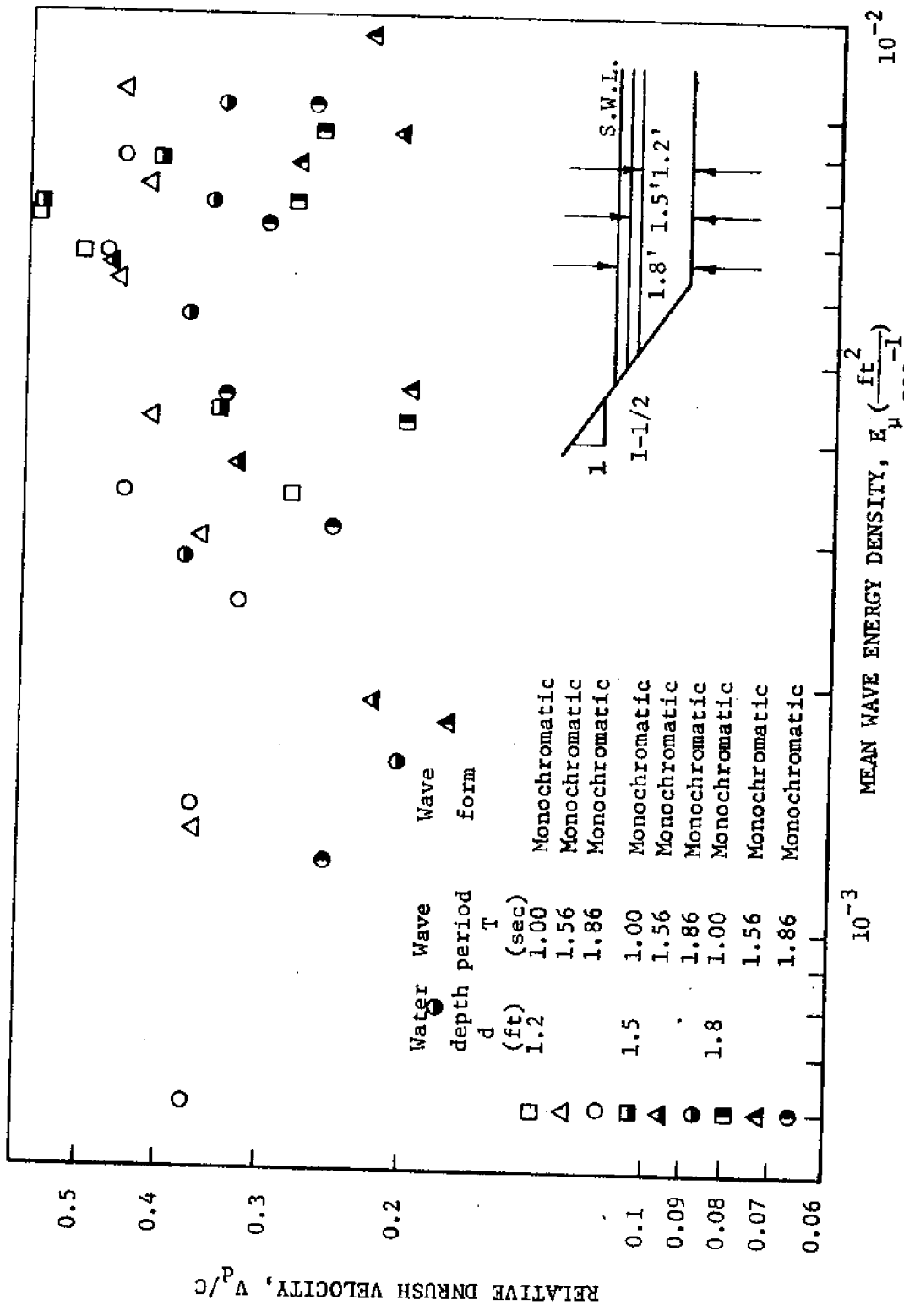

FIG. 36.--RELATIVE DNRUSH VELOCITY FOR A ROUGHENED (STRIPS) 1 ON 1-1/2 SLOPE (d = 1.2, 1.5 and 1.8')

As the mean wave energy density (E_μ) increased from 0.001 ft^2/sec^{-1} to 0.01 ft^2/sec^{-1} the relative uprush velocity (V_u/C) increased from 0.49 to 0.56 as shown in Fig. 35. Due to the scatter of the relative dnrush velocity (V_d/C) it was not evaluated (see Fig. 36).

The uprush and dnrush velocity distribution for the 1.2 ft water depth is shown in Figs. 155 through 168 (Appendix VII).

Effect of water depth (d) on relative wave run-up (R/H_o'). The effect of water depth (d) on relative wave run-up (R/H_o') on a roughened (1 on 1-1/2) slope was studied by comparing relative wave run-up (R/H_o') data from the three water depths (d) tested (see Fig. 37). The comparison was made between the best fit curves (lines) obtained from least squares regression analysis of the data.

Some effect of water depth (d) on relative wave run-up (R/H_o') was noted in the lower range of mean wave energy densities (E_μ) between the lowest and highest depths tested, but since the correlation coefficients from the best fit curves (lines) were very low (< 0.1) the differences in relative wave run-up (R/H_o') were not considered significant. Although there was no change in relative wave run-up (R/H_o') between the 1.2 ft and 1.5 ft water depths there was an apparent increase in relative wave run-up (R/H_o') between the 1.5 ft and 1.8 ft water depths. This anomaly was attributed to the scatter of the data.

A study of Fig. 37 suggests a strong possibility that water depths (d) may have a pronounced effect on relative wave run-up (R/H_o') in low wave energy densities (E_μ) representing long waves

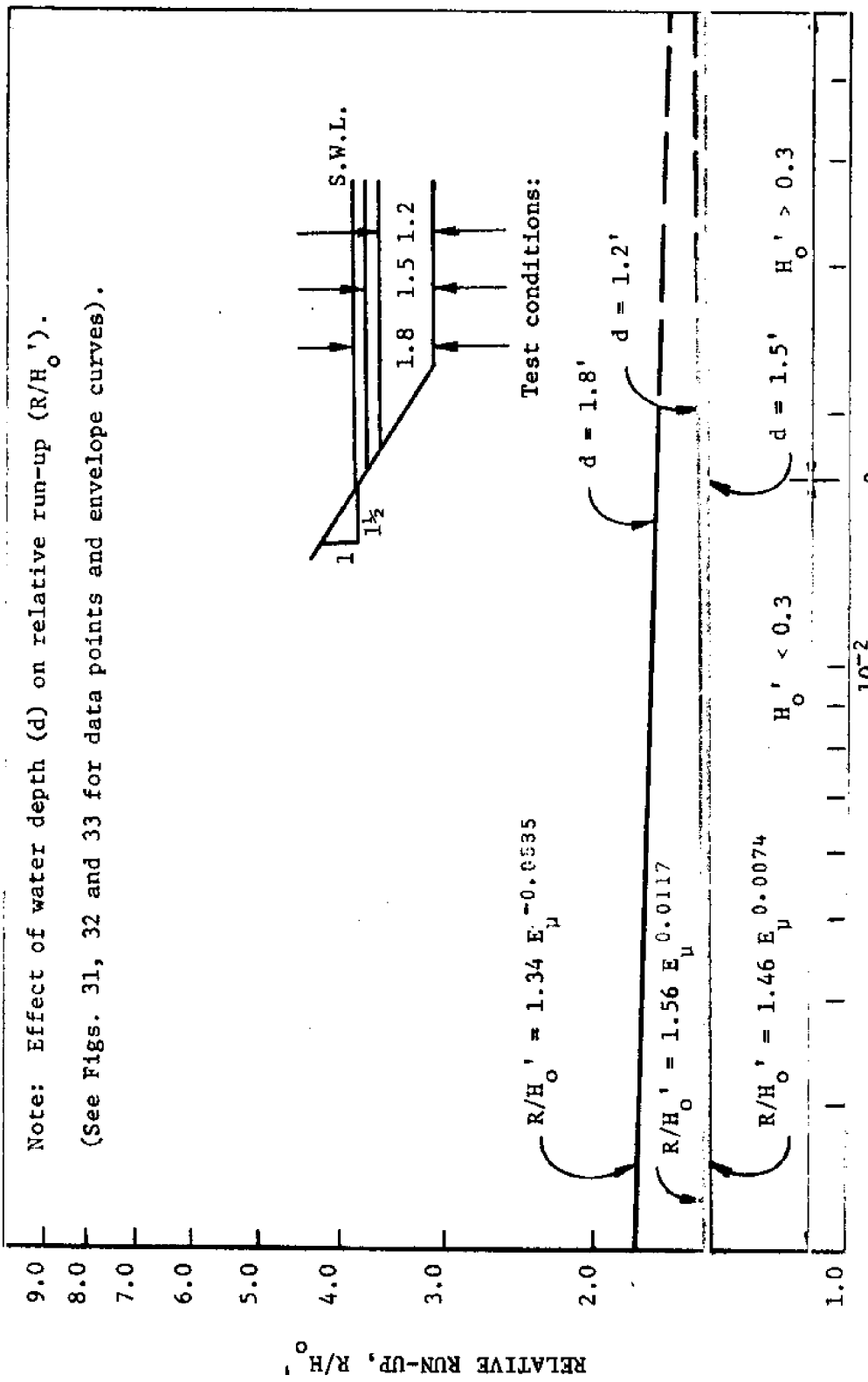

FIG. 37.--RELATIVE RUN-UP ON A ROUGHENED (STACKED) 1 on 1½/2 SLOPE
(d = 1.2, 1.5 and 1.8 ft)

($d < < \lambda$) with small wave heights ($H_o' < < d$).

Effect of significant parameters (d/λ, H_o'/d, and H_o'/T^2) on relative wave run-up (R/H_o'). The effects of three significant parameters (d/λ, H_o'/d and H_o'/T^2) on relative wave run-up (R/H_o') were studied. The relative wave run-up (R/H_o') data was plotted as a dependent variable for its respective relative wave energy density (E_μ/C^2T^3) which was plotted as an independent variable as shown in Figs. 38, 39, and 40 (at this point, it should be noted that by non-dimensionalizing the mean wave energy density (E_μ) with the time (t) variable the wave steepness (H_o'/T^2) values were ordered by magnitude). Arbitrary curves for each relative depth (d/λ) were developed as shown in Figs. 38, 39 and 40. Since these curves were independent of each other, it was concluded that the relative wave run-up (R/H_o') was affected by the relative depth (d/λ) parameter:

$$\frac{R}{H_o'} = f\left(\frac{d}{\lambda}, \ldots\right) \qquad \ldots\ldots\ldots \qquad (45)$$

As the wave steepness (H_o'/T^2) and the relative wave height (H_o'/d) increased for each constant relative depth (d/λ), the relative wave run-up (R/H_o') increased to a maximum value for a particular wave steepness (H_o'/T^2) and relative wave height (H_o'/d) and then decreased. It was therefore concluded that the relative wave run-up (R/H_o') was affected by the wave steepness (H_o'/T^2) and the relative wave height (H_o'/d) parameters:

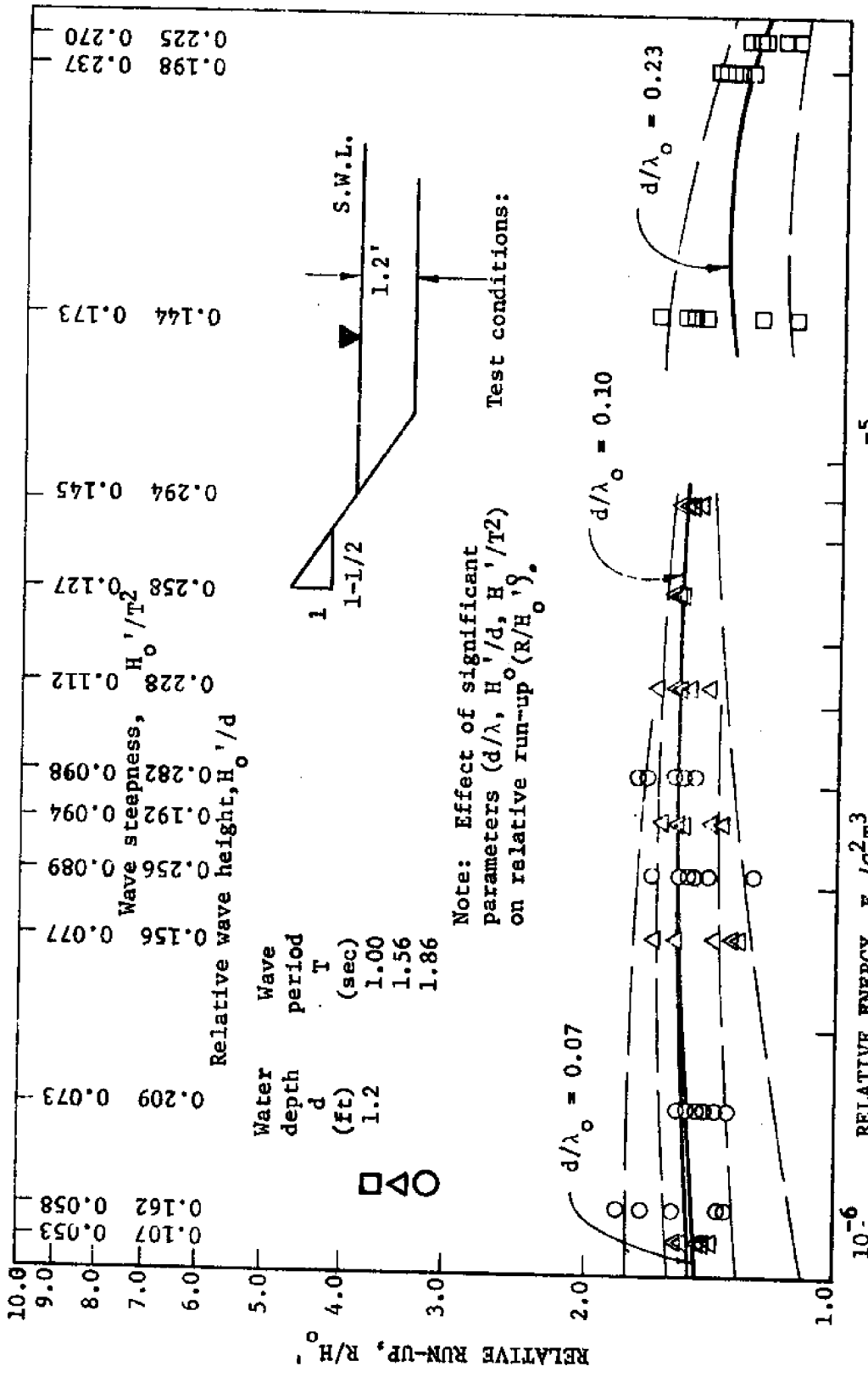

FIG. 38.--RELATIVE RUN-UP ON A ROUGHENED (STRIPS) 1 ON 1-1/2 SLOPE (d = 1.2 ft)

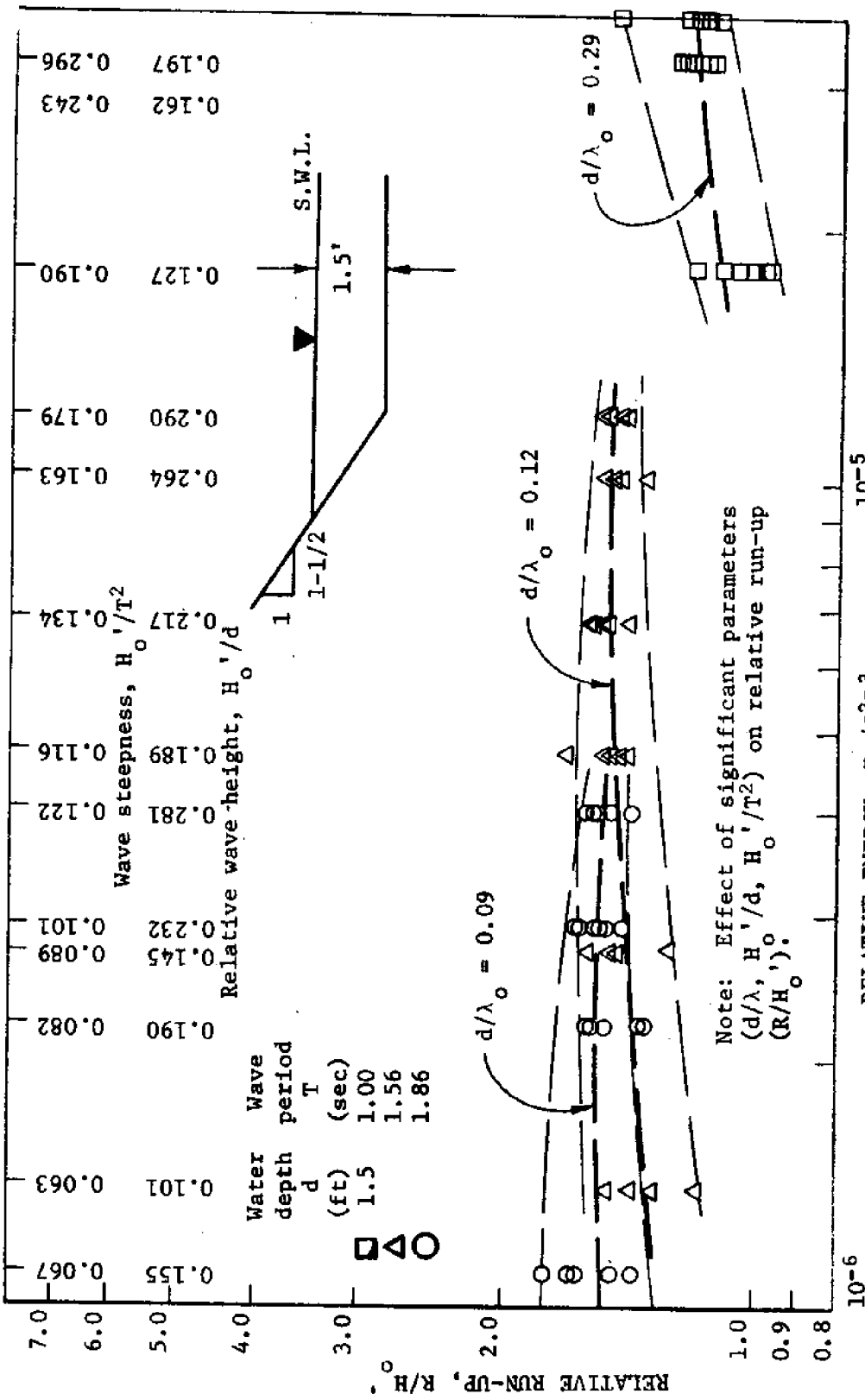

FIG. 39.--RELATIVE RUN-UP ON A ROUGHENED (STRIPS) 1 ON 1-1/2 SLOPE (d = 1.5 ft)

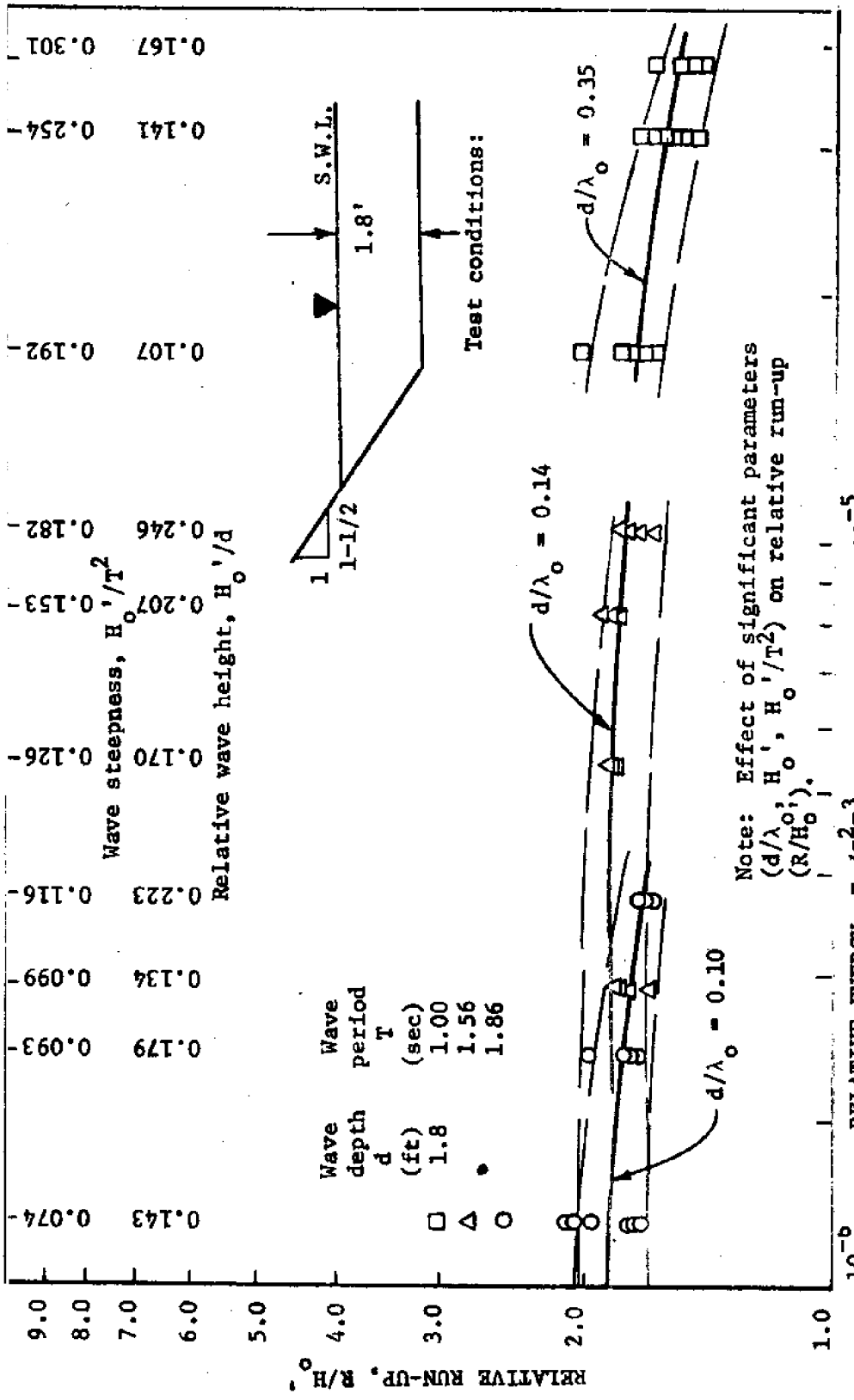

FIG. 40.--RELATIVE RUN-UP ON A ROUGHENED (STRIPS) 1 ON 1-1/2 SLOPE (d = 1.8 ft)

$$R/H_o' = f\left(\frac{H_o'}{T^2},\ H_o'/d \right) . \qquad \ldots\ldots \qquad (46)$$

Physical observations. The following significant observations were made and recorded during testing:

1. The leading edge of the wave run-up (R) was initially irregular but was observed to become regular as the wave advanced up the slope (see Fig. 41).

2. The phenomena of transverse waves was unexpectedly (and unavoidably) observed at various times during testing although the wave lengths tested were not harmonics of the wave flume width.

3. Wave reflection was observed in the flume shortly after the leading wave was reflected.

4. A water 'set-up' was observed in the wave flume during the testing using the wind (irregular) waves.

5. A considerable spray up the slope was observed during the wave run-up (R) tests using the wind (irregular) wave generator, even though the 'venturi' effect was eliminated by providing a comparable flow way above the slope.

The following methods of energy dissipation were observed during testing:

1. Dissipation of energy by the vertical face of the upslope strip.

2. Dissipation of energy by vortices (turbulence) generated by the strips.

3. Dissipation of energy by air entrainment caused by the strips.

4. Dissipation of energy by opposing backwash (from water retained by the strips).

These methods of energy dissipation were significant contributors to the reduction of wave run-up (R) by surface strips.

FIG. 41.--MONOCHROMATIC (REGULAR) WAVE RUN-UP ON A SINGLE (1 ON 1-1/2) ROUGHENED (STRIPS) SLOPE

Wave Energy Dissipation on a Single (1 on 1-1/2) Roughened (Blocks) Slope

Relative wave run-up (R/H_o'). To determine the effects of slope roughness on wave run-up (see objectives 1 and 4) a series of tests were run using a (1 on 1-1/2) slope containing a symmetric pattern of surface blocks. Wave run-up (R) data for both monochromatic (regular) waves and wind (irregular) waves was obtained for the roughened slope configuration shown in Fig. 52 (page 133).

The monochromatic (regular) wave tests were run using wave periods (T) of 1.00 sec, 1.56 sec and 1.86 sec in water depths (d) of 1.2 ft, 1.5 ft and 1.8 ft. Equivalent deepwater wave heights (H_o') were varied from 0.113 ft to 0.443 ft for the water depths tested [see Table 9 (Appendix III)].

The wind (irregular) wave tests were run using surface wind velocities ($V_{0.30}$) of 39.8 ft/sec, 41.3 ft/sec and 54.5 ft/sec obtained for water depths of 1.2 ft, 1.5 ft and 1.8 ft, respectively. The equivalent wave periods (T) obtained from the wave energy spectrum were 0.72 sec, 0.77 sec and 0.83 sec for water depths of 1.2 ft, 1.5 ft and 1.8 ft, respectively, while the equivalent deepwater wave heights (H_e') obtained from the wave energy spectrum were respectively 0.287 ft, 0.296 ft and 0.344 ft [see Table 10 (Appendix III)].

The mean wave energy density (E_μ) was obtained from the wave energy spectrum for both the monochromatic (regular) waves and for

the wind (irregular) waves. For the monochromatic (regular) waves the mean wave energy density (E_μ) varied from 0.0006 ft^2/sec^{-1} to 0.0165 ft^2/sec^{-1} while for the wind (irregular) waves the mean wave energy density (E_μ) varied from 0.0124 ft^2/sec^{-1} to 0.0200 ft^2/sec^{-1} [see Tables 9 and 10 (Appendix III)].

Relative wave run-up (R/H_o' and R/H_e') was calculated from the wave run-up (R) tests for both the monochromatic (regular) waves and the wind (irregular) waves [see Tables 15, 16, 17 and 18 (Appendix VI)]. Each relative run-up value (R/H_o' and R/H_e') was plotted as a dependent variable for its respective incident mean wave energy density (E_μ) which was plotted as an independent variable.

Relative wave run-up (R/H_o' and R/H_e') values for water depths (d) of 1.2 ft, 1.5 ft, and 1.8 ft are shown, respectively, in Figs. 42, 43 and 44. From the relative monochromatic wave run-up (R/H_o') data for each water depth (d) an empirical equation expressing the relative run-up (R/H_o') in terms of the oncoming wave energy density (E_μ) was obtained from a multiple least squares regression analysis of the data [see Table 21 (Appendix VI) for statistics]. The empirical equations:

$$d = 1.2 \text{ ft} \qquad R/H_o' = 1.46\, E_\mu^{0.01749} \quad . \ . \ . \qquad (47)$$

$$d = 1.5 \text{ ft} \qquad R/H_o' = 1.54\, E_\mu^{0.0135} \quad . \ . \ . \qquad (48)$$

$$d = 1.8 \text{ ft} \qquad R/H_o' = 1.35\, E_\mu^{-0.0446} \quad . \ . \ . \qquad (49)$$

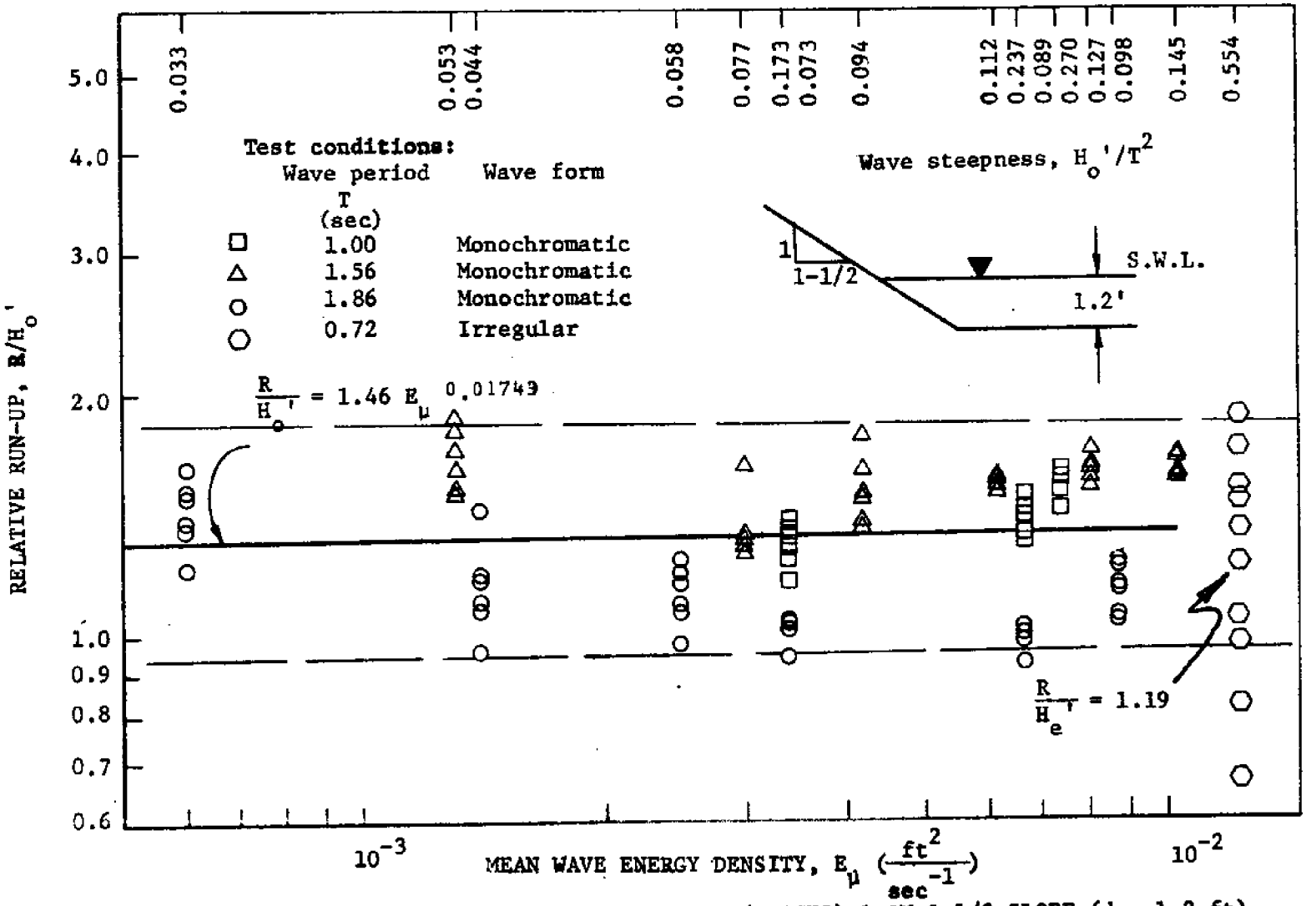

FIG. 42.--RELATIVE RUN-UP ON A ROUGHENED (BLOCKS) 1 ON 1-1/2 SLOPE (d = 1.2 ft)

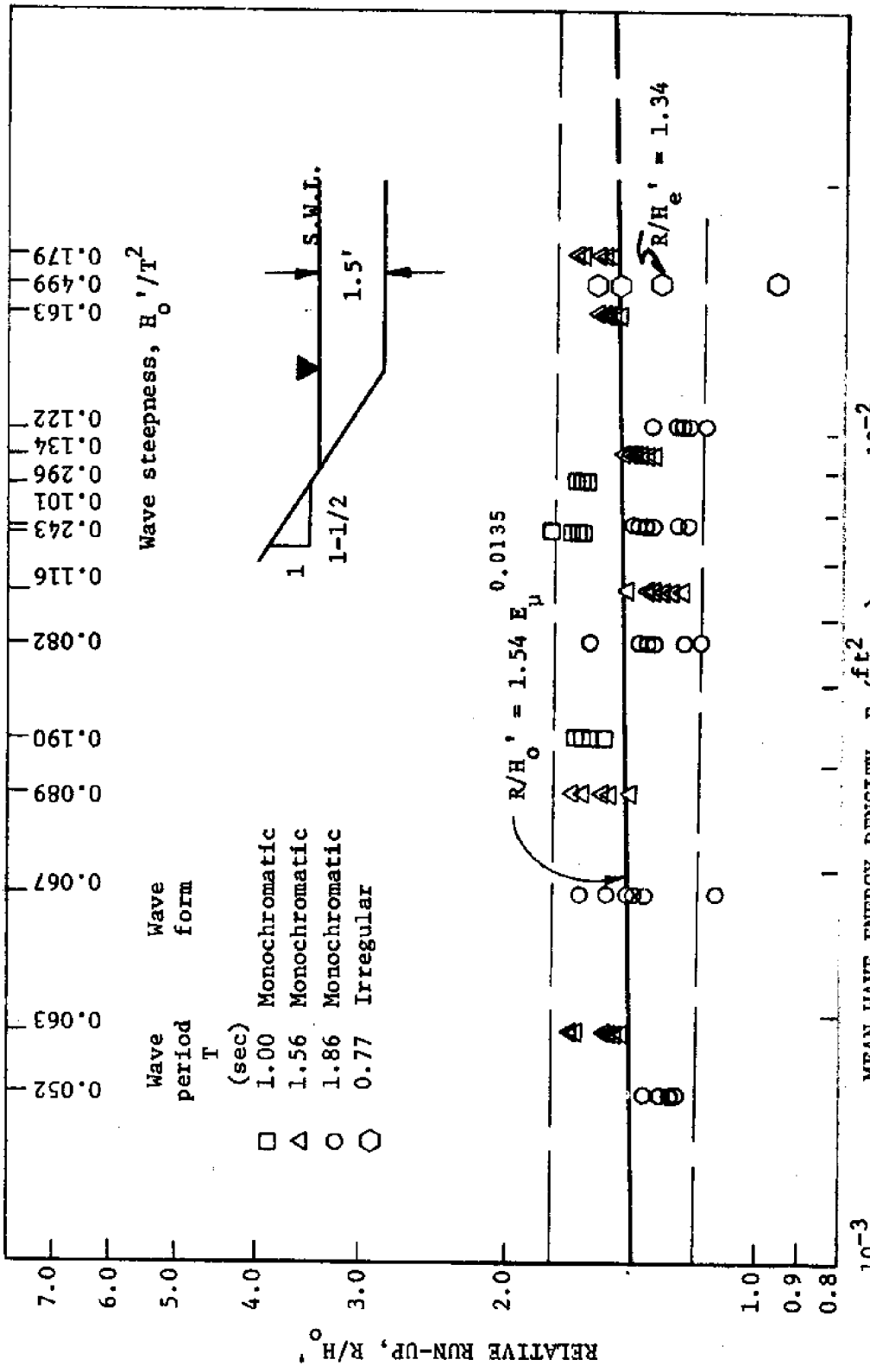

FIG. 43.- RELATIVE RUN-UP ON ROUGHENED (BLOCKS) 1 ON 1-1/2 SLOPE (d = 1.5 ft)

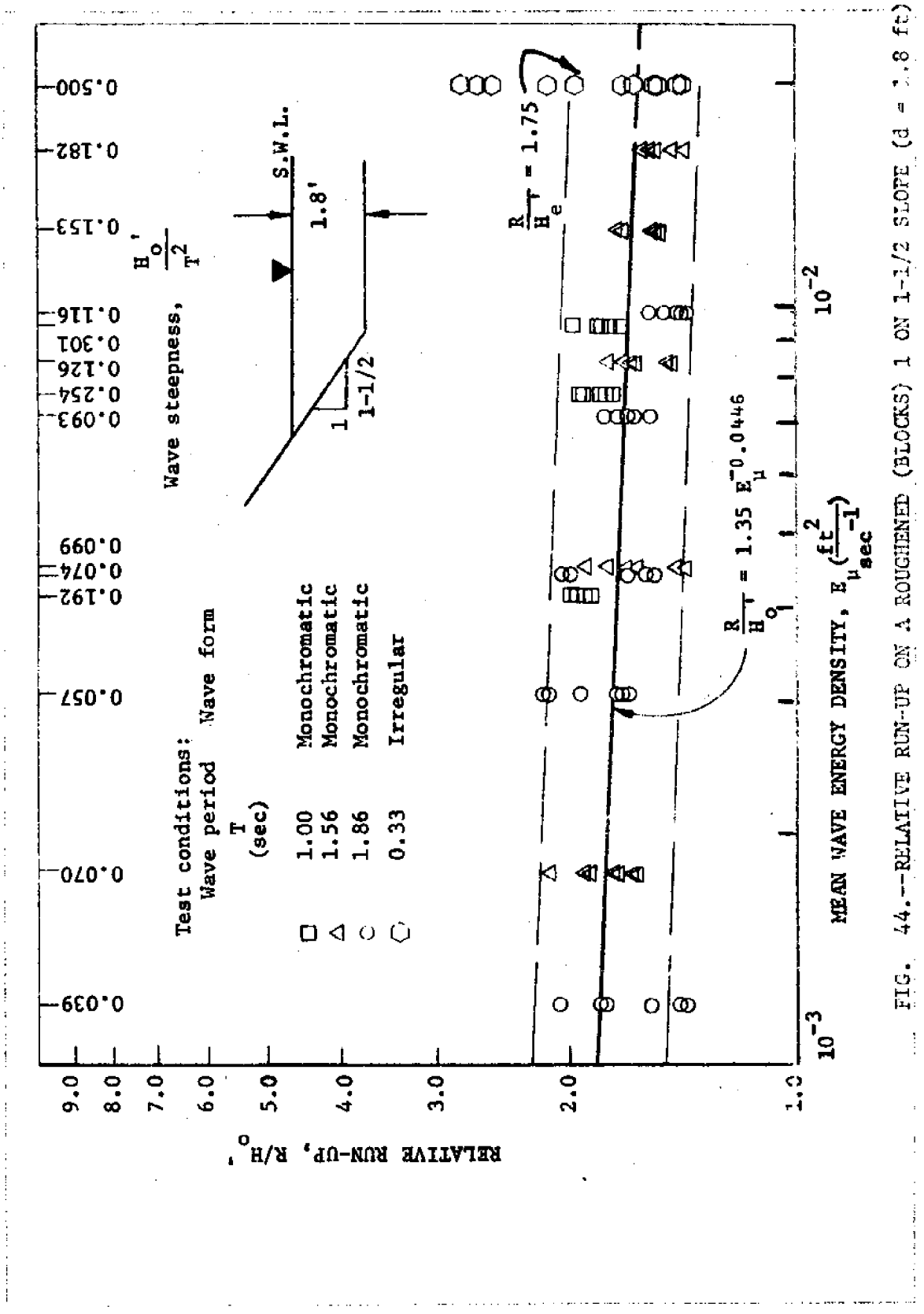

FIG. 44.--RELATIVE RUN-UP ON A ROUGHENED (BLOCKS) 1 ON 1-1/2 SLOPE (d = 1.8 ft)

were obtained, respectively, from 451, 445 and 374 monochromatic wave run-up (R/H_o') values. Due to the nature of the monochromatic wave run-up (R) phenomena there was a distribution (scatter) of the monochromatic wave run-up (R) values for each mean wave energy density (E_μ). Envelope curves (lines) were arbitrarily drawn to enclose the relative monochromatic wave run-up (R/H_o') data. The envelope curves delineated the deviation of the data from the best fit line obtained from the regression analysis. For the 1.2 ft water depth the relative monochromatic wave run-up (R/H_o') values deviated as much as 46 per cent above and 25 per cent below the best fit line for the data. For the 1.5 ft and 1.8 ft water depths the relative monochromatic wave run-up (R/H_o') values deviated 20 per cent above and 20 per cent below and 22 per cent above and 18 per cent below, respectively. Due to the scatter of the data the correlation coefficients were very low (< 0.1) for all depths. Analysis of variance was computed for each water depth. Results of the F test are shown in Table 22 (Appendix VI). From the relative wind wave run-up (R/H_e') data for each water depth (d) an average relative wave run-up (R/H_e') value was computed for the oncoming mean wave energy density (E_μ). The average relative wave run-up (R/H_e') values:

$$d = 1.2 \text{ ft}$$
$$E = 0.0124 \frac{ft^2}{sec^{-1}} \qquad R/H_e' = 1.19 \qquad \ldots\ldots \qquad (50)$$

$d = 1.5$ ft
$E = 0.0152 \frac{ft^2}{sec^{-1}}$ $\quad R/H_e' = 1.34 \quad . \; . \; . \; . \; . \; .$ (51)

$d = 1.8$ ft
$E = 0.0200 \frac{ft^2}{sec^{-1}}$ $\quad R/H_e' = 1.75 \quad . \; . \; . \; . \; . \; .$ (52)

were obtained, respectively, from 50, 35 and 45 wave run-up (R) readings [see Tables 17 and 18 (Appendix VI)].

Comparing the relative run-up values (R/H_o' and R/H_e'):

$R/H_o' = 1.35 \quad . \; . \; . \; . \; . \; .$ (53)
$d = 1.2$ ft
$E_\mu = 0.0124 \frac{ft^2}{sec^{-1}}$
$R/H_e' = 1.19 \quad . \; . \; . \; . \; . \; .$ (50)

$R/H_o' = 1.46 \quad . \; . \; . \; . \; . \; .$ (54)
$d = 1.5$ ft
$E_\mu = 0.0152 \frac{ft^2}{sec^{-1}}$
$R/H_e' = 1.34 \quad . \; . \; . \; . \; . \; .$ (51)

$R/H_o' = 1.62 \quad . \; . \; . \; . \; . \; .$ (55)
$d = 1.8$ ft
$E_\mu = 0.0200 \frac{ft^2}{sec^{-1}}$
$R/H_e' = 1.75 \quad . \; . \; . \; . \; . \; .$ (52)

indicates no significant difference in relative wave run-up (R/H_o' and R/H_e') values.

Wave reflection. To determine the effects of slope roughness

on reflecting capability (power) a series of wave reflection (H_r/H_i) tests were run using a (1 on 1-1/2) slope containing a symmetric pattern of surface blocks. Wave reflection (H_r/H_i) data for monochromatic (regular) waves was obtained for the roughened slope configuration shown in Fig. 52 (page 133).

The wave reflection tests were run using wave periods of 1.00 sec, 1.56 sec and 1.85 sec in water depths of 1.2 ft, 1.5 ft and 1.8 ft. Equivalent deepwater wave heights (H_o') were varied from 0.113 ft to 0.443 ft while the mean wave energy densities (E_μ) varied from 0.0006 ft^2/sec^{-1} to 0.0165 ft^2/sec^{-1}, respectively, for the water depths tested [see Table 9 (Appendix III)].

The reflecting capability (power) of the roughened (1 on 1-1/2) slope was evaluated from wave records obtained by moving the instrument carriage containing the wave height sensor through a train of waves to obtain the incident and reflected wave heights. A reflecting coefficient (ratio of the reflected wave height to the incident wave height) was calculated for each test run [see Table 14 (Appendix V)]. Each reflecting coefficient (*i.e.*, coefficient of reflection) value ($C_r = H_r/H_i$) was plotted as a dependent variable for its respective incident mean wave energy density (E_μ) which was plotted as an independent variable as shown in Fig. 45. Fig. 45 therefore represents the reflecting capability (power) of the slope containing a symmetric pattern of surface blocks.

As the mean wave energy density (E_μ) increased from 0.001

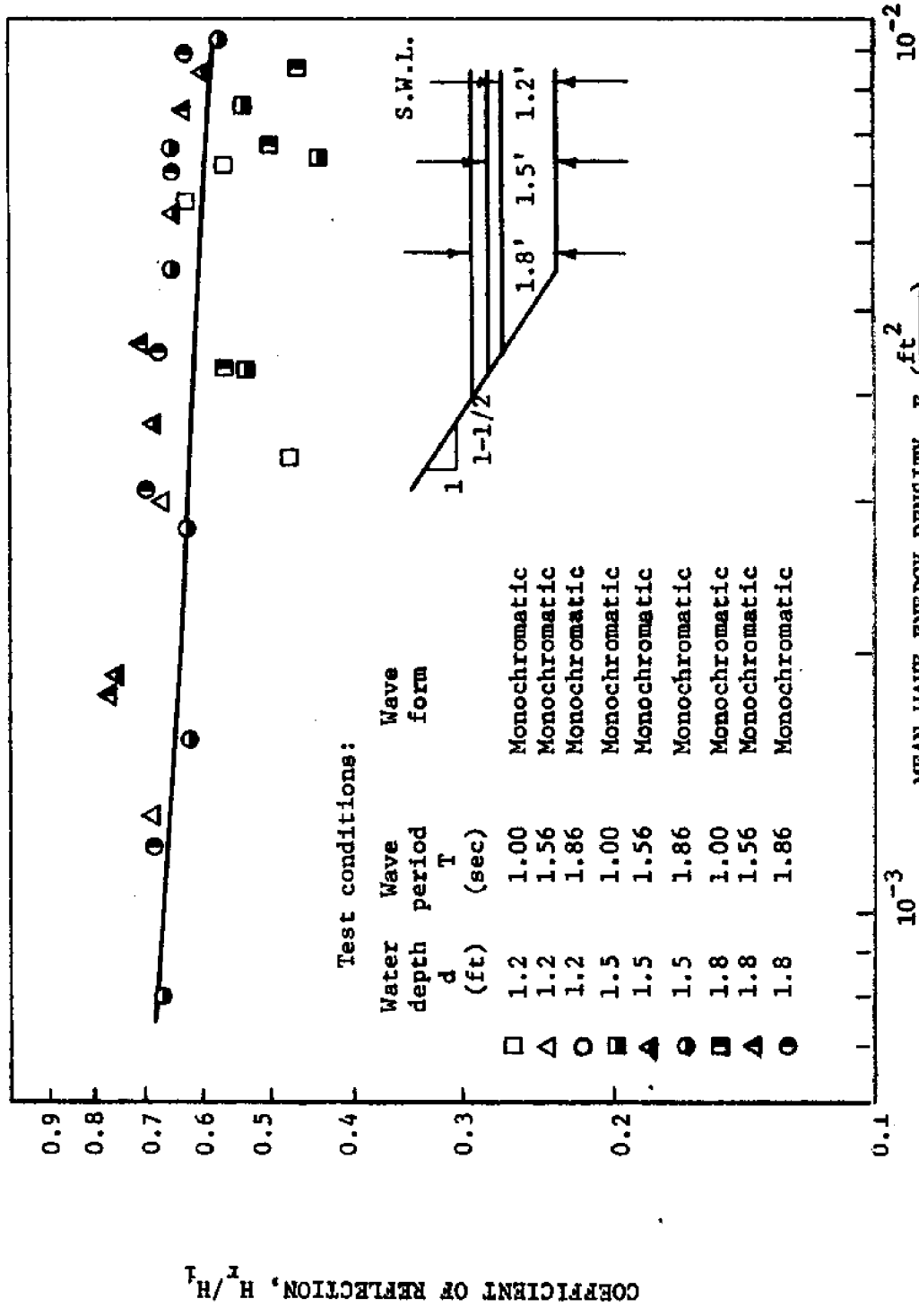

FIG. 45.--COEFFICIENT OF REFLECTION FOR A ROUGHENED (BLOCKS)
1 ON 1-1/2 SLOPE (d = 1.2, 1.5 and 1.8 ft)

ft^2/sec^{-1} to 0.01 ft^2/sec^{-1} the reflecting capability (power) was decreased approximately 10 per cent.

Energy dissipation by turbulence and bottom friction. The level of turbulence (intensity of turbulence) was increased with the introduction of surface blocks. Each block functioned as a vortex generator.

The effect of turbulence and bottom friction on the wave run-up (R) could not be measured due to the fluctuating nature of the uprush velocity. Since the effect of turbulence on the wave run-up (R) was coupled with the effect of drag on the wave run-up (R) the combined effect was studied. In all cases the combined effects of drag and increased turbulence reduced the wave run-up (R).

Uprush and dnrush velocity (V_u and V_d). To determine the effects of slope roughness on the maximum velocities in the uprush zone [see objective 2] a series of tests were run using a (1 on 1-1/2) slope containing a symmetric pattern of surface blocks. Wave uprush and dnrush velocity (V_u and V_d) data for monochromatic (regular) waves was obtained for the roughened slope configuration shown in Fig. 52 (page 133).

The uprush and dnrush velocity tests were run using wave periods (T) of 1.00 sec, 1.56 sec and 1.86 sec in water depths (d) of 1.2 ft, 1.5 ft and 1.8 ft. Equivalent deepwater wave heights (H_o') were varied from 0.113 ft to 0.443 ft while the mean wave energy densities (E_μ) varied from 0.0006 ft^2/sec^{-1} to 0.0165 ft^2/sec^{-1}, respectively,

for the water depths tested [see Table 9 (Appendix III)].

Velocities in the uprush zone were evaluated from profiles obtained using the turbulent velocity sensor (hot-film sensor). In the first series of tests to measure the uprush and dnrush velocities the sensor was maintained at a height of 0.035 ft above a slope gauge reading of 0.05 ft, thus the velocity component parallel to the slope (just above the S.W.L.) was measured. In the second series of tests the sensor height was varied from 0.035 ft to 0.255 ft, thus the velocity component parallel to the slope at various heights was obtained. The maximum uprush and dnrush velocities (V_u and V_d) were evaluated from profiles for the first test runs [see Table 23 and Figs. 169 through 183 (Appendix VII)].

A relative uprush velocity (V_u/C) value and a relative dnrush velocity (V_d/C) value was obtained for each test run and plotted as a dependent variable for its respective incident mean wave energy density (E_μ) which was plotted as an independent variable as shown in Figs. 46 and 47.

As the mean wave energy density (E_μ) increased from 0.001 ft^2/sec^{-1} to 0.01 ft^2/sec^{-1} the relative uprush velocity (V_u/C) increased from 0.56 to 0.63 as shown in Fig. 46. Due to the scatter of the relative dnrush velocity (V_d/C) it was not evaluated [see Fig. 47].

The uprush and dnrush velocity distribution profiles for the 1.2 ft water depth are shown in Figs. 169 through 183 (Appendix VII).

Effect of water depth (d) on relative wave run-up (R/H_o'). The

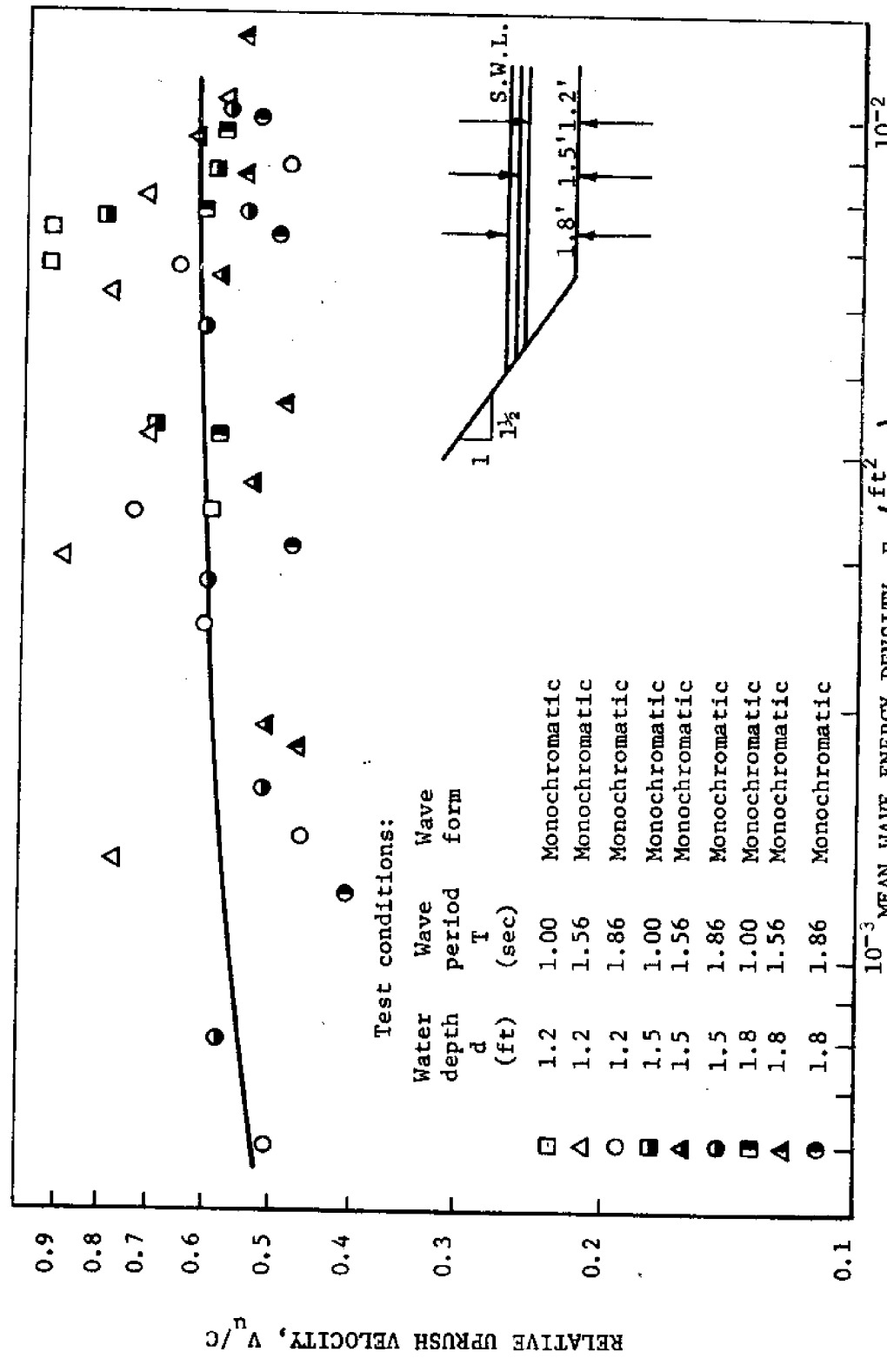

FIG. 46.--RELATIVE UPRUSH VELOCITY FOR A ROUGHENED (BLOCKS) 1 ON 1-1/2 SLOPE (d = 1.2,1.5 and 1.8 ft)

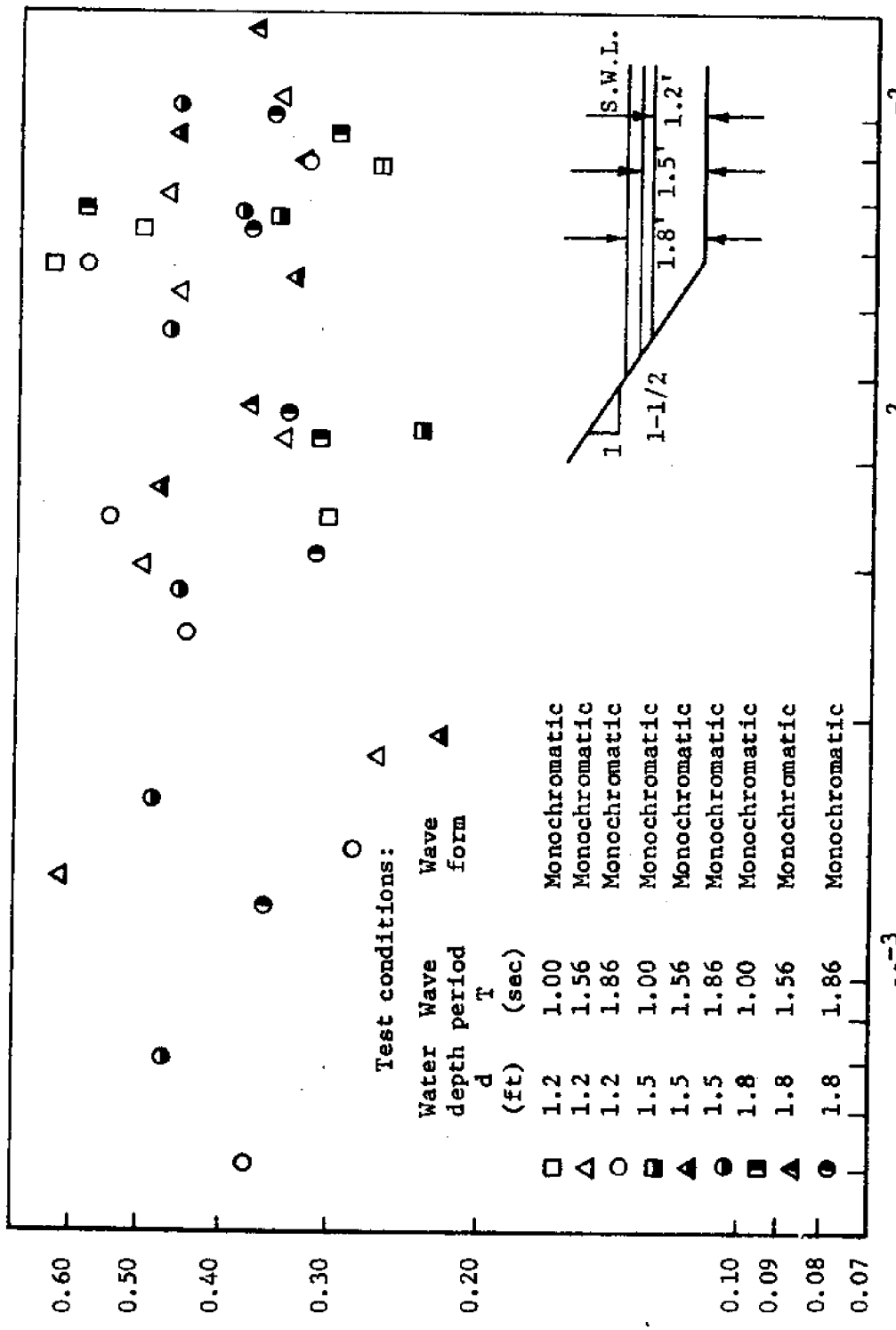

FIG. 47.--RELATIVE DNRUSH VELOCITY FOR A ROUGHENED (BLOCKS) 1 ON 1-1/2 SLOPE (d = 1.2, 1.5 and 1.8 ft)

effect of water depth (d) on relative wave run-up (R/H_o') on a roughened (1 on 1-1/2) slope was studied by comparing relative wave run-up (R/H_o') data from the three water depths (d) tested (see Fig. 48). The comparison was made between the best fit curves (lines) obtained from least squares regression analysis of the data.

Some effect of water depth (d) on relative wave run-up (R/H_o') was noted in the lower range of mean wave energy densities (E_μ) but here again the effect of water depth (d) was not considered significant due to the low correlation coefficients (< 0.1) obtained for the best fit curves (lines). A study of Fig. 48 suggests a strong possibility that water depth (d) may have a pronounced effect on relative wave run-up (R/H_o') in low wave energy densities (E_μ) representing long waves ($d << \lambda$) with small wave heights ($H_o' << d$).

Effect of significant parameters (d/λ, H_o'/d and H_o'/T^2) on relative run-up (R/H_o'). The effects of three significant parameters (d/λ, H_o'/d and H_o'/T^2) on relative wave run-up (R/H_o') were studied. The relative wave run-up (R/H_o') data was plotted as a dependent variable for its respective relative wave energy density (E_μ/C^2T^3) which was plotted as an independent variable as shown in Figs. 49, 50, and 51. (At this point, it should be noted that by nondimensionalizing the mean wave energy density (E_μ) with the time (t) variable the wave steepness (H_o'/T^2) values were ordered by magnitude.) Arbitrary curves for each relative depth (d/λ) were developed as shown in Figs. 49, 50 and 51. Since these curves were

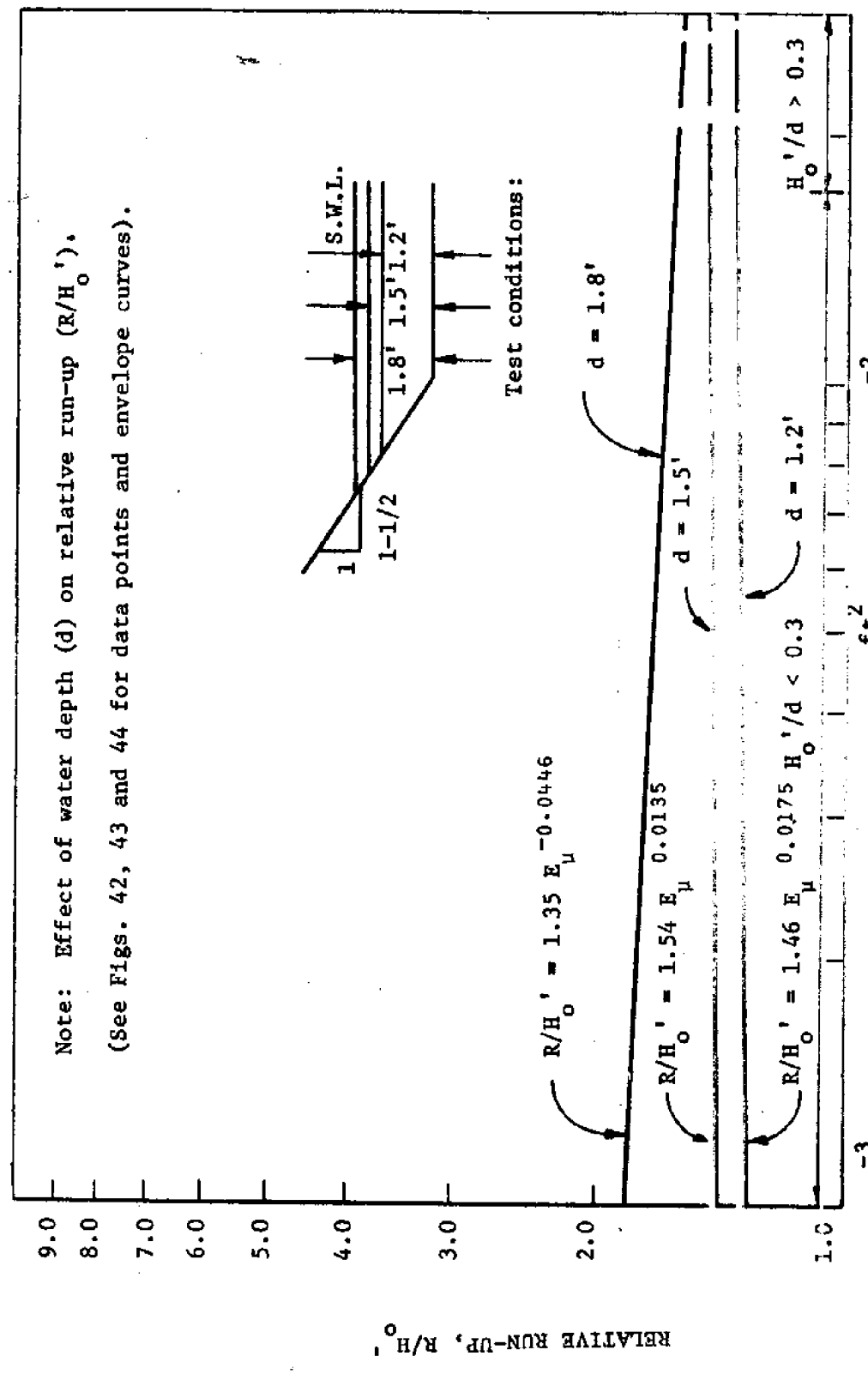

FIG. 48.--RELATIVE RUN-UP ON A ROUGHENED (BLOCKS) 1 ON 1-1/2 SLOPE
(d = 1.2, 1.5 and 1.8 ft)

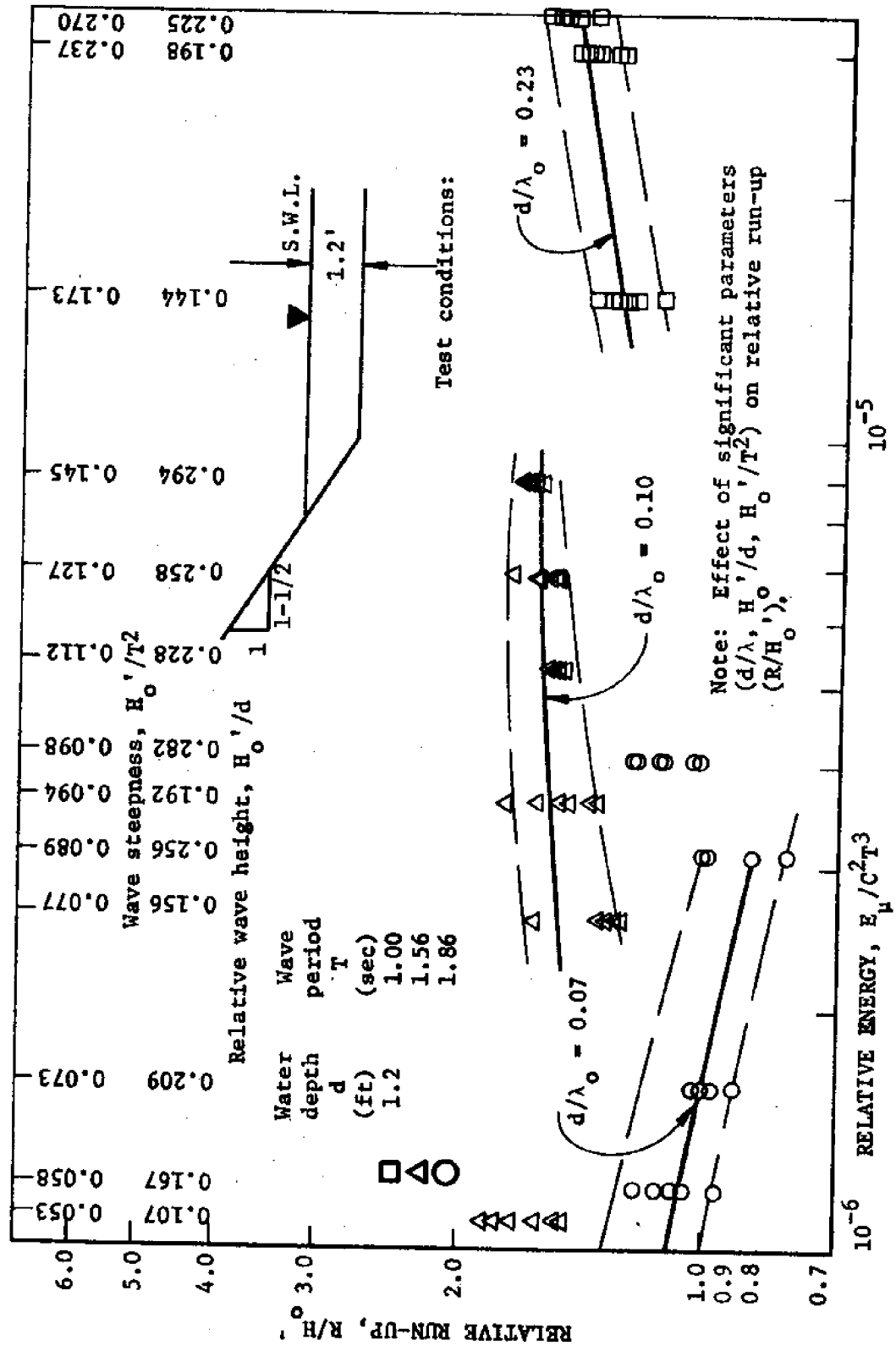

FIG. 49.--RELATIVE RUN-UP ON A ROUGHENED (BLOCKS) 1 ON 1-1/2 SLOPE (d = 1.2 ft)

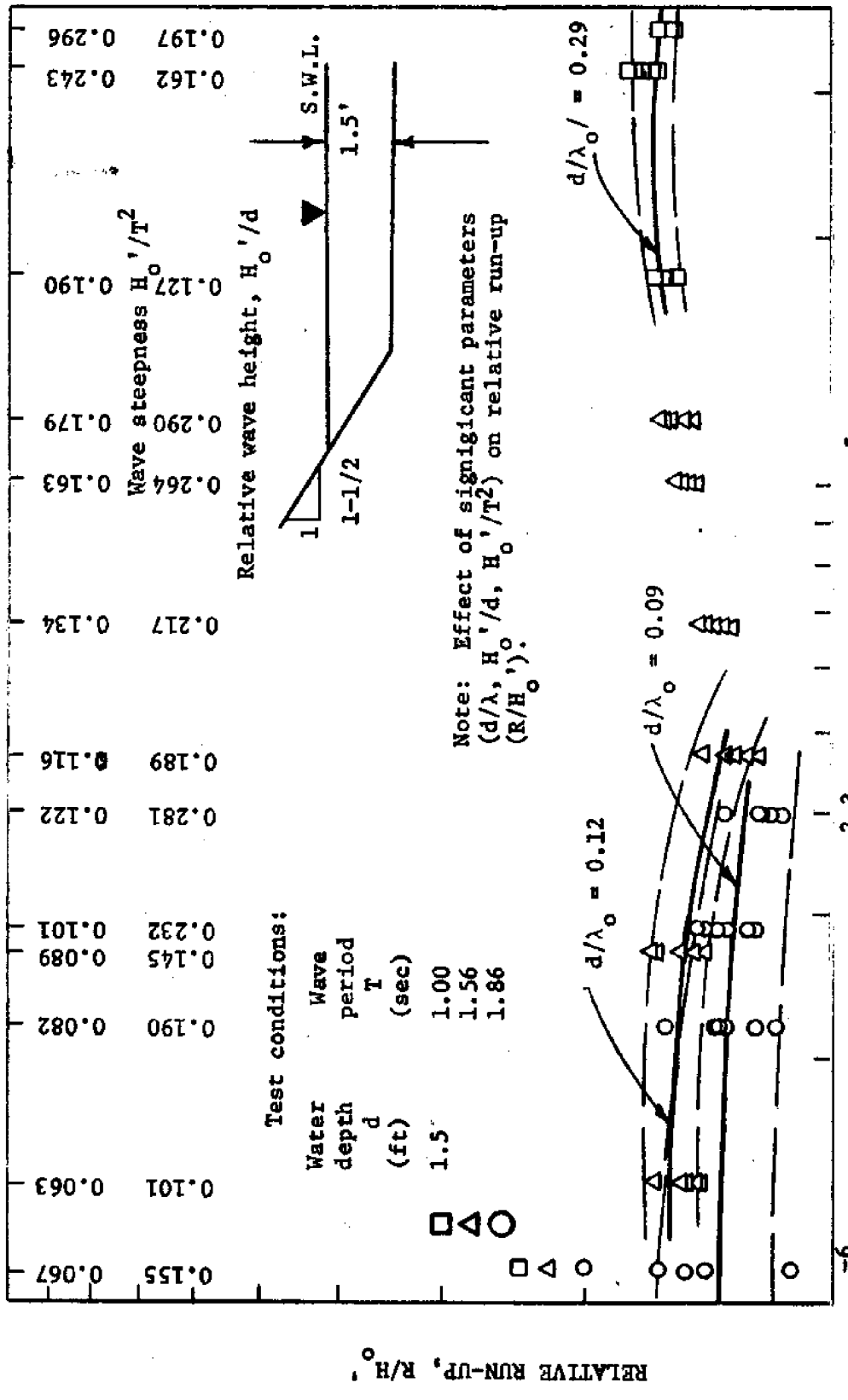

FIG. 50. RELATIVE RUN-UP ON A ROUGHENED (BLOCKS) 1 ON 1-1/2 SLOPE (d = 1.5 ft)

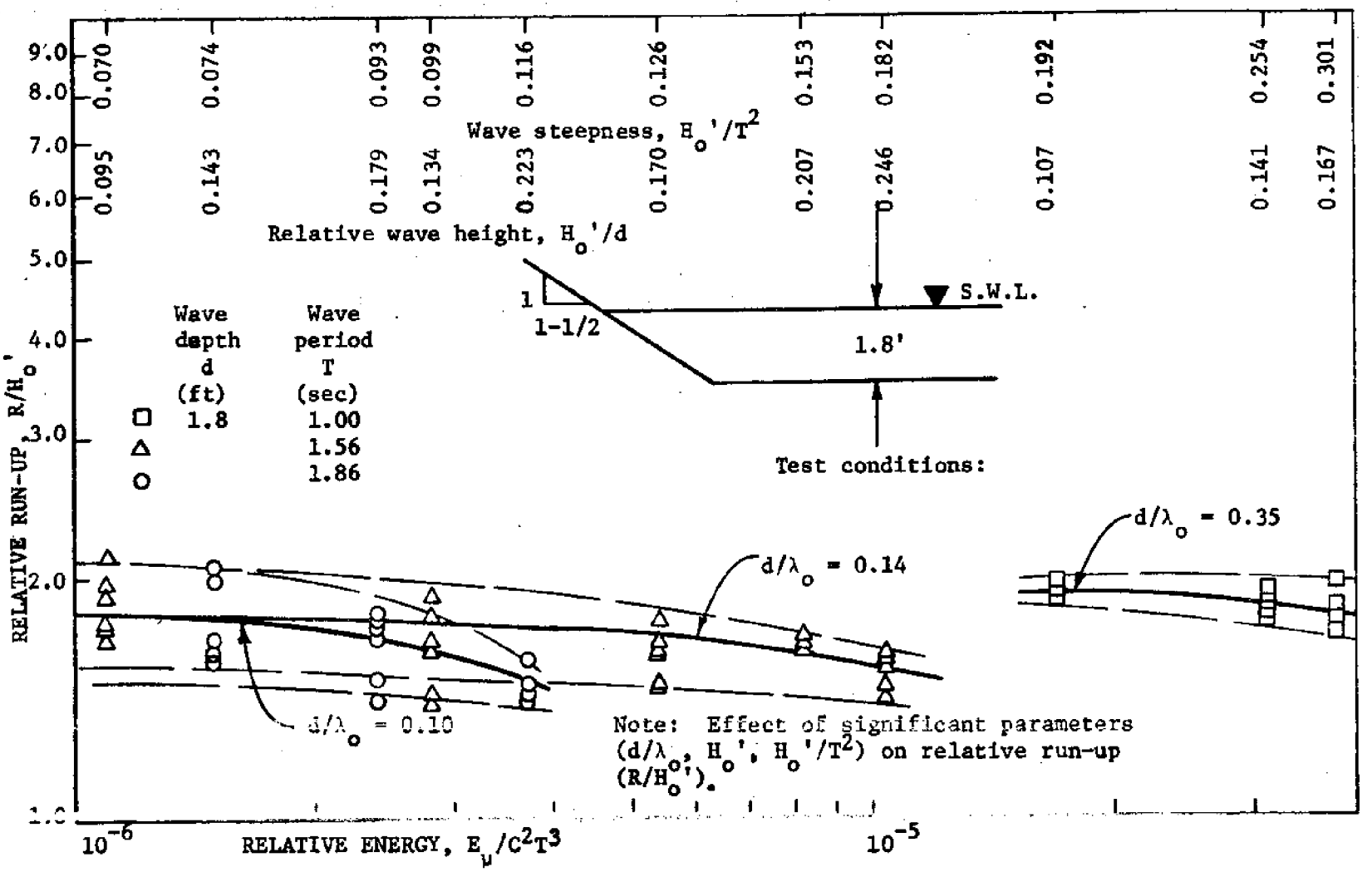

FIG. 31. RELATIVE RUN-UP ON A ROUGHENED (SMOOTH) 1 ON 1-1/2 SLOPE (d = 1.8 ft)

independent of each other, it was concluded that the relative wave run-up (R/H_o') was affected by the relative depth (d/λ) parameters.

$$\frac{R}{H_o'} = f\left(\frac{d}{\lambda}, \ldots\right) \quad \ldots\ldots\ldots \quad (56)$$

As the wave steepness (H_o'/T^2) and the relative wave height (H_o'/d) increased for each constant relative depth (d/λ), the relative wave run-up (R/H_o') increased to a maximum value for a particular wave steepness (H_o'/T^2) and relative wave height (H_o'/d) and then decreased. It was therefore concluded that the relative wave run-up (R/H_o') was affected by the wave steepness (H_o'/T^2) and the relative wave height (H_o'/d) parameters:

$$\frac{R}{H_o'} = f\left(\frac{H_o'}{T^2}, H_o'/d \ \ldots\right) \ldots\ldots \quad (57)$$

Physical observations. The following significant observations were made and recorded during testing:

1. The leading edge of the wave run-up (R) was observed to be irregular (see Fig. 52).

2. The phenomena of transverse waves was unexpectedly (and unavoidably) observed at various times during testing although the wave lengths tested were not harmonics of the wave flume width.

3. Wave reflection was observed in the flume shortly after the leading wave was reflected.

4. A water 'set-up' was observed in the wave flume during the testing using the wind (irregular) waves.

5. A considerable spray up the slope was observed during the wave run-up (R) tests using the wind (irregular) wave generator even though the

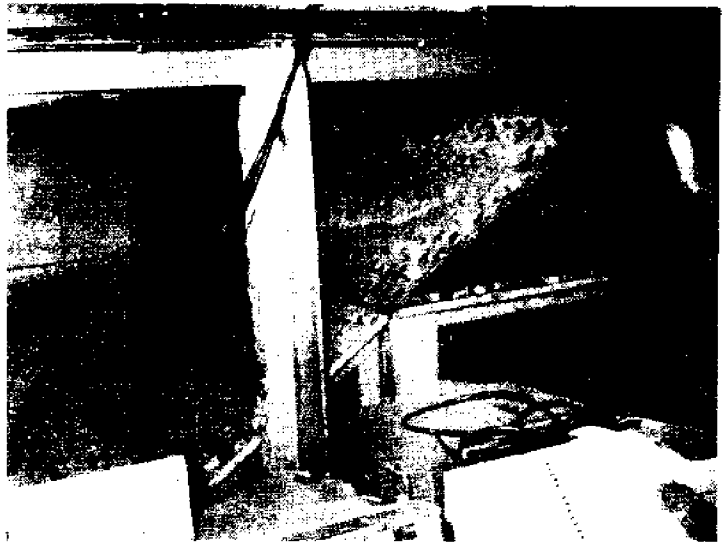

FIG. 52.--MONOCHROMATIC (REGULAR) WAVE RUN-UP ON A SINGLE (1 ON 1-1/2) ROUGHENED (BLOCKS) SLOPE

'venturi' effect was eliminated by providing a comparable flow way above the slope.

The following methods of energy dissipation were observed during testing:

1. Dissipation of energy by jets channeled between the blocks which hit the vertical face of the upslope block.
2. Dissipation of energy by vortices (turbulence) generated by the blocks.
3. Dissipation of energy by air entrainment (heterogeneous mixing of air and water) caused by the blocks.
4. Dissipation of energy by opposing backwash (water running down the slope between the blocks).

These methods of energy dissipation were significant contributors to the reduction of wave run-up (R) by surface blocks.

Comparison of Relative Wave Run-up (R/H_o') on Artificially Roughened (1 on 1-1/2) Slopes with Relative Wave Run-up (R/H_o') on a Smooth (1 on 1-1/2) Slope

The effects of slope roughness (r) on relative wave run-up (R/H_o') were studied by comparing relative wave run-up (R/H_o') data from the three slope conditions for a constant water depth (see Figs. 53, 54 and 55). For the monochromatic (regular) waves the comparison was made between the best fit curves (lines) obtained from the least squares regression analysis of the data while for the wind (irregular) waves the comparison was made between the average relative wave run-up (R/H_e') values.

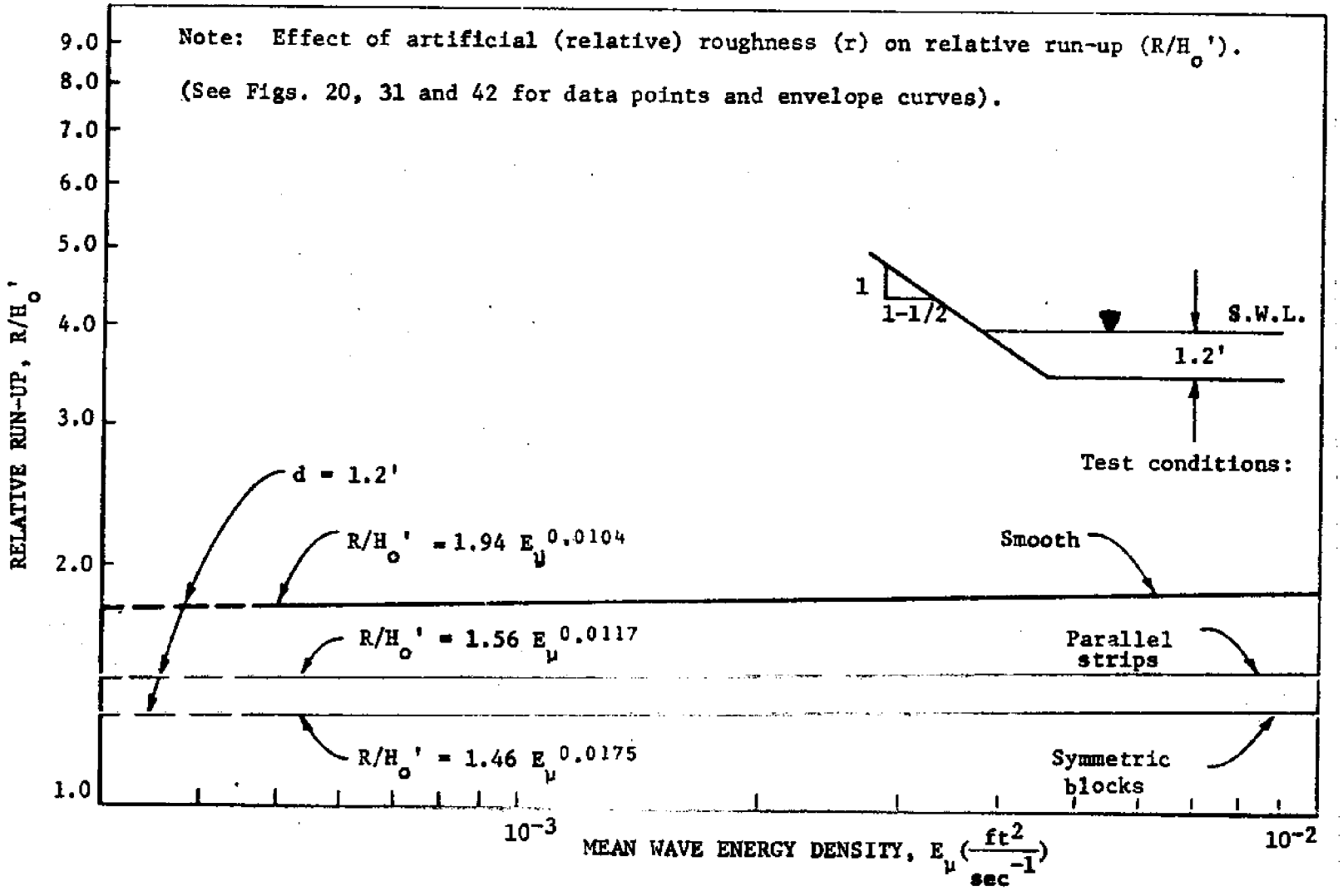

FIG. 53.--RELATIVE RUN-UP ON A SMOOTH AND ROUGHENED (BLOCKS AND STRIPS) 1 ON 1-1/2 SLOPE (d = 1.2 ft)

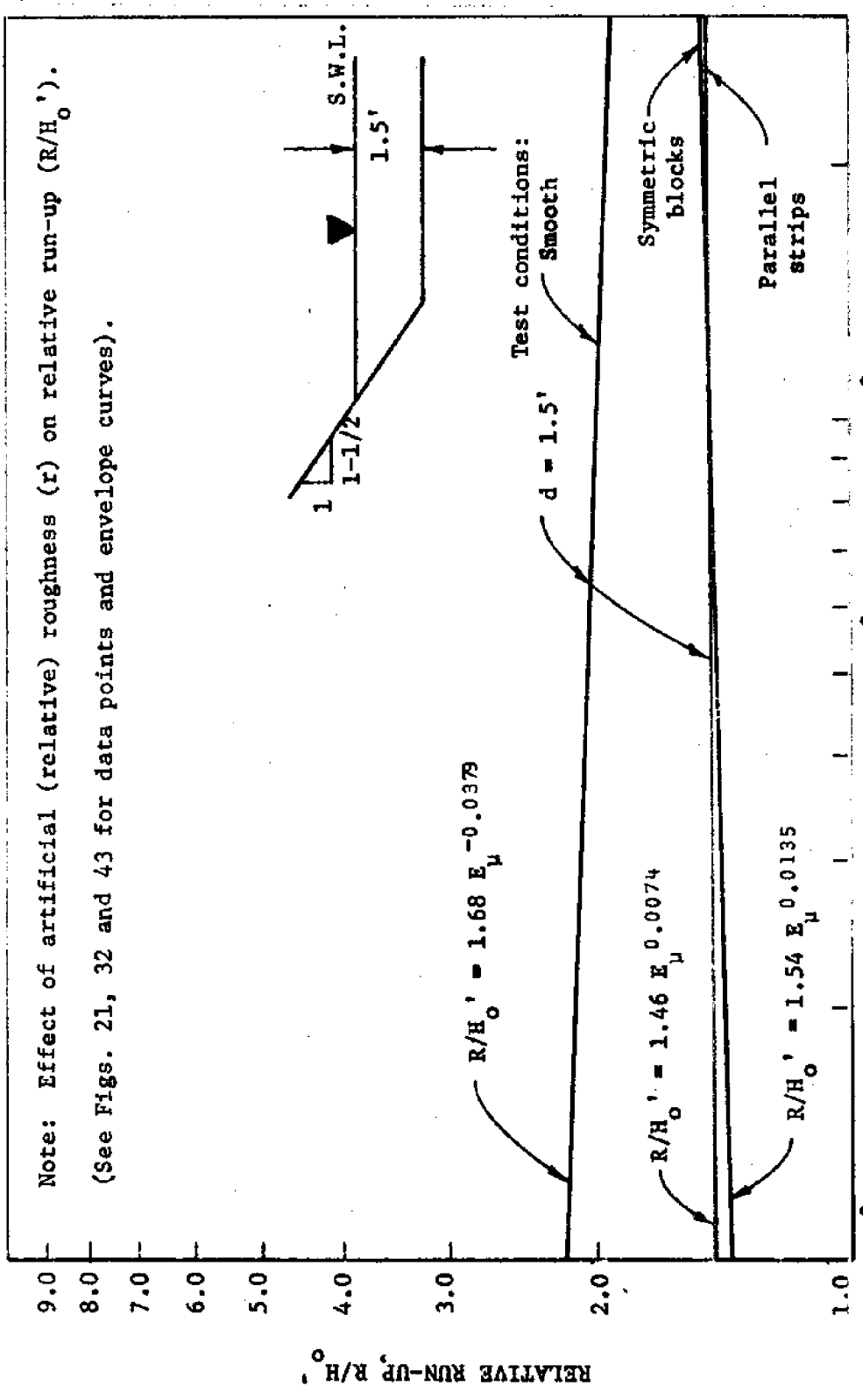

FIG. 54.--RELATIVE RUN-UP ON A SMOOTH AND ROUGHENED (BLOCKS AND STRIPS) 1 ON 1-1/2 SLOPE (d = 1.5 ft)

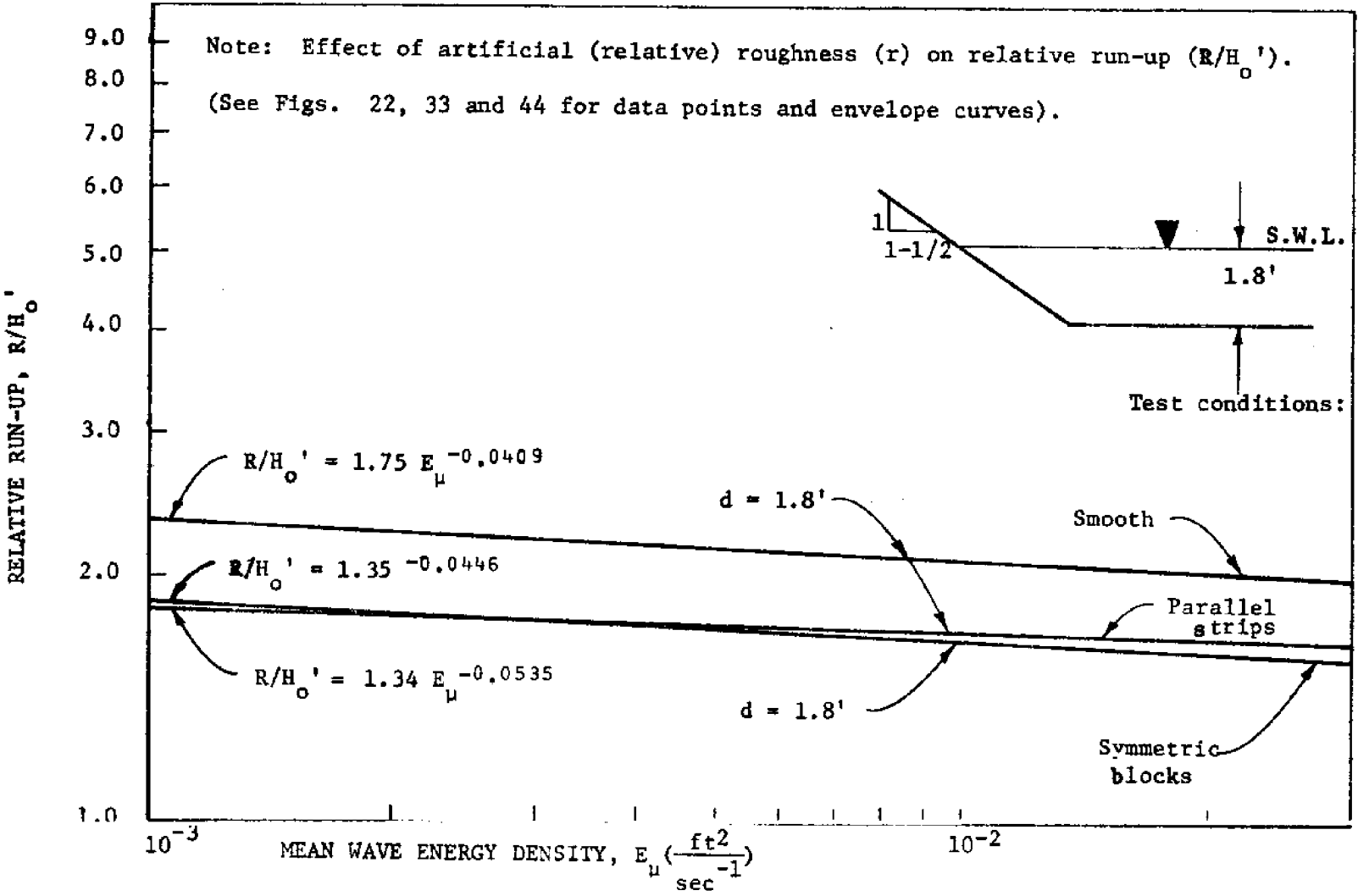

FIG. 55.--RELATIVE RUN-UP ON A SMOOTH AND ROUGHENED (BLOCKS AND STRIPS)
1 ON 1-1/2 SLOPE (d = 1.8 ft)

For each water depth (d) the comparison was made using the relative wave run-up (R/H_o') data for the smooth (1 on 1-1/2) slope (see Figs. 20, 21, and 22), the roughened (1 on 1-1/2) slope containing the parallel strips (see Figs. 31, 32 and 33) and the roughened (1 on 1-1/2) slope containing the symmetric pattern of blocks (see Figs 42, 43 and 44).

For the 1.2 ft water depth the parallel strips reduced the relative monochromatic wave run-up (R/H_o') approximately 20 per cent while the symmetric pattern of blocks reduced the relative monochromatic wave run-up (R/H_o') approximately 27 per cent. The reduction was, respectively, 42 per cent and 46 per cent for the wind (irregular) waves. The symmetric pattern of blocks provided the greatest reduction in relative wave run-up (R/H_o' and R/H_e') on the slope.

For the 1.5 ft water depth the reduction in relative monochromatic wave run-up (R/H_o') was approximately 29 per cent for both the parallel strips and the symmetric pattern of blocks whereas for the wind (irregular) waves the reduction in relative wave run-up (R/H_e') was approximately 21 per cent for the parallel strips and 40 per cent for the symmetric pattern of blocks.

For the 1.8 ft water depth the reduction in relative monochromatic wave run-up (R/H_o') was approximately 16 per cent for both the parallel strips and the symmetric pattern of blocks whereas for the wind (irregular) waves the reduction in relative wave run-up (R/H_e') was approximately 37 per cent for the slope containing the

parallel strips and 33 per cent for the slope containing the symmetric pattern of blocks.

Both the parallel strips and the symmetric pattern of blocks effectively reduced the relative wave uprush (R/H_o' and R/H_e') by 15 per cent or better as shown in Table 8.

Comparison of Wave Reflection from Artificially Roughened (1 on 1-1/2) Slopes with Wave Reflection from a Smooth (1 on 1-1/2) Slope

The effects of slope roughness (r) on the reflecting capability (power) of a single (1 on 1-1/2) slope were studied by comparing reflection data from the three slope conditions tested (see Fig. 56). A comparison was made between the coefficient of reflection data for the smooth (1 on 1-1/2) slope (see Fig. 23), the roughened (1 on 1-1/2) slope containing parallel strips (see Fig. 34) and the roughened (1 on 1-1/2) slope containing a symmetric pattern of blocks (see Fig. 45).

As shown in Fig. 56 the slope roughness did not affect the reflecting capability (power) of the slope. The dissipation of energy by wave reflection was therefore not significantly affected by the slope roughness.

Comparison of Relative Uprush Velocity (V_u/C) for Artificially Roughened (1 on 1-1/2) Slopes with Relative Uprush Velocity (V_u/C) for a Smooth (1 on 1-1/2) Slope

The effects of slope roughness (r) on the maximum velocities

TABLE 8.--COMPARISON OF RELATIVE WAVE RUN-UP (R/H_o', R/H_e') ON ARTIFICIALLY ROUGHENED (1 on 1½) SLOPES WITH RELATIVE WAVE RUN-UP (R/H_o', R/H_e') ON A SMOOTH (1 on 1½) SLOPE

Depth of water d (ft) (1)	Mean wave energy density, E_μ (ft^2/sec^{-1}) (2)	Relative wave run-up: On a smooth (1 on 1½) slope (3)	Relative wave run-up: On a (1 on 1½) slope with parallel strips (4)	Decrease in relative wave run-up (5)	Relative wave run-up: On a (1 on 1½) slope with symmetric blocks (6)	Decrease in relative wave run-up (7)
			Monochromatic (regular) waves			
1.2	0.0005	1.78	1.45	0.33 (0.19)[a]	1.30	0.48 (0.27)[a]
	0.0010	1.80	1.45	0.35 (0.20)	1.32	0.48 (0.27)
	0.0050	1.87	1.48	0.39 (0.21)	1.34	0.53 (0.28)
	0.0100	1.90	1.50	0.40 (0.21)	1.35	0.55 (0.29)
1.5	0.0010	2.19	1.44	0.75 (0.30)	1.39	0.80 (0.31)
	0.0050	2.06	1.44	0.62 (0.30)	1.43	0.63 (0.31)
	0.0100	2.00	1.46	0.54 (0.27)	1.46	0.54 (0.27)
	0.0500	1.90	1.47	0.43 (0.15)	1.52	0.38 (0.20)

TABLE 8.--CONTINUED

Depth of water d (ft) (1)	Mean wave energy density, E_μ (ft^2/sec^{-1}) (2)	Relative wave run-up: On a smooth (1 on 1½) slope (3)	Relative wave run-up: On a (1 on 1½) slope with parallel strips (4)	Decrease in relative wave run-up (5)	Relative wave run-up: On a (1 on 1½) slope with symmetric blocks (6)	Decrease in relative wave run-up (7)
1.8	0.0010	2.18	1.83	0.35 (0.16)	1.87	0.31 (0.14)
	0.0050	2.08	1.75	0.33 (0.16)	1.74	0.34 (0.16)
	0.0100	2.05	1.72	0.33 (0.16)	1.67	0.38 (0.19)
	0.0500	1.96	1.67	0.29 (0.15)	1.57	0.39 (0.20)
			Wind (irregular) waves			
1.2	0.0131	2.21	----	----	----	----
	0.0124	----	1.29	0.92 (0.42)	----	----
	0.0124	----	----	----	1.19	1.02 (0.46)

TABLE 8.--CONTINUED

Depth of water d (ft) (1)	Mean wave energy density, E_μ (ft^2/sec^{-1}) (2)	Relative wave run-up: On a smooth (1 on 1½) slope (3)	Relative wave run-up: On a (1 on 1½) slope with parallel strips (4)	Decrease in relative wave run-up (5)	Relative wave run-up: On a (1 on 1½) slope with symmetric blocks (6)	Decrease in relative wave run-up (7)
1.5	0.0138	2.23	----	----	----	----
	0.0152	----	1.76	0.47 (0.21)	----	----
	0.0152	----	----	----	1.34	0.89 (0.40)
1.8	0.0232	2.60	----	----	----	----
	0.0200	----	1.64	0.96 (0.37)	----	----
	0.0200	----	----	----	1.75	0.85 (0.33)

[a]Per cent.

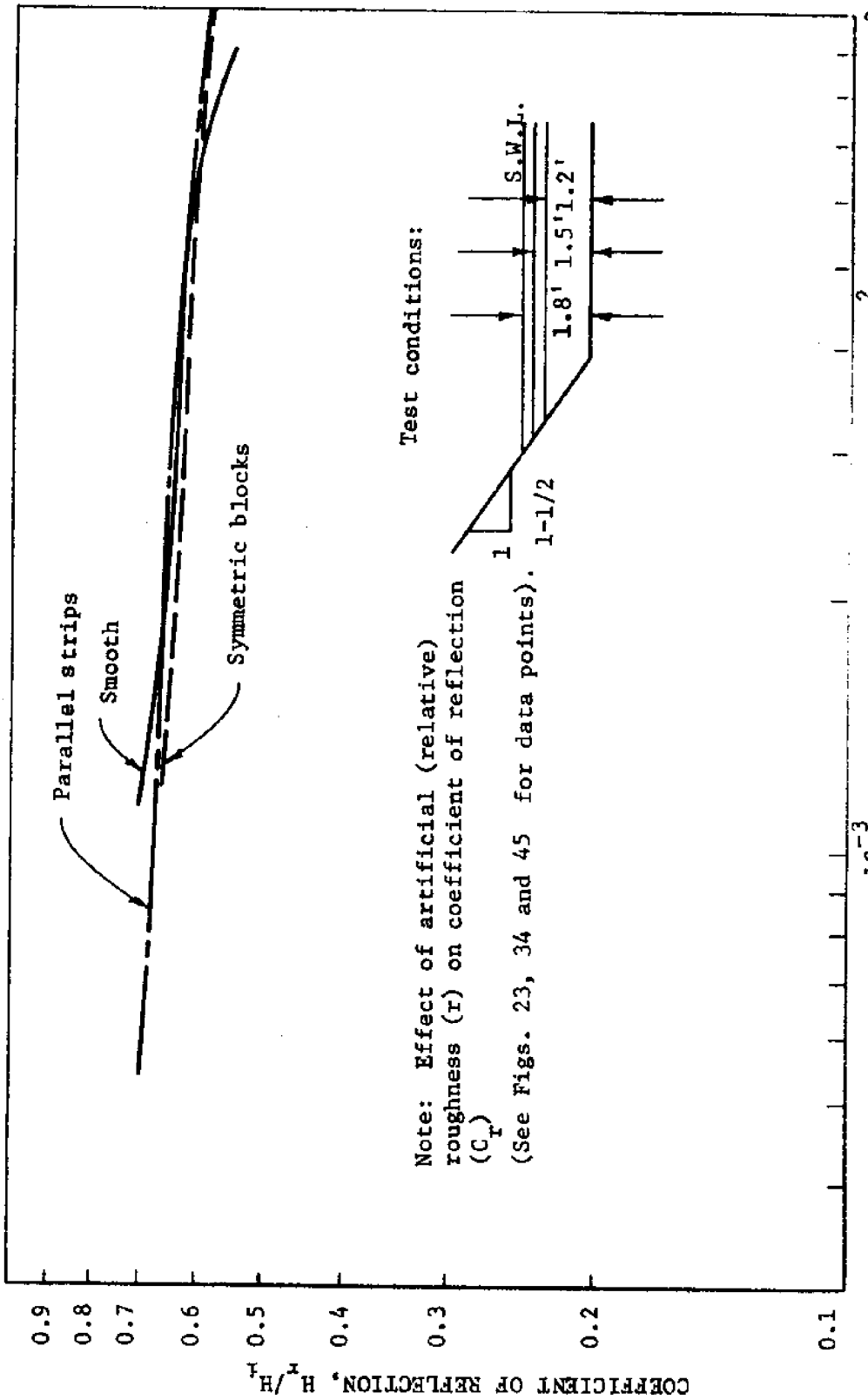

FIG. 56.--COEFFICIENT OF REFLECTION FOR SMOOTH AND ROUGHENED (BLOCKS AND STRIPS) 1 ON 1-1/2 SLOPE (d = 1.2, 1.5 and 1.8 ft)

in the uprush zone of a single (1 on 1-1/2) slope were studied by comparing the relative uprush velocity (V_u/C) data from the three slope conditions tested (see Fig. 57). A comparison was made between the relative uprush velocity (V_u/C) data from the smooth (1 on 1-1/2) slope (see Fig. 24), the roughened (1 on 1-1/2) slope containing parallel strips (see Fig. 35) and the roughened (1 on 1-1/2) slope containing a symmetric pattern of blocks (see Fig. 46).

As shown in Fig. 57, the slope roughness (r) reduced the relative uprush velocity (V_u/C) on the slope. The symmetric pattern of blocks reduced the relative uprush velocity (V_u/C) approximately 15 per cent while the parallel strips reduced the relative uprush velocity (V_u/C) approximately 25 per cent. The reduction in the uprush velocity component (measured parallel to the slope at a height of 0.035 ft above the slope) was primarily due to (1) an increase in form drag, (2) an increase in air entrainment and (3) an increase in the intensity of turbulence caused by the slope roughness.

Wave Energy Dissipation on a Composite (1 on 1-1/2 Smooth Slopes with 1.5 ft Berm) Section

Wave run-up (R). To establish a standard for comparison purposes and to verify the work of previous investigators, a series of wave run-up (R) tests were run using a composite (1 on 1-1/2 smooth slopes with 1.5 ft berm) section. Wave run-up (R) data for both

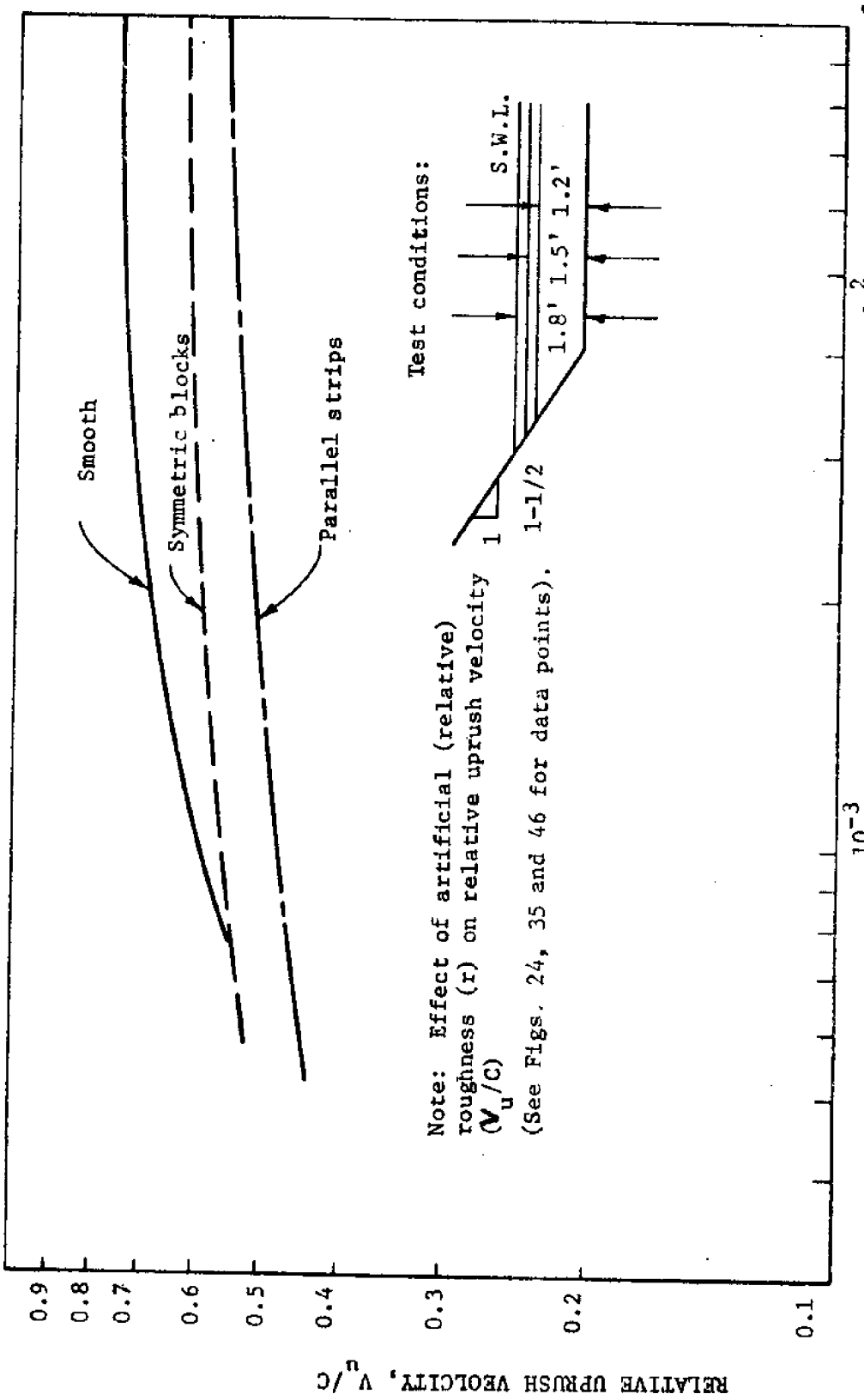

FIG. 57.--RELATIVE UPRUSH VELOCITY FOR SMOOTH AND ROUGHENED (BLOCKS AND STRIPS) 1 ON 1-1/2 SLOPE
(d = 1.2, 1.5 and 1.8 ft)

monochromatic (regular) waves and wind (irregular) waves was obtained for the composite (1 on 1-1/2 smooth slopes with 1.5 ft berm) section.

The monochromatic (regular) wave tests were run using wave periods (T) of 1.00 sec, 1.56 sec and 1.86 sec in water depths (d) of 1.2 ft, 1.5 ft and 1.8 ft. Equivalent deep water wave heights (H_o') were varied from 0.113 ft to 0.443 ft for the water depths tested [see Table 9 Appendix III)].

The wind (irregular) wave tests were run using surface wind velocities ($V_{0.30}$) of 39.8 ft/sec, 41.3 ft/sec and 54.5 ft/sec obtained for water depths of 1.2 ft, 1.5 ft and 1.8 ft, respectively. The equivalent wave periods (T) obtained from the wave energy spectrum were 0.72 sec, 0.77 sec and 0.83 sec for water depths of 1.2 ft, 1.5 ft and 1.8 ft, respectively, while the equivalent deep-water wave heights (H_e') obtained from the wave energy spectrum were, respectively, 0.362 ft, 0.316 ft and 0.357 ft [see Table 10 (Appendix III)].

The mean wave energy density (E_μ) was obtained from the wave energy spectrum for both the monochromatic (regular) waves and for the wind (irregular) waves. For the monochromatic (regular) waves the mean wave energy density (E_μ) varied from 0.0006 ft^2/sec^{-1} to 0.0165 ft^2/sec^{-1} while for the wind (irregular) waves the mean wave energy density (E_μ) varied from 0.0151 ft^2/sec^{-1} to 0.0208 ft^2/sec^{-1} [see Tables 9 and 10 (Appendix III)].

Each wave run-up (R) value was plotted as a dependent variable

for its respective incident mean wave energy density (E_μ) which was plotted as an independent variable as shown in Figs. 58, 59 and 60. Due to the nature of the monochromatic wave run-up (R) phenomena there was a distribution (scatter) of the monochromatic wave run-up (R) values for each mean wave energy density (E_μ).

For the 1.2 ft water depth the wave run-up (R) phenomena was affected by the berm as shown in Fig. 58. Between mean wave energy densities (E_μ) of 0.0006 ft^2/sec^{-1} and 0.00225 ft^2/sec^{-1} the wave run-up (R) energy was dissipated on the front slope of the composite section. Between mean wave energy densities (E_μ) of 0.0025 ft^2/sec^{-1} and 0.00420 ft^2/sec^{-1} the wave run-up (R) energy was dissipated by the characteristics (length, roughness, etc.) of the berm. Between mean wave energy densities (E_μ) of 0.00420 ft^2/sec^{-1} and 0.0100 ft^2/sec^{-1} the wave run-up (R) energy was dissipated on the rear slope of the composite section. For the wind waves the run-up (R) energy was dissipated on the rear slope.

For the 1.5 ft water depth the wave run-up (R) phenomena was affected by the berm as shown in Fig. 59. Comparing the wave run-up values for a mean wave energy density (E_μ) of 0.0151 ft^2/sec^{-1}:

$$R = 0.264 \text{ ft} \quad \text{for} \quad \lambda_o = 3.04 \text{ ft} \quad \ldots\ldots \quad (58)$$

$$R = 0.355 \text{ ft} \quad \text{for} \quad \lambda_o = 5.12 \text{ ft} \quad \ldots\ldots \quad (59)$$

$$R = 0.662 \text{ ft} \quad \text{for} \quad \lambda_o = 12.46 \text{ ft} \quad \ldots\ldots \quad (60)$$

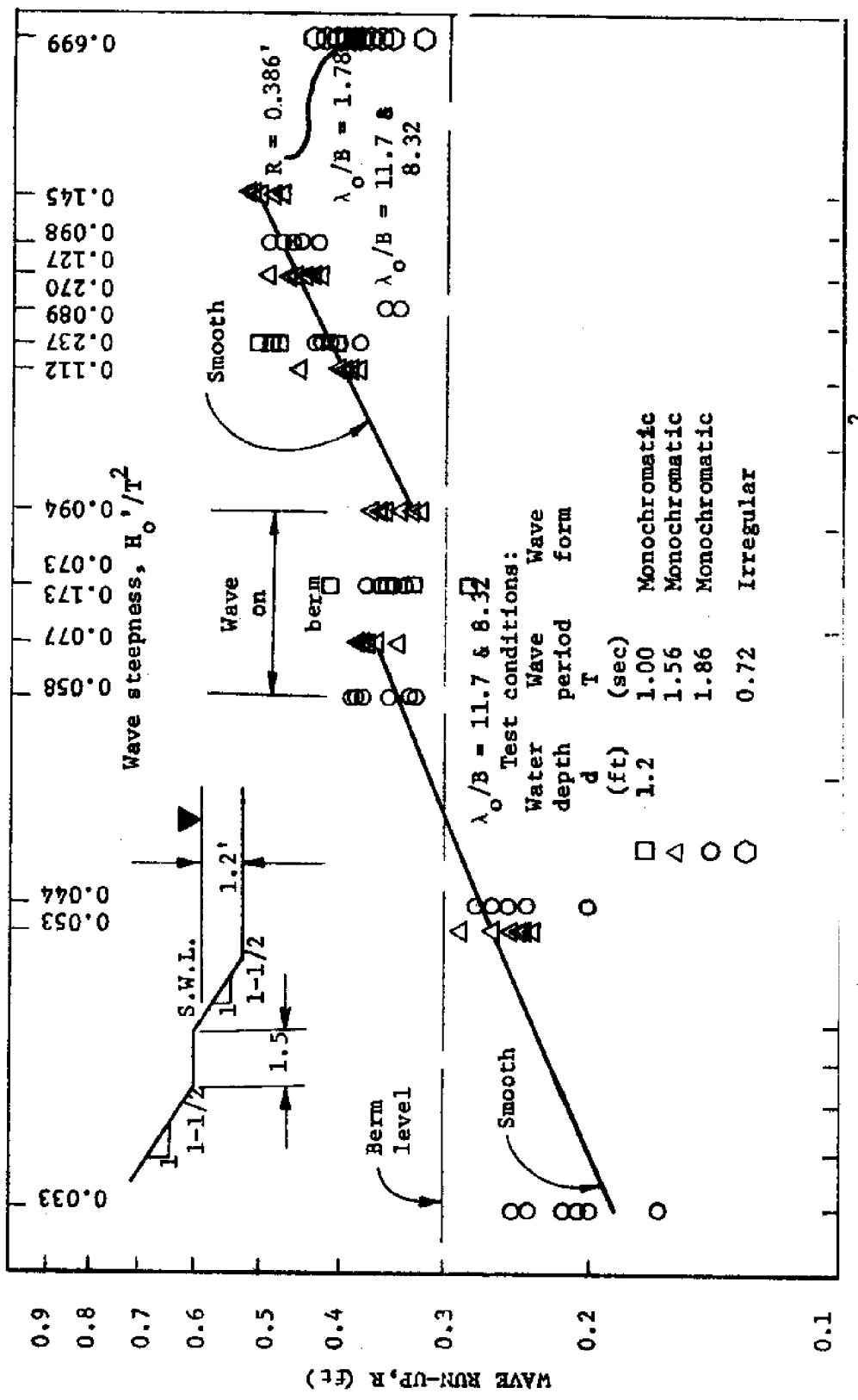

FIG. 58.--WAVE RUN-UP ON A COMPOSITE (1 ON 1-1/2 SMOOTH SLOPES WITH 1.5 FT BERM) SECTION
(d = 1.2 ft)

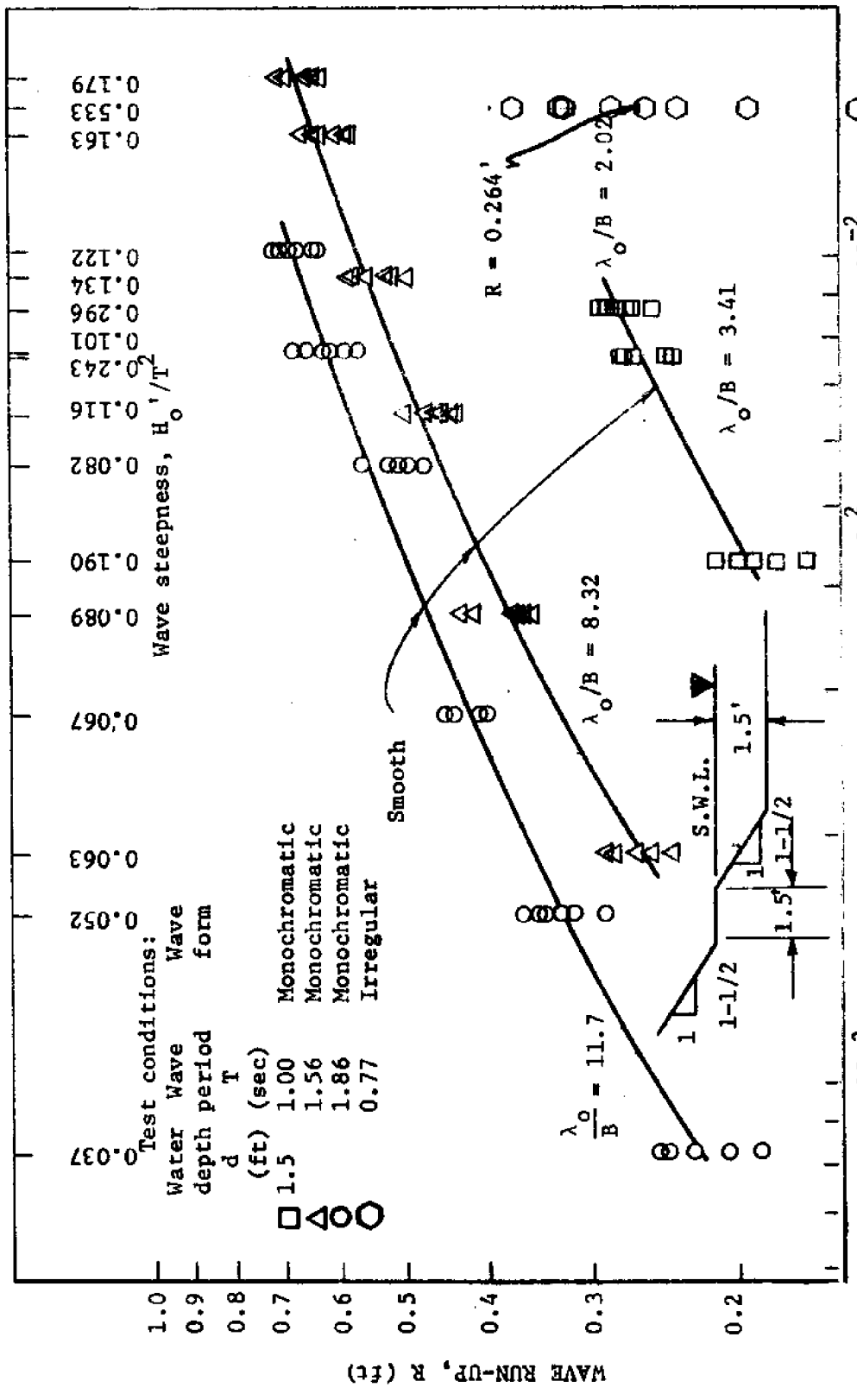

FIG. 59.--WAVE RUN-UP ON A COMPOSITE (1 ON 1-1/2 SMOOTH SLOPES WITH 1.5 FT BERM) SECTION (d = 1.5 ft)

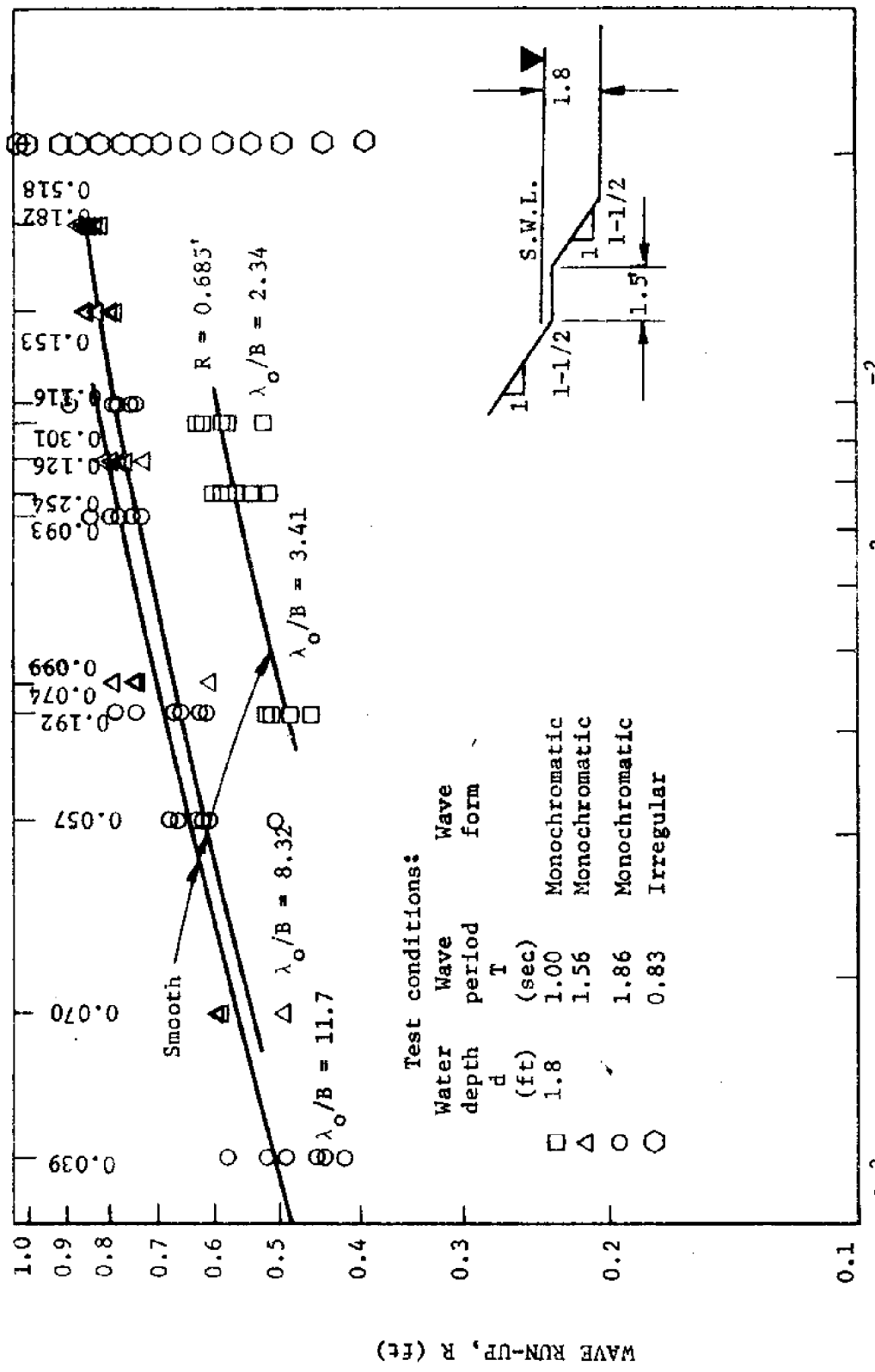

FIG. 60.--WAVE RUN-UP ON A COMPOSITE (1 ON 1-1/2 SMOOTH SLOPES WITH 1.5 FT BERM) SECTION (d = 1.8 ft)

$$R = 0.785 \text{ ft} \quad \text{for} \quad \lambda_o = 17.71 \text{ ft} \quad . \quad . \quad . \quad . \quad . \quad (61)$$

indicates that the wave run-up (R) was a function of the wave length (λ_o).

For the 1.8 ft water depth the wave run-up (R) phenomena was affected by the berm as shown in Fig. 60. Comparing the wave run-up (R) values for a mean wave energy density (E_μ) of 0.0208 ft^2/sec^{-1}:

$$R = 0.685 \text{ ft} \quad \lambda_o = 0.35 \text{ ft} \quad . \quad . \quad . \quad . \quad . \quad . \quad . \quad . \quad (62)$$

$$R = 0.665 \text{ ft} \quad \lambda_o = 5.12 \text{ ft} \quad . \quad . \quad . \quad . \quad . \quad . \quad . \quad . \quad (63)$$

$$R = 0.860 \text{ ft} \quad \lambda_o = 12.46 \text{ ft} \quad . \quad . \quad . \quad . \quad . \quad . \quad . \quad . \quad (64)$$

$$R = 0.910 \text{ ft} \quad \lambda_o = 17.71 \text{ ft} \quad . \quad . \quad . \quad . \quad . \quad . \quad . \quad . \quad (65)$$

indicates that the wave run-up (R) was a function of the wave length (λ_o). The wave run-up (R) increased with increasing wave length (λ_o).

Wave reflection. To establish a standard for comparison purposes and to determine the reflecting capability (power) of a composite (1 on 1-1/2 smooth slopes with 1.5 ft berm) section, a series of wave reflection (H_r/H_i) tests were run using monochromatic (regular) waves.

The wave reflection tests were run using wave periods (T) of 1.00 sec, 1.56 sec, and 1.86 sec on water depths of 1.2 ft, 1.5 ft and 1.8 ft. Equivalent deep water wave heights (H_o') were varied from 0.113 ft to 0.443 ft while the mean wave energy densities (E_μ) varied from 0.0006 ft^2/sec^{-1} to 0.0165 ft^2/sec^{-1}, respectively, for the water depths tested [see Table 9 (Appendix III)].

The reflecting capability (power) of the composite (1 on 1-1/2 smooth slopes with 1.5 ft berm) section was evaluated from wave records obtained by moving the instrument carriage containing the wave height sensor through a train of waves to obtain the incident and reflected wave heights. A reflecting coefficient (ratio of the reflected wave height to the incident wave height) was calculated for each test run [see Table 14 (Appendix V)]. Each reflecting coefficient (*i.e.*, coefficient of reflection) value ($C_r = H_r/H_i$) was plotted as a dependent variable for its respective incident mean wave energy density (E_μ) which was plotted as an independent variable as shown in Fig. 61. Fig. 61, therefore represents the reflecting capability (power) of the composite (1 on 1-1/2 smooth slopes with 1.5 ft berm) section.

As the mean wave energy density (E_μ) increased from 0.001 ft^2/sec^{-1} to 0.010 ft^2/sec^{-1} the reflecting capability (power) of the composite section was decreased. For the 1.2 ft water depth the reflecting capability was not significantly reduced, but for the 1.5 ft and 1.8 ft water depths the reflecting capability was decreased approximately 16 per cent and 32 per cent, respectively.

Effect of berm (width and elevation) on wave run-up (R). The effect of berm width and elevation on wave run-up (R) was investigated. Water depths (d) above and below the berm elevation were used in the study.

For the 1.2 ft water depth (0.3 ft below the berm) the wave run-up (R) was not affected by the berm between the mean wave energy

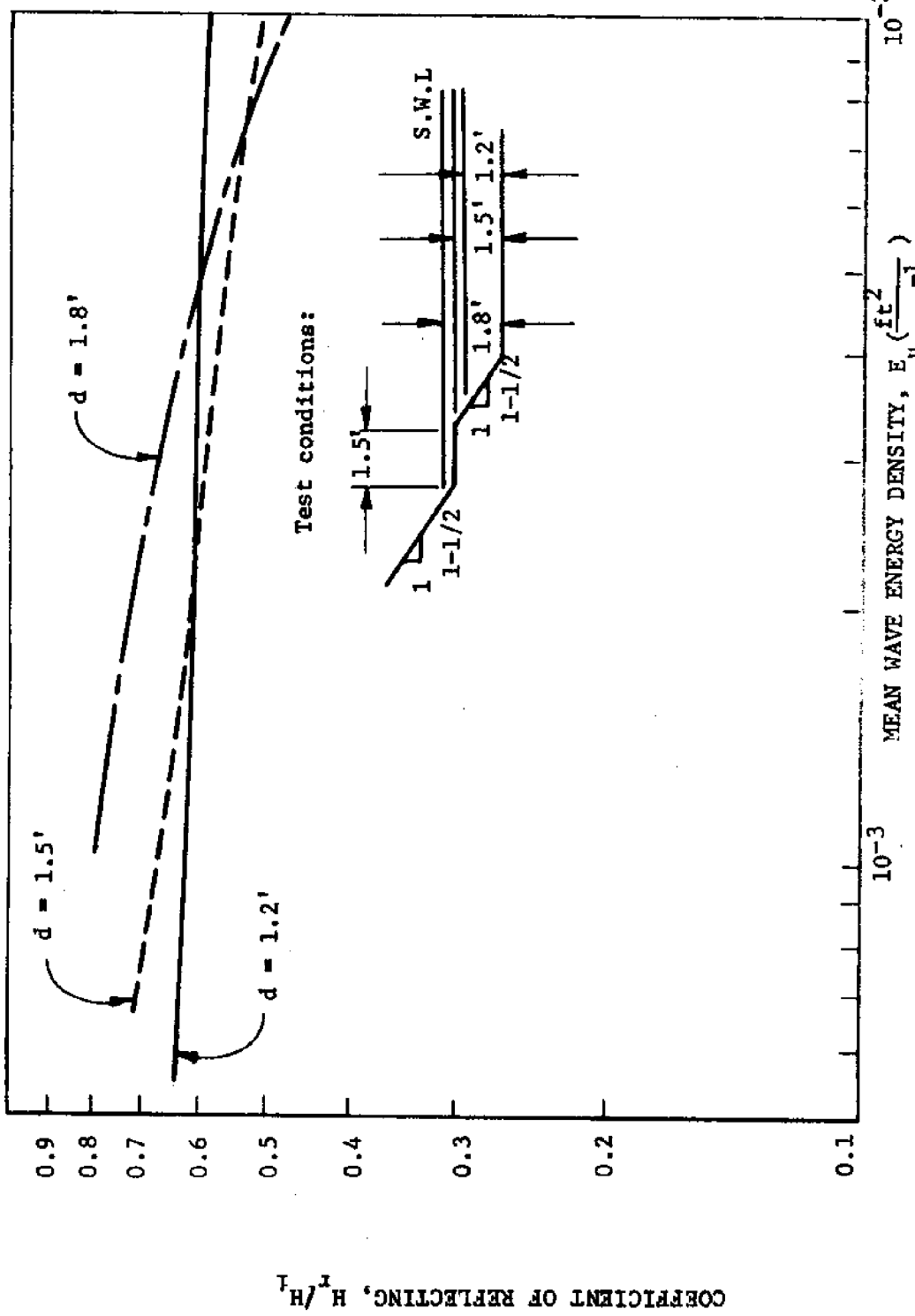

FIG. 61.--COEFFICIENT OF REFLECTION FOR A COMPOSITE (1 ON 1-1/2 SMOOTH SLOPES WITH 1.5 FT BERM) (d = 1.2, 1.5 and 1.8 ft)

densities of 0.0006 ft^2/sec^{-1} and 0.00225 ft^2/sec^{-1}. In this range of mean wave energy densities (E_μ) the wave run-up (R) was on the front slope. Between the mean wave energy densities (E_μ) of 0.00225 ft^2/sec^{-1} and 0.00420 ft^2/sec^{-1} the wave run-up (R) was reduced by the berm. In the range of mean wave energy densities (E_μ) the wave energy was dissipated on the berm. Between the mean wave energy densities (E_μ) of 0.0042 ft^2/sec^{-1} and 0.0154 ft^2/sec^{-1} the wave run-up (R) was on the rear slope. In this range of mean wave energy densities (E_μ) the wave run-up (R) was reduced by the berm as shown in Fig. 58.

For the 1.5 ft water depth (same water depth as berm elevation) the berm had a significant affect on the wave run-up (R). The maximum reduction in wave run-up (R) was experienced for the short wave lengths ($\lambda > d$) while the least reduction in wave run-up (R) was experienced for the long wave lengths ($\lambda > > d$) as shown in Fig. 59.

For the 1.8 ft water depth (0.3 ft above the berm) the berm had a significant affect on the wave run-up (R). The maximum reduction in wave run-up (R) was experienced for the short wave lengths ($\lambda > d$) while the least reduction in wave run-up (R) was experienced for the long wave lengths ($\lambda > > d$) as shown in Fig. 60.

From a comparison of wave run-up (R) values for smooth single and composite sections it was determined that the berm elevation should be set at still water level. For the short wave lengths ($\lambda > d$) the composite section with the berm elevation at still water level reduced the wave run-up (R) approximately 50 per cent.

For the long wave lengths ($\lambda > > d$) the composite section with the berm elevation at still water level reduced the wave run-up (R) approximately 20 per cent.

Physical observations. The following significant observations were made and recorded during testing:

1. The leading edge of the wave run-up (R) was observed to be irregular.

2. The phenomena of transverse waves was unexpectedly (and unavoidably) observed at various times during testing although the wave lengths tested were not harmonics of the wave flume width.

3. Wave reflection was observed in the flume shortly after the leading wave was reflected.

4. A water 'set-up' was observed in the wave flume during the testing using the wind (irregular) waves.

5. A considerable spray up the slope was observed during the wave run-up (R) tests using the wind (irregular) wave generator even though the 'venturi' effect was eliminated by providing a comparable flow way above the slope.

6. For the long waves a vortex was generated on the forward slope (below the berm elevation) due to the collision of the breaking wave and the backwash from the berm.

7. Five different wave run-up (R) cases were noted. These cases were discussed in detail by Herbich[14].

Wave Energy Dissipation on a Composite (1 on 1-1/2 Roughened Strips) Slopes with 1.5 ft Berm Section

Wave run-up (R). To determine the effects of slope roughness on wave run-up (see objectives 1 and 4), a series of tests were run

using a composite (1 on 1-1/2 slopes with 1.5 ft berm) section containing parallel surface strips. Wave run-up (R) data for both monochromatic (regular) waves and wind (irregular) waves was obtained for the roughened slope configuration.

The monochromatic (regular) wave tests were run using wave periods (T) of 1.00 sec, 1.56 sec and 1.86 sec in water depths (d) of 1.2 ft, 1.5 ft and 1.8 ft. Equivalent deep water wave heights (H_o') were varied from 0.113 ft to 0.443 ft for the water depths tested [see Table 9 (Appendix III)].

The wind (irregular) wave tests were run using surface wind velocities ($V_{0.30}$) of 39.8 ft/sec, 41.3 ft/sec and 54.5 ft/sec obtained for water depths of 1.2 ft, 1.5 ft and 1.8 ft, respectively. The equivalent wave periods (T) obtained from the wave energy spectrum were 0.77 sec, 0.77 sec and 0.83 sec for the water depths of 1.2 ft, 1.5 and 1.8 ft, respectively, while the equivalent deep water wave heights (H_e') obtained from the wave energy spectrum were, respectively, 0.331 ft, 0.327 ft and 0.371 ft [see Table 10 (Appendix III)].

The mean wave energy density (E_μ) was obtained from the wave energy spectrum for both the monochromatic (regular) waves and for the wind (irregular) waves. For the monochromatic (regular) waves the mean wave energy density (E_μ) varied from 0.0006 ft^2/sec^{-1} to 0.0165 ft^2/sec^{-1} while for the wind (irregular) waves the mean wave energy density (E_μ) varied from 0.0114 ft^2/sec^{-1} to 0.0228 ft^2/sec^{-1}. [see Tables 9 and 10 (Appendix III)].

Each wave run-up (R) value was plotted as a dependent variable for its respective incident mean wave energy density (E_μ) which was plotted as an independent variable as shown in Figs. 62, 63 and 64. Due to the nature of the monochromatic wave run-up (R) phenomena there was a distribution (scatter) of the monochromatic wave run-up (R) values for each mean wave energy density (E_μ).

By comparing the wave run-up (R) values for a constant wave energy density (E_μ) for each water depth, it was noted that the wave run-up (R) was a function of the wave length (λ_o). For all water depths the wave run-up (R) increased with increasing wave length (λ_o).

Wave reflection. To determine the effects of slope roughness on the reflecting capability (power) of a composite (1 on 1-1/2 slopes with 1.5 ft berm) section containing parallel surface strips, a series of wave reflection (H_r/H_i) tests were run using monochromatic (regular) waves.

The wave reflection tests were run using wave periods (T) of 1.00 sec, 1.56 sec and 1.86 sec in water depths of 1.2 ft, 1.5 ft and 1.8 ft. Equivalent deep water wave heights (H_o') were varied from 0.113 ft to 0.443 ft while the mean wave energy densities (E_μ) varied from 0.0006 ft^2/sec^{-1} to 0.0165 ft^2/sec^{-1}, respectively, for the water depths tested [see Table 9 (Appendix III)].

The reflecting capability (power) of the composite (1 on 1-1/2 slopes with 1.5 ft berm) section containing parallel surface strips

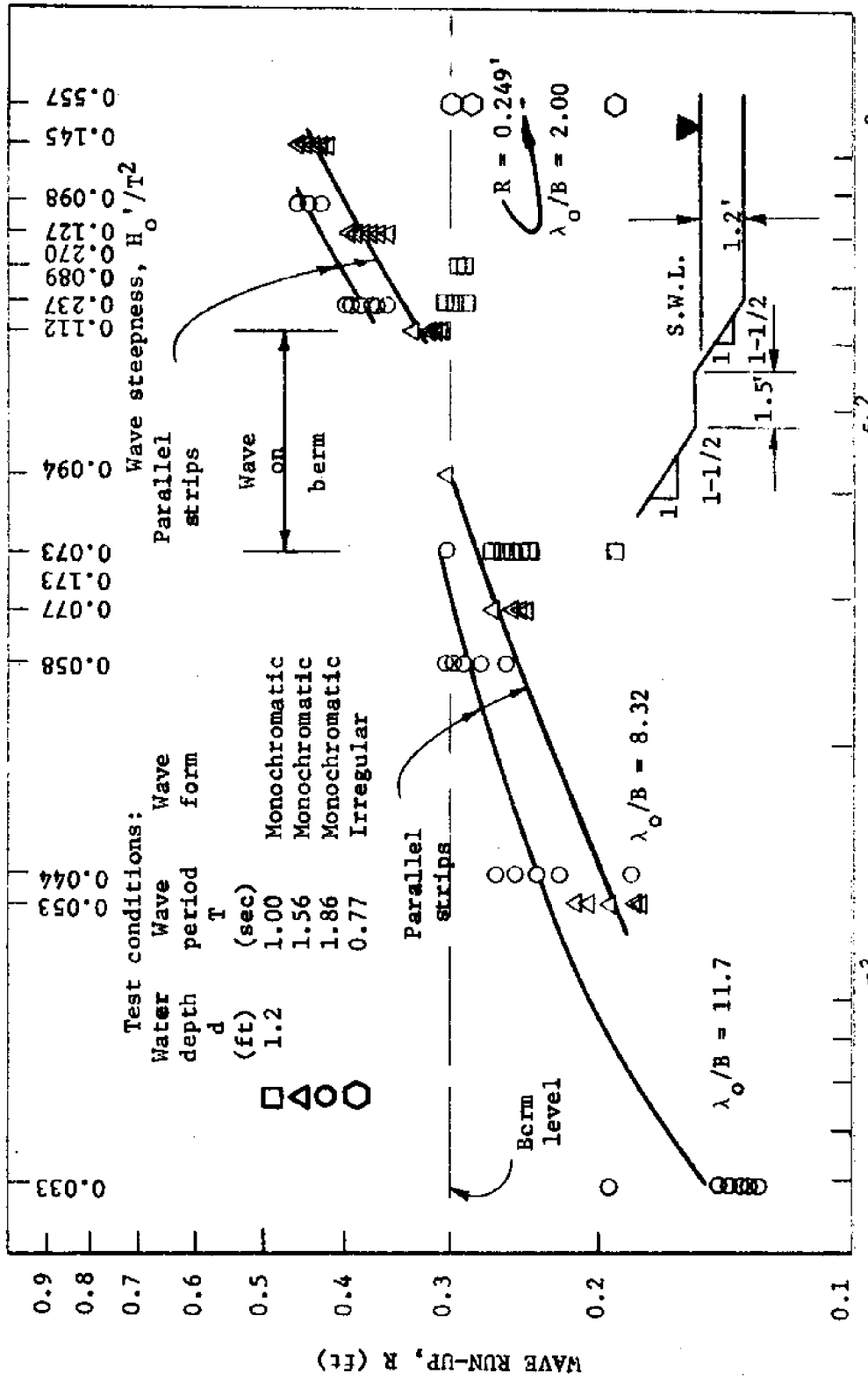

FIG. 62.--WAVE RUN-UP ON A COMPOSITE (1 ON 1-1/2 ROUGHENED (STRIPS) SLOPES WITH 1.5 FT BERM) SECTION (d = 1.2 ft)

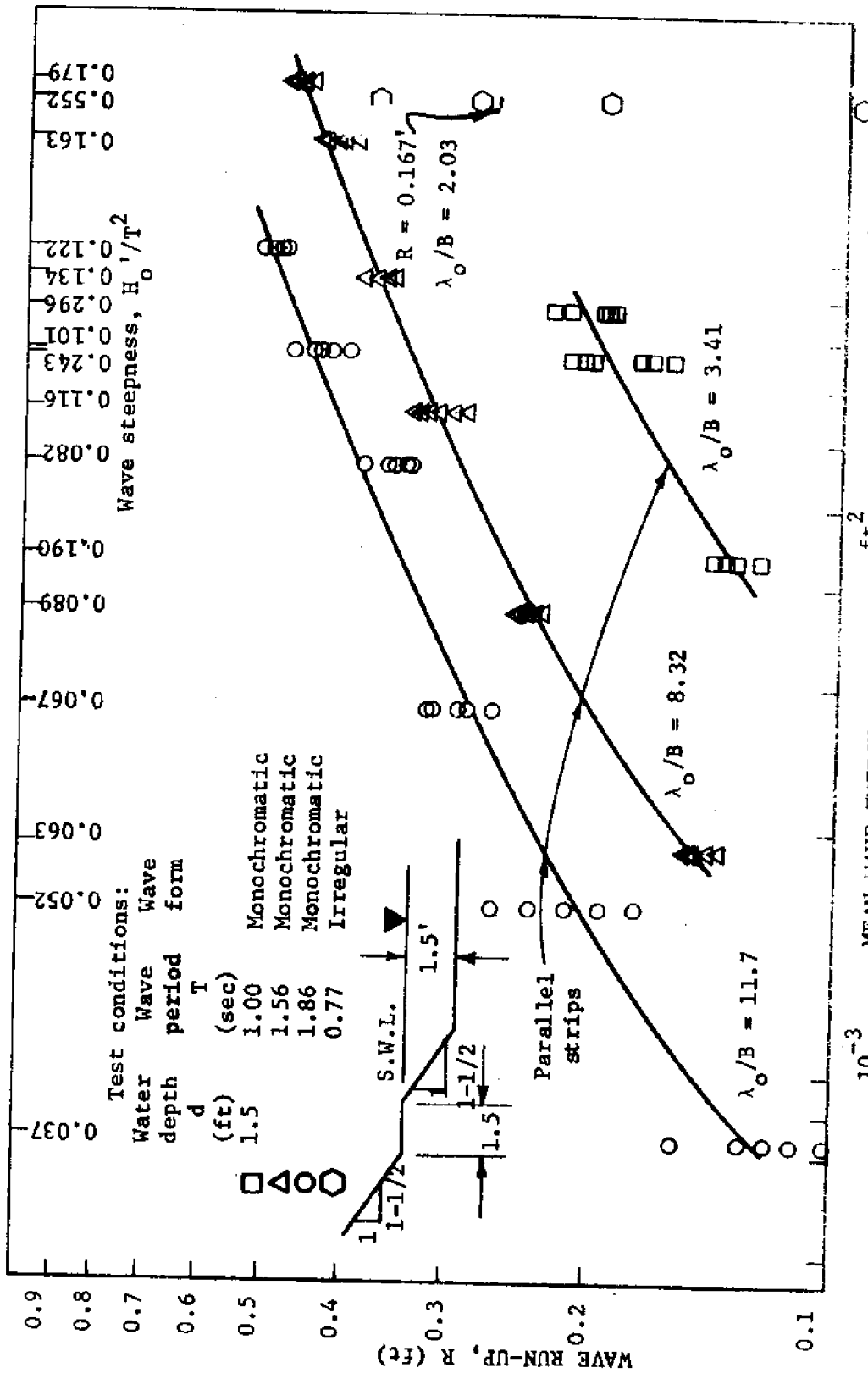

FIG. 63.--WAVE RUN-UP ON A COMPOSITE (1 ON 1-1/2 ROUGHENED (STRIPS) SLOPES WITH 1.5 FT BERM) SECTION (d = 1.5 ft)

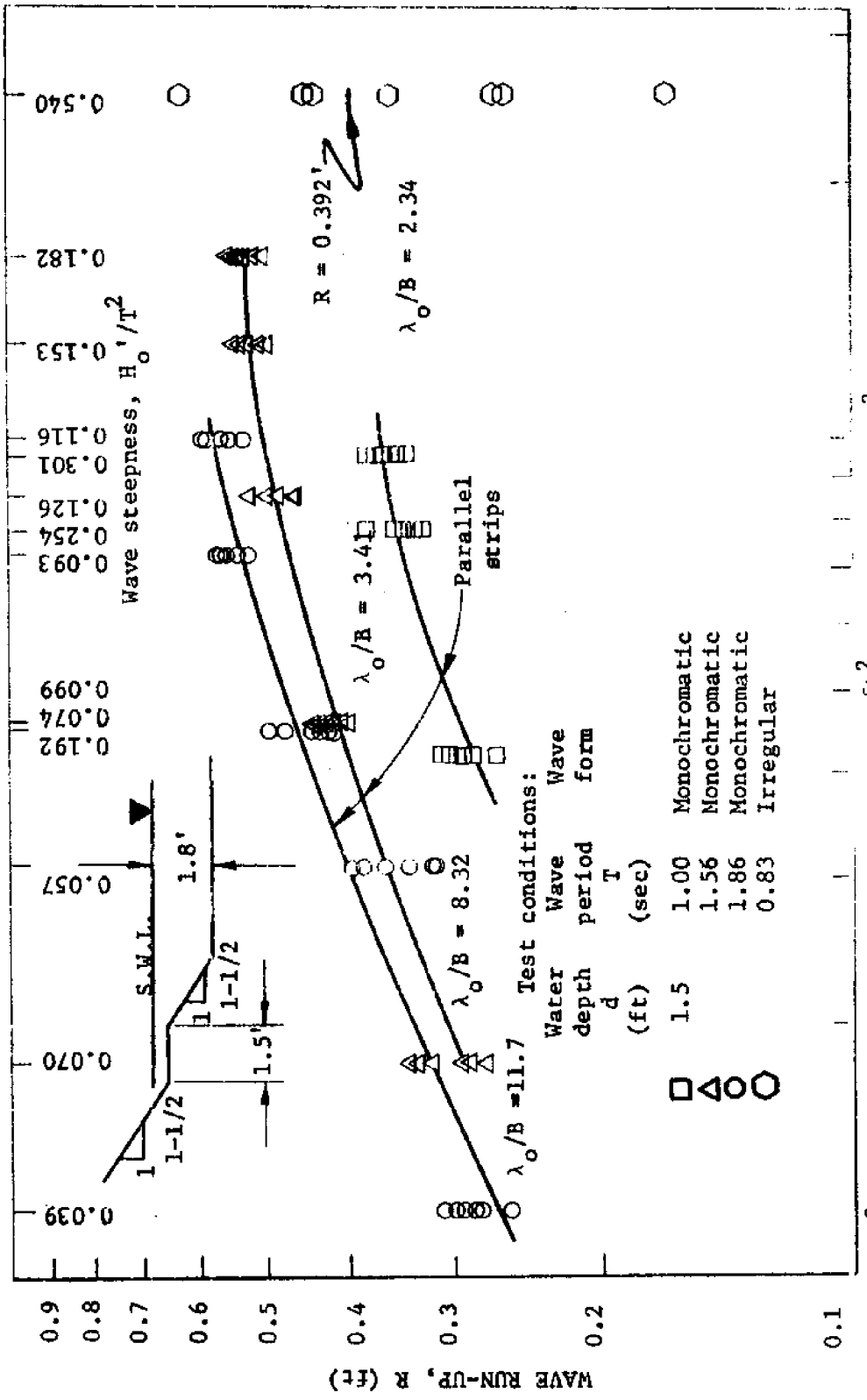

FIG. 64.--WAVE RUN-UP ON A COMPOSITE (1 ON 1-1/2 ROUGHENED (STRIPS) SLOPES WITH 1.5 FT BERM) SECTION (d = 1.8 ft)

was evaluated from wave records obtained by moving the instrument carriage containing the wave height sensor through a train of waves to obtain the incident and reflected wave heights. A reflecting coefficient (ratio of the reflected wave height to the incident wave height) was calculated for each test run [see Table 14 (Appendix V)]. Each reflecting coefficient (*i.e.*, coefficient of reflection) value ($C_r = H_r/H_i$) was plotted as an independent variable as shown in Fig. 65. Fig. 65, therefore represents the reflecting capability (power) of the composite (1 on 1-1/2 roughened (strips) slopes with 1.5 ft berm) section.

As the mean wave energy density (E_μ) increased from 0.001 ft^2/sec^{-1} to 0.010 ft^2/sec^{-1} the reflecting capability (power) of the composite section was decreased. For the 1.2 ft water depth the reflecting capability was not significantly reduced, but for the 1.5 ft and 1.8 ft water depths the reflecting capability was decreased approximately 5 per cent and 14 per cent, respectively. For the 1.5 ft and 1.8 ft water depths the berm and the parallel strips reduced the reflecting capability (power) of the composite section approximately 16 per cent.

Effect of berm (width and elevation) on wave run-up (R). The effect of berm width and elevation on wave run-up (R) was investigated. Water depths (d) above and below the berm elevation were used in the study.

For water depths of 1.2 ft (0.3 ft below the berm), 1.5 ft (same water depth as berm elevation) and 1.8 ft (0.3 ft above the

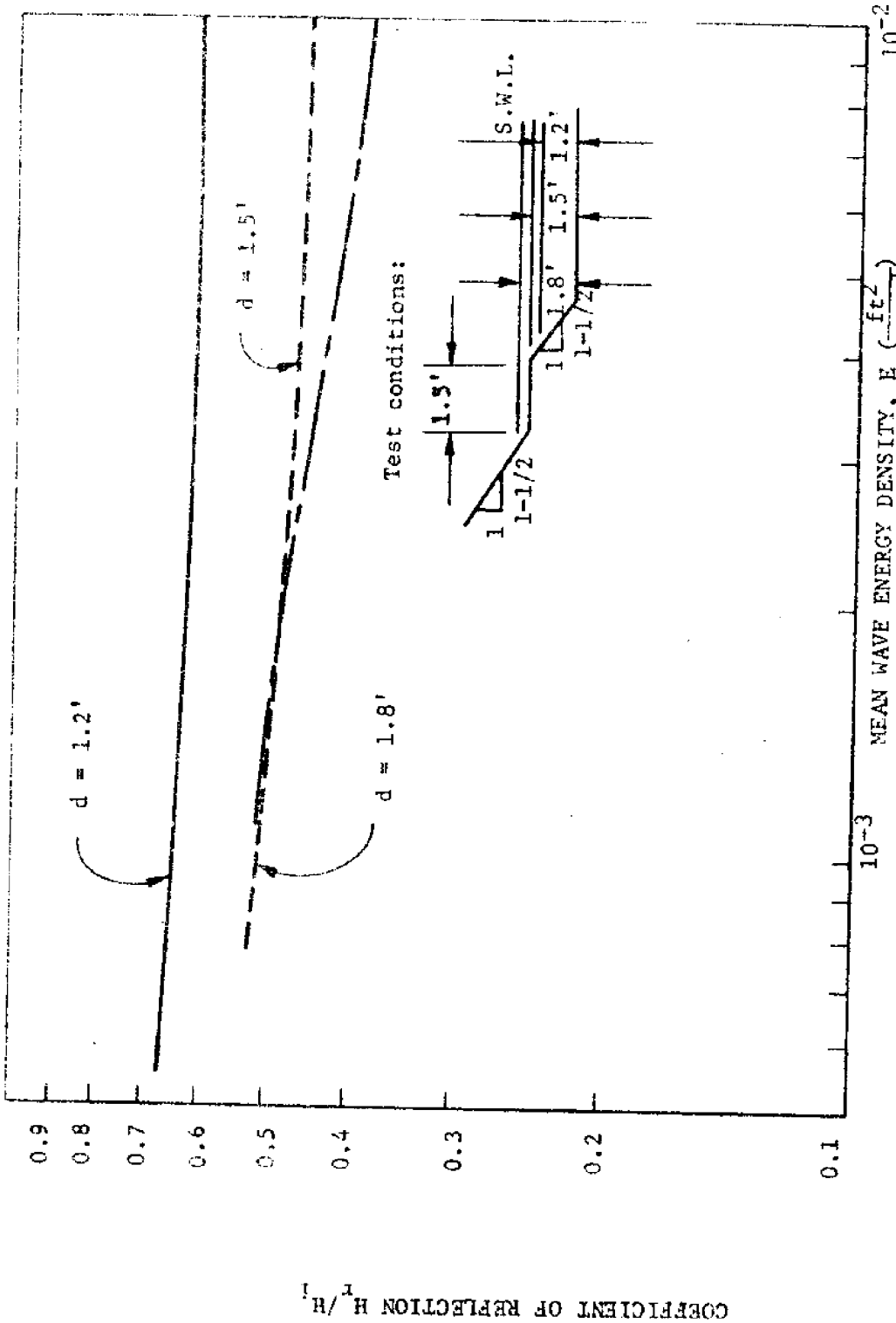

FIG. 65.--COEFFICIENT OF REFLECTION FOR A COMPOSITE (1 ON 1-1/2 ROUGHENED (STRIPS) SLOPES WITH 1.5 FT BERM) SECTION (d = 1.2, 1.5 and 1.8 ft)

berm) the berm had a significant effect on the wave run-up (R). The maximum reduction in wave run-up (R) was experienced for the short wave lengths ($\lambda > d$) while the least reduction in wave run-up (R) was experienced for the long wave lengths ($\lambda >> d$) as shown in Figs. 62, 63 and 64.

From a comparison of wave run-up (R) values for single and composite sections containing the same parallels strip pattern it was determined that the berm elevation should be set at still water level. For the short wave lengths ($\lambda > d$) the composite section with the berm elevation at still water level reduced the wave run-up (R) approximately 30 per cent. For the long wave lengths ($\lambda >> d$) the composite section with the berm elevation at still water level reduced the wave run-up (R) approximately 20 per cent.

Physical observations. The following significant observations were made and recorded during testing:

1. The phenomena of transverse waves was unexpectedly (and unavoidably) observed at various times during testing although the wave lengths tested were not harmonics of the wave flume width.

2. Wave reflection was observed in the flume shortly after the leading wave was reflected.

3. A water 'set-up' was observed in the wave flume during the testing using the wind (irregular) waves.

4. A considerable spray up the slope was observed during the wave run-up (R) tests using the wind (irregular) wave generator even though the 'venturi' effect was eliminated by providing a comparable flow way above the slope.

5. For the long waves a vortex was generated on the forward slope (below the berm elevation)

due to the collision of the breaking wave and the backwash from the berm.

6. Five different wave run-up (R) cases were noted. These cases were discussed in detail by Herbich[14].

The following methods of energy dissipation were observed during testing:

1. Dissipation of energy by wave front collision with the vertical face of the strip.

2. Dissipation of energy by vortices (turbulence) generated by the strips.

3. Dissipation of energy by air entrainment (heterogeneous mixing of air and water) caused by the strips.

4. Dissipation of energy by waves breaking on the structure (breaking occurred at the break in slope).

5. Dissipation of energy by opposing backwash (water running back across the berm over the strips).

Wave Energy Dissipation on a Composite (1 on 1-1/2 Roughened (Blocks) Slopes with 1.5 ft Berm) Section

Wave run-up (R). To determine the effects of slope roughness on wave run-up (see objectives 1 and 4), a series of tests were run using a composite (1 on 1-1/2 slopes with 1.5 ft berm) section containing a symmetric pattern of surface blocks. Wave run-up (R) data for both monochromatic (regular) waves and wind(irregular) waves was obtained for the roughened slope configuration.

The monochromatic (regular) wave tests were run using wave periods (T) of 1.00 sec, 1.56 sec and 1.86 sec in water depths (d)

of 1.2 ft, 1.5 ft and 1.8 ft. Equivalent deep water wave heights (H_o') were varied from 0.113 ft to 0.443 ft for the water depths tested [see Table 9(Appendix III)].

The wind (irregular) wave tests were run using surface wind velocities ($V_{0.30}$) of 39.8 ft/sec, 41.3 ft/sec and 54.5 ft/sec obtained for water depths of 1.2 ft, 1.5 ft and 1.8 ft, respectively. The equivalent wave periods (T) obtained from the wave energy spectrum were 0.77 sec, 0.77 sec and 0.83 sec for water depths of 1.2 ft, 1.5 ft and 1.8 ft, respectively, while the equivalent deep water wave heights (H_e') obtained from the wave energy spectrum were, respectively, 0.331 ft, 0.327 ft and 0.371 ft [see Table 10 (Appendix III)].

The mean wave energy densities (E_μ) was obtained from the wave energy spectrum for both the monochromatic (regular) waves and for the wind (irregular) waves. For the monochromatic (regular) waves the mean wave energy density (E_μ) varied from 0.0006 ft^2/sec^{-1} to 0.0165 ft^2/sec^{-1} while for the wind (irregular) waves the mean wave energy density (E_μ) varied from 0.0114 ft^2/sec^{-1} to 0.0228 ft^2/sec^{-1} [see Tables 9 and 10 (Appendix III)].

Each wave run-up (R) value was plotted as a dependent variable for its respective incident mean wave energy density (E_μ) which was plotted as an independent variable as shown in Figs. 66, 67 and 68. Due to the nature of the monochromatic wave run-up (R) phenomena there was a distribution (scatter) of the monochromatic wave run-up (R) values for each mean wave energy density (E_μ).

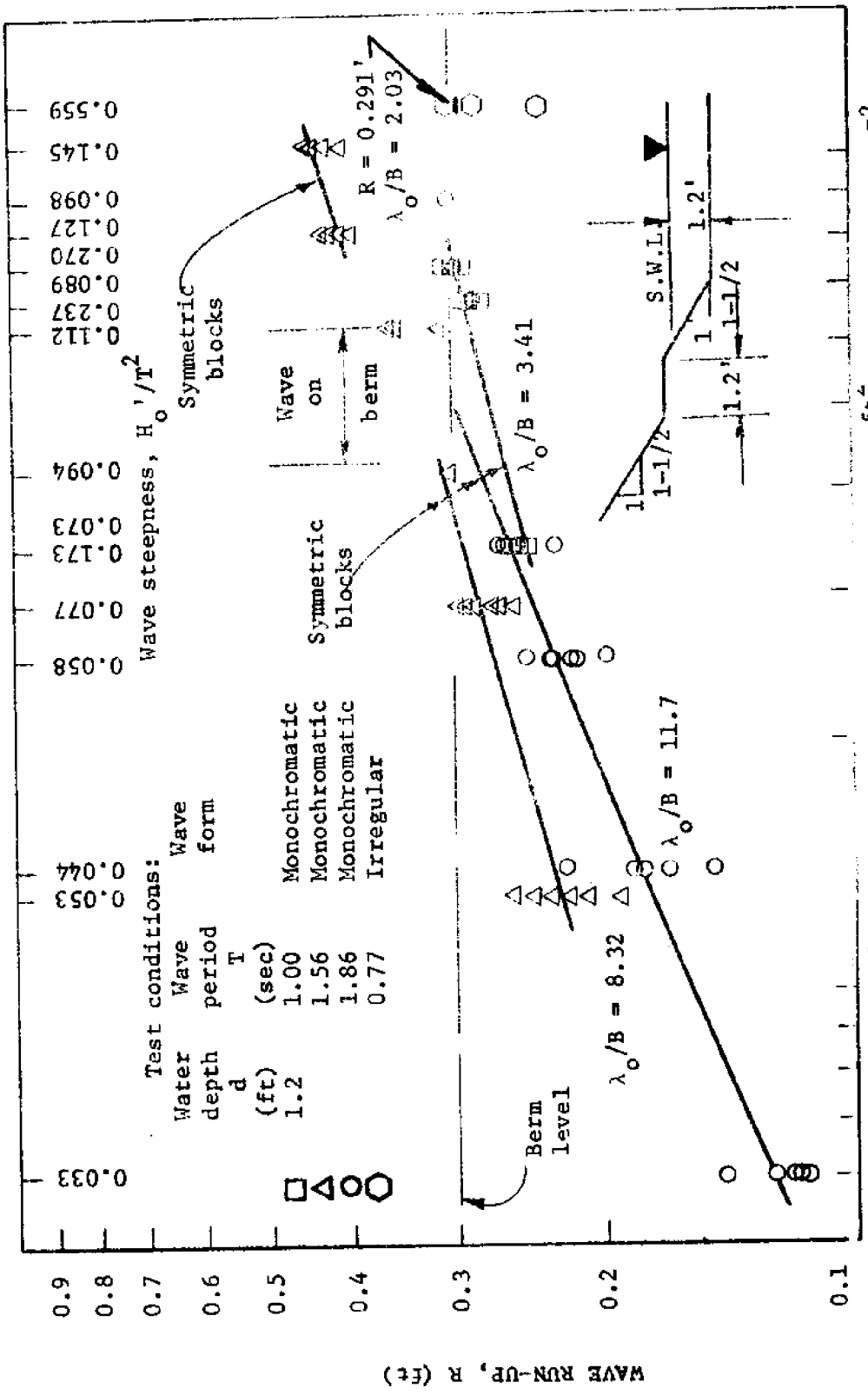

FIG. 66.--WAVE RUN-UP ON A CONCRETE [illegible] ROUGHENED (BLOCKS) SLOPES [illegible] BERM SECTION (d = 1.2 ft)

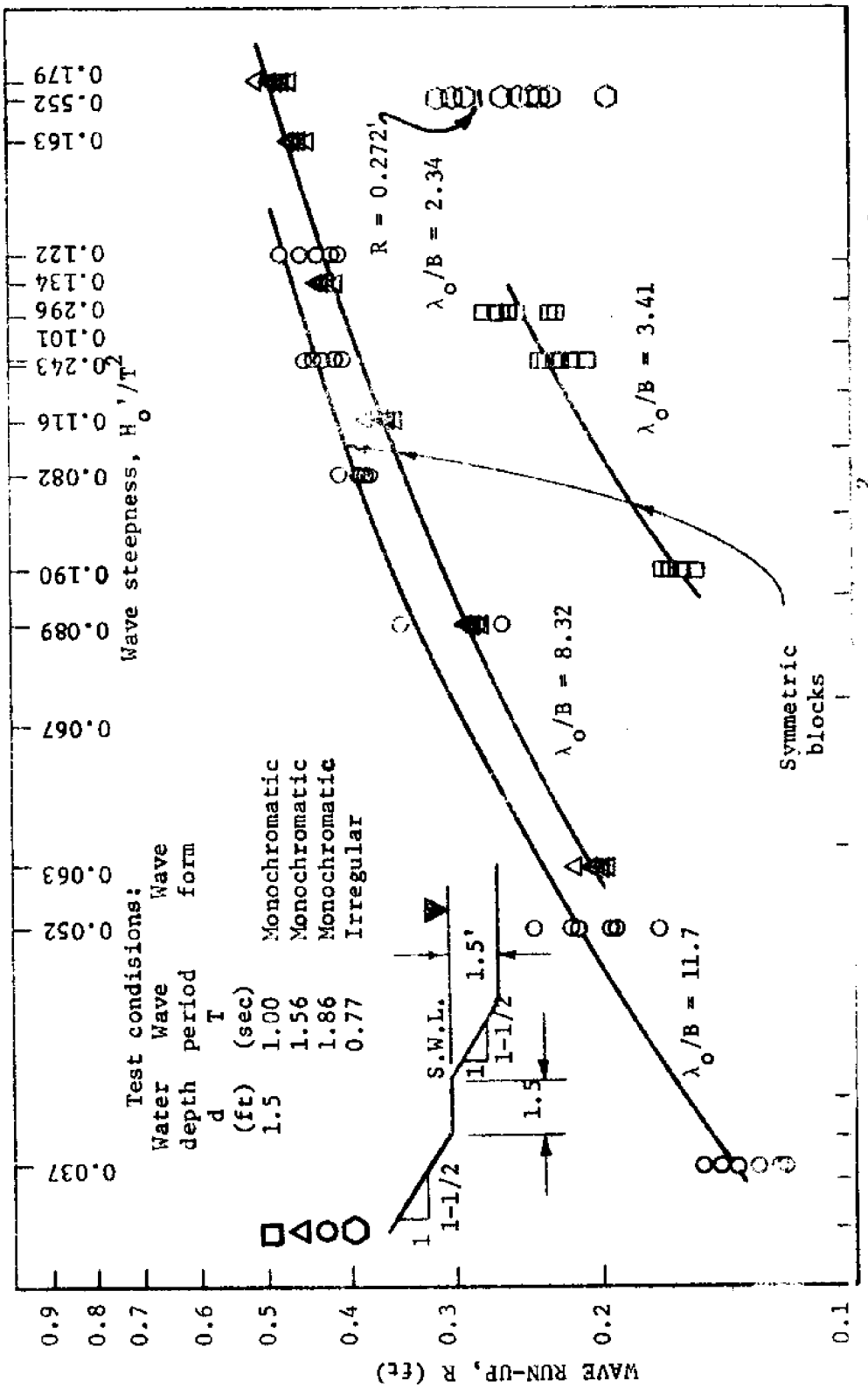

FIG. 67.--WAVE RUN-UP ON A COMPOSITE (1 ON 1-1/2 ROUGHENED (BLOCKS) SLOPES WITH 1.5 FT BERM) SECTION (d = 1.5 ft)

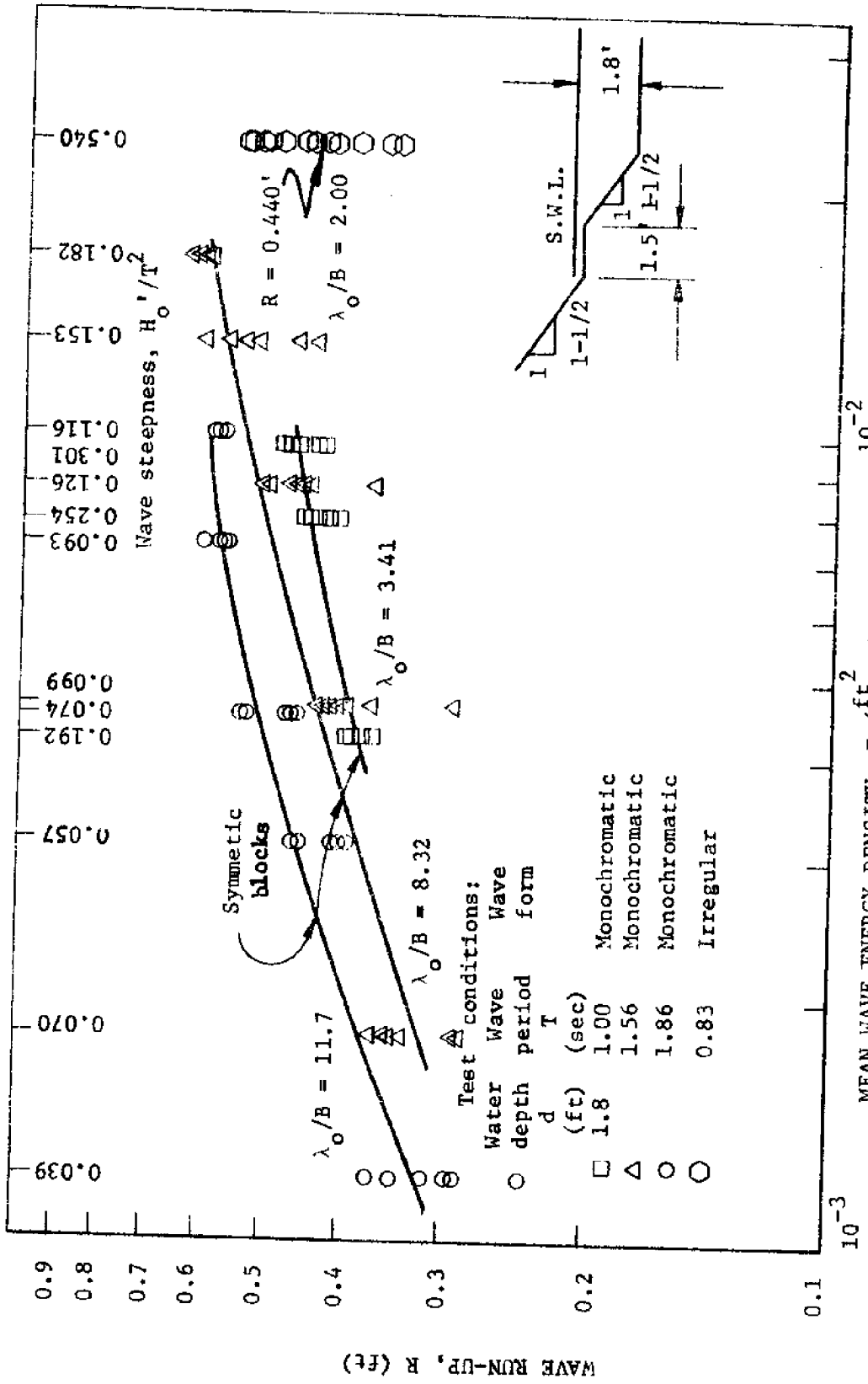

FIG. 68.--WAVE RUN-UP ON A COMPOSITE (1 ON 1-1/2 ROUGHENED (BLOCKS) SLOPES WITH 1.5 FT BERM) SECTION (d = 1.8 ft)

By comparing the wave run-up (R) values for a constant wave energy density (E_μ) for each water depth, it was noted that the wave run-up (R) was a function of the wave length (λ_o). For water depths of 1.5 ft and 1.8 ft the wave run-up (R) increased with increasing wave length (λ_o).

Wave reflection. To determine the effects of slope roughness on the reflecting capability (power) of a composite (1 on 1-1/2 slopes with 1.5 ft berm) section containing a symmetric pattern of blocks, a series of wave reflection (H_r/H_i) tests were run using monochromatic (regular) waves.

The wave reflection tests were run using wave periods (T) of 1.00 sec, 1.56 sec, and 1.86 sec in water depths of 1.2 ft, 1.5 ft and 1.8 ft. Equivalent deep water wave heights (H_o') were varied from 0.113 ft to 0.443 ft while the mean wave energy densities (E_μ) varied from 0.0006 ft^2/sec^{-1} to 0.0165 ft^2/sec^{-1}, respectively, for the water depths tested [see Table 9 (Appendix III)].

The reflecting capability (power) of the roughened (1 on 1-1/2) slope was evaluated from wave records obtained by moving the instrument carriage containing the wave height sensor through a train of waves to obtain the incident and reflected wave heights. A reflecting coefficient (ratio of the reflected wave height to the incident wave height) was calculated for each test run [see Table 14 (Appendix V)]. Each reflecting coefficient (*i.e.*, coefficient of reflection) value ($C_r = H_r/H_i$) was plotted as a dependent variable for its

respective incident mean wave energy density (E_μ) which was plotted as an independent variable as shown in Fig. 69. Fig. 69, therefore represents the reflecting capability (power) of the composite (1 on 1-1/2 roughened (blocks) slopes with 1.5 berm) section.

As the mean wave energy density (E_μ) increased from 0.001 ft^2/sec^{-1} to 0.010 ft^2/sec^{-1} the reflecting capability (power) of the composite section was decreased. For the 1.2 ft water depth the reflecting capability was decreased approximately 24 per cent while for the 1.5 ft and 1.8 ft water depths the reflecting capability was decreased approximately 10 per cent.

Effect of berm (width and elevation) on wave run-up (R). The effect of berm width and elevation on wave run-up (R) was investigated. Water depths (d) above and below the berm elevation were used in the study.

For water depths of 1.5 ft (same water depth as berm elevation) and 1.8 ft (0.3 ft above the berm) the berm had a significant affect on the wave run-up (R). The maximum reduction in wave run-up (R) was experienced for the short wave lengths ($\lambda > d$) while the least reduction in wave run-up (R) was experienced for the long wave lengths ($\lambda >> d$) as shown in Figs. 67 and 68. The reason for the anomaly in Fig. 66 for the 1.2 ft water depth was not determined.

From a comparison of wave run-up (R) values for single and composite sections containing the same symmetric block patterns it was determined that the berm elevation should be set at still water level. For the short wave lengths ($\lambda > d$) the composite section

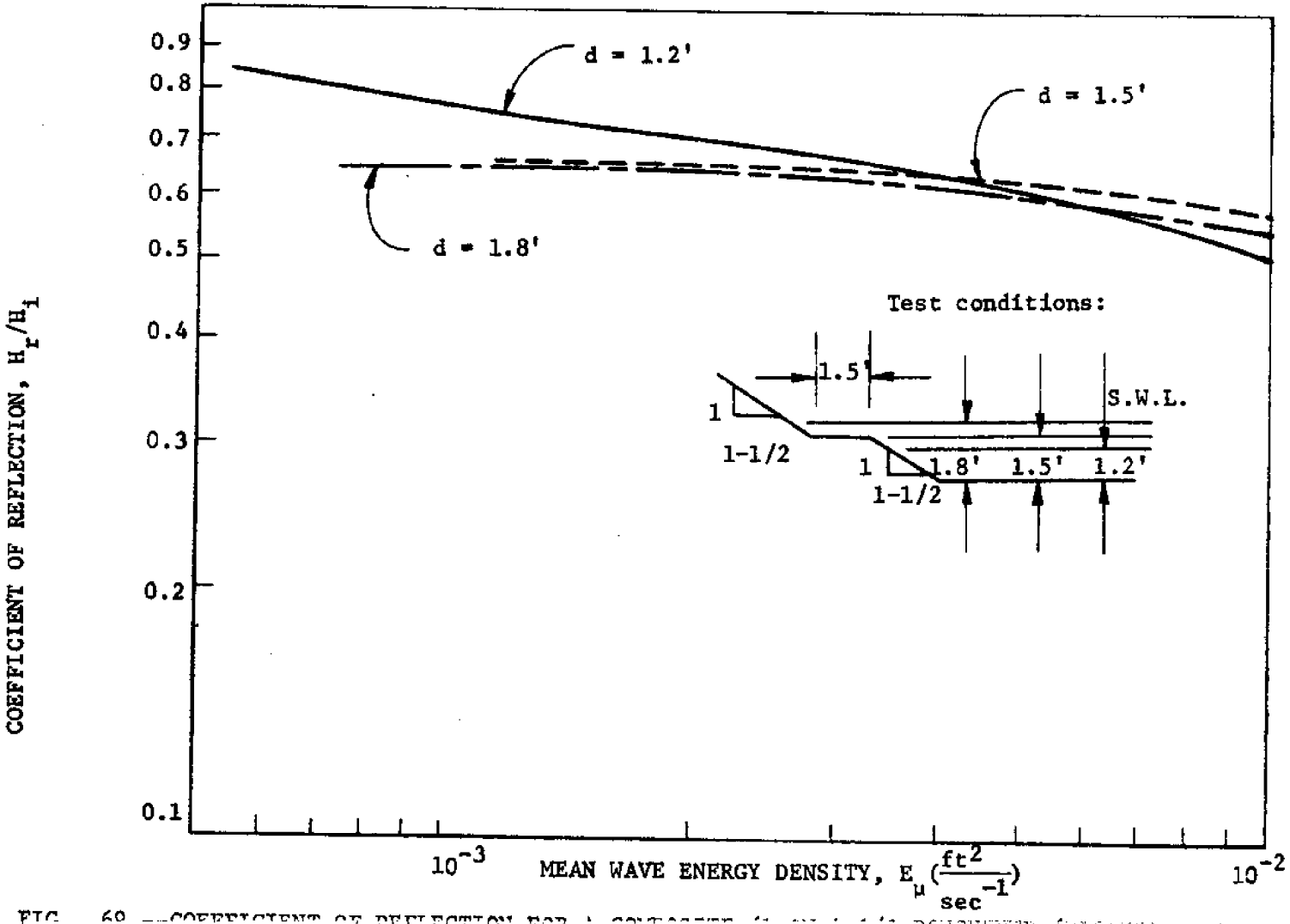

FIG. 69 --COEFFICIENT OF REFLECTION FOR A COMPOSITE (1 ON 1-1/2 ROUGHENED (BLOCKS) SLOPES WITH 1.5 FT BERM) SECTION (d = 1.2, 1.5 and 1.8 ft)

with the berm elevation at still water level reduced the wave run-up (R) approximately 40 per cent. For the long wave lengths ($\lambda >> d$) the composite section with the berm elevation at still water level reduced the wave run-up (R) approximately 20 per cent.

Physical observations. The following significant observations were made and recorded during testing:

1. The leading edge of the wave run-up (R) was observed to be irregular.

2. The phenomena of transverse waves was unexpectedly (and unavoidably) observed at various times during testing although the wave lengths tested were not harmonics of the wave flume width.

3. Wave reflection was observed in the flume shortly after the leading wave was reflected.

4. A water 'set-up' was observed in the wave flume during the testing using the wind (irregular) waves.

5. A considerable spray up the slope was observed during the wave run-up (R) tests using the wind (irregular) wave generator even though the 'venturi' effect was eliminated by providing a comparable flow way above the slope.

6. For the long waves a vortex was generated on the forward slope (below the berm elevation) due to the collision of the breaking wave and the back-wash from the berm.

7. Five different wave run-up (R) cases were noted. These cases were discussed in detail by Herbich[14].

The following methods of energy dissipation were observed during testing:

1. Dissipation of energy by jets channeled between the blocks which hit the vertical face of the upslope block.

2. Dissipation of energy by air entrainment (heterogeneous mixing of air and water) caused by the blocks.

3. Dissipation of energy by vortices (turbulence) generated by the blocks.

4. Dissipation of energy by waves breaking on the structure (breaking occurred at the break in slope).

5. Dissipation of energy by opposing backwash (water running back across the berm between the blocks).

Comparison of Wave Run-up (R) on Artificially Roughened Composite (1 on 1-1/2 Slopes with 1.5 ft Berm) Sections with Wave Run-up on a Smooth Composite (1 on 1-1/2 Slopes with 1.5 ft Berm) Section

The effect of slope roughness (r) on wave run-up (R) was studied by comparing wave run-up (R) data from the three slope conditions using wave periods (T) of 1.00 sec, 1.56 sec and 1.86 sec in water depths (d) of 1.2 ft, 1.5 ft and 1.8 ft (see Figs. 70 through 78). For the 1.2 ft water depth the symmetric pattern of blocks provided the greatest reduction in wave run-up (R) as shown in Figs. 70, 71 and 72. Since these were the only tests in which the blocks provided the greatest reduction in wave run-up (R) it was concluded that the tests were biased by human or experimental error.

For the 1.5 ft and 1.8 ft water depths the parallel strips provided the greatest reduction in wave run-up (R) as shown in Figs. 73 through 78. As the wave length (λ_o) increased the effect of the symmetric block pattern increased as shown in Figs. 75 and 78.

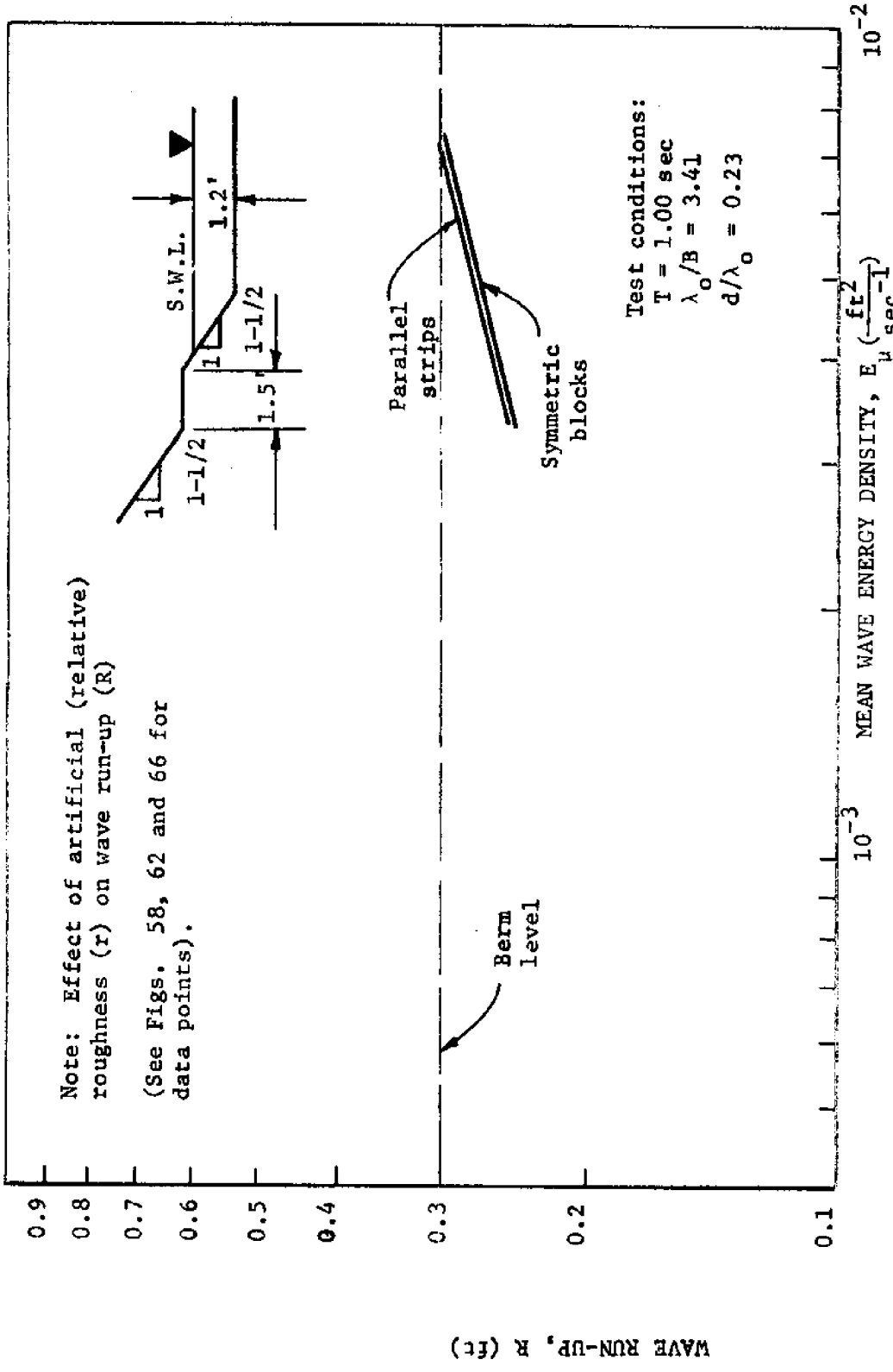

FIG. 70.--WAVE RUN-UP ON A COMPOSITE (1 ON 1-1/2 SLOPES WITH 1.5 FT BERM) SECTION (d = 1.2 ft and T = 1.00 sec)

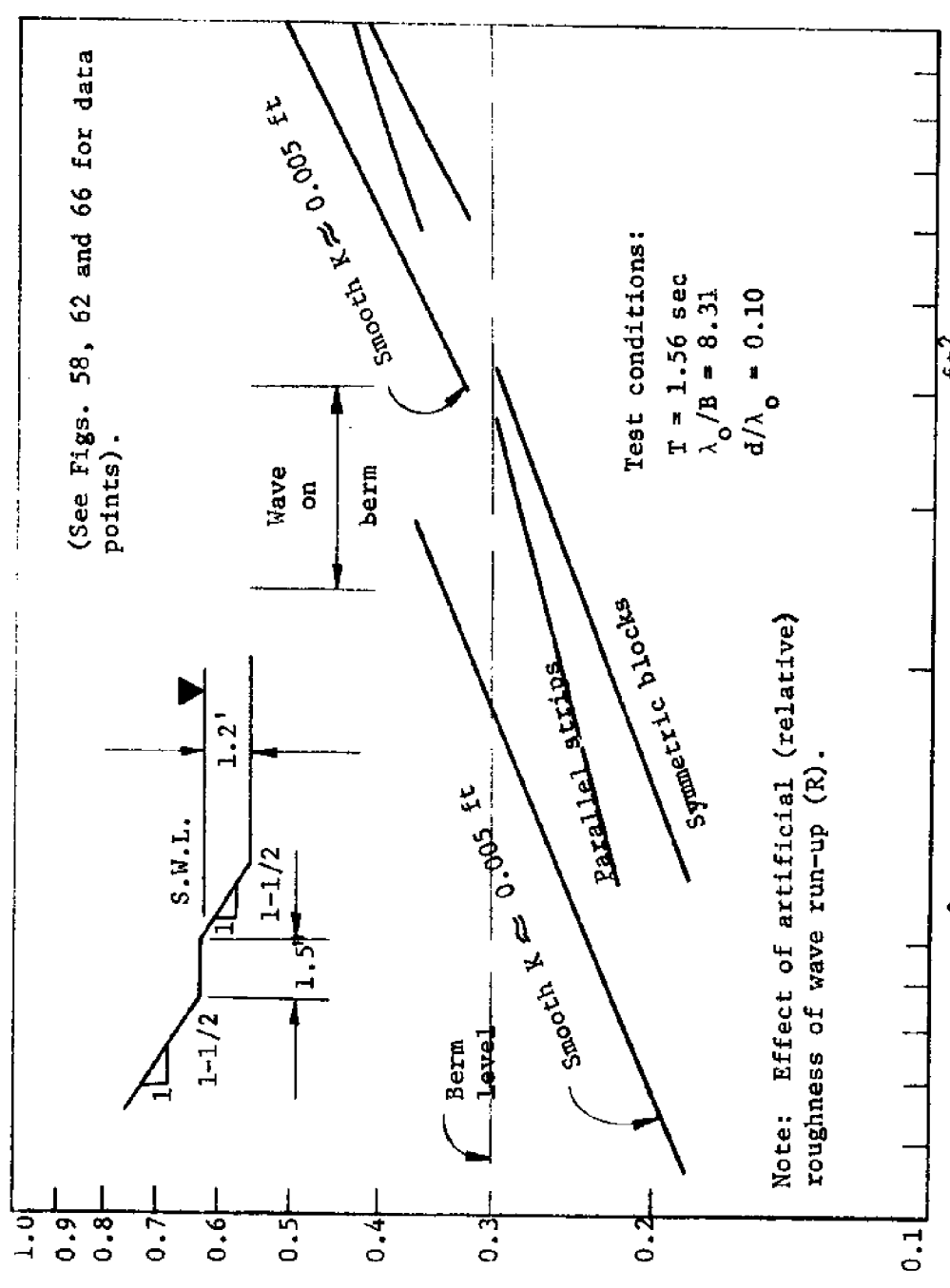

FIG. 71.--WAVE RUN-UP ON A COMPOSITE (1 ON 1-1/2 SLOPES WITH 1.5 FT BERM) SECTION (d = 1.2 ft and T = 1.56 sec)

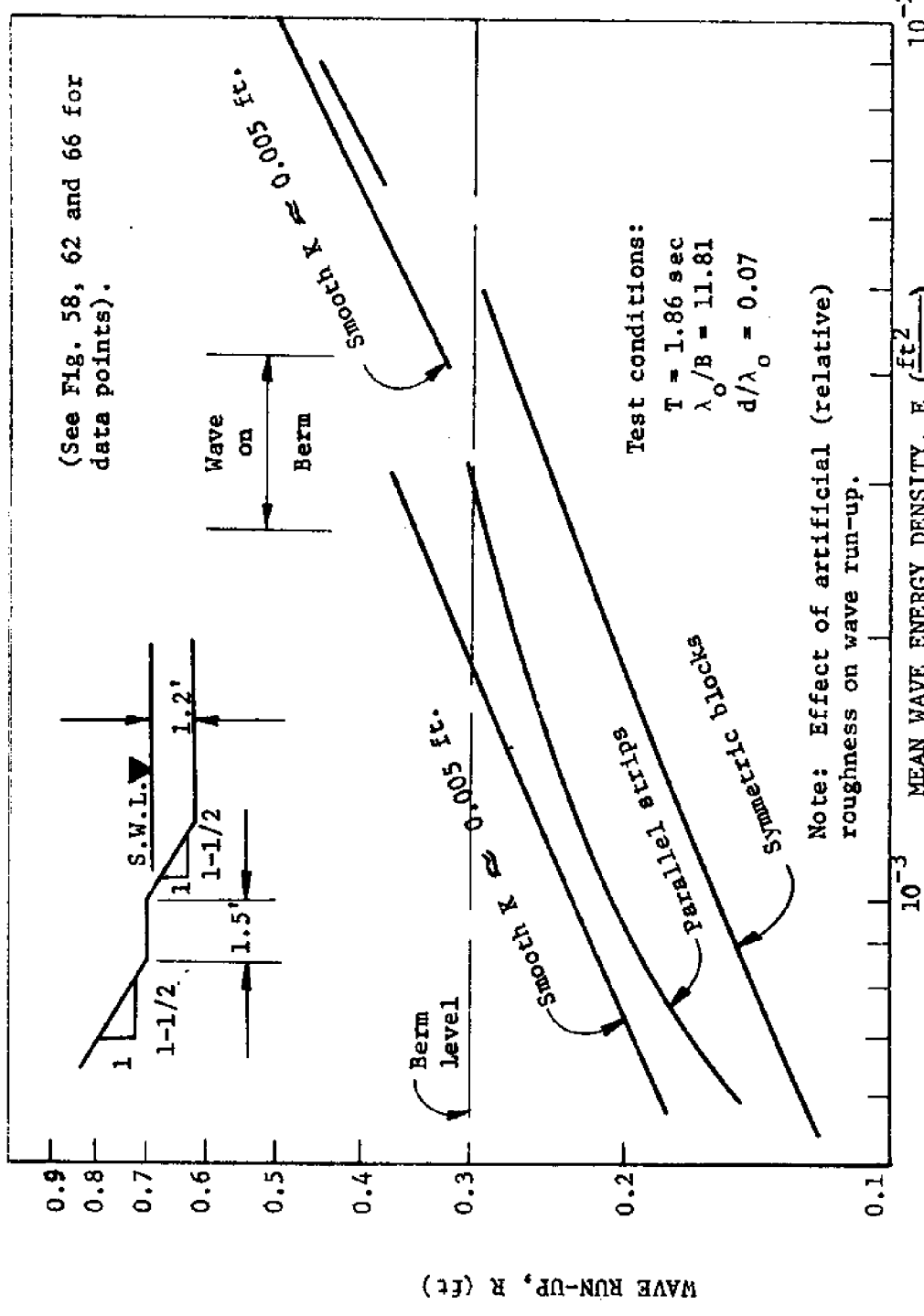

FIG. 72.--WAVE RUN-UP ON A COMPOSITE (1 ON 1-1/2 SLOPES WITH 1.5 FT BERM) SECTION (d = 1.2 ft and T = 1.86 sec)

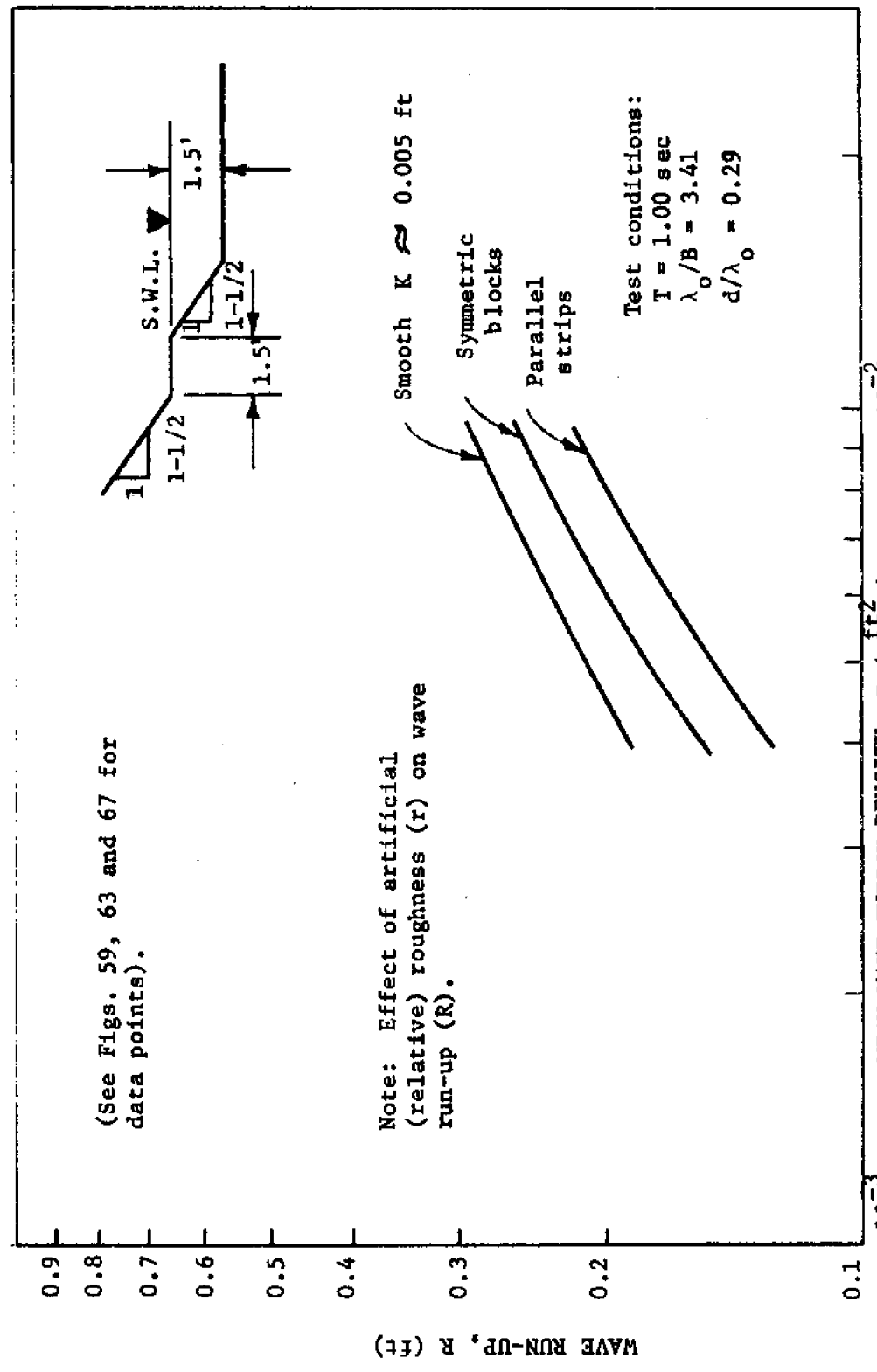

FIG. 73.--WAVE RUN-UP ON A COMPOSITE (1 ON 1-1/2 SLOPES WITH 1.5 FT BERM) SECTION (d = 1.5 ft and T = 1.00 sec)

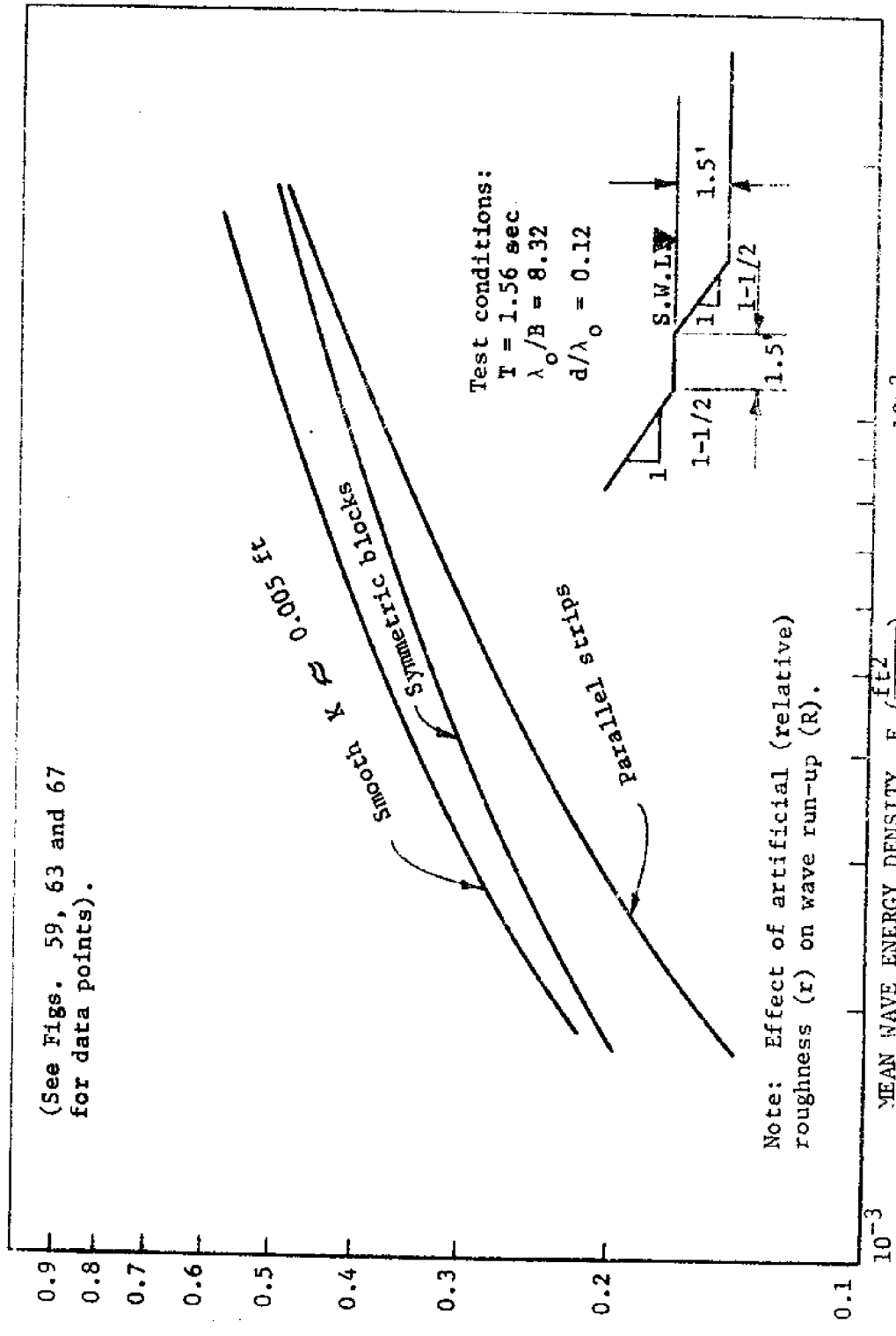

FIG. 74.--WAVE RUN-UP ON A COMPOSITE (1 ON 1-1/2 SLOPES WITH 1.5 FT BERM) SECTION (d = 1.5 ft and T = 1.56 sec)

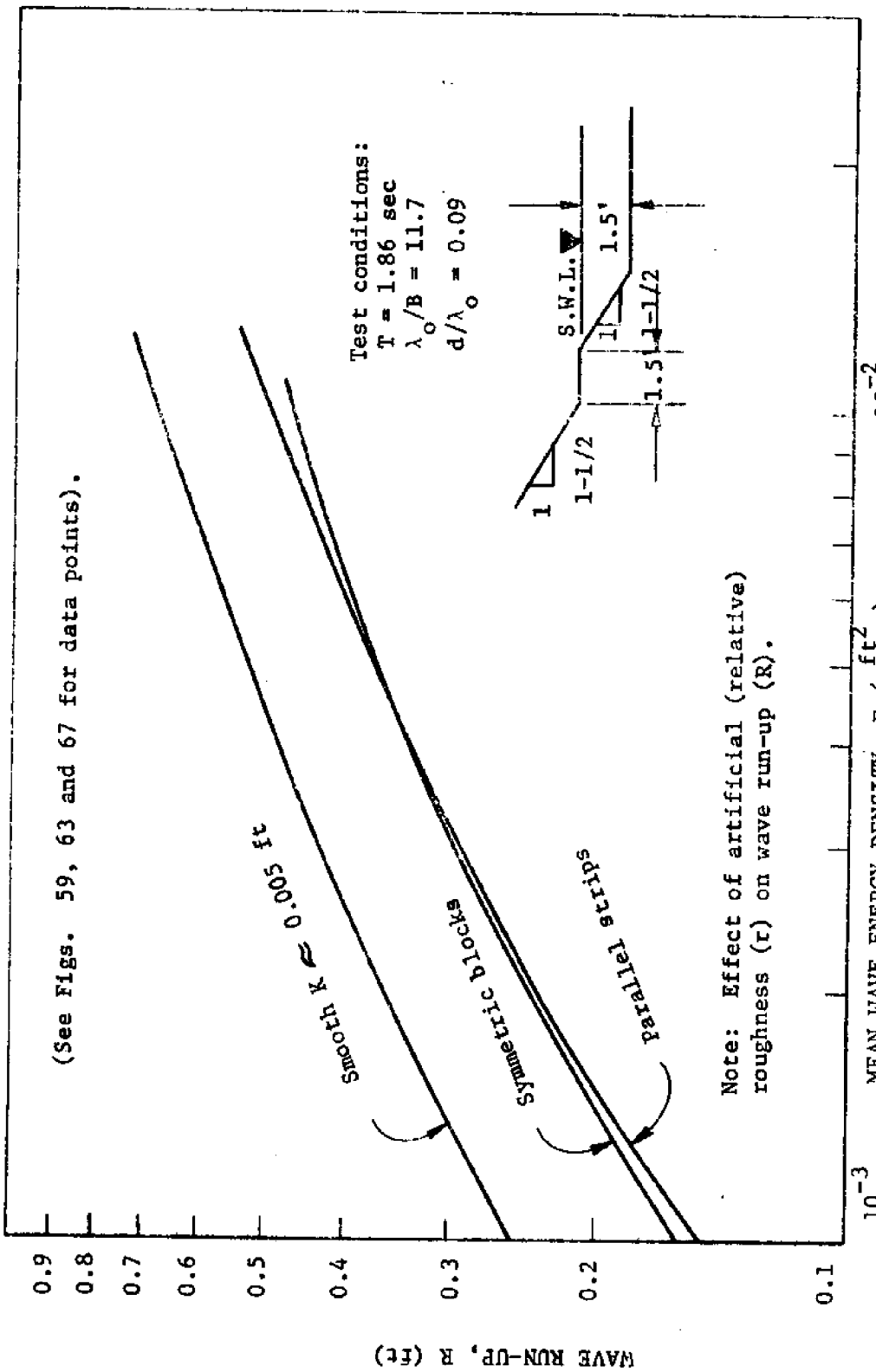

FIG. 75.--WAVE RUN-UP ON A COMPOSITE (1 ON 1-1/2 SLOPES WITH 1.5 FT BERM) SECTION (d = 1.5 ft and T = 1.86 sec)

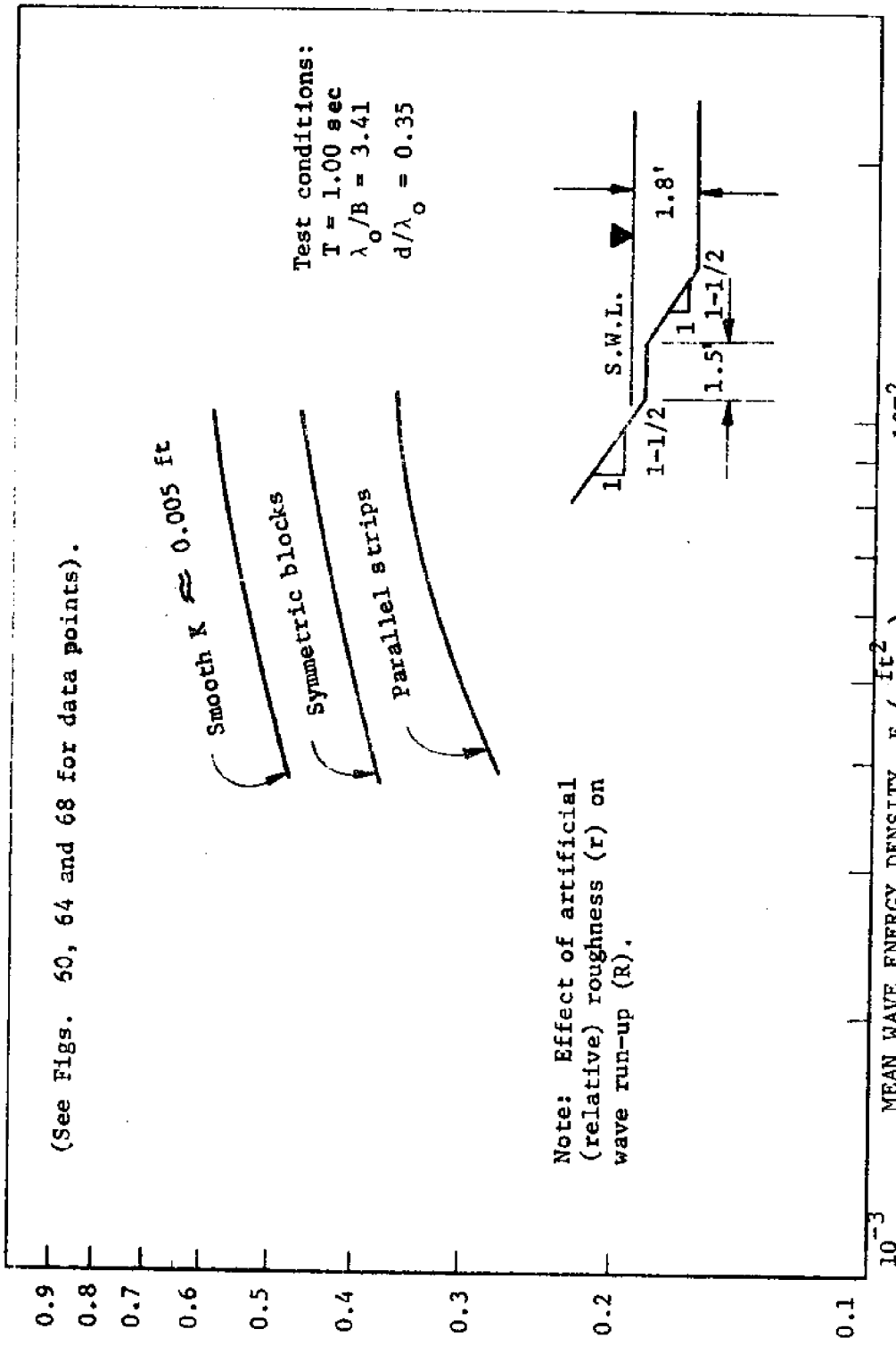

FIG. 76.--WAVE RUN-UP ON A COMPOSITE (1 ON 1-1/2 SLOPES WITH 1.5 FT BERM) SECTION (d = 1.8 ft and T = 1.00 sec)

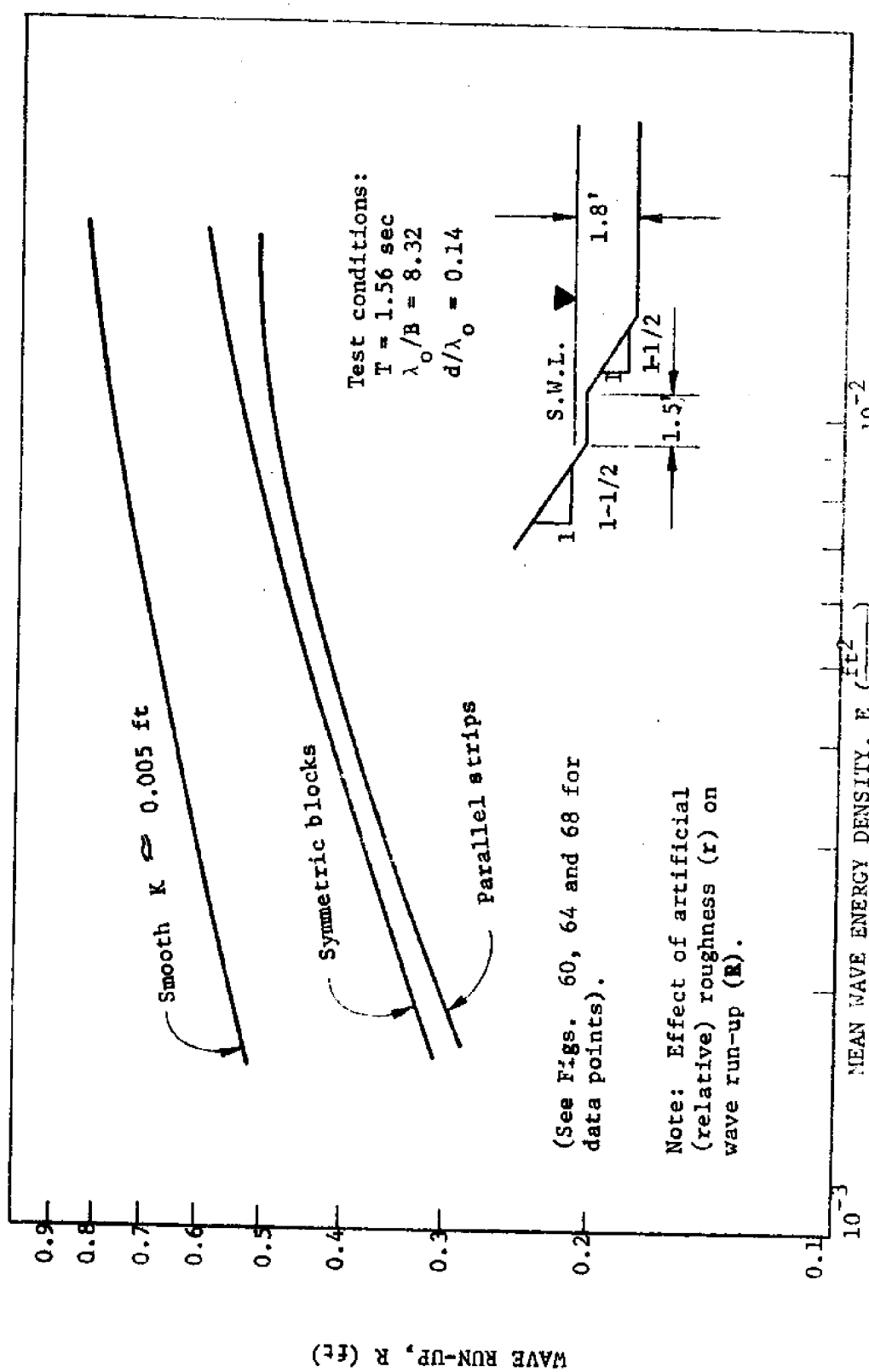

FIG. 77.--WAVE RUN-UP ON A COMPOSITE (1 ON 1-1/2 SLOPES WITH 1.5 FT BERM) SECTION (d = 1.8 ft and T = 1.56 sec)

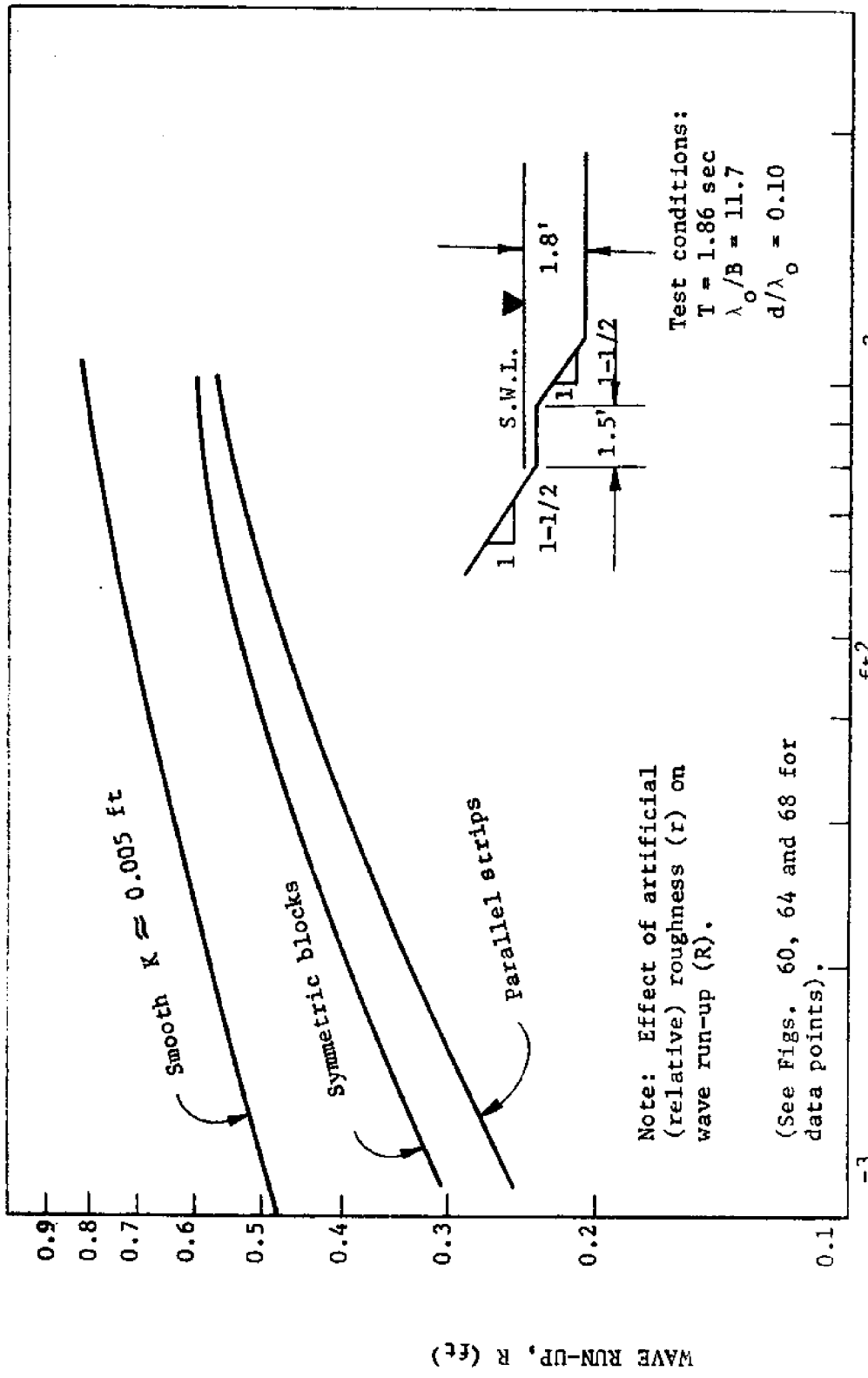

FIG. 78.--WAVE RUN-UP ON A COMPOSITE (1 ON 1-1/2) SLOPES WITH 1.5 FT BERM) SECTION (d = 1.8 ft and T = 1.86 sec)

Comparison of Coefficients of Reflection (C_r) for Artificially Roughened Composite (1 on 1-1/2 Slopes with 1.5 ft Berm) Sections with Coefficients of Reflection (C_r) on a Smooth Composite (1 on 1-1/2 Slopes with 1.5 ft Berm) Section

The effect of slope roughness (r) and berm elevation on the reflecting capability (power) of the composite (1 on 1-1/2 slopes with 1.5 ft berm) section was studied by comparing reflection data for three slope conditions and for water depths (d) of 1.2 ft, 1.5 ft and 1.8 ft (see Fig. 79). For each test condition the reflecting capability (power) of the composite section decreased as the mean wave energy density (E_μ) increased. The reflecting capability (power) of the composite section was not significantly affected by the slope roughness (C_r). In one test series, the elevation of the berm had a significant affect on the reflecting capability (power) of the composite section while in two test series the elevation of the berm did not have a significant affect on the reflecting capability (power) of the composite section. The reason for this anomaly was not determined.

Wave Energy Dissipation on a Composite (1 on 1-1/2 Smooth Slopes with 3.0 ft Berm) Section

Wave run-up (R). To establish a standard for comparison purposes and to verify the work of previous investigators, a series of wave run-up (R) tests were run using a composite (1 on 1-1/2 smooth

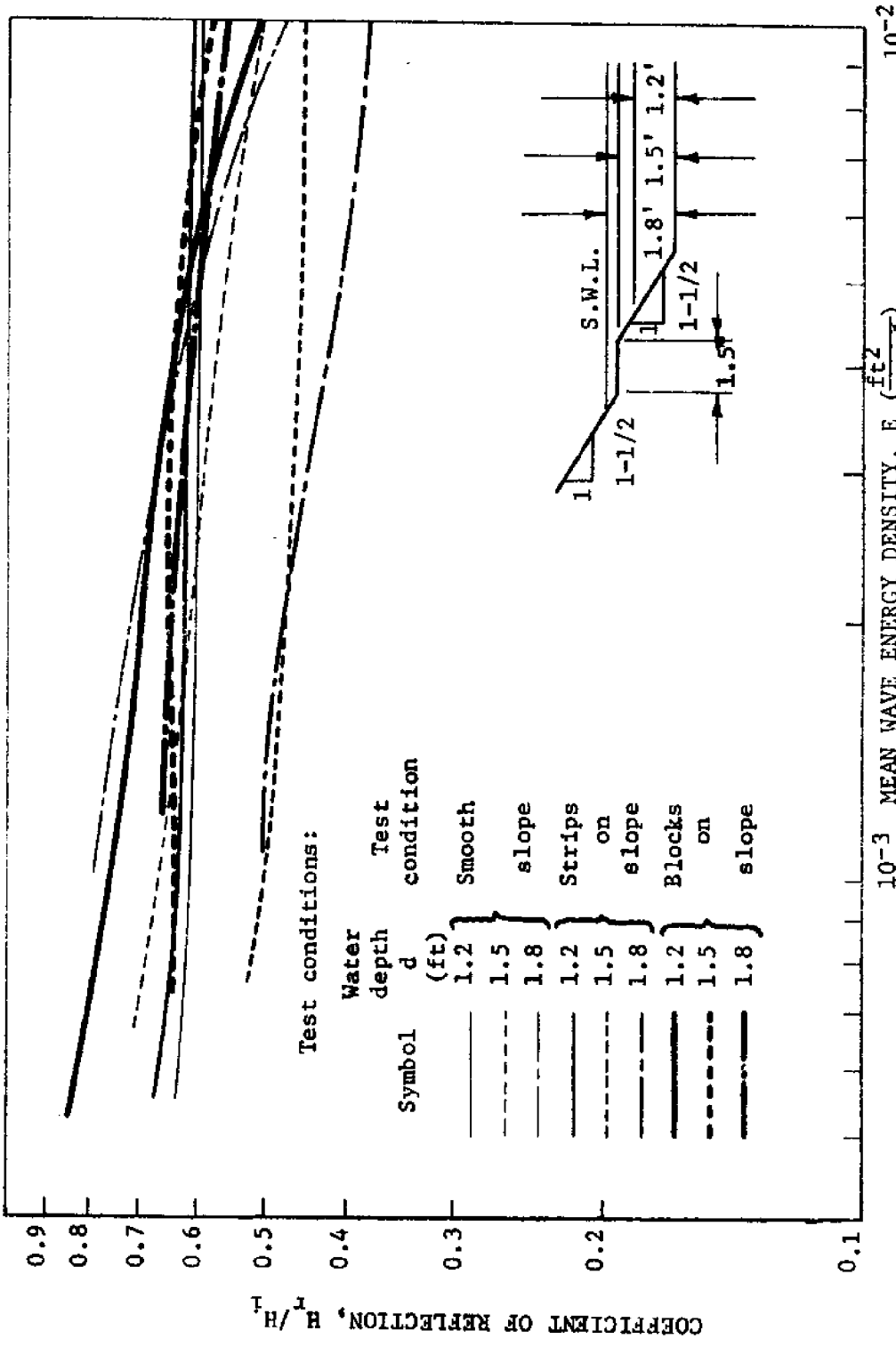

FIG. 79.--COEFFICIENT OF REFLECTION FOR SMOOTH AND ROUGHENED (BLOCKS AND STRIPS) COMPOSITE (1 ON 1-1/2 SLOPES WITH 1.5 FT BERM) SECTION

slopes with 3.0 ft berm) section. Wave run-up (R) data for both monochromatic (regular) waves and wind (irregular) waves was obtained for the composite (1 on 1-1/2 smooth slopes with 3.0 ft berm) section.

The monochromatic (regular) wave tests were run using wave periods (T) of 1.00 sec, 1.56 sec and 1.86 sec in water depths (d) of 1.2 ft, 1.5 ft and 1.8 ft. Equivalent deep water wave heights (H_o') were varied from 0.113 ft to 0.443 ft for the water depths tested [see Table 9 (Appendix III)].

The wind (irregular) wave tests were run using surface wind velocities ($V_{0.30}$) of 39.8 ft/sec, 41.3 ft/sec and 54.5 ft/sec obtained for water depths of 1.2 ft, 1.5 ft and 1.8 ft, respectively. The equivalent wave periods (T) obtained from the wave energy spectrum were 0.72 sec, 0.78 sec and 0.83 sec for water depths of 1.2 ft, 1.5 ft and 1.8 ft, respectively, while the equivalent deep water wave heights (H_e') obtained from the wave energy spectrum were, respectively, 0.340 ft, 0.342 ft and 0.396 ft [see Table 10 (Appendix III)].

The mean wave energy density (E_μ) was obtained from the wave energy spectrum for both the monochromatic (regular) waves and for the wind (irregular) waves. For the monochromatic (regular) waves the mean wave energy density (E_μ) varied from 0.0006 ft^2/sec^{-1} to 0.0165 ft^2/sec^{-1} while for the wind (irregular) waves the mean wave energy density (E_μ) varied from 0.0124 ft^2/sec^{-1} to 0.0228 ft^2/sec^{-1} [see Tables 9 and 10 (Appendix III)].

Each wave run-up (R) value was plotted as a dependent variable for its respective incident mean wave energy density (E_μ) which was

plotted as an independent variable as shown in Figs. 80, 81 and 82. Due to the nature of the monochromatic wave run-up (R) phenomena there was a distribution (scatter) of the monochromatic wave run-up (R) values for each mean wave energy density (E_μ).

For the 1.2 ft water depth the wave run-up (R) phenomena was affected by the berm as shown in Fig. 80. Between mean wave energy densities (E_μ) of 0.0006 ft^2/sec^{-1} and 0.0025 ft^2/sec^{-1} the wave run-up (R) energy was dissipated on the front slope of the composite section. Between mean wave energy densities (E_μ) of 0.0025 ft^2/sec^{-1} and 0.0062 ft^2/sec^{1} the wave run-up (R) energy was dissipated on the berm while between mean wave energy densities (E_μ) of 0.0062 and 0.0101 ft^2/sec^{-1} the wave run-up (R) energy was dissipated on the rear slope of the composite section.

For the 1.5 ft water depth the wave run-up (R) phenomena was affected by the berm as shown in Fig. 81. The wave run-up (R) was a function of the wave length (λ_o). For a constant mean wave energy density (E_μ), the highest wave run-up (R) was experienced with the longest waves tested. As the wave length (λ_o) was decreased the wave run-up (R) decreased.

For the 1.8 ft water depth the wave run-up (R) phenomena was affected by the berm as shown in Fig. 82. The wave run-up (R) was a function of the wave length (λ_o). For a constant mean wave energy density (E_μ) the highest wave run-up (R) was experienced with the longest waves tested. As the wave length (λ_o) was decreased the wave run-up (R) decreased.

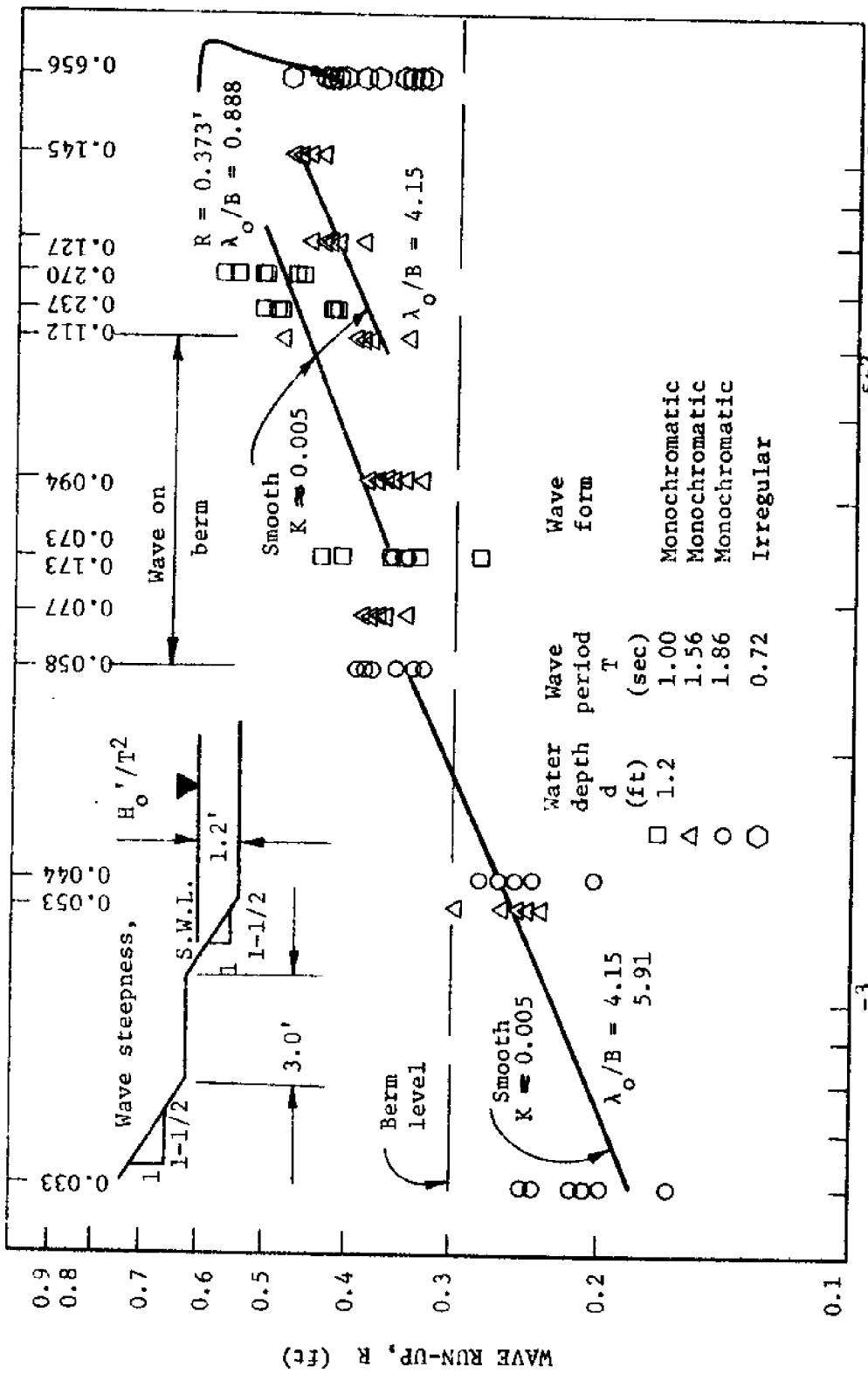

FIG. 80.--WAVE RUN-UP ON A COMPOSITE (1 ON 1-1/2 SMOOTH SLOPES WITH 3.0 FT BERM) SECTION (d = 1.2 ft)

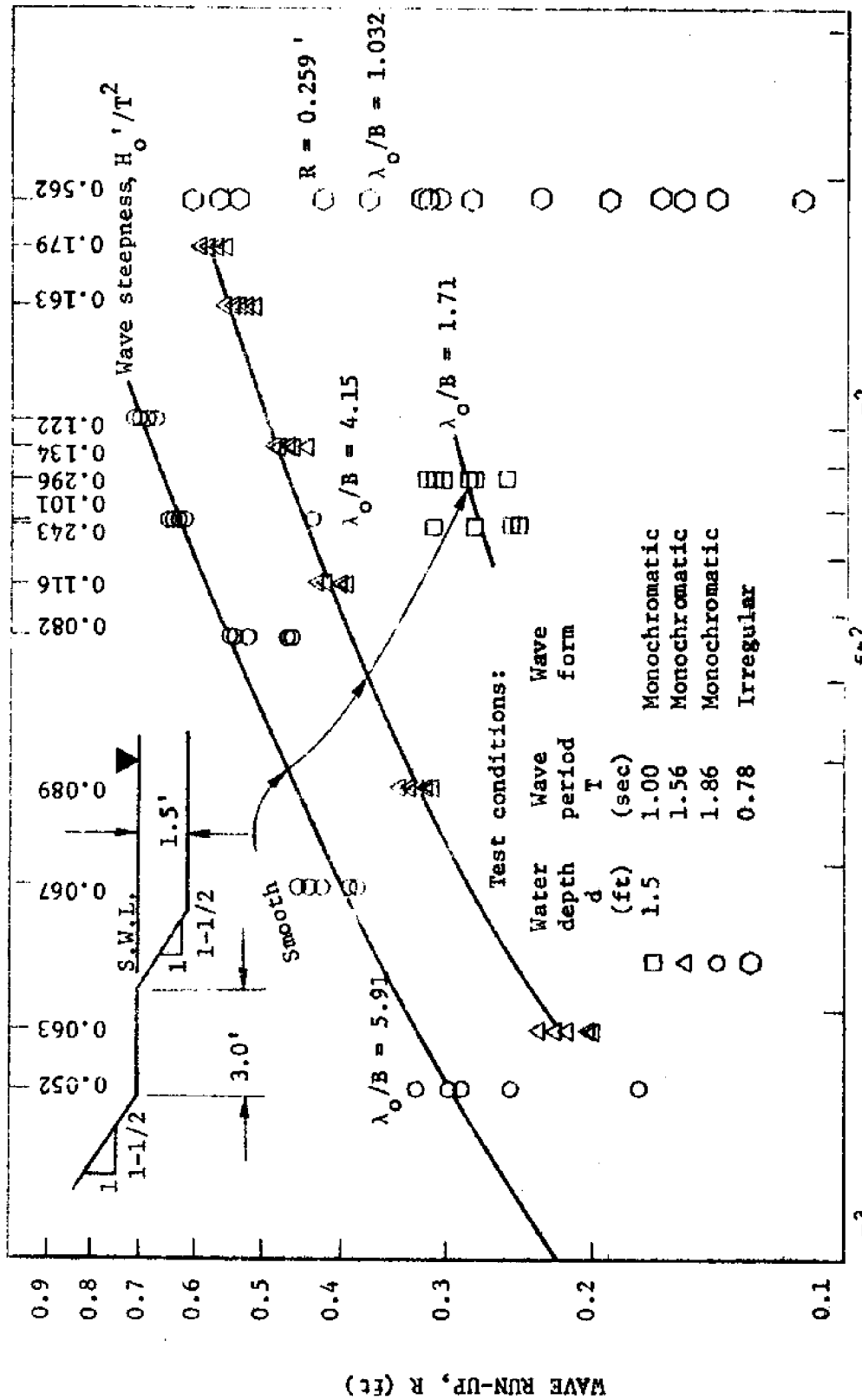

FIG. 81.--WAVE RUN-UP ON A COMPOSITE (2 ON 1-1/2 SMOOTH SLOPES WITH 3.0 FT BERM) SECTION (d = 1.5 ft)

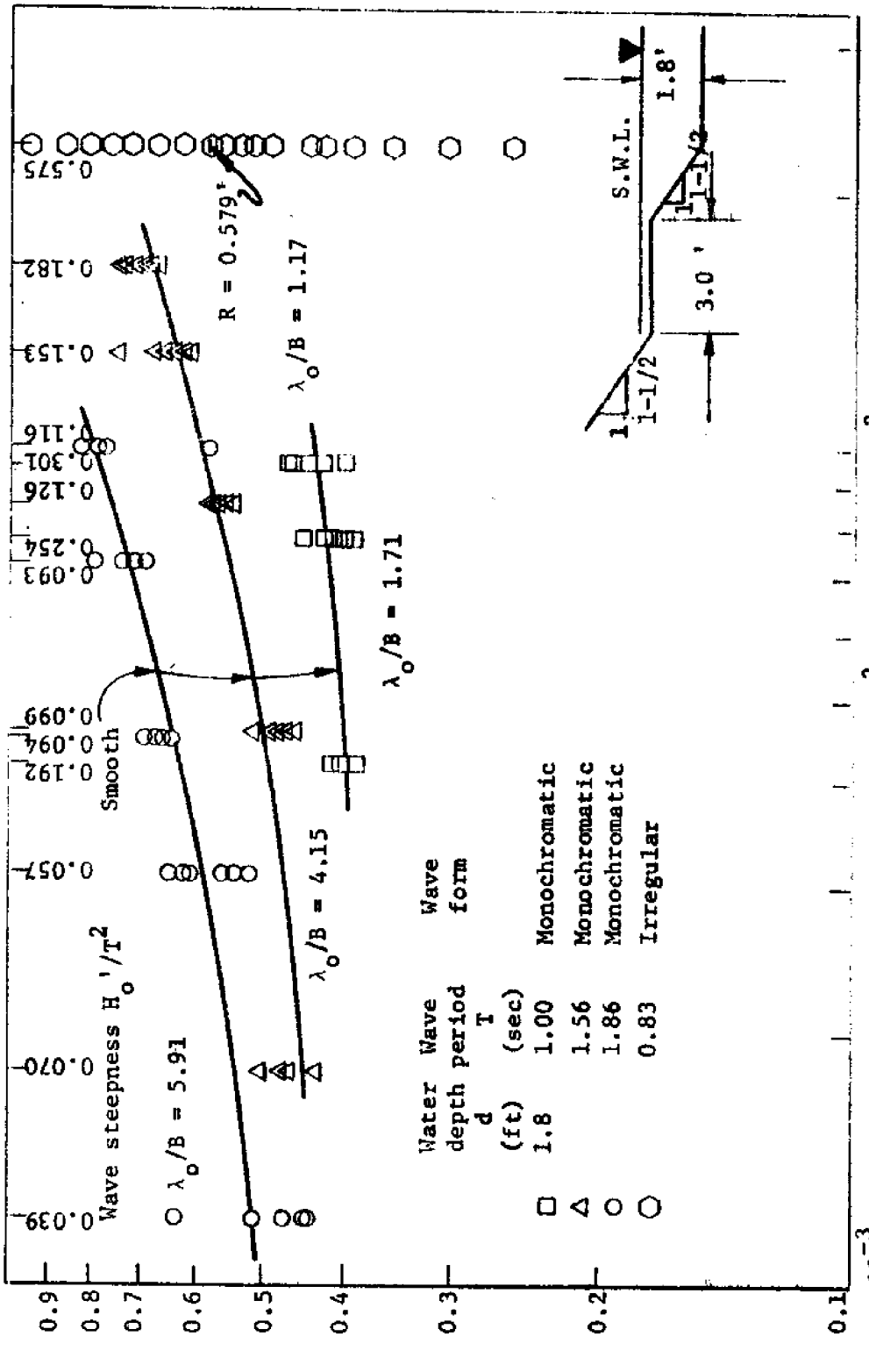

FIG. 82.--WAVE RUN-UP ON A COMPOSITE ($\frac{1}{d}$ ON 1-1/2 SMOOTH SLOPES WITH 3.0 FT BERM) SECTION
($d = 1.8$ ft)

Wave reflection. To establish a standard for comparison purposes and to determine the reflecting capability (power) of a composite (1 on 1-1/2 smooth slopes with 3.0 ft berm) section, a series of wave reflection (H_r/H_i) tests were run using monochromatic (regular) waves.

The wave reflection tests were run using wave periods (T) of 1.00 sec, 1.56 sec and 1.86 sec in water depths of 1.2 ft, 1.5 ft and 1.8 ft. Equivalent deep water wave heights (H_o') were varied from 0.113 ft to 0.443 ft while the mean wave energy densities (E_μ) varied from 0.0006 ft^2/sec^{-1} to 0.0165 ft^2/sec^{-1}, respectively, for the water depths tested [see Table 9 (Appendix III)].

The reflecting capability (power) of the composite (1 on 1-1/2 smooth slopes with 3.0 ft berm) section was evaluated from wave records obtained by moving the instrument carriage containing the wave height sensor through a train of waves to obtain the incident and reflected wave heights. A reflecting coefficient (ratio of the reflected wave height to the incident wave height) was calculated for each test run [see Table 14 (Appendix V)]. Each reflecting coefficient (*i.e.*, coefficient of reflection) value ($C_r = H_r/H_i$) was plotted as a dependent variable for its respective incident mean wave energy density (E_μ) which was plotted as an independent variable as shown in Fig. 83.

The reflecting capability (power) of the composite section decreased as the mean wave energy density (E_μ) increased. As the mean wave energy density (E_μ) increased from 0.001 ft^2/sec^{-1} to 0.01

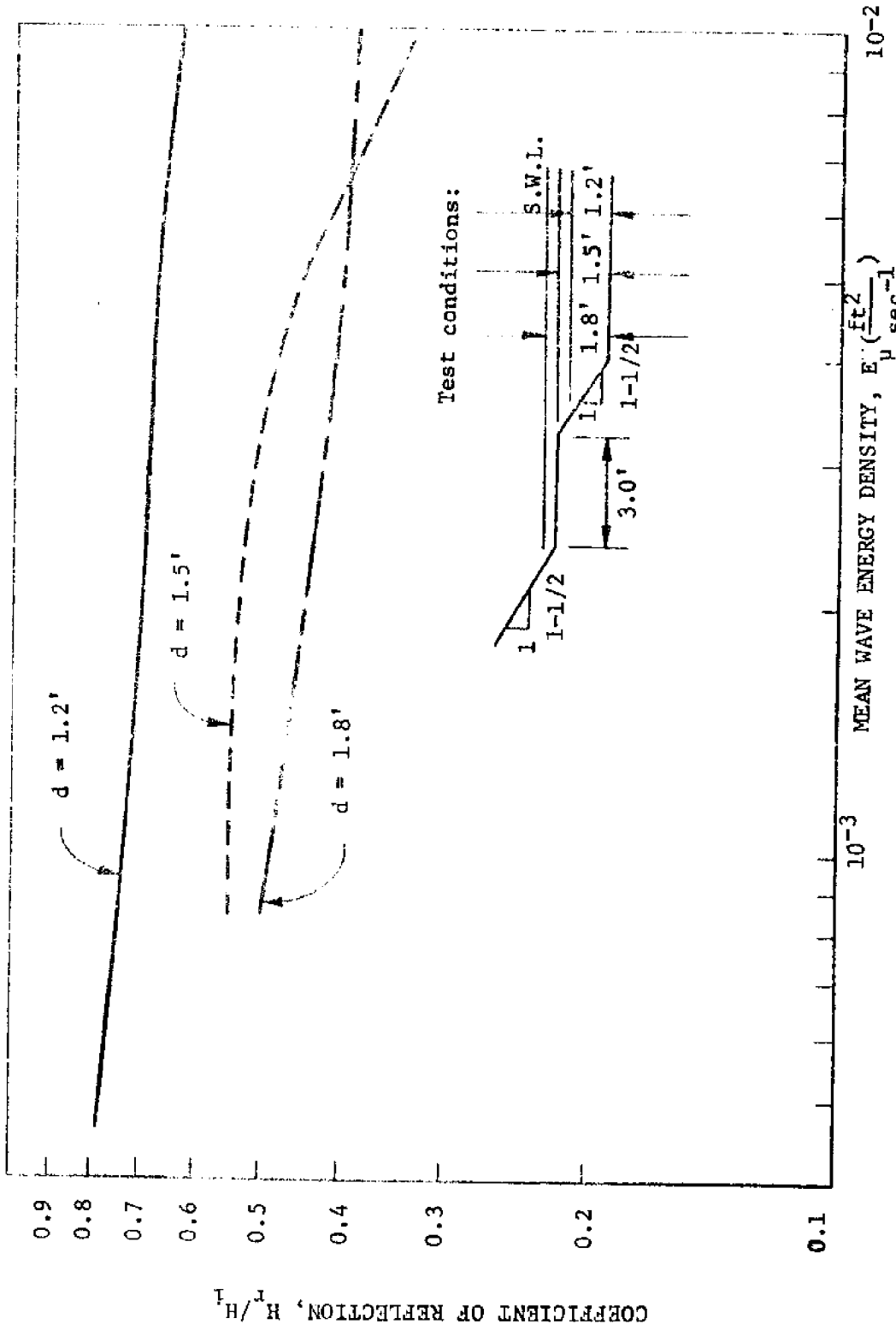

FIG. 83.--COEFFICIENT OF REFLECTION FOR A COMPOSITE (1 ON 1-1/2 SMOOTH SLOPES WITH 3.0 FT BERM) (d = 1.2, 1.5 and 1.8 ft)

ft^2/sec^{-1}, the coefficient of reflection for the 1.2 ft water depth decreased approximately 10 per cent while for the 1.5 ft and 1.8 ft water depths the decrease was, respectively, 22 per cent and 9 per cent.

Physical observations. The following significant observations were made and recorded during testing:

1. The leading edge of the wave run-up (R) was observed to be irregular.

2. The phenomena of transverse waves was unexpectedly (and unavoidably) observed at various times during testing although the wave lengths tested were not harmonics of the wave flume width.

3. Wave reflection was observed in the flume shortly after the leading wave was reflected.

4. A water 'set-up' was observed in the wave flume during the testing using the wind (irregular) waves.

5. A considerable spray up the slope was observed during the wave run-up (R) tests using the wind (irregular) wave generator even though the 'venturi' effect was eliminated by providing a comparable flow way above the slope.

6. For the long waves a vortex was generated on the forward slope (below the berm elevation) due to the collision of the breaking wave and the back-wash from the berm.

7. Five different wave run-up (R) cases were noted. These cases were discussed in detail by Herbich [14].

Wave Energy Dissipation on a Composite [1 on 1-1/2 Roughened (Strips) Slopes with a 3.0 ft Berm] Section

Wave run-up (R). To determine the effects of slope roughness on wave run-up (see objectives 1 and 4), a series of tests were run using a composite (1 on 1-1/2 slopes with 3.0 ft berm) section containing parallel surface strips. Wave run-up (R) data for both monochromatic (regular) waves and wind (irregular) waves was obtained for the roughened slope configuration.

The monochromatic (regular) wave tests were run using wave periods (T) of 1.00 sec, 1.56 sec and 1.86 sec in water depths (d) of 1.2 ft, 1.5 ft and 1.8 ft. Equivalent deep water wave heights (H_o') were varied from 0.113 ft to 0.443 ft for the wave depths tested [see Table 9 (Appendix III)].

The wind (irregular) wave tests were run using surface wind velocities ($V_{0.30}$) of 39.8 ft/sec, 41.3 ft/sec and 54.5 ft/sec obtained for water depths of 1.2 ft, 1.5 ft and 1.8 ft, respectively. The equivalent wave periods (T) obtained from the wave energy spectrum were 0.72 sec, 0.72 sec and 0.83 sec for water depths of 1.2 ft, 1.5 ft and 1.8 ft, respectively, while the equivalent deep water wave heights (H_e') obtained from the wave energy spectrum were, respectively, 0.290 ft, 0.349 ft and 0.361 ft [see Table 10 (Appendix III)].

The mean wave energy density (E_μ) was obtained from the wave energy spectrum for both the monochromatic (regular) waves and for

the wind (irregular) waves. For the monochromatic (regular) waves the mean wave energy density (E_μ) varied from 0.0006 ft^2/sec^{-1} to 0.0165 ft^2/sec^{-1}, while for the wind (irregular) waves the mean wave energy density (E_μ) varied from 0.0100 ft^2/sec^{-1} to 0.0224 ft^2/sec^{-1} [see Tables 9 and 10 (Appendix III)].

Each wave run-up (R) value was plotted as a dependent variable for its respective incident mean wave energy density (E_μ) which was plotted as an independent variable as shown in Figs. 84, 85 and 86. Due to the nature of the monochromatic wave run-up (R) phenomena there was a distribution (scatter) of the monochromatic wave run-up (R) values for each mean wave energy density (E_μ).

For the 1.2 ft water depth the wave run-up (R) phenomena was affected by the berm as shown in Fig. 84. Between mean wave energy densities (E_μ) of 0.0006 ft^2/sec^{-1} and 0.0042 ft^2/sec^{-1} the wave energy was dissipated on the front slope. Between mean wave energy densities (E_μ) of 0.0042 ft^2/sec^{-1} and 0.0090 ft^2/sec^{-1} the wave run-up (R) energy was dissipated on the berm while between mean wave energy densities (E_μ) of 0.0090 ft^2/sec^{-1} and 0.0101 ft^2/sec^{-1} the wave run-up (R) energy was dissipated on the rear slope of the composite section.

For the 1.5 ft and 1.8 ft water depths the wave run-up (R) phenomena was affected by the berm as shown in Figs. 85 and 86. For each depth the wave run-up (R) was a function of the wave length (λ_o). For a constant mean wave energy density (E_μ) for each depth, the highest wave run-up (R) was experienced with the longest waves

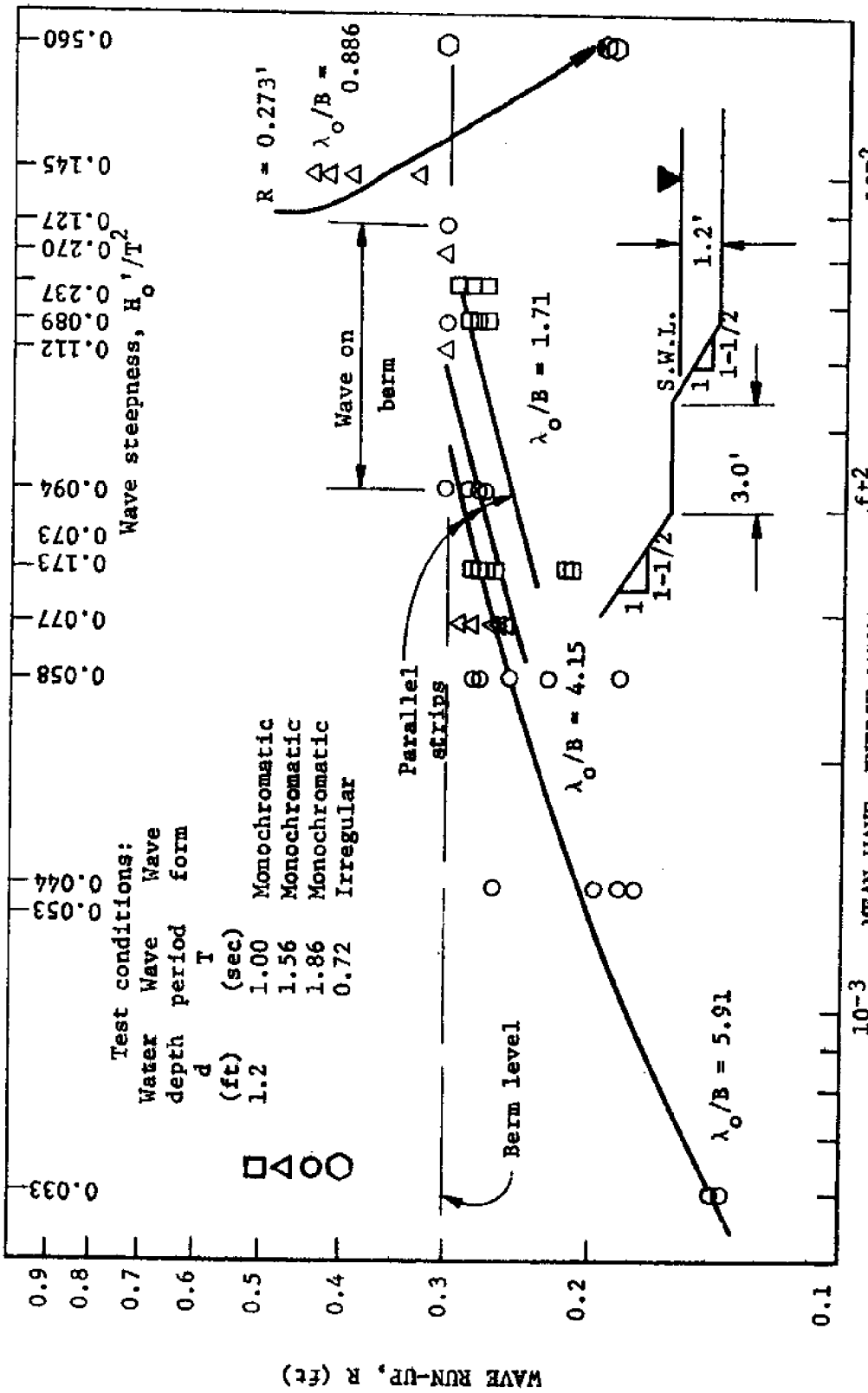

FIG. 84.--WAVE RUN-UP ON A COMPOSITE (1 ON 1-1/2 ROUGHENED (STRIPS) SLOPES WITH 3.0 FT BERM) SECTION (d = 1.2 ft)

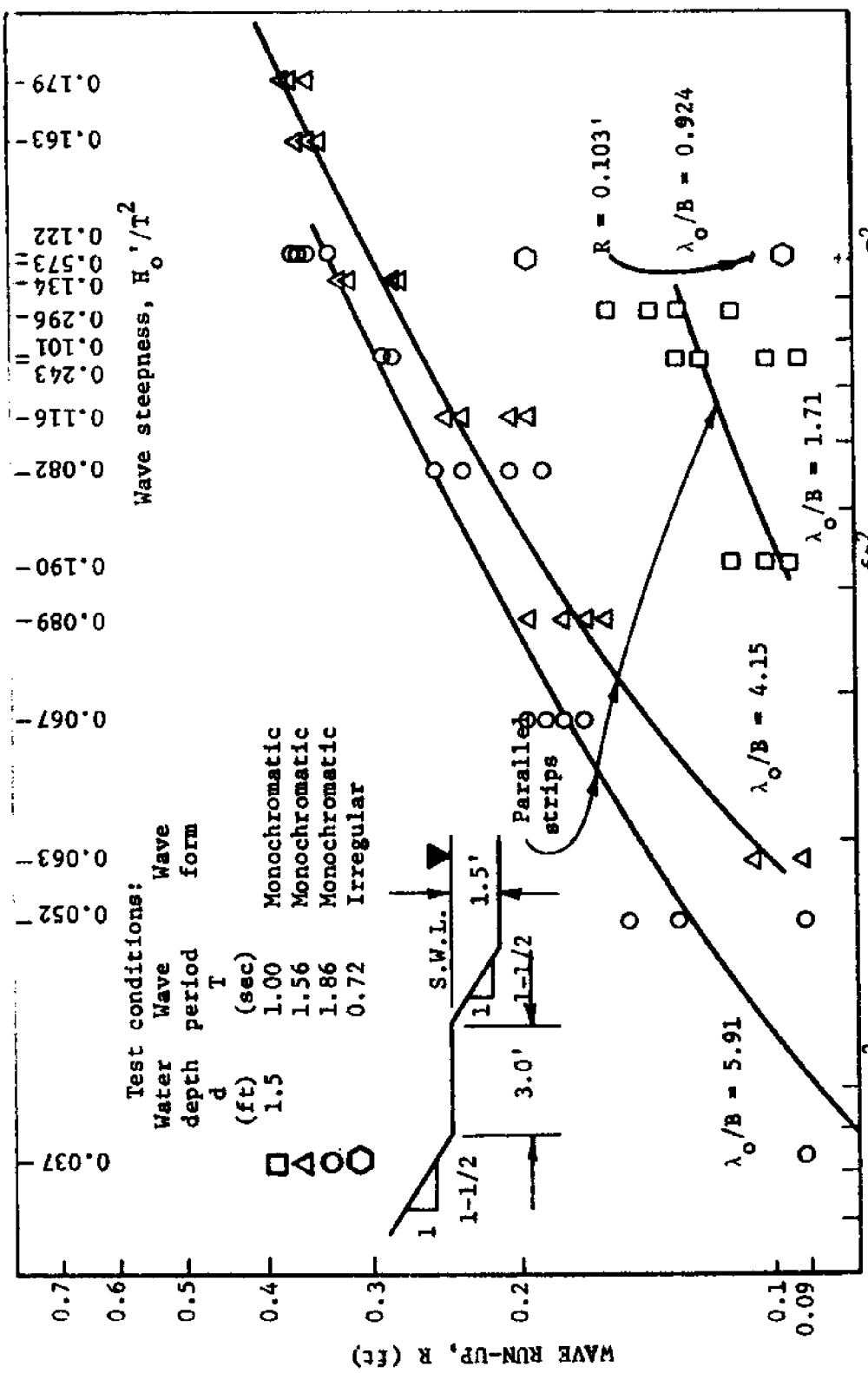

FIG. 85.--WAVE RUN-UP ON A COMPOSITE (1 ON 1-1/2 ROUGHENED (STRIPS) SLOPES WITH 3.0 FT BERM) SECTION (d = 1.5 ft)

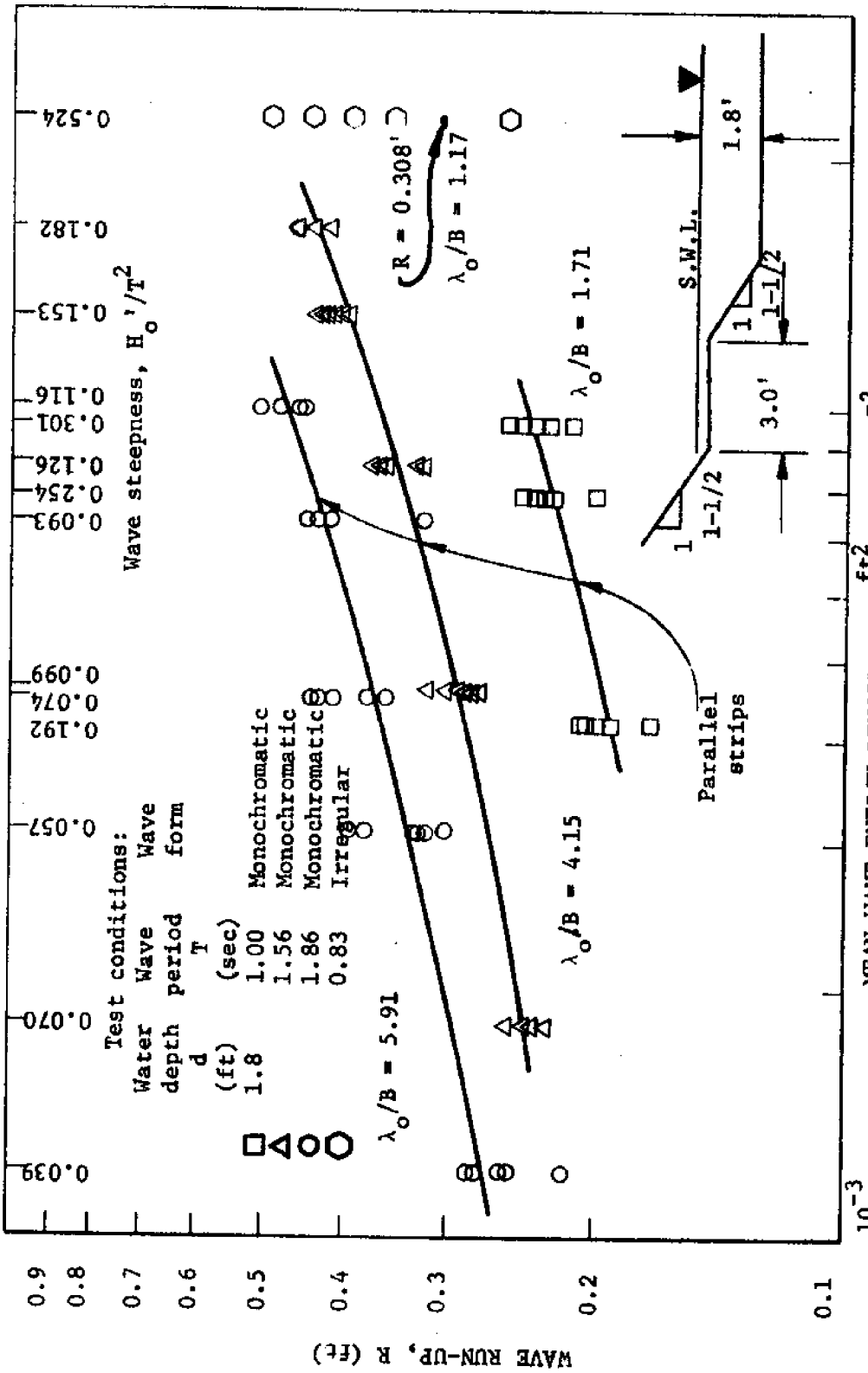

FIG. 86.--WAVE RUN-UP ON A COMPOSITE (1 ON 1-1/2 ROUGHENED (STRIPS) SLOPES WITH 3.0 FT BERM) SECTION (d= 1.8 ft)

tested. As the wave length (λ_o) was decreased the wave run-up (R) was decreased.

Wave reflection. To determine the effects of slope roughness on the reflecting capability (power) of a composite (1 on 1-1/2 slopes with 3.0 ft berm) section containing parallel surface strips, a series of wave reflection (H_r/H_i) tests were run using monochromatic (regular) waves.

The wave reflection tests were run using wave periods (T) of 1.00 sec, 1.56 sec and 1.86 sec in water depths of 1.2 ft, 1.5 ft and 1.8 ft. Equivalent deep water wave heights (H_o') were varied from 0.113 ft to 0.443 ft while the mean wave energy densities (E_μ) varied from 0.0006 ft^2/sec^{-1} to 0.0164 ft^2/sec^{-1}, respectively, for the water depths tested [see Table 9 (Appendix III)].

The reflecting capability (power) of the composite (1 on 1-1/2 slopes with 3.0 ft berm) section containing parallel strips was evaluated from wave records obtained by moving the instrument carriage containing the wave height sensor through a train of waves to obtain the incident and reflected wave heights. A reflecting coefficient (ratio of the reflected wave height to the incident wave height) was calculated for each test run [see Table 14 (Appendix V)]. Each reflecting coefficient (*i.e.*, coefficient of reflection) value ($C_r = H_r/H_i$) was plotted as a dependent variable for its respective incident mean wave energy density (E_μ) which was plotted as an independent variable as shown in Fig. 87.

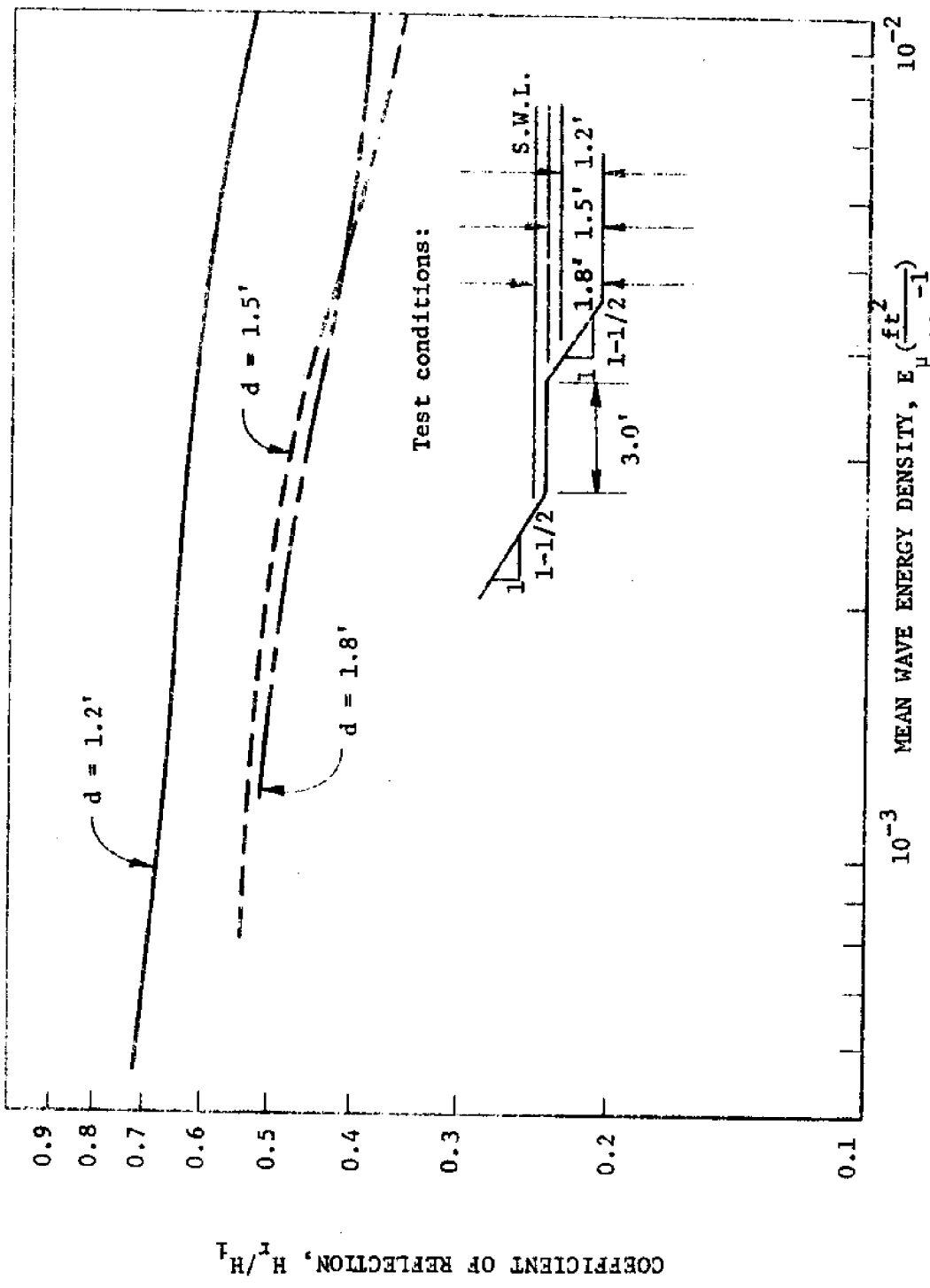

FIG. 87.—COEFFICIENT OF REFLECTION FOR A COMPOSITE (1 ON 1-1/2 ROUGHENED (STRIPS) SLOPES WITH 3.0 FT BERM) SECTION (d = 1.2, 1.5 and 1.8 ft)

The reflecting capability (power) of the composite section decreased as the mean wave energy density (E_μ) increased. As the mean wave energy density (E_μ) increased from 0.001 ft^2/sec^{-1} to 0.01 ft^2/sec^{-1} the coefficient of reflection for the 1.2 ft water depth decreased approximately 15 per cent while for the 1.5 ft and 1.8 ft water depths the decrease was, respectively, 18 per cent and 13 per cent.

Physical observations. The following significant observations were made and recorded during testing:

1. The leading edge of the wave run-up (R) was observed to be irregular on the lower slope.

2. The phenomena of transverse waves was unexpectedly (and unavoidably) observed at various times during testing although the wave lengths tested were not harmonics of the wave flume width.

3. Wave reflection was observed in the flume shortly after the leading wave was reflected.

4. A water 'set-up' was observed in the wave flume during the testing using the wind (irregular) waves.

5. A considerable spray up the slope was observed during the wave run-up (R) tests using the wind (irregular) wave generator even though the 'venturi' effect was eliminated by providing a comparable flow way above the slope.

6. For the long waves a vortex was generated on the forward slope (below the berm elevation) due to the collision of the breaking wave and the backwash from the berm.

7. Five different wave run-up (R) cases were noted. These cases were discussed in detail by Herbich[14].

The following methods of energy dissipation were observed during testing:

1. Dissipation of energy by wave front collision with the vertical face of the upslope strip.
2. Dissipation of energy by vortices (turbulence) generated by the strips.
3. Dissipation of energy by air entrainment (heterogeneous mixing of air and water) caused by the strips.
4. Dissipation of energy by waves breaking on the structure (breaking occurred at the break in slope).
5. Dissipation of energy by opposing backwash (water running back across the berm over the strips).

Wave Energy Dissipation on a Composite [1 on 1-1/2 Roughened (Blocks) Slopes with a 3.0 ft Berm] Section

Wave run-up (R). To determine the effects of slope roughness on wave run-up (see objectives 1 and 4), a series of tests were run using a composite (1 on 1-1/2 slopes with 3.0 ft berm) section containing a symmetric pattern of surface blocks. Wave run-up (R) data for both monochromatic (regular) waves and wind (irregular) waves was obtained for the roughened slope configuration.

The monochromatic (regular) wave tests were run using wave periods (T) of 1.00 sec, 1.56 sec and 1.86 sec in water depths (d) of 1.2 ft, 1.5 ft and 1.8 ft. Equivalent deep water wave heights (H_o') were varied from 0.113 ft to 0.443 ft for the water depths tested [see Table 9(Appendix III)].

The wind (irregular) wave tests were run using surface wind velocities ($V_{0.30}$) of 39.8 ft/sec, 41.3 ft/sec and 54.5 ft/sec obtained for water depths of 1.2 ft, 1.5 ft and 1.8 ft, respectively. The equivalent wave periods (T) obtained from the wave energy spectrum were 0.72 sec, 0.72 sec and 0.83 sec for water depths of 1.2 ft, 1.5 ft and 1.8 ft, respectively, while the equivalent deep water wave heights (H_e') obtained from the wave energy spectrum were, respectively, 0.290 ft, 0.349 ft and 0.361 ft [see Table 10 (Appendix III)].

The mean wave energy density (E_μ) was obtained from the wave energy spectrum for both the monochromatic (regular) waves and for the wind (irregular) waves. For the monochromatic (regular) waves the mean wave energy density (E_μ) varied from 0.0006 ft^2/sec^{-1} to 0.0165 ft^2/sec^{-1} while for the wind (irregular) waves the mean wave energy density (E_μ) varied from 0.0100 ft^2/sec^{-1} to 0.0224 ft^2/sec^{-1} [see Tables 9 and 10 (Appendix III)].

Each wave run-up (R) value was plotted as a dependent variable for its respective incident mean wave energy density (E_μ) which was plotted as an independent variable as shown in Figs. 88, 89 and 90. Due to the nature of the monochromatic wave run-up (R) phenomena there was a distribution (scatter) of the monochromatic wave run-up (R) values for each mean wave energy density (E_μ).

For the 1.2 ft water depth the wave run-up (R) phenomena was affected by the berm as shown in Fig. 88. Between mean wave energy densities (E_μ) of 0.0006 ft^2/sec^{-1} and 0.0034 ft^2/sec^{-1} the wave

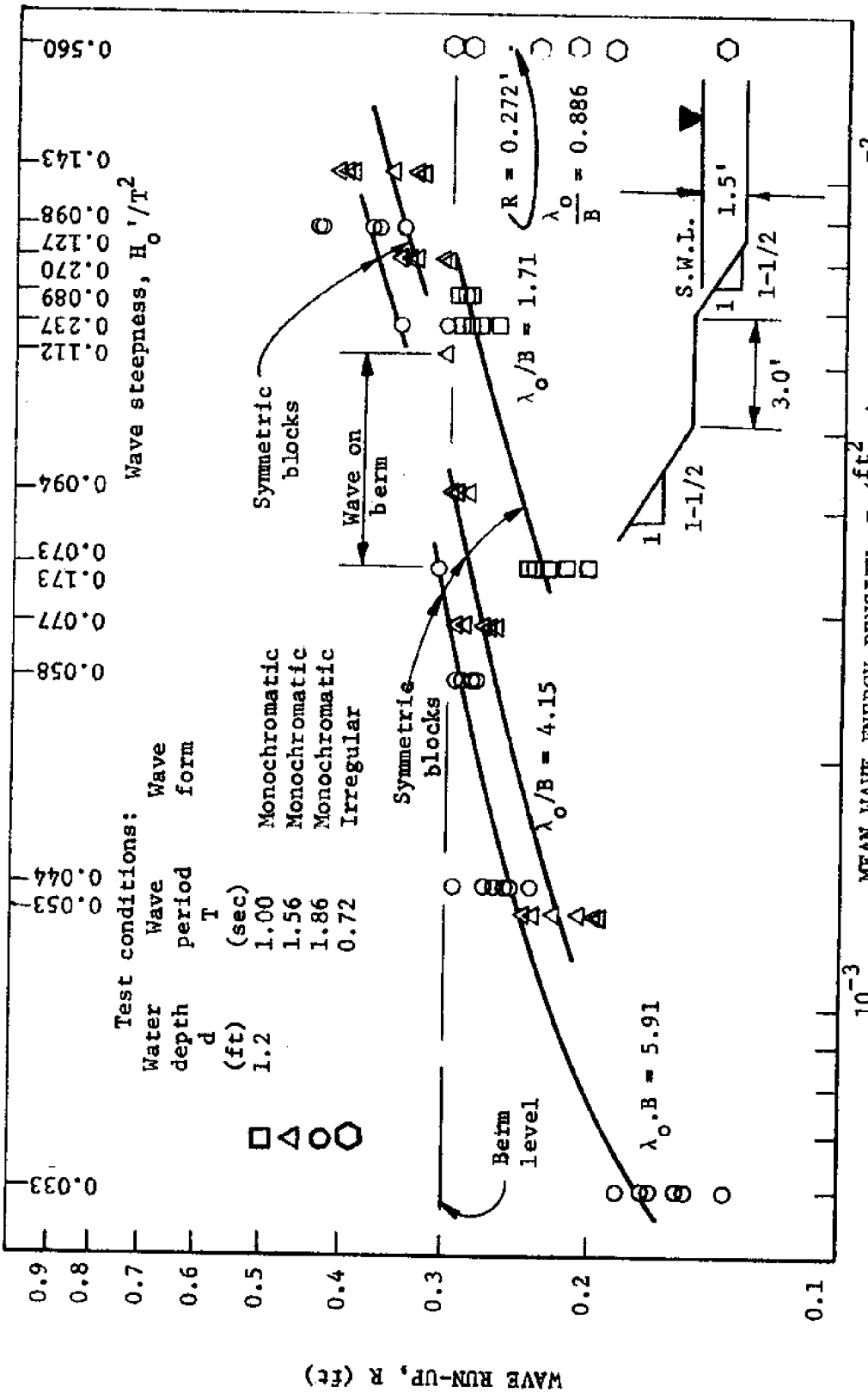

FIG. 88.--WAVE RUN-UP ON A COMPOSITE (1 ON 1-1/2 ROUGHENED (BLOCKS) SLOPES WITH 3.0 FT BERM) SECTION (d = 1.2 ft)

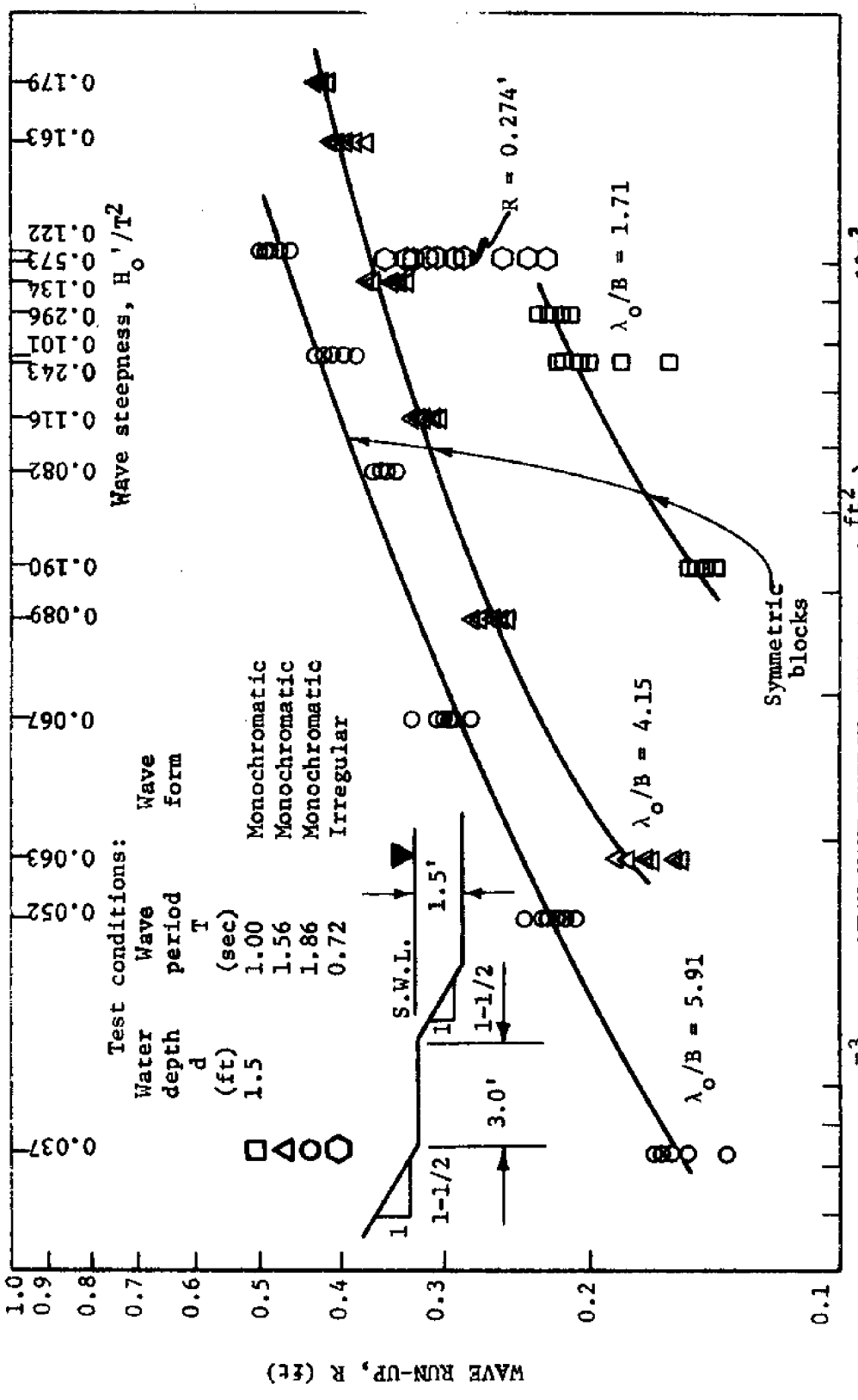

FIG. 89.--WAVE RUN-UP ON A COMPOSITE (1 ON 1-1/2 ROUGHENED (BLOCKS) SLOPES WITH 3.0 FT BERM) SECTION (d = 1.5 ft)

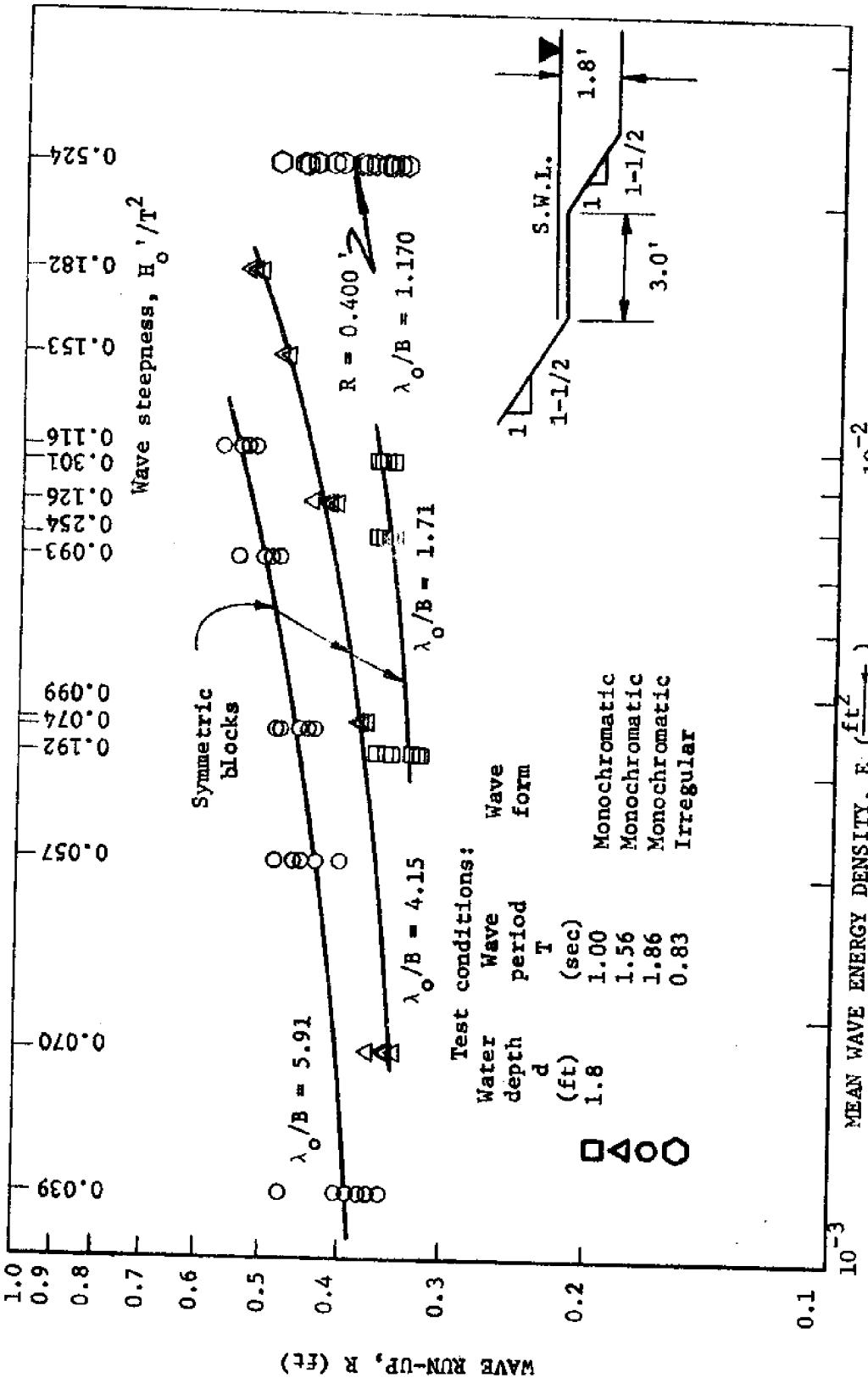

FIG. 90.--WAVE RUN-UP ON A COMPOSITE (1 ON 1-1/2 ROUGHENED (BLOCKS) SLOPES WITH 3.0 FT BERM) SECTION (d = 1.8 ft)

run-up (R) energy was dissipated on the front slope of the composite section. Between mean wave energy densities (E_μ) of 0.0034 ft^2/sec^{-1} and 0.0062 ft^2/sec^{-1} the wave run-up (R) energy was dissipated on the berm while between mean wave energy densities (E_μ) of 0.0062 ft^2/sec^{-1} and 0.0101 ft^2/sec^{-1} the wave run-up (R) energy was dissipated on the rear slope of the composite section.

For the 1.5 ft and 1.8 ft water depths the wave run-up (R) phenomena was affected by the berm as shown in Figs. 89 and 90. The wave run-up (R) was a function of the wave length (λ_o). For a constant mean wave energy density (E_μ) for each depth, the highest wave run-up (R) was experienced with the longest waves tested. As the wave length (λ_o) was decreased the wave run-up (R) was decreased.

Wave reflection. To determine the effects of slope roughness on the reflecting capability (power) of a composite (1 on 1-1/2 slopes with 3.0 ft berm) section containing a symmetric pattern of blocks, a series of wave reflection (H_r/H_i) tests were run using monochromatic (regular) waves.

The wave reflection tests were run using wave periods (T) of 1.00 sec, 1.56 sec and 1.86 sec in water depths of 1.2 ft, 1.5 ft and 1.8 ft. Equivalent deep water wave heights (H_o') were varied from 0.113 ft to 0.443 ft while the mean wave energy densities (E_μ) varied from 0.0006 ft^2/sec^{-1} to 0.0165 ft^2/sec^{-1}, respectively, for the water depths tested [see Table 9 (Appendix III)].

The reflecting capability (power) of the composite (1 on 1-1/2 slopes with 3.0 ft berm) section containing a symmetric pattern of

blocks was evaluated from wave records obtained by moving the instrument carriage containing the wave height sensor through a train of waves to obtain the incident and reflected wave heights. A reflecting coefficient (ratio of the reflected wave height to the incident wave height) was calculated for each test run [see Table 14 (Appendix V)]. Each reflecting coefficient (*i.e.*, coefficient of reflection) value ($C_r = H_r/H_i$) was plotted as a dependent variable for its respective incident mean wave energy density (E_μ) which was plotted as an independent variable as shown in Fig. 91.

The reflecting capability (power) of the composite section decreased as the mean wave energy density (E_μ) increased. As the mean wave energy density (E_μ) increased from 0.001 ft^2/sec^{-1} to 0.01 ft^2/sec^{-1} the coefficient of reflection for the 1.2 ft water depth decreased approximately 16 per cent while for the 1.5 ft and 1.8 ft water depths the decrease was, respectively 16 per cent and 17 per cent.

Physical observations. The following significant observations were made and recorded during testing:

1. The leading edge of the wave run-up (R) was observed to be irregular.

2. The phenomena of transverse waves was unexpectedly (and unavoidably) observed at various times during testing although the wave lengths tested were not harmonics of the wave flume width.

3. Wave reflection was observed in the flume shortly after the leading wave was reflected.

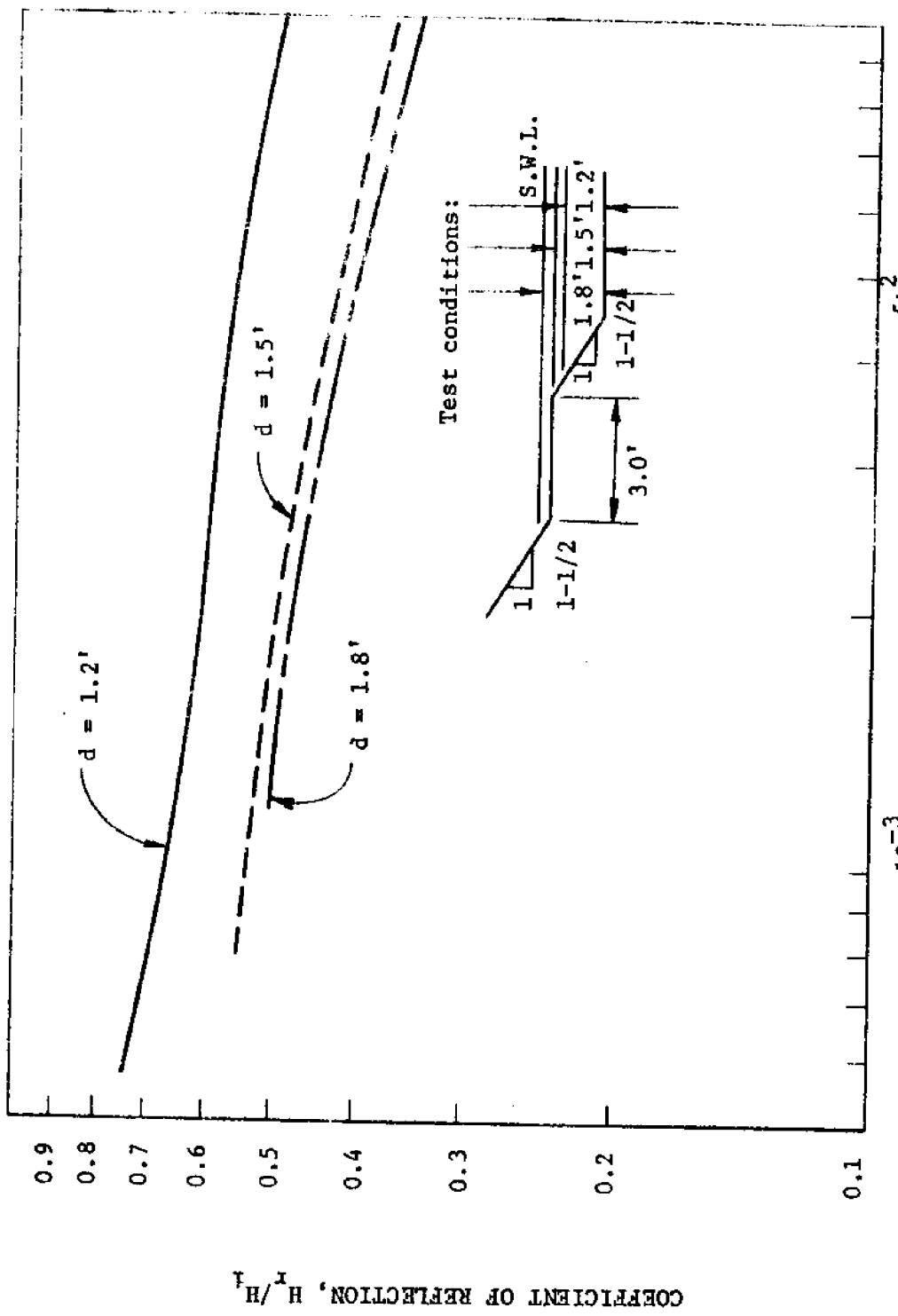

FIG. 91.—COEFFICIENT OF REFLECTION FOR A COMPOSITE (1 ON 1-1/2 ROUGHENED (BLOCKS) SLOPES WITH 3.0 FT BERM) SECTION (d = 1.2, 1.5 and 1.8 ft)

4. A water set-up was observed in the wave flume during the testing using the wind (irregular) waves.

5. A considerable spray up the slope was observed during the wave run-up (R) tests using the wind (irregular) wave generator even though the 'venturi' effect was eliminated by providing a comparable flow way above the slope.

6. For the long waves a vortex was generated on the forward slope (below the berm elevation) due to the collision of the breaking wave and the backwash from the berm.

7. Five different wave run-up (R) cases were noted. These cases were discussed in detail by Herbich[14].

The following methods of energy dissipation were observed during testing:

1. Dissipation of energy by jets channeled between the blocks which hit the vertical face of the up-slope block.

2. Dissipation of energy by vortices (turbulence) generated by the blocks.

3. Dissipation of energy by air entrainment (heterogeneous mixing of air and water) caused by the blocks.

4. Dissipation of energy by waves breaking on the structure (breaking occurred at the break in slope).

5. Dissipation of energy by opposing backwash (water running back across the berm between the blocks).

Comparison of Wave Run-up (R) on Artificially Roughened Composite (1 on 1-1/2 Slopes with 3.0 ft Berm) Section with Wave Run-up (R) on a Smooth Composite (1 on 1-1/2 Slopes with 3.0 ft Berm) Section

The effect of slope roughness (r) on wave run-up (R) was studied

by comparing wave run-up (R) data from the three slope conditions using wave periods (T) of 1.00 sec, 1.56 sec and 1.86 sec in water depths (d) of 1.2 ft, 1.5 ft and 1.8 ft (see Figs. 92 through 100).

For the 1.2 ft, 1.5 ft and 1.8 ft water depths the parallel strips provided the greatest reduction in wave run-up (R) as shown in Figs. 92 through 100.

Comparison of Coefficients of Reflection (C_r) for Artificially Roughened Composite (1 on 1-1/2 Slopes with 3.0 ft Berm) Sections With Coefficients of Reflection (C_r) for a Smooth Composite (1 on 1-1/2 Slopes with 3.0 ft Berm) Section

The effect of slope roughness (r) and berm elevation on the reflection capability (power) of the composite (1 on 1-1/2 slopes with 3.0 ft berm) section was studied by comparing reflecting data for three slope conditions and for water depths (d) of 1.2 ft, 1.5 ft and 1.8 (see Fig. 101). For each test condition the reflecting capability (power) of the composite section decreased as the mean wave energy density (E_μ) increased. The reflecting capability (power) of the composite section was not significantly affected by the slope roughness (r). In all test series the elevation of the berm had a significant affect on the reflecting capability (power) of the composite section. As the still water level increased from below the berm to above the berm the reflecting capability of the composite section was decreased.

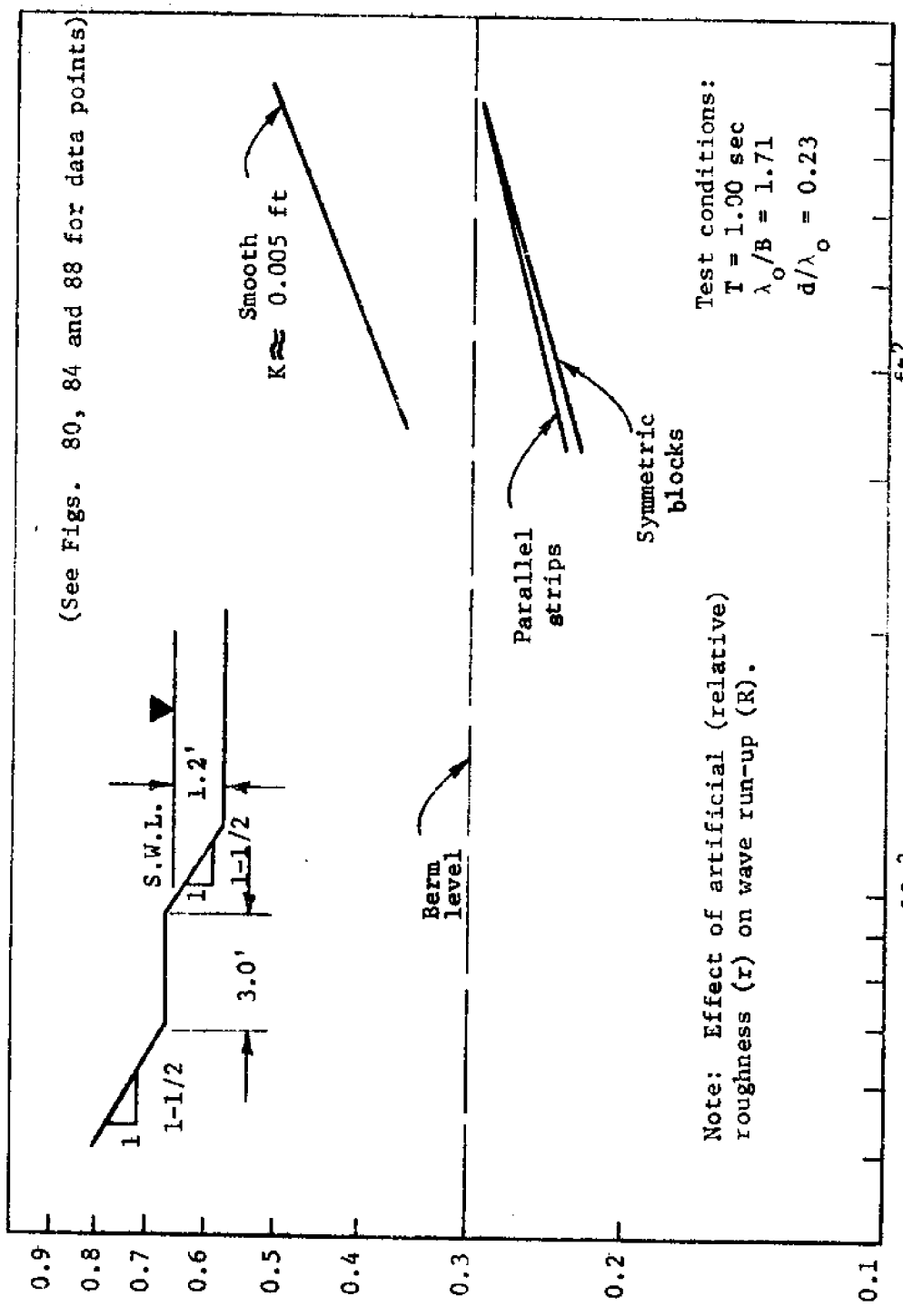

FIG. 92.--WAVE RUN-UP ON A COMPOSITE (1 ON 1-1/2 SLOPES WITH 3.0 FT BERM) SECTION (d = 1.2 ft and T = 1.00 sec)

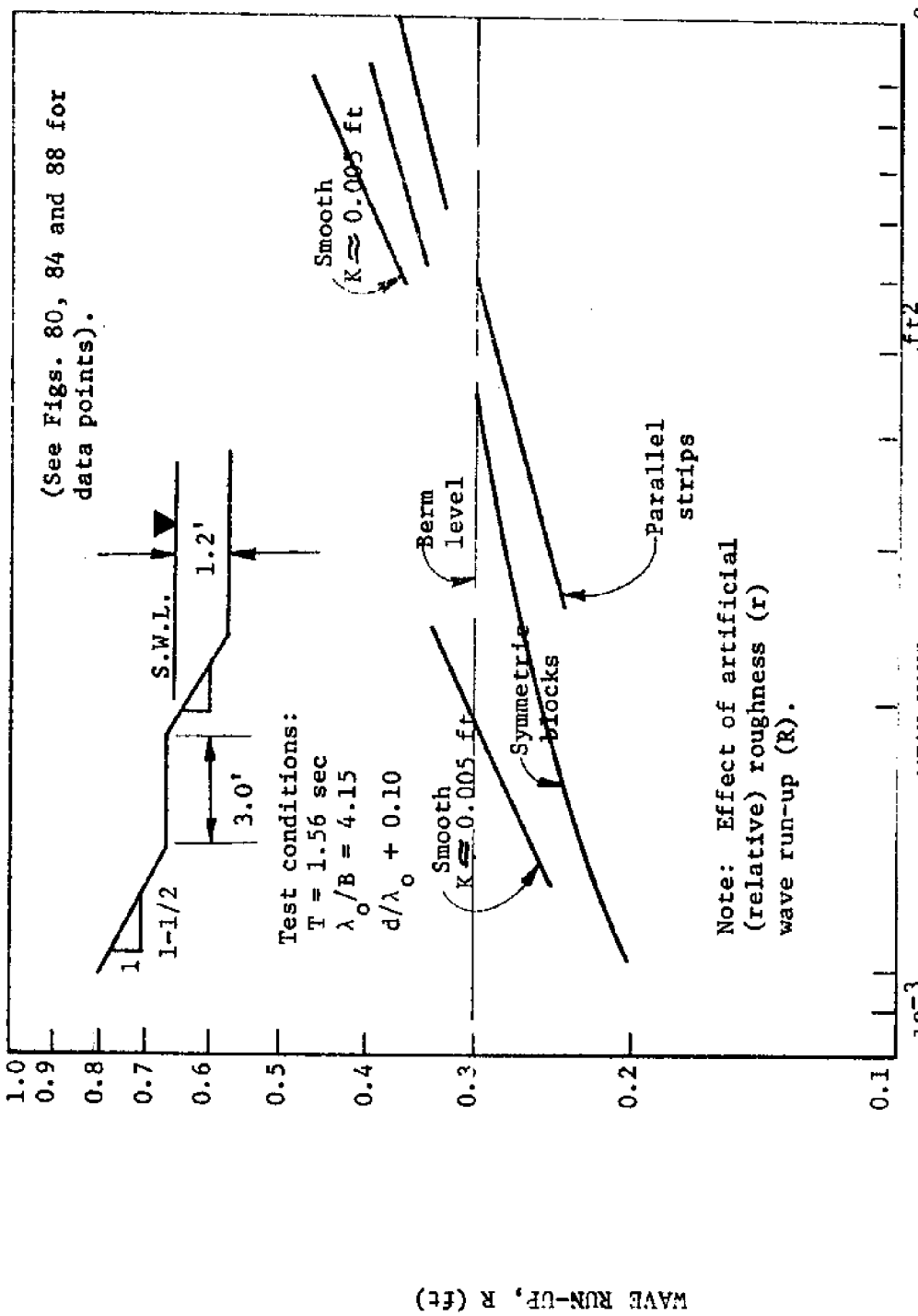

FIG. 93.--WAVE RUN-UP ON A COMPOSITE (1 ON 1-1/2 SLOPES WITH 3.0 FT BERM) SECTION (d = 1.2 ft and T = 1.56 sec)

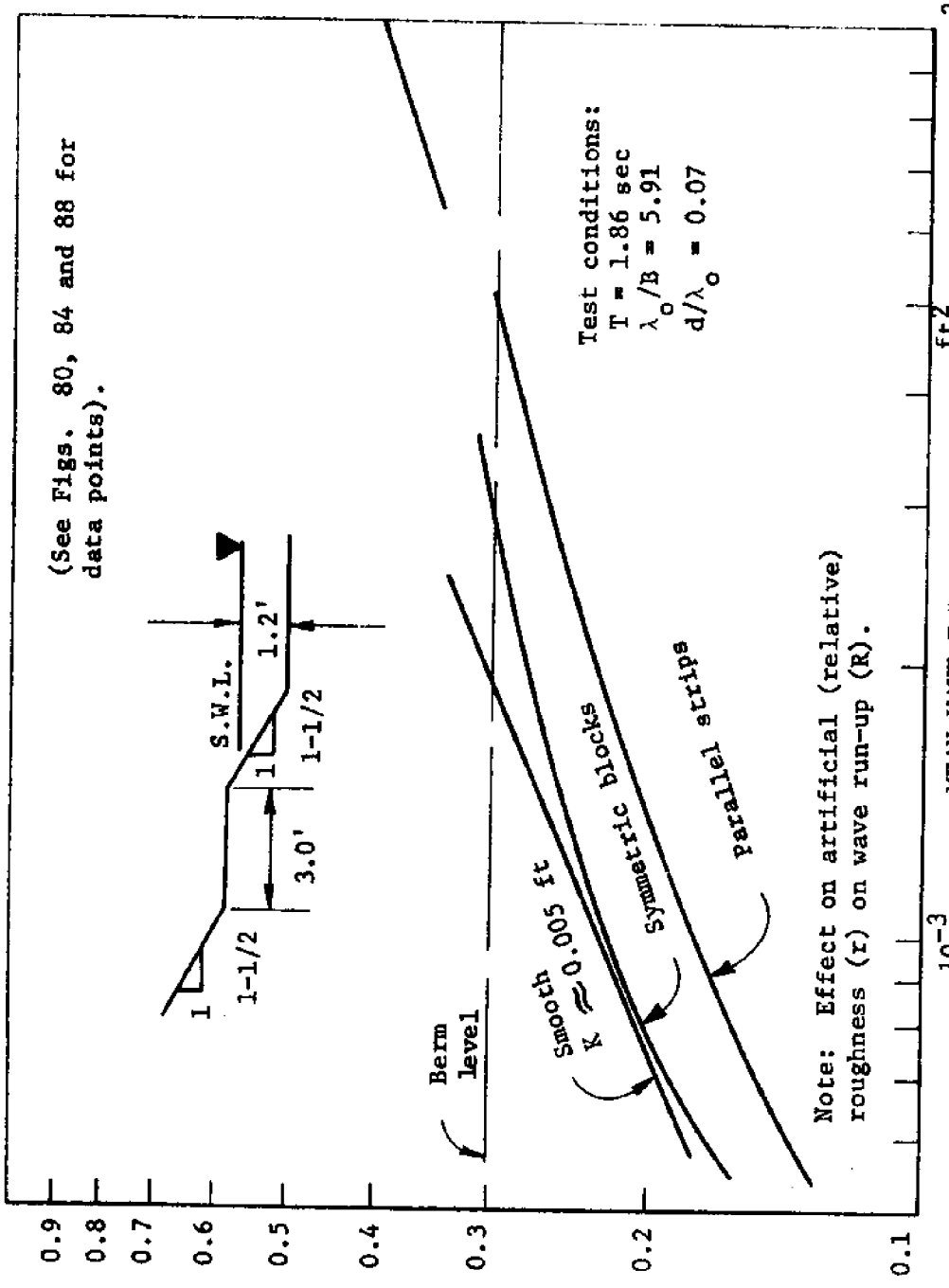

FIG. 94.--WAVE RUN-UP ON A COMPOSITE (1 ON 1-1/2 SLOPES WITH 3.0 FT BERM) SECTION (d = 1.2 ft and T = 1.86 sec)

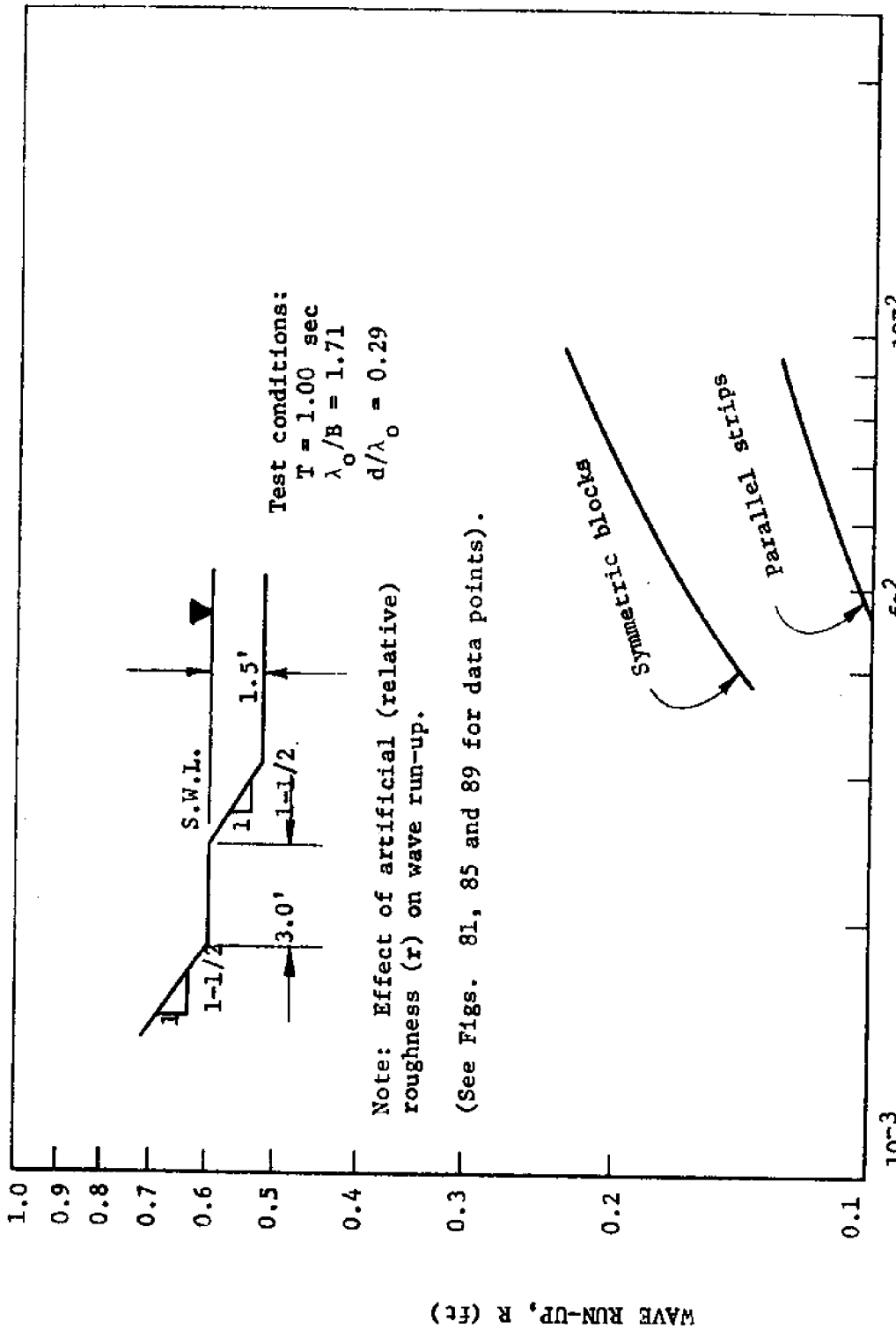

FIG. 95.--WAVE RUN-UP ON A COMPOSITE (1 ON 1-1/2 SLOPES WITH 3.0 FT BERM) SECTION
(d = 1.5 ft and T = 1.00 sec)

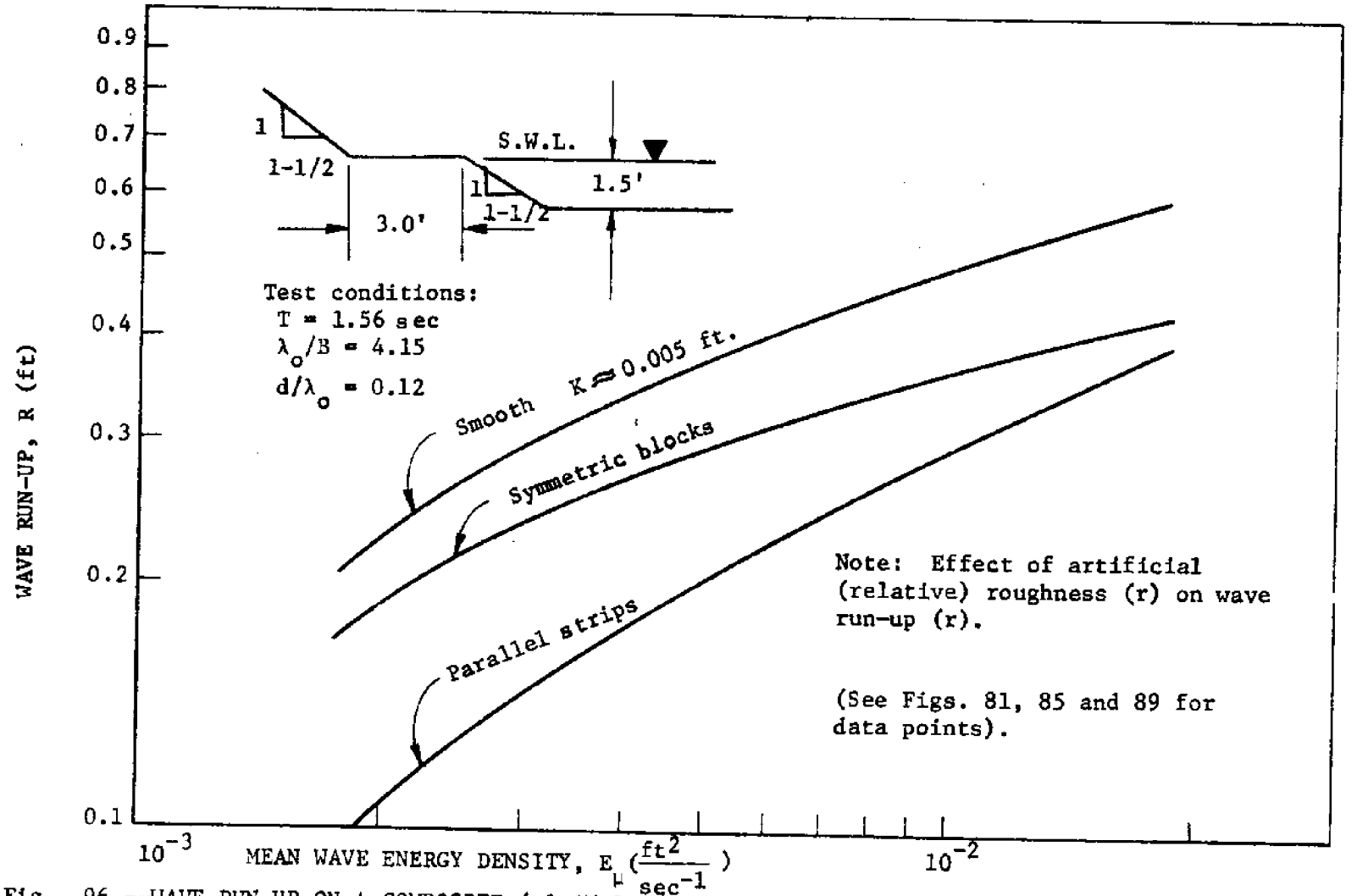

Fig. 96.--WAVE RUN-UP ON A COMPOSITE (1 ON 1-1/2 SLOPES WITH 3.0 FT BERM) SECTION (d = 1.5 ft and T = 1.56 sec)

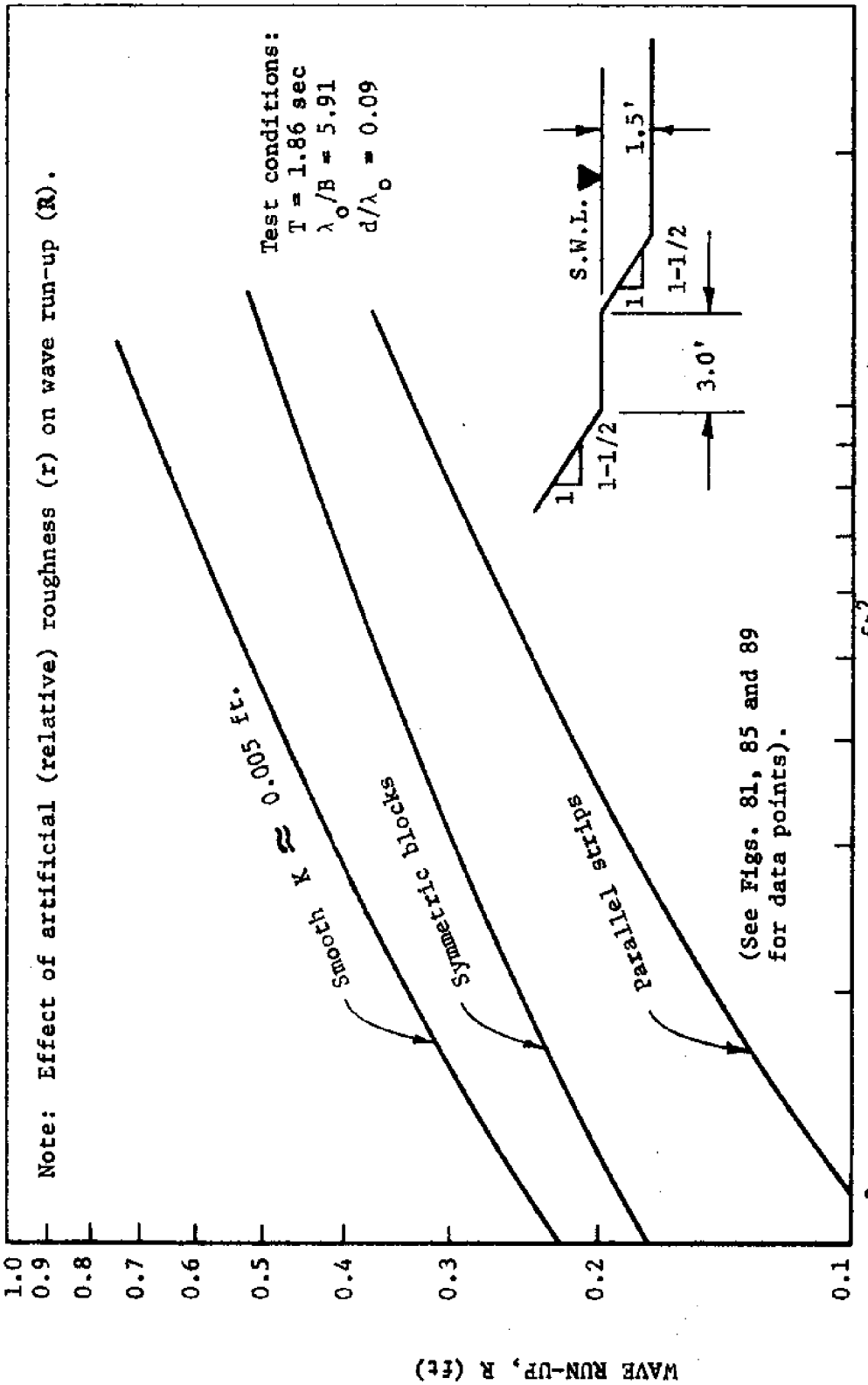

FIG. 97.--WAVE RUN-UP ON A COMPOSITE (1 ON 1-1/2 SLOPES WITH 3.0 FT BERM) SECTION (d = 1.5 ft and T = 1.86 sec)

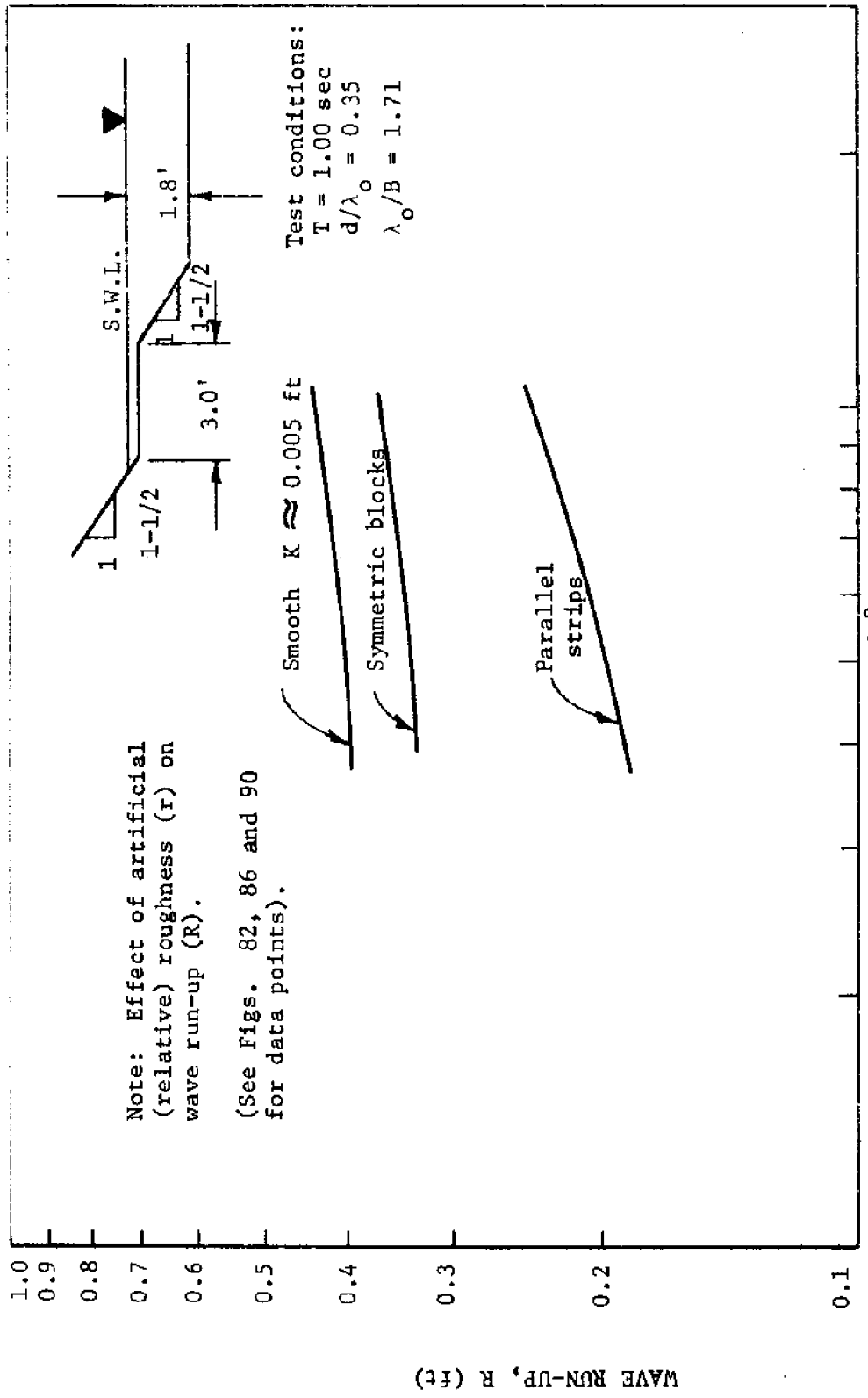

FIG. 98.--WAVE RUN-UP ON A COMPOSITE (1 ON 1-1/2 SLOPES WITH 3.0 FT BERM) SECTION (d = 1.8 ft and T = 1.00 sec)

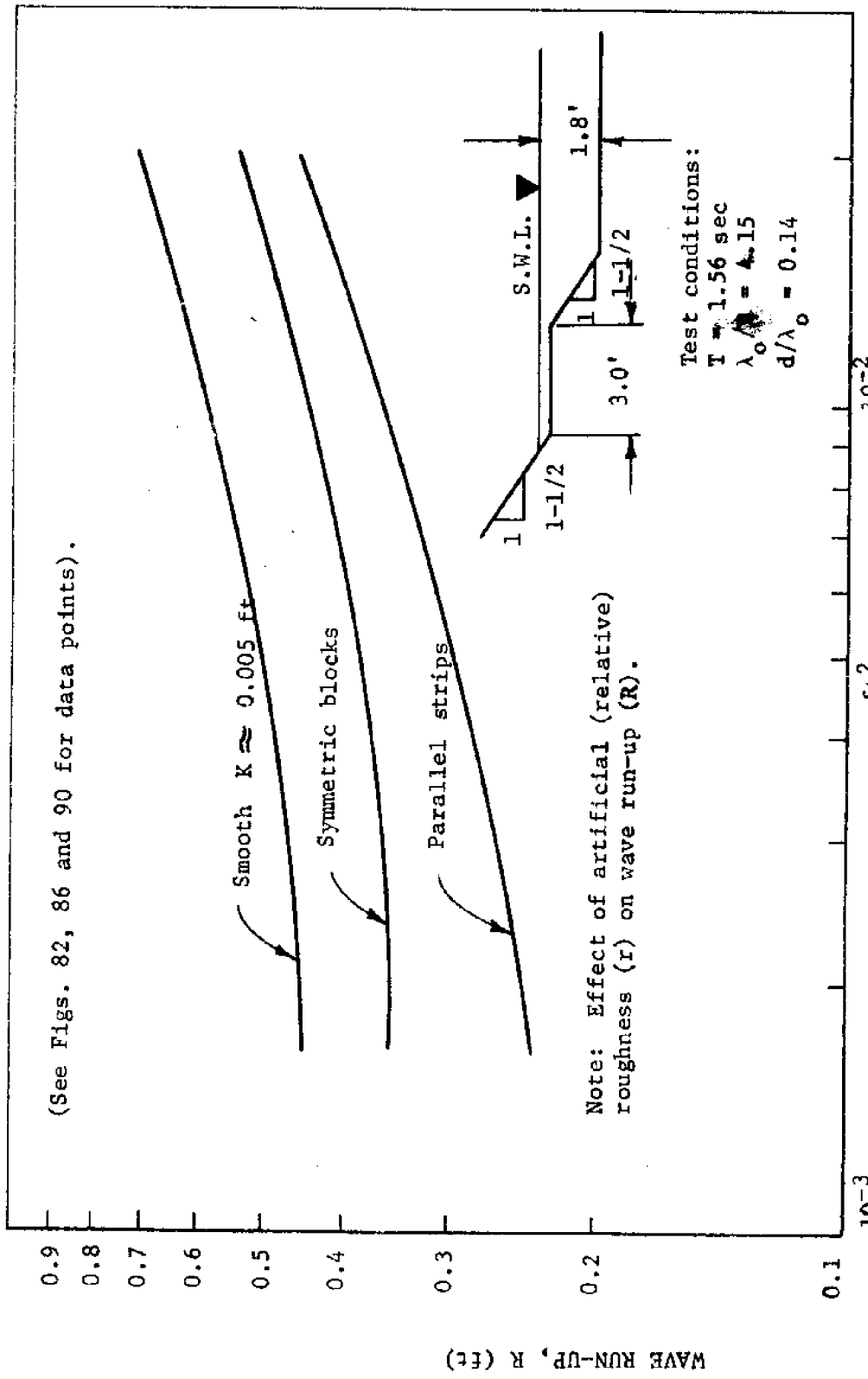

FIG. 99.--WAVE RUN-UP ON A COMPOSITE (1 ON 1-1/2 SLOPES WITH 3.0 FT BERM) SECTION (d = 1.8 ft and T = 1.56 sec)

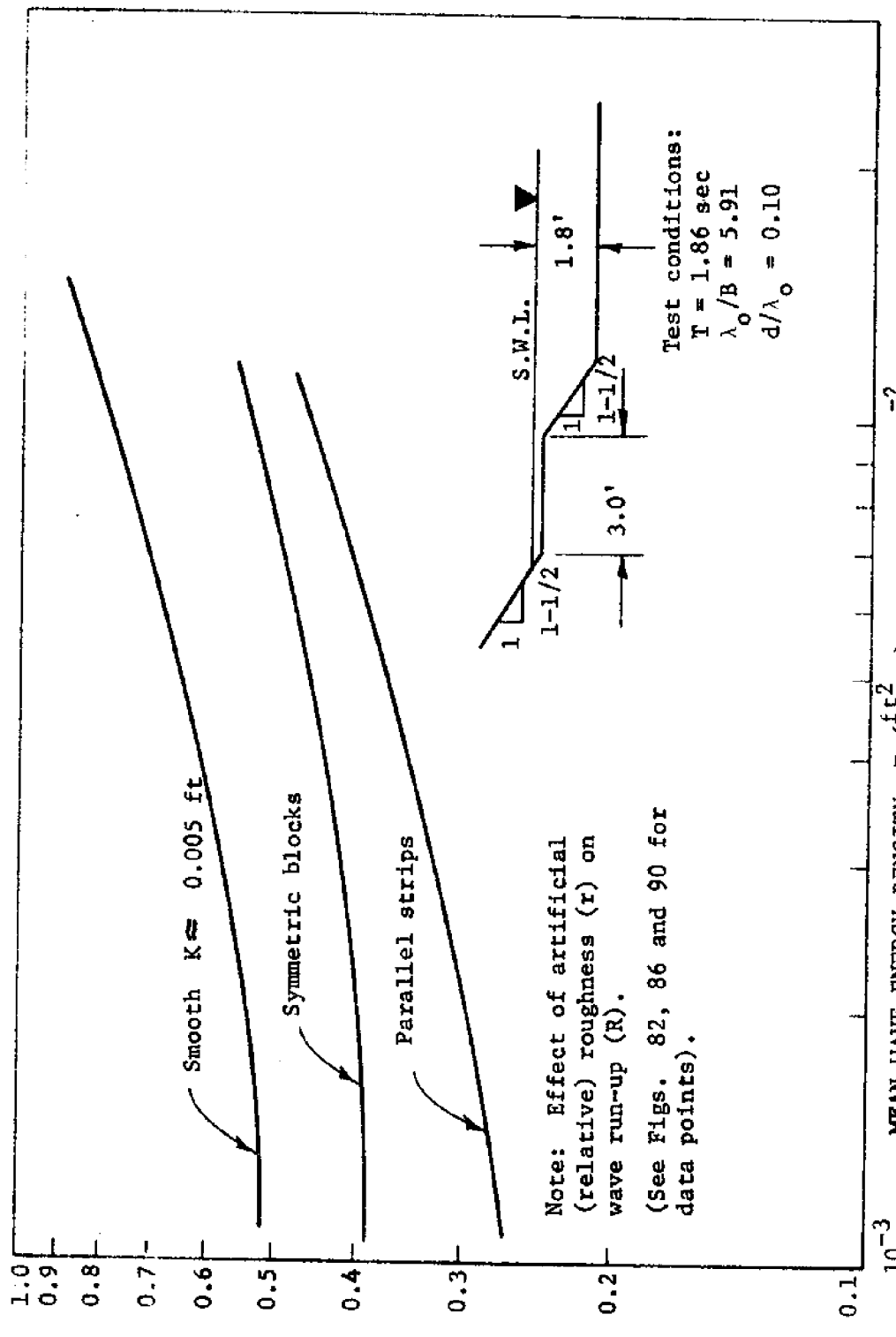

FIG. 100.--WAVE RUN-UP ON A COMPOSITE (1 ON 1-1/2 SLOPES WITH 3.0 FT BERM) SECTION (d = 1.8 ft and T = 1.86 sec)

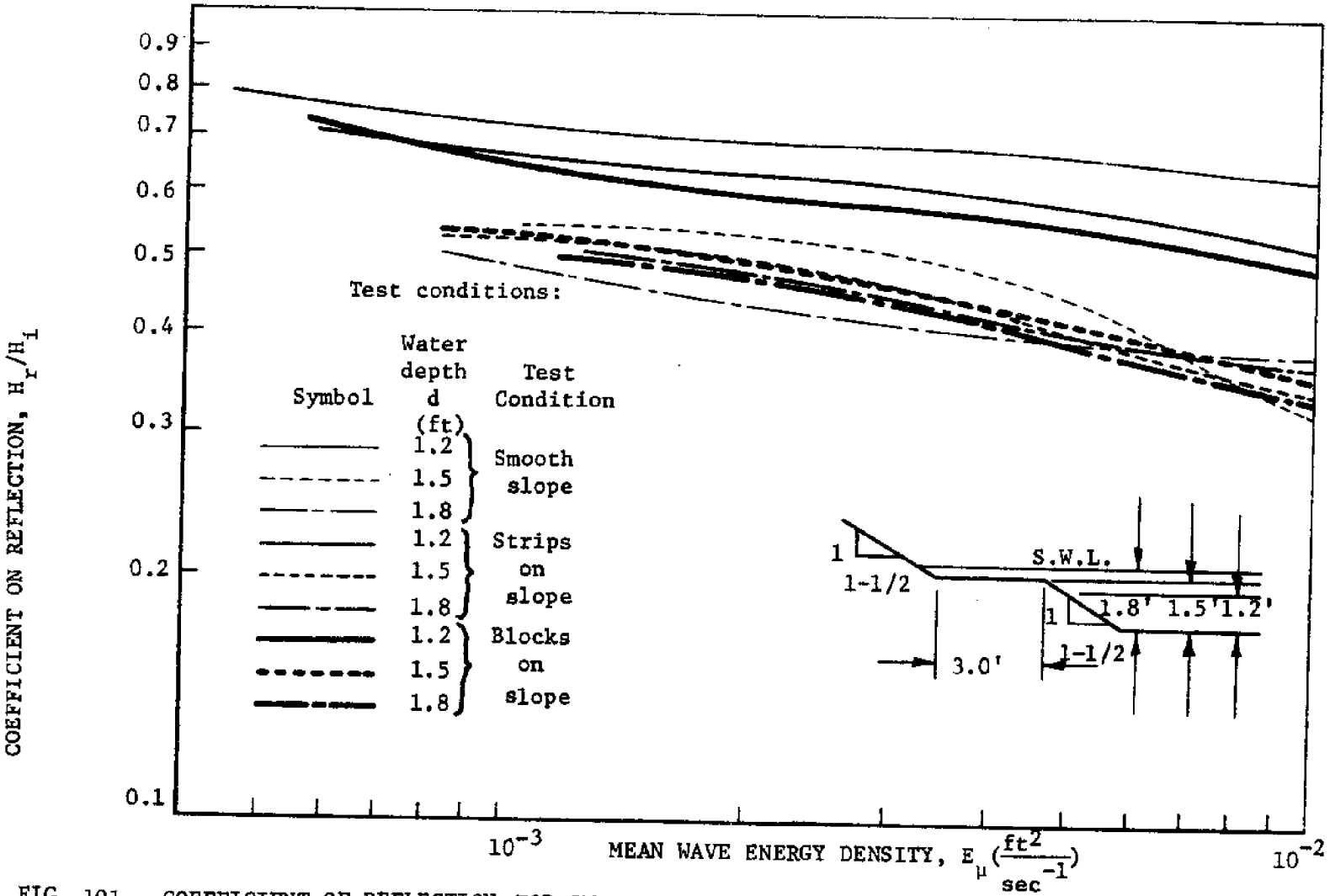

FIG. 101.--COEFFICIENT OF REFLECTION FOR SMOOTH AND ROUGHENED (BLOCKS AND STRIPS) COMPOSITE (1 ON 1-1/2 SLOPES WITH 3.0 FT BERM) SECTION

Run-up Ratios for a Smooth Composite Section

Run-up ratios [wave run (R) on a composite (1 on 1-1/2 slopes with berm) section divided by wave run-up (R) on a single (1 on 1-1/2) slope section] *versus* berm-width ratios [berm width (B) divided by deep water wave length (λ_o)] for the smooth slope configuration are shown in Fig. 102 for a 1.5 ft water depth (still water level at the berm). As shown in Fig. 102, the berm had a significant effect on the run-up ratio. As the berm-width ratio increased the run-up ratio decreased (but at a decreasing rate). With the berm width (B) approximately one-half (1/2) of the deep water wave length (λ_o) the wave run-up on the composite section was approximately one-half (1/2) of the wave run-up (R) on a single (1 on 1-1/2) slope.

Methods for Determining Wave Run-up on a Single (1 on 1-1/2) Slope

Wave spectra method. To determine the wave run-up (R) on a single (1 on 1-1/2) slope the following procedure should be used:

1. Compute mean wave energy density (E_μ) from wave history and power spectrum computer program [see Fig. 124 (Appendix IV)].
2. Compute wave run-up (R) from Equation (66).

$$\frac{R}{H_o'} = 1.9\ E_\mu^{-0.0043} \quad \ldots\ldots \quad (66)$$

Significant parameters method. To determine the wave run-up (R) on a single (1 on 1-1/2) slope (when the wave history is not available) the following procedure should be used:

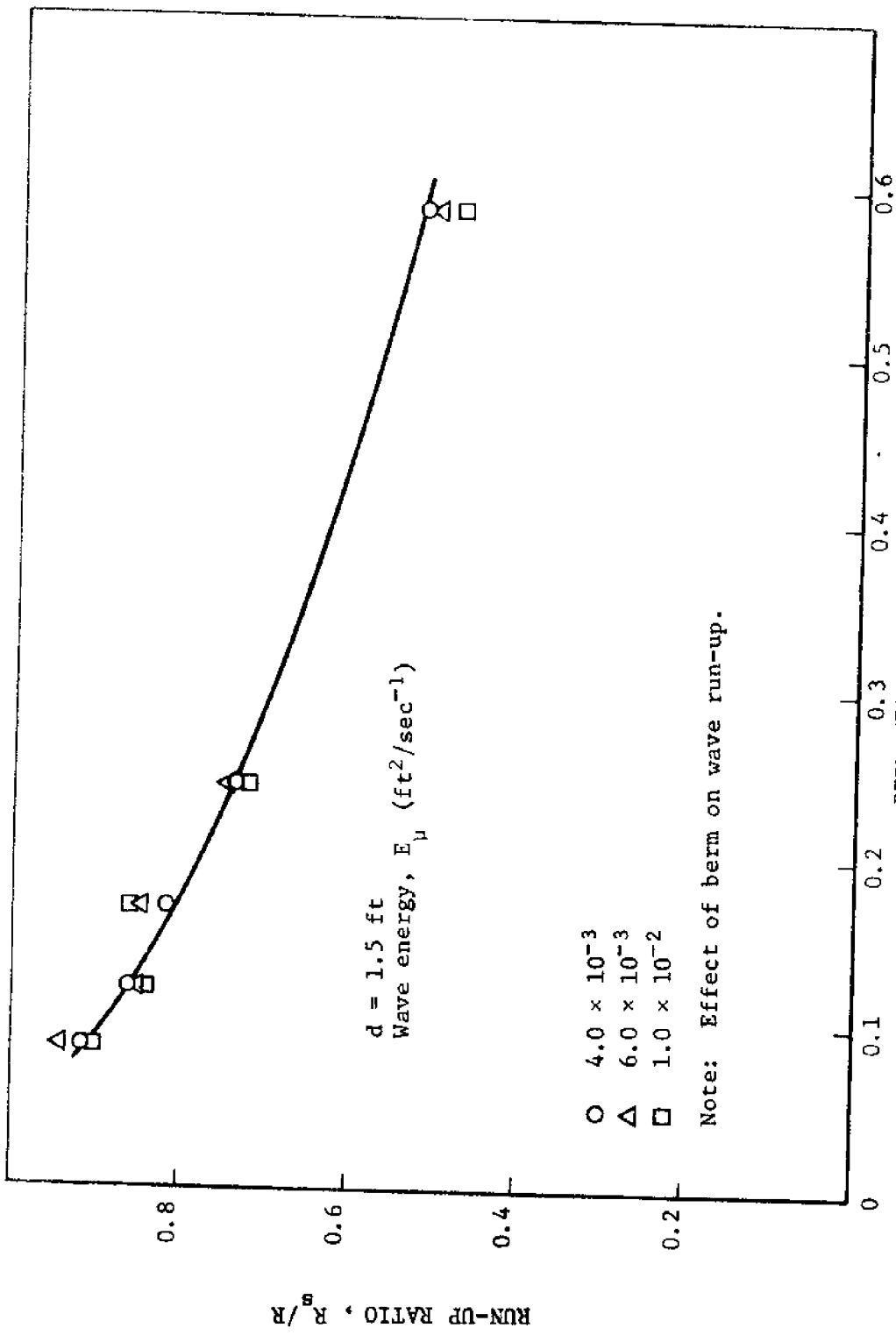

FIG. 102.--RUN-UP RATIO *VERSUS* RELATIVE BERM-WIDTH RATIO FOR SMOOTH COMPOSITE SECTION

1. Compute the relative wave height (H_o'/d) and relative depth (d/λ_o). Use Fig. 103 to obtain the relative energy coefficient. (E_μ/C^2T^3).

2. Obtain the mean wave energy density (E_μ) from the relative energy coefficient (E_μ/C^2T^3).

3. Compute wave run-up (R) from Equation (66).

Instrument Error

Errors in the instruments are often difficult to detect and almost impossible to measure.

Errors in wave height measurement. Wave heights were measured by changes in the capacitance of a thin insulated wire immersed in the wave tank. Sources of error in the wave height instrumentation were surface film contamination (which caused a change in the ground potential), meniscus effects, capacitance changes in the cable to the measuring bridge, defects in the recorder and pen drag. In addition there was a dynamic error caused by electrical impedance and mechanical inertia. Due to the instrument error a difference between the true water surface and the position signalled by the analogue trace was experienced. This difference has been estimated to be less than ± 0.01 ft.

Errors in velocity and turbulence measurement. Point velocities and turbulence fluctuations in the mean flow direction were measured with a constant temperature cylindrical (hot-film) sensor. The heat transfer between the sensor and the water was converted into velocity and turbulence data. The sources of possible error affecting system

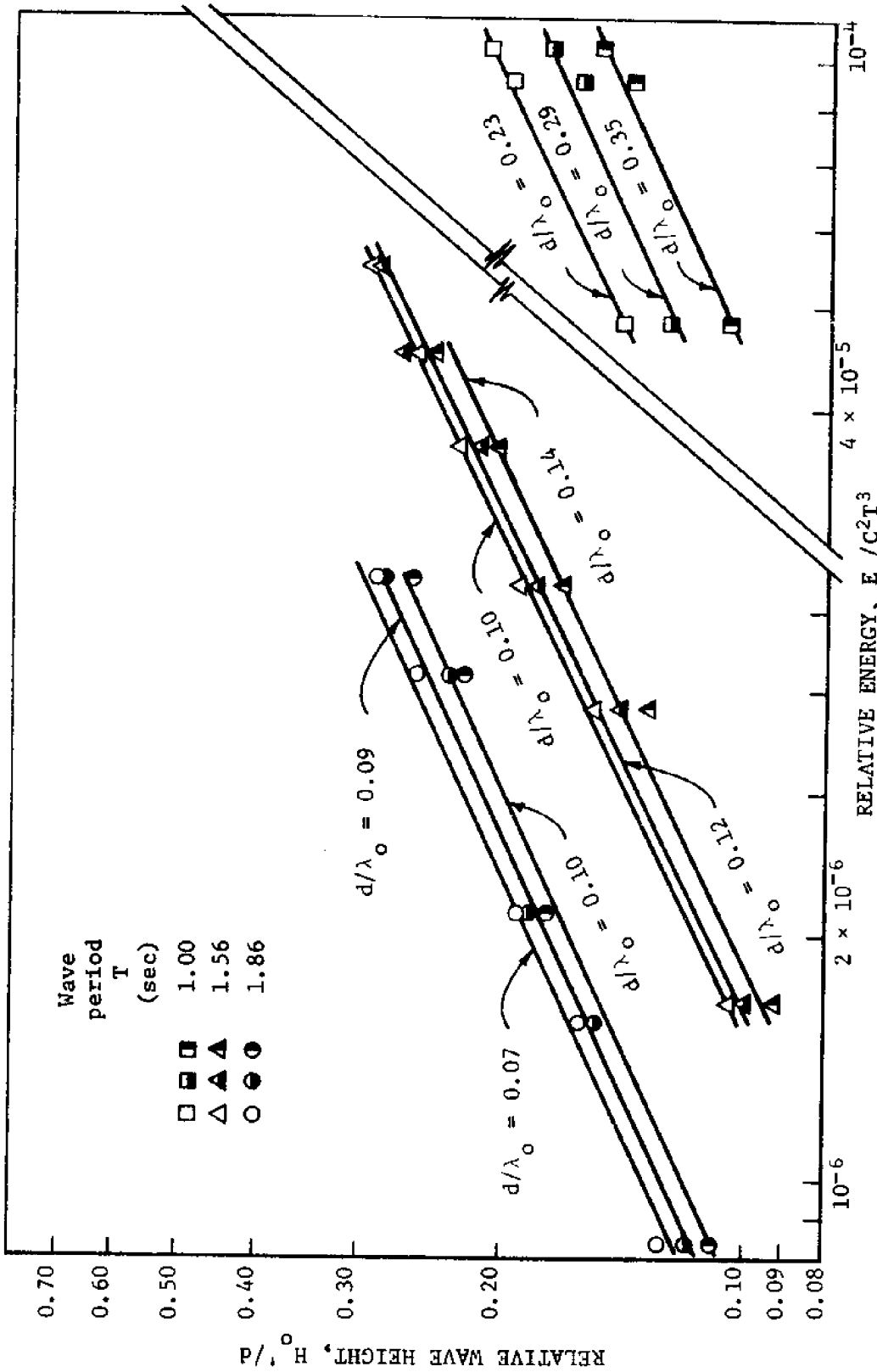

FIG. 103.--RELATIVE WAVE ENERGY COEFFICIENTS FOR SIGNIFICANT WAVE PARAMETERS

accuracy were (1) sensor contamination by the environment, (2) resistance shifts in the sensor or bridge resistors and (3) errors associated with calibration accuracy. No attempt was made to estimate the magnitude of these errors.

Errors in wave generation. The monochromatic wave generator introduced unwanted two-frequency components into the water through a pumping action which was found to excite the normal longitudinal and lateral modes of the tank. Since the normal modes decayed at different exponential rates (moduli depend on the damping coefficients for each mode), a continually varying still water reference level was introduced into the study.

Scale Effect

Large scale run-up tests conducted by W.E.S.[51] in connection with the design of Lake Okeechobee Levees, have shown the existence of scale effect in model studies of wave run-up on smooth slopes. W.E.S. found a general increase in wave run-up of about 9 per cent on a 1 on 6 slope due to a change in model scale from 1 on 17 to 1 on 30. Saville[43] reports that unpublished data from the B.E.B. indicates that actual wave run-up from prototype waves will be greater than that predicted by small scale tests by about 10 per cent for a 1 on 6 slope and about 20 per cent for a 1 on 3 slope. Corrections for model scale effect (based on limited data) have been presented by the Coastal Engineering Research Center[7] for slopes ranging from 1 on 15 to 1 on 1-1/4. It should be remembered that

the degree of correction actually depends on the actual scale increase involved.

SUMMARY AND CONCLUSIONS

Summary

A comprehensive study of the wave run-up (R) phenomena on single and composite slopes was conducted in order (1) to determine the effects of slope roughness (r) on regular and irregular wave run-up (R) on composite sections, (2) to determine the effects of slope roughness (r) on the velocity distribution in the uprush zone, (3) to investigate the energy loss in the uprush zone due to turbulence and bottom dissipation and (4) to compare regular and irregular wave run-up (R) on roughened slopes with the wave run-up (R) on smooth slopes. Both monochromatic and wind wave tests were run. Three model structures and three slope conditions were tested.

Conclusions

The following conclusions were drawn from the general investigation of the wave run-up (R) phenomena:

1. The water depth (d) affected the relative wave run-up (R/H_o') from the waves in the lower range of mean wave energy densities [*i.e.*, long waves ($\lambda > > d$) with small wave heights ($H_o' < < d$)].

2. The relative wave run-up (R/H_o') was found to be a function of the relative depth (d/λ_o), the relative wave height (H_o'/d) and the relative wave steepness (H_o'/T^2).

3. The reflecting capability (power) of the single (1 on 1-1/2) slope decreased as the wave energy density (E_u) increased.

4. The reflecting capability (power) of the single (1 on 1-1/2) slope was not significantly affected by the slope roughness.

5. The reflecting capability (power) of the composite (1 on 1-1/2 slopes with berm) section was not significantly affected by slope roughness.

6. The reflecting capability (power) of the composite section was affected by the berm elevation. As the still water level was increased from below the berm to above the berm the reflecting capability (power) of the composite section decreased.

7. The symmetric pattern of blocks and the parallel strips reduced the relative wave run-up (R/H_o') on the single slope. The relative monochromatic wave run-up (R/H_o') was reduced approximately 15 per cent while the relative wind wave run-up (R/H_e') was reduced approximately 35 per cent.

8. The wave run-up (R) was significantly reduced by the berm. Maximum reduction of wave run-up (R) occurred with the water depth located at the berm. The maximum reduction of wave run-up (R) also occurred for the short wave lengths ($d < \lambda$) whereas the least reduction in the wave run-up (R) occurred for the long wave lengths ($d << \lambda$).

First objective. The following conclusions were drawn from the wave run-up (R) phenomena on a composite section:

1. The symmetric pattern of blocks and the parallel strips reduced the wave run-up (R) on the composite (1 on 1-1/2 slopes with berm) section.

2. The parallel strip roughness element was the most efficient dissipator of the relative wave run-up

(R) energy on the composite (1 on 1-1/2 slopes with berm) section.

3. No significant differerence between the relative wave run-up (R/H_o') of monochromatic waves and the relative wave run-up (R/H_e') of wind waves was noted on the composite (1 on 1-1/2 slope with berm) section.

Second objective. The following conclusions were drawn from the investigation of the velocity distribution in the uprush zone:

1. The wave uprush velocity (V_u) on the 1 on 1-1/2 slope increased as the mean wave energy density (E_μ) increased.

2. The wave uprush velocity (V_u) for the smooth (1 on 1-1/2) slope was approximately seven-tenths of the wave celerity ($V = 0.7C$).

3. The slope roughness (r) reduced the maximum relative uprush velocity (V_u/C) on the 1 on 1-1/2 slope. The symmetric pattern of blocks reduced the relative uprush velocity (V_u/C) approximately 15 per cent while the parallel strips reduced the relative uprush velocity (V_u/C) approximately 25 per cent.

Third objective. The following conclusions were drawn from the investigation of the energy loss due to turbulence and bottom dissipation:

1. Due to the changing mean velocity in the uprush zone the level of turbulence could not be measured or calculated.

2. The roughness elements acted as vortex generators and increased the level of turbulence.

3. The roughness elements increased the bottom dissipation of energy.

Fourth objective. The following conclusion was drawn from the investigation of regular and irregular wave run-up (R) on composite sections:

No significant difference in relative wave run-up (R/H_e') was obtained from the wind (irregular) waves on either the single (1 on 1-1/2) slope or the composite (1 on 1-1/2 slopes with berm) section.

Recommendations for Further Research

The following research should be conducted:

1. Investigate the effects of slope roughness (random roughness elements) on wave run-up (R).

2. Investigate the effects of permeability on wave run-up (R).

3. Develop a technique to measure the level of turbulence (intensity) in the uprush zone.

4. Investigate the effect of an inclined berm on wave run-up (R).

APPENDIX I.--REFERENCES

REFERENCES

1. Adam, K. M., "A Model Study of Wave Run-up on Smooth and Rough Slopes," unpublished M.S. thesis, University of Manitoba, Winnipeg, Canada, 1963, pp. 1-114.

2. Amein, M., "A Method for Determining the Behavior of Long Waves Climbing a Sloping Beach," *Journal of Geophysical Research*, Vol. 71, No. 2., Jan. 15, 1966, pp. 401-410.

3. Blackman, R. B., and Tukey, J. W., "The Measurement of Power Spectra," *Dover*, New York, 1958.

4. Bowen, A. J., Inman, D. L., and Simmons, V. P., "Wave 'Set-down' and Set-up," *Journal of Geophysical Research*, Vol. 73, No. 8, April 15, 1968, pp. 2569-2577.

5. Bruun, P., "Breakwaters for Coastal Protection," *Proceedings*, XVIII International Navigation Congress, Sect. 2, Question 1, Rome 1953, pp. 25-35.

6. Carrier, G. F. and Greenspan, H. P., "Water Waves of Finite Amplitude on a Sloping Beach," *Journal of Fluid Mechanics*, Vol. 4, 1958, pp. 97-109.

7. Coastal Engineering Research Center, "Shore Protection, Planning and Design," *CERC Technical Report No. 4*, U.S. Army Coastal Engineering Research Center, 1966, pp. 194 and 195.

8. Freeman, J. C., and Le Méhauté, B., "Wave Breakers on a Beach and Surges on a Dry Bed," *Journal of the Hydraulics Division*, ASCE, Vol. 90, March 1964, pp. 187-216.

9. Friedrichs, K. O., "Water Waves on a Shallow Sloping Beach," *Communication Applied Mathematics*, Vol. 1, 1948, pp. 109-134.

10. Galvin, C. J., Jr., "Finite-amplitude, Shallow Water Waves of Periodically Recurring Form," unpublished report, U.S. Army Corps of Engineers Coastal Engineering Research Center, 1968.

11. Granthem, K. N., "Wave Run-up on Sloping Structures," *Transactions, American Geophysical Union*, Vol. 34, No. 5., October 1953, pp. 720-724.

12. Hall, J. V. and Watts, G. M., "Laboratory Investigation of the Vertical Rise of Solitary Waves on Impermeable Slopes," *BEB Technical Memorandum No. 33*, U.S. Army Corps of Engineers Beach Erosion Board, March 1953, pp. 1-14.

13. Haws, E. T., "Discussion on Mangle," *Proceedings of the Institute of Civil Engineers*, Vol. 41, Sept. 1968, pp. 145-148.

14. Herbich, J. B., Sorensen, R. M., and Willenbrock, J. H., "Effect of Berm on Wave Run-up on Composite Beaches," *Journal of the Waterways and Harbors Division*, ASCE, Vol. 89, No. WW2, May 1963, pp. 55-72.

15. Ho, D. V., and Meyer, R. E., "Climb of a Bore on a Beach," *Journal of Fluid Mechanics*, Vol. 14, 1962, pp. 305-318.

16. Ho, D. V., Meyer, R. E., and Shen, M. C., "Long Surf," *Journal of Marine Research*, Vol. 21, No. 3, 1963, pp. 219-23 .

17. Hosoi, M., and Mitsui, H., "Wave Run-up on Sea Dikes Located in the Surf Zone or on the Shore," *Coastal Engineering in Japan*, Vol. 6, 1963, pp. 1-6.

18. Hudson, R. Y., "Laboratory Investigation of Rubble-mound Breakwaters," *Journal of the Waterways and Harbors Division*, ASCE, Vol. 85, No. WW3, Sept. 1959, pp. 108-113.

19. Hunt, I. A., "Design of Seawalls and Breakwaters," *Journal of the Waterways and Harbors Division*, ASCE, Vol. 85, No. WW3, Sept. 1959, pp. 123-152.

20. Isaacson, E., "Water Waves over a Sloping Bottom," *Comm. Pure and Applied Mathematics*, Vol. 3, 1950, pp. 1-32.

21. Jackson, R. A., "Design of Cover Layers for Rubble-mound Breakwaters Subjected to Non-breaking Waves," *WES Research Report No. 2-11*, U.S. Army Waterways Experiment Station, Vicksburg, Mississippi, June 1968, pp. 29 and 30.

22. Johnson, J. W., "Rectangular Artificial Roughness in Open Channels," *Transactions of the American Geophysical Union*, Vol. 34, May 1945, pp. 907-914.

23. Jordaan, J. M., Jr., "Feasibility of Modeling Run-up Effects of Dispersive Water Waves," *USNCEL Technical Note N-691*, U.S. Naval Civil Engineering Lab., Port Hueneme, May 1965, pp. 1-61.

24. Kaplan, K., "Generalized Laboratory Study of Tsunami Run-up," *BEB Technical Memorandum No. 60*, U.S. Army Corps of Engineers Beach Erosion Board, Jan. 1955, pp. 1-30.

25. Keller, H. B., Levine, D. A., and Whitham, G. B., "Motion of a Bore on a Sloping Beach," *Journal of Fluid Mechanics*, Vol. 7, 1960, pp. 302-316.

26. Keller, J. B., and Keller, H. B., "Water Wave Run-up on a Beach, Part II," *Service Bureau Corporation Research Report*, New York, 1965, pp. 1-40.

27. Keller, J. B., and Keller, H. B., "Water Wave Run-up on a Beach," *Service Bureau Corporation Research Report*, New York, 1964, pp. 1-A13.

28. Keller, J. B., "Tsunamis-Water Waves Produced by Earthquakes," *Proceedings*, Conference on Tsunami Hydrodynamics, 1961.

29. King, L. V., "On the Convection of Heat from Small Cylinders in a Stream of Fluid: Determination of the Convective Constants of Small Platinum Wires with Application to Hot-wire Anemometry," *Proceeding Royal Society (London)*, Vol. 214A, No. 14, 1914, p. 373.

30. Le Méhauté, B., Koh, B. C. Y. and Li-San Hwang, "A Synthesis on Wave Run-up," *Journal of the Waterways and Harbors Division*, ASCE, No. WW1, Vol. 94, Feb. 1968, pp. 77-92.

31. Le Méhauté, B., and Divoky, D., "Effects of Explosion-Generated Waves on the Hawaiian Islands," *NESCO Report No. SN-30*, National Engineering Science Co., Pasadena, California, Dec. 1966, pp. 1-74.

32. Le Méhauté, B., "On Non-saturated Breakers and the Wave Run-ups," *Proceedings*, Eighth Conference on Coastal Engineering, Council on Wave Research, Chapter 6, 1963, pp. 77-92.

33. Lewy, H., "Water Waves on a Sloping Beach," *Bulletin American Mathematical Society*, Vol. 52, 1946, pp. 737-775.

34. Miche, R., "Le Pouvoir Reflechissant Des Ouvrages Maritimes," *Ann. Des Ponts Et Ch.*, May to June 1951, pp. 285-319.

35. Miche, R., "Mouvements Ondulatores de la Mer," *Ann. Des Ponts Et Ch.*, Jan. to Aug. 1944.

36. Miller, R. L., "Experimental Determination of Run-up of Undular and Fully Developed Bores," *Journal of Geophysical Research*, Vol. 73, No. 14, July 15, 1968, pp. 4497-4510.

37. Multer, B., "Wave Run-up," *CERC Memorandum for Record*, U.S. Army Corps of Engineers Coastal Engineering Research Center, 1967, pp. 1-15.

38. Robson, L. E., and Jones, D. B., "Laboratory Study of Seiching Induced on an Offshore Shelf," *USNCEL Technical Note N-895*, U.S. Naval Civil Engineering Lab., Port Hueneme, California, 1967, pp. 1-46.

39. Savage, R. P., "Wave Run-up on Roughened and Permeable Slopes," *Journal of the Waterways and Harbors Division*, ASCE, Vol. 84, No. WW3, May 1958, pp. 1640-1 -- 1640-38.

40. Savage, R. P., "Laboratory Data on Wave Run-up on Roughened and Permeable Slopes," *BEB Technical Memorandum No. 109*, U.S. Army Corps of Engineers Beach Erosion Board, March 1959, pp. 1-28.

41. Saville, T., Jr., Discussion To, "Laboratory Investigation of Rubble-mound Breakwaters," *Journal of the Waterways and Harbor Division*, ASCE, Vol. 86, No. WW3, Sept. 1960, pp. 151-156.

42. Saville, T., Jr., "Wave Run-up on Composite Slopes," *Proceedings*, Sixth Conference on Coastal Engineering, Council on Wave Research, Chapter 41, 1957, pp. 691-699.

43. Saville, T., Jr., "Wave Run-up on Shore Structures," *Journal of the Waterways and Harbors Division*, ASCE, Vol. 82, No. WW2, April 1956, pp. 9251-92514.

44. Shen, M. C., and Meyer, R. E., "Climb of a Bore on a Beach," Part 3, *Journal of Fluid Mechanics*, Vol. 16, 1963, pp. 173-175.

45. Sibul, O., "Flow over Reefs and Structures by Wave Action," *Transactions of the American Geophysical Union*, Vol. 36, No. 1, Feb. 1955, pp. 61-71.

46. Sibul, O. J., and Tickner, E. G., "A Model Study of the Run-up of Wind-generated Waves on Levees with Slopes of 1:3 and 1:6," *BEB Technical Memorandum No. 67*, U.S. Army Corps of Engineers Beach Erosion Board, Dec. 1955, pp. 1-19.

47. Stoker, J. J., "Water Waves," *Interscience*, New York, 1957.

48. Van Dorn, W. G., "Theoretical and Experimental Study of Wave Enhancement and Run-up on Uniformly Sloping Impermeable Beaches," *SIO-66-11* Scripps Institute of Oceanography, San Diego, California, 1966, pp. 1-95.

49. Wallace, N. R., "Deformation of Solitary Waves, Part I: Reflection from a Vertical Wall," *URS-631-1*, United Research Services, Burlingame, California, 1963, pp. 1-56.

50. Wassing, F., "Model Investigations on Wave Run-up Carried Out in the Netherlands During the Past Twenty Years," *Proceedings*, Sixth Conference on Coastal Engineering, Council on Wave Research, 1957, pp. 700-713.

51. Waterways Experiment Station, "Wave Run-up and Overtopping Levee Sections Lake Okeechobee, Florida," *USWES Technical Report No. 2-449*, U.S. Waterways Experiment Station, Vicksburg, Miss., Jan. 1957, pp. 1-26.

52. Whitham, J. B., "On the Propagation of Shock Waves Through Regions of Non-uniform Area or Flow, *Journal of Fluid Mechanics*, Vol. 4, 1958, pp. 337-360.

53. _____, "Hot Film and Hot Wire Anemometry Theory and Application," *TSI Bulletin TB-5*, Thermo-systems Inc. Saint Paul, Minnesota, 1969, pp. 1-13.

APPENDIX II.--NOTATIONS

NOTATIONS

The following symbols are used:

Symbol	Description	Dimensions
a	Height of hydraulic roughness element	L
A	Amplification factor $(A = J_o^2\ (\gamma/\alpha) + J_1^2\ (\gamma/\alpha)^{-1/2})$	-
A'	Constant [f(anemometer velocity sensor and flow characteristics)]	-
b	Width of hydraulic roughness element	L
B	Width of berm	L
B'	Constant [f(anemometer velocity sensor and flow characteristics)]	-
c	Clear distance betwen hydraulic roughness elements	L
C	Wave celerity	L/T
C_r	Coefficient of reflection $(C_r = H_r/H_i)$	-
d	Depth of water (measured from stillwater level to the bottom)	L
d_1	Depth of water (measured from the still-water level to the toe of the beach slope)	L
d_2	Depth of water (measured from the still-water level to the toe of the levee)	L
d'	Mean diameter of roughness particle	L
d_b	Depth of water at a breaker's position	L
E_a	Anemometer output voltage	-
E	Wave energy Also: Wave energy density	LF/T L^2T

Symbol	Description	Dimensions
E_w	Mean wave energy density	L^2T
F_r	Froude number ($F_r = V/\sqrt{gd}$)	-
f	Wave frequency	$1/T$
f_*	Coefficient of friction	-
f_1	Function of one or more variables	-
f_2	Function of one or more variables	-
g	Acceleration of gravity Also: Function	$\frac{L}{T^2}$
H	Wave height	L
H_1	Wave height of primary wave [measured when secondary waves (solitons) are present]	L
H_2	Wave height of secondary waves	L
H_3	Wave height (measured from the bottom) ($H_3 = H + d$)	L
H_e	Equivalent wave height (measured from wave spectrum)	L
H_e'	Equivalent deep water wave height (measured from wave spectrum)	L
H_i	Incident wave height	L
H_o'	Equivalent deep water wave height	L
H_r	Reflected wave height	L
ξ	Critical slope	-
J_o	Bessel function (on the order of zero)	-

Symbol	Description	Dimensions
J_1	Bessel function (on the order of one)	-
k	Function	-
K	Equivalent sand roughness	L
K_o	Root of equation $K_o \tanh\gamma K_o = 1.0$	-
L_r	Length ratio	-
n	Coefficient of permeability Also: side slope porosity Also: exponent	-
N	A number	-
r	Hydraulic roughness Also: slope roughness Also: relative roughness Also: correlation coefficient Also: surface roughness	-
R	Wave run-up (the vertical height of the limit of uprush reached by a wave on a slope) Also: wave uprush	L
R_s	Wave run-up on single slope	L
S	Beach slope Also: bottom slope	-
t	Time	T
t_e	Fluid temperature	-
t_s	Temperature of anemometer velocity sensor	-
T	Wave period	T

Symbol	Description	Dimensions
U_o	'Characteristic' bore velocity	$\frac{L}{T}$
V	Wind velocity (surface velocity)	$\frac{L}{T}$
V_u	Uprush velocity (measured in uprush zone on structure)	$\frac{L}{T}$
V_{ur}	Relative uprush velocity ($V_{ur} = V_u/C$)	-
V_d	Dnrush velocity (measured in uprush zone on structure)	$\frac{L}{T}$
V_{dr}	Relative dnrush velocity ($V_{dr} = V_d/C$)	-
$\overline{V}$	Temporal mean velocity (measured past anemometer velocity sensor)	$\frac{L}{T}$
V_r	Velocity ratio	-
X	A horizontal distance	L
X_b	Horizontal distance (measured from point of breaking to toe of structure)	L
X_o	A point	
X_r	Horizontal distance (measured from the toe of the structure to the extent of maximum wave run-up)	L
Y_r	Vertical scale ratio	-
α	Slope angle (measured from horizontal) Also: Structure slope	-
δ	Displacement (measured from slope)	L
γ	Dimensionless wave frequency ($2\pi/T\sqrt{g/d}$)	-

Symbol	Description	Dimensions
η	Water surface elevation (measured from still water level) Also: Wave amplitude	L
θ	Wave phase angle	-
λ	Wave length	L
λ_o	Deep water wave length	L
μ	Dynamic viscosity	FT/L^2
π	3.1416	
ρ	Mass density	FT^2/L^4
ϕ	Coefficient of artificial roughness	-
ψ	A function	-
ζ	Random variable	-
∞	Infinity	-

NOTE: APPENDICES III, IV, V, VI and VII were not reproduced in this report but are available on loan from the Coastal and Ocean Engineering Division at Texas A&M University.